NASA Technical Memorandum 58275

Application of Radar for Automotive Collision Avoidance - Phase 1 Final Report Volume I: Technical Report

Edited by

Christopher L. Lichtenberg
Lyndon B. Johnson Space Center
Houston, Texas

Principal Investigator

Paul Shores
Head, Tracking Systems
Lyndon B. Johnson Space Center
Houston, Texas

DISCLAIMER

The findings in this report are not to be construed as standards, requirements, or official NASA position unless so designated by other authorized documents. This document is disseminated under the sponsorship of the Department of Transportation in the interest of information exchange. The United States Government assumes no liability for its contents or use thereof. The opinions, findings, and conclusions expressed in this publication are those of the authors and not necessarily those of the National Aeronautics and Space Administation (NASA) or the National Highway Traffic Safety Administration (NHTSA).

TRADE NAMES

Use of trade names or manufacturers in this report does not constitute an offical endorsement or approval of the use of such commercial hardware or software.

FOREWORD

This publication was prepared by the Tracking and Communications Division of the NASA Lyndon B. Johnson Space Center (JSC). It fulfills the Interagency Agreement DTNH22-85-X-07163 between the Department of Transportation (DOT) and the National Aeronautics and Space Administration (NASA). The initial or Phase 1 effort covers the period November 1984 through December 1985. Significant tasks undertaken during Phase 1 were the (1) generation of several reports and short studies, (2) design, fabrication, testing, and implementation of a data collection engineering breadboard radar, and (3) analysis of collected data and conclusions and recommendations derived therefrom. The main goal of this program is to fundamentally contribute to the development of a potentially commercial, practical collision avoidance radar for automobiles.

Volume I is the technical report consisting of 13 sections covering all the Phase 1 tasks.

Volume II consists of the development plan submitted to the Department of Transportation during Phase 1 of the NASA/DOT Interagency Agreement DTNH22-85-X-07163 and five progress reports. The progress reports provide additional technical or program management detail to that given in Volume I: Technical Report.

ACKNOWLEDGEMENTS

Special thanks are given to the many individuals who assisted this effort. Several people at the Department of Transportation made this project possible and contributed guidance and assistance, especially Drs. J. Bascunana and K. Brewer.

Thanks to W. Culpepper who, with the help of others at Lockheed Engineering and Management Services Company, handled all the test equipment preparation, data collection, and data analysis which are detailed in sections 9, 10, and 11.

P. Shores organized and managed most of the effort at JSC. His contribution of section 2 is appreciated.

Drs. E. T. Dickerson and C. Hallum from the University of Houston - Clear Lake are recognized for their contributions of sections 4 and 5 as well as their efforts regarding the literature search and collection.

Additionally, H. Nitschke and H. Erwin are recognized for managing and providing final direction necessary for completing this phase of the work.

Appreciation is extended to C. Lichtenberg of NASA-JSC for his radar design and analysis and preparation of most of sections 1, 3, 6, 7, 8, 12, and 13.

D. O'Connell, while with NASA-JSC, provided the early work on the slotted waveguide array antenna and radar accuracy analysis, among other things.

Technical review was provided by Dr. K. Krishen, R. Fenner, A. Feivesen, and Dr. W. Marker of NASA-JSC, and Dr. H. Schaeper of Lockheed - EMSCO.

CONTENTS
VOLUME 1

TABLES

FIGURES

ACRONYMS/ABBREVIATIONS

AC	alternating current
A/D	analog-to-digital
AGC	automatic gain control
ANSI	American National Standards Institute
B/B	breadboard
CAD	computer-aided-design
CAR	crash avoidance radar
CARDFILE	Crash Avoidance Research Data File
CRT	cathode ray tube
CW	continuous wave
DC	direct current
DMA	direct memory access
DoD	Department of Defense
DOT	Department of Transportation
ERP	effective radiated power
FARS	Fatal Accident Reporting System
FFD	far field distance
FFT	fast Fourier transform
FM	frequency modulated
GFE	Government-furnished equipment
HW	hardware
IF	intermediate frequency
JSC	Johnson Space Center
KRAESP	Kinetic Research Accident Environment Simulation and Projection
LEMSCO	Lockheed Engineering and Management Services Company
LOS	line-of-sight
MSA	midsized automobile
NASA	National Aeronautics and Space Administration
NASS	National Accident Sampling System
NEC	numerical electromagnetics code
NHTSA	National Highway Traffic Safety Administration
OHSA	Occupational Safety and Health Administration

PRF	pulse repetition frequency
PRR	pulse repetition rate
PW	pulse width
RCS	radar cross-section
RCV	receive
RF	radio frequency
RFP	request for proposal
RH	relative humidity
RSS	root sum squared
RSV	research safety vehicle
SAE	Society of Automotive Engineers
SAR	specific absorption rate
S/N	signal-to-noise
SW	software
TBD	to be determined
TLV	threshold limit value
T/R	transmit/receiver
UH-CL	University of Houston-Clear Lake
U.S.	United States
USASI	United States of America Standards Institute
U.S.S.R	Union of Soviet Socialist Republics
VCR	video cassette recorder
VHF	very high frequency
VSWR	voltage standing wave ratio
W/G	waveguide
XMIT	transmit

SECTION 1
INTRODUCTION

BACKGROUND

The cost of automobile accidents in death, personal trauma, and property damage in the United States alone is alarmingly high. A figure for 1982 puts this cost at more than $80 billion. The Department of Transportation (DOT) has been sponsoring research for several years aimed at reducing accident frequency and severity. Many safety innovations in the areas of auto-body structural design, airbags, braking systems, lighting systems, steering, and suspension have already been implemented. Nevertheless, accident frequency and severity has remained at unacceptably high levels.

It is believed by the DOT, others, and us that a system capable of alerting a driver in a timely fashion to the existence of an impending collision would have the potential for drastically reducing accident seriousness as well as frequency.

CANDIDATE SYSTEM

A radar is the leading candidate for such a collision avoidance system. It is felt that system characteristics such as sufficiently small size, reasonable price, high sensitivity, and high reliability can be accommodated with judicious effort given to radar design, development, test, and manufacturing. The thrust of this project has been directed toward initial system design and laboratory testing. Since automobile radar collision avoidance systems have been investigated by previous authors, the logical approach is to attempt to extend the capabilities of systems already investigated while focusing on alleviating the problems which have plagued them. To date no truly effective system has been developed and marketed which can offer a driver/driver's vehicle a warning within adequate time for him/his vehicle to react and avoid or significantly mitigate the effects of typical urban/highway collisions. The system techniques and concepts researched in any depth thus far offer a much too limited performance to be of practical use. Additionally, they suffer from unacceptably high false alarm rates. The consensus is not that radar -- whether microwave, millimeter-wave, or micron-wave (lidar) -- is inappropriate for the task, but rather that the correct radar system designs and techniques have not yet been adequately developed and applied to this unique problem.

WHY RADAR?

As currently envisioned, the collision avoidance system must be effective in several areas. It shall (1) detect large objects at a distance, e.g., a car, truck, or motorcycle at typically 300 feet (or to be determined (TBD)); (2) determine the distance to this object; (3) determine some useful measurement of some component of the object's velocity with respect to the radar; (4) be capable of tracking multiple objects simultaneously; (5) observe a horizontally-oriented sector, or scan, of at least several highway lanes; (6) only give a warning when a collision trajectory is

determined; (7) operate through fog, rain, snow, hail, sandstorm, dust-storm, or other inclement weather conditions; (8) be a technology that can be miniaturized enough to be compatible with midsized automobile equipment space; (9) be reasonably priced when the technology is brought to maturation and the system is produced in consumer quantities; (10) be effective and reliable; (11) be safe. Radar is the only technique which presently has a hope of simultaneously meeting these requirements.

OBJECTIVES

The main objective of the Phase I effort was to design, develop, and evaluate the performance of a potentially commercial radar system which could provide advanced warning of impending collisions with motor vehicles or other traffic hazards. A potentially commercial system must use components and techniques which are now, or will be in the future, fairly inexpensive, relatively non-exotic, and can be mass produced. For example, traveling-wave-tube-amplifier active array antennas with cryogenically cooled parametric amplifier receiver modules by nature are an exotic and costly technology, now and into the foreseeable future. On the other hand, a Gunn diode/Impatt diode transmitter module with a GaAs transistor receiver amplifier represents a lower cost technology which is becoming cheaper each year coincident with the maximum performance capabilities of the components improving each year.

APPROACH AND TASK AREAS

The approach taken to this project and the tasks performed were as follows.

a. Literature searches were performed and procurement of many of the useful documents occurred. Searches covering automobile collision avoidance devices and biological effects of microwave radiation were the main areas of concentration. Contacts were made with DOT, university, and independent researchers to obtain additional literature sources pertinent to the problems.

b. Geometrically-oriented analyses were performed on the relationships of targets relative to the radar-equipped vehicle to derive information related to determining parameters such as range, range rate, angle, angle rate, and time to impact.

c. A critical review of previous radar efforts was performed internally and was used to guide decisions relating to selection of the data collection radar design.

d. A review of traffic accident reports was performed to assist in the determination of radar parameters such as detection distance, area of coverage, speed of collision objects, etc.

e. A study of weather effects on radar performance was prepared to assist in determination of possible carrier frequencies, modulation methods, detection distance, and disruption of radar operation during inclement weather conditions.

f. A report was prepared addressing preliminary considerations of the collision trajectory models and associated decision logic.

g. A data collection radar and instrumentation system were designed, fabricated, and installed on a test vehicle. They were used to collect engineering data useful for determining system operation and target return signal information. Static tests primarily were performed. A limited amount of dynamic, or moving radar, tests were conducted.

h. The test data were recorded, then analyzed off-line using equipment in the radar data processing facility, which consists of microcomputers, analog-to-digital conversion equipment, software packages, video display equipment, and ancillary equipment.

i. Conclusions and recommendations for future development efforts based on items a through h were derived.

SECTION 2
PRELIMINARY DESIGN REQUIREMENTS ASSESSMENT

INTRODUCTION

A review of the available literature and test results of this previous work was conducted to establish a 1985 baseline of radar technology. The purpose of this review is to minimize duplicating previous work and at the same time strive to determine system characteristics that will eliminate problem areas of previous systems.

HISTORICAL DATA BASE

The major effort to date for this phase of the program has been the review and collection of documents relating to historical efforts in implementing a crash avoidance radar (CAR) to provide automatic braking and/or warning of impending automotive collisions. A summary of the characteristics of the various radars either existing or under development in 1980 was prepared by Kinetic Research for the DOT.[1] This summary is reproduced as table 2-1 and is supplemented by information obtained from more recent publications.[2,3] This supplemental information is also contained in table 2-1. The final entry in table 2-1 is the design goal performance characteristics for the NASA Phase 1 experimental radar which was used for data collection only.

A literature search revealed that relatively many documents have been published in the last 15 years relating to the utilization of radar for automotive crash avoidance. A listing of the majority of the publications collected and reviewed in this effort is contained in the bibliography.

A comprehensive review of these documents reveals some interesting facts. During the first 10 years of automotive radar research the only serious development efforts were directed towards one-dimensional radar systems (range and range rate). The ten radars analyzed by Kinetic Research[1] were of this type. False targets were inhibited by a combination of reducing the maximum detection range as a function of steering angles and velocities and reducing the average coverage volume to a 5-degree cone or less in the forward direction of the vehicle. Although it was recognized by several investigators that improvements could be made in the ratio of false-to-real target detection process by the addition of the capability to measure both the forward and lateral components of range and velocity, there appears to have been only one serious development effort to date.[3] The Nissan Motor Company, Kyoto, Japan, is designing and testing a stereo radar system that measures the lateral component of velocity by using two pulse-Doppler radars and detecting the phase difference of the two Doppler signals.

TABLE 2-1.- AUTOMOTIVE RADAR SYSTEMS

Description	Nissan-Mitsubishi	Benz-Sel
System		
Principle	Pulse Doppler/stereo	FM-CW (sawtooth)
Range	5 to 127 m	10 to 100 m
Accuracy	1 m	± 2.5 m
Relative speed	+ 1 to + 127 km/h	- 30 to 160 km/h
Accuracy	1 km/h	+ 2.5 km/h
Sensitivity - Pr/Pt	-78 dB	
Antenna		
Number and type	1 parabola/2 stereo	2 parabola
Beam width	H3.4°, V6°	H2.5°, V4°
Polarization	45°	V
Tx and Rx		
Main oscillator	Gunn	Gunn
Frequency	24.15 GHz	35 GHz
Output power	20 mW	20 mW
Pulse width	20 ns	CW
Receiver	Homodyne	Superheterodyne
Range cut by steering angles	Contained in program	Contained
Notes		
Supported by	MITI	Benz-Sel plus Government
Started in	1974	1975

TABLE 2-1.- Continued

Description	Telefunken	VDO
System		
Principle	Pulse	Pulse
Range	5 to 120 m	5 to 120 m
Accuracy	+ 1 m	± 1 m
Relative speed	150 km/h	130 km/h
Accuracy	± 3.6 km/h	130 km/h
Sensitivity - Pr/Pt		
Antenna		
Number and type	2 parabola	2 parabola
Beam width	H2.5°, V4°	H2.5°, V4°
Polarization	V	V
Tx and Rx		
Main oscillator	Gunn	Gunn
Frequency	35.6 GHz	35 GHz
Output power	300 mW	200 mW
Pulse width	20 ns	30 ns
Receiver	Superheterodyne	Superheterodyne
	250 kHz PRF	
		1.5 mW average
Range cut by steering angles	Contained	Contained
Notes		
Supported by	Bosch-Telefunken plus Government	BMW-VDO plus Government
Started in	1975	1968

TABLE 2-1.- Continued

Description	Bendix	CA Research	RCA
System			
Principle	Diplex	Pulse, gated	FM-CW
Range	30 to 75 m	6 to 96 m	6 to 30 m
Accuracy			0.2 m
Relative speed			0 to 60 km/h
Accuracy			2.5 km/h
Sensitivity-Pr/Pt			
Antenna			
Number and type	1 parabola		2 printed
Beam width	H2.5°, V4°	H1°	H3°, V5°
Polarization	45°	45°	45°
Tx and Rx			
Main oscillator	Gunn	Gunn	Gunn
Frequency	36 GHz	24 GHz	17.5 GHz
Output power	25 mW	100 mW to 2.5 W	20 mW
Pulse width	730 ns	25 ns	
Receiver	Homodyne		Homodyne
Range cut by steering angles	Contained		Contained
Notes			
Supported by	(Independent)	(Independent)	(Independent)
Started in			1971

TABLE 2-1.- Continued

Description	Sperry	British	Rashid
System			
Principle	Base-band	FM-CW (sawtooth)	FM-CW
Range	45 m		
Accuracy	0.1 m		
Relative speed			
Accuracy			
Sensitivity-Pr/Pt			
Antenna			
Number and type	3 dipole	2 parabola	1 dielectric lens
Beam width	H2.5°		
Polarization			
Tx and Rx			
Main oscillator	Differentiating antenna Base-band radiation	Gunn	Gunn
Frequency		41.8 to 33.4 GHz Sweep of 0.25	X-band/K-band
Output power			
Pulse width		15 ms	
Receiver	Super-regenerative receiver		
Notes			
Supported by	DOT	Lucas	(Independent)
Started in	1974		1970

TABLE 2-1.- Continued

Description	Toyota	Arno
System		
Principle	FM-CW (triangular)	Narrow dc pulse
Range	3 to 60 m	
Accuracy	0.5 m	
Relative speed	± 60 km/hr	
Accuracy	5 km/hr	
Sensitivity-Pr/Pt		
Antenna		
Number and type	2 cross beams	
Beam width	2 degrees	
Polarization	Diagonal	
Tx and Rx		
Main oscillator	Gunn	Tunnel diode
Frequency	49.5 GHz	L-band to S-band
Output power	30 mW	Very small (?)
Pulse width/PRF	750 Hz modulation	
Receiver		

TABLE 2-1.- Concluded

Description	NASA Experimental Radar (used for Data Collection Purposes Only)
System	
Principle	Phase monopulse
Range	50 to 500 ft
Accuracy	± 4.5 ft
Relative Speed	0 to 176 fps
Accuracy	
Angle (relative)	(see data analysis section)
Accuracy	
Antenna	
Type	1 waveguide array or 3 separate elements used as functional replacement
Beam width	H120° V4° or H12° V8°
Polarization	Horizontal
TX and RX	
Main oscillator	Gunn
Frequency	24 GHz
Output power	(2 W design) 200 mW-used
Pulse width	20 ns
Receiver	Heterodyne - 150 MHz intermediate frequency (IF)

SYSTEM PERFORMANCE CRITERIA

In the formulation of the specific system design, consideration will be given to the following general guidelines provided by the DOT.

a. Capability of the selected system to operate satisfactorily under conditions including rain, snow, hail, blowing sand, etc.

b. Capability of the selected system to be compatible with the requirements and use of the vehicle, stand the environmental effects, and have electromagnetic compatibility with the expected environment.

c. Human safety for the highest continuous radar exposure levels that could occur in real world traffic situations.

d. As a minimum the following accident types must be considered in the design approach: passenger car head-on, rear end, sideswipe, and angle collisions; single vehicle collision accidents involving trees, utility poles, nonfixed objects, bridge abutments, and guardrails; and accidents involving motorcycles and pedestrians.

e. Expected life, size, weight, and estimated original and maintenance costs, if the system was designed for production quantities of at least 100,000 units, should be consistent with the economic use of the system.

f. The design must consider the location of the components within a typical midsized passenger car with a minimum impact to the normal day-to-day operation of the vehicle.

REAL VERSUS FALSE ALARMS

The predominant task is to design a crash avoidance radar which detects hazards with small false-to-real hazard detection ratios. System designs prior to 1981 were one-dimensional (range and its derivatives) and had no means of determining angle or lateral position of an object. As a result of the one-dimensional measurements the warning algorithms were subsets of linear combinations of range, velocity, and various mechanical parameters such as steering angle. Reduction of the false alarm rate was accomplished by limiting coverage volume (beam width), reducing maximum range capability, and reducing parameter limits as a function of steering angle. Although these schemes worked to some degree, it forced a trade-off of desirable characteristics and an overall reduction of the effectiveness of the warning system. It is felt to be mandatory that targets are tracked in angle in addition to range. Otherwise, false alarm rates will continue to be high and sensitivity to targets displaced widely in angle will be low.

Radar Signature Discrimination

Several documents have suggested the possible use of target signatures to discriminate against false targets. There are many disadvantages to this technique. The first and most obvious is that any target is a real hazard if it is involved in a collision. Visually the experienced driver recognizes

a guardrail as a non-hazard by the perception of rate of change of angle and not because it is a guardrail.

The radar cross-section of an object is determined by the magnitude of the returned signal and varies as a function of aspect angle, its size, geometrical shape, and its electrical properties such as permittivity. Examples of the variation of cross-section magnitude as a function of aspect angle for a standard sized automobile were presented by E. E. Martin of Georgia Tech[5]. Peak-to-mean value variations were approximately 20 dB, and peak-to-minimum fluctuations ran approximately 40 to 50 dB depending on frequency.

Phase, the other important parameter of radar target signature analysis, was not measured in these tests, but should exhibit similar fluctuations as a function of aspect angle. The target signatures would vary widely due to the many different designs of bridges, guardrails, roadside signs, and such details as damaged sections, bends, curves, etc. Due to the limitation of radar resolution and increased complexity of signal processing, it is not considered practical at this time to use pattern recognition for the reduction of false alarms. It may be possible though to use the variations in amplitude and phase as an indication of variation in the aspect angle of the target which in turn implies lateral motion.

Experimental Evaluations

JSC engineers performed a series of tests on their data collection radar which in effect evaluated both the phase and amplitude characteristics of the reflected radar signals. In the period of time from 1975 to the present at least three systems have been proposed by others that have the potential to reduce the frequency of false alarms. These systems are unique in that the measurement of the lateral position component could be possible.

A stereo radar system under development by Nissan Motor Company[3] appears to be the only system of this type that has advanced beyond the proposal stage. The principle of operation of their stereo radar is to measure the phase difference between two pulse-Doppler radars mounted on the front of the vehicle. A coherent continuous wave (CW) version of this technique was fabricated and tested on the JSC antenna range. Preliminary analysis of the data indicates the technique warrants further study.

The second method as proposed in 1975 by Mark Krage[4] would utilize two 10 GHz radars and detect lateral motion by measuring the difference of the two Doppler frequencies. A 24 GHz version of this method was assembled in the laboratory and tested very briefly at the JSC antenna test range. The initial examination of the data indicates that with conventional frequency difference techniques the time required to detect the Doppler frequency difference is excessive. A novel circuit was devised that is capable of detecting differences as small as 1 Hz. The resulting reduction in detection time was significant. To further reduce the detection time a 100 GHz version could be fabricated and tested. The increase in the operating frequency should reduce the detection time by a factor of four due to the increase in detected Doppler frequencies.

The third technique proposed by D. M. Grimes and V. P. McGinn[2] would be a swept-beam system operating in the 80 to 100 GHz frequency region. It was suggested that the beam could be swept approximately ± 5 degrees and provide an angle sensing output to provide lateral or cross-range information. No details of the suggested implementation approaches were available. However, a narrow, scanned beam system seems to hold the most promise for high performance if one is willing to accept the increased hardware and signal processor/software complexity.

From this brief review of the historical information and other data available, the conclusion can be drawn that the most promising technique for the reduction of false alarms must include a method of determining the lateral components of relative position.

CHARACTERIZATION OF THE ENVIRONMENT

Characterization of the environment is the analysis required to determine the equations of relative motion of the various targets within the field-of-view of the radar. Once these equations have been established, they can be used to determine the required parameters to be measured and the corresponding measurement accuracy requirements.

The Technical Problem

At first glance, the problem of designing a radar for automotive crash warning does not appear difficult: simply detect an object in your path coming toward you and sound the warning. The problem becomes difficult when you consider the environment in which there is a large number of potential targets most of which present no hazard. A radar "target" is anything which provides a radar reflection. "Clutter" is any radar target which is unwanted. In the present case, this could be other buildings, road signs, rain, debris, bridge abutments, guardrails, or even the road surfaces. To further complicate the problem these clutter objects have the potential of being a desired target if circumstances should place the object on a collision trajectory with the radar vehicle.

Therefore, if one intends to blank out clutter through some method, he must be sure he does not discard true hazards in the process. A radar system can be designed to provide the following information about the targets it detects: signal strength, range (relative distance), range rate (relative velocity), angle, and angle rate. The distinction between hazardous and nonhazardous targets must be made on the basis of some form or combination of these parameters.

Geometry of the Traffic Environment

This section presents an examination of the geometry and dynamic environment of traffic situations in order to evaluate the parameters of a radar system which would warn of impending collisions. The aim here is to recognize relevant considerations and not to evaluate particular systems.

Relative Geometrical Relationships of Fixed Roadside Targets

Range and angle from the radar-equipped vehicle must be appropriately defined for discussion. These parameters will be referenced to a radar-centered, radar-fixed coordinate system. The center of the coordinate system will be taken to be the location of the phase center of the radar antenna system. The X-dimension will lie along the radar vehicle's velocity vector. Y is then perpendicular to the vehicle's motion.

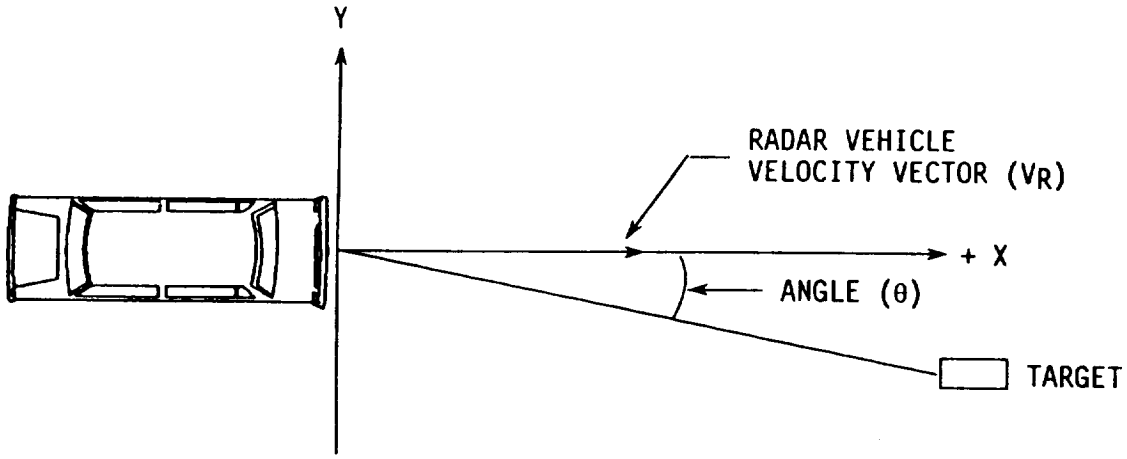

Figure 2-1.- Vehicle-centered, vehicle-fixed coordinate system.

Range in this system will then refer to the distance of the target in question to the origin. Angle will be defined as the arctangent of the Y-coordinate over the X-coordinate.

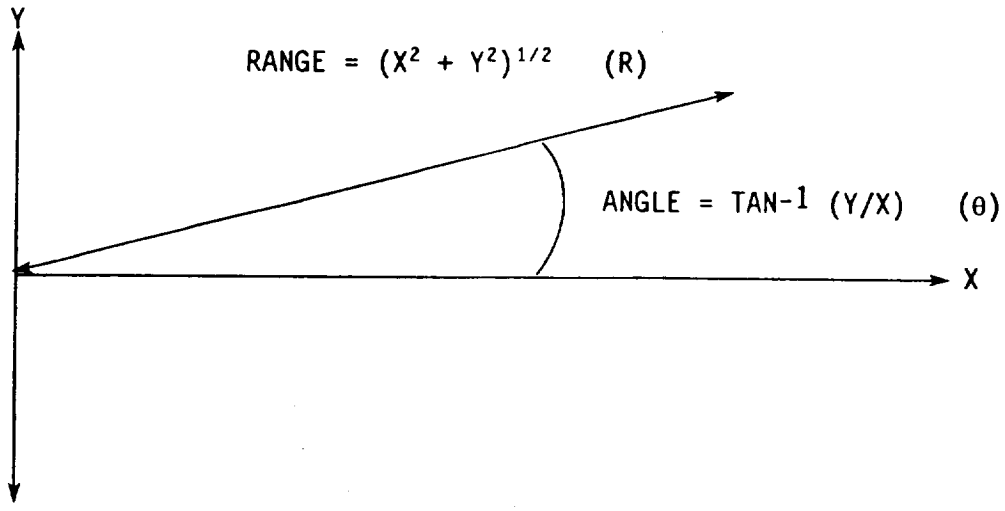

Figure 2-2.- Range and angle definitions.

For the purpose of determining which of the radar measured parameters of range, angle, and their derivatives would be indicators of potential hazards, a series of computer-generated plots with various affects were made and are included as figures 2-3 through 2-7.

These geometrical relationships were studied using a computer simulation to derive a preliminary set of required measurement accuracies (table 2-2).

A copy of the report is included as an appendix.

TABLE 2-2.- ACCURACIES DERIVED FROM ELEMENTARY ANALYSIS

	Strictest design tolerance	Loosest design tolerance
Range	.005 ft	15 ft
Range rate	.01 fps	3.8 fps
Angle	.1°	.1°

These required measurement accuracies were arrived at using simplifications of the actual expected radar environment. They serve as a starting point for future considerations of the accuracies actually required for an operational radar. They should not be considered as the required accuracies for an operational system.

Radar Spatial Coverage

The purpose of the following discussion is to discuss the spatial coverage for the radar which in turn could be used to calculate the required antenna pattern. The following statements were derived from previous studies and reports. They will be presented in this section without proof:

a. Majority of side impacts occur in the region of 30 to 50 degrees.

b. Most benefits are derived from radars in the case of head-on or rear impacts.

c. Orthogonal impacts occur more frequently at intersections and with velocities less than 30 mph.

d. Pedestrian accidents occur more frequently in cities and towns with vehicle velocities less than 25 mph and initial ranges of less than 50 feet.

e. Some radar braking studies in the past suggest that a maximum range cut-off at 200 feet provides adequate range coverage. Increasing the range cut-off to 400 feet does not add much and decreasing it to 100 feet results in a significant loss of benefits. However, these values were arrived at for simple, non-angle sensing radars. They can only be used as a starting point for future analysis of the requirements.

The following will be assumed throughout this section:

a. Velocity extremes are between 176 fps (two cars approaching each other going 60 mph) and 5 fps (3.5 mph).

b. Targets are assumed to be idealized points (invalid assumption, in general).

c. The radar vehicle velocity vector is aligned with the phase center of the radar antenna and the origin of the coordinate system.

To estimate the vertical coverage it is necessary to examine the anticipated environment. The Bendix Corporation Phase II study conducted in 1976 recorded the number of false alarms from an experimental radar over three test courses and with variations of radar parameters. A significant factor from the results of this data is the large number of false alarms due to overhead targets such as overpasses, overhead signs, and bridges. As reported in the Bendix report 55 percent of all false alarms from their tests were identified as overhead targets. Smaller percentages of false alarms were attributed to vehicles on the side of the road, guardrails, and traffic in adjacent lanes.

Although there is a finite number of true targets in the vertical plane (entrance and exit ramps, etc.), these for the most part are limited to vertical angles of less than 3 or 4 degrees. Two of the radar parameters varied in the Bendix studies were maximum detection range and antenna beam width. The beam widths were 2.5, 4.5, and 10.0 degrees and were fairly symmetrical in both the horizontal and vertical planes. As illustrated in figure 2-11, the average number of false alarms increases rapidly as the beam width and maximum detection range get larger. Note that this was derived for simple, non-angle sensing radar. The general trend of more false alarms resulting from wider beam widths or coverage areas would tend to hold for angle sensing, more sophisticated radar. The major difference between angle and non-angle sensing radars is that the angle sensing radars would presumably have false alarm levels orders of magnitude less than the non-angle sensing radars. This would arise from the ability of the angle sensing radar to discard targets that are not on a collision path with the radar-equipped vehicle.

The limit to which the vertical antenna beam width may be reduced is limited by the area available to mount the antenna and the degree of difficulty in aligning the radar boresight. Additionally, a beam width of less than one degree would be in the range of variations due to the distribution of loads. The typical height of overhead signs and overpasses is approximately 15 feet. Comparing the beam spreading as a function of beam width and distance, the 10 degree beam width exceeds this height at 100 feet and the 4.5 degree beam width at 200 feet. The 2.5 degree beam width is approximately equal to 15 feet at a distance of 300 feet. This correlates very closely with the Bendix measured data. The trade-off of these factors leads to the conclusion of a vertical beam width of 2 to 3 degrees.

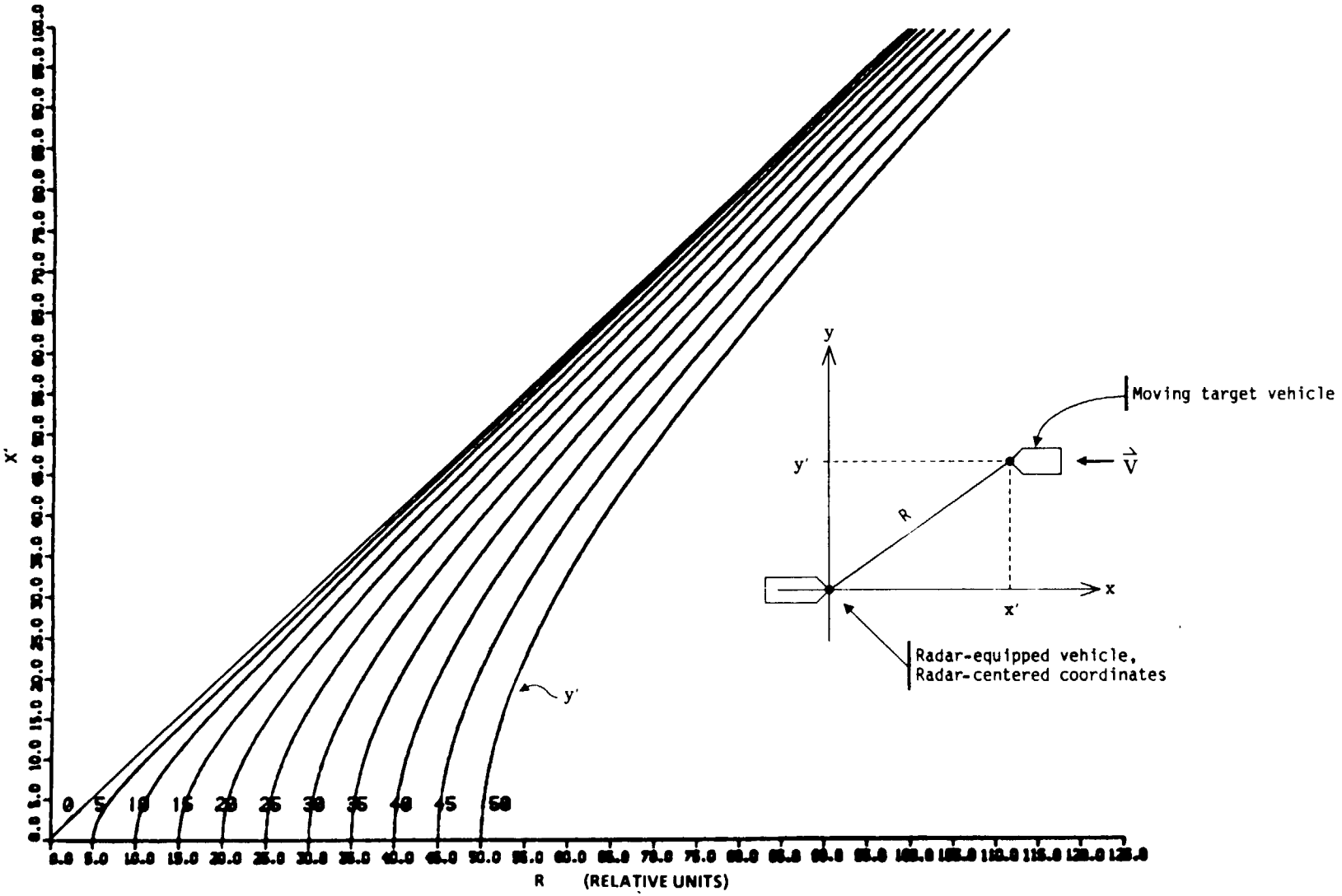

Figure 2-3.- Range trajectories as a function of target offset.

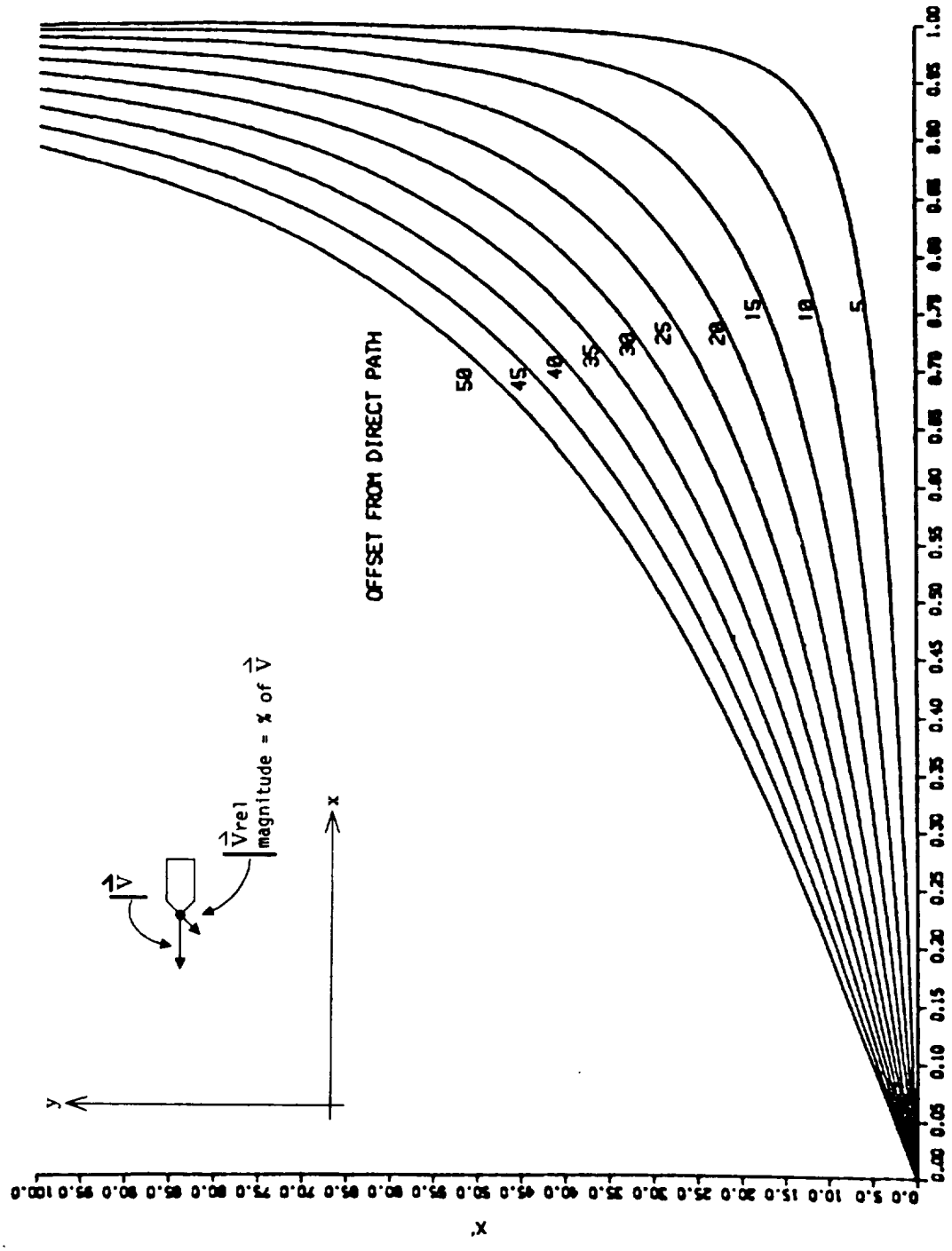

Figure 2-4.- Variation of velocity as a function of target offset.

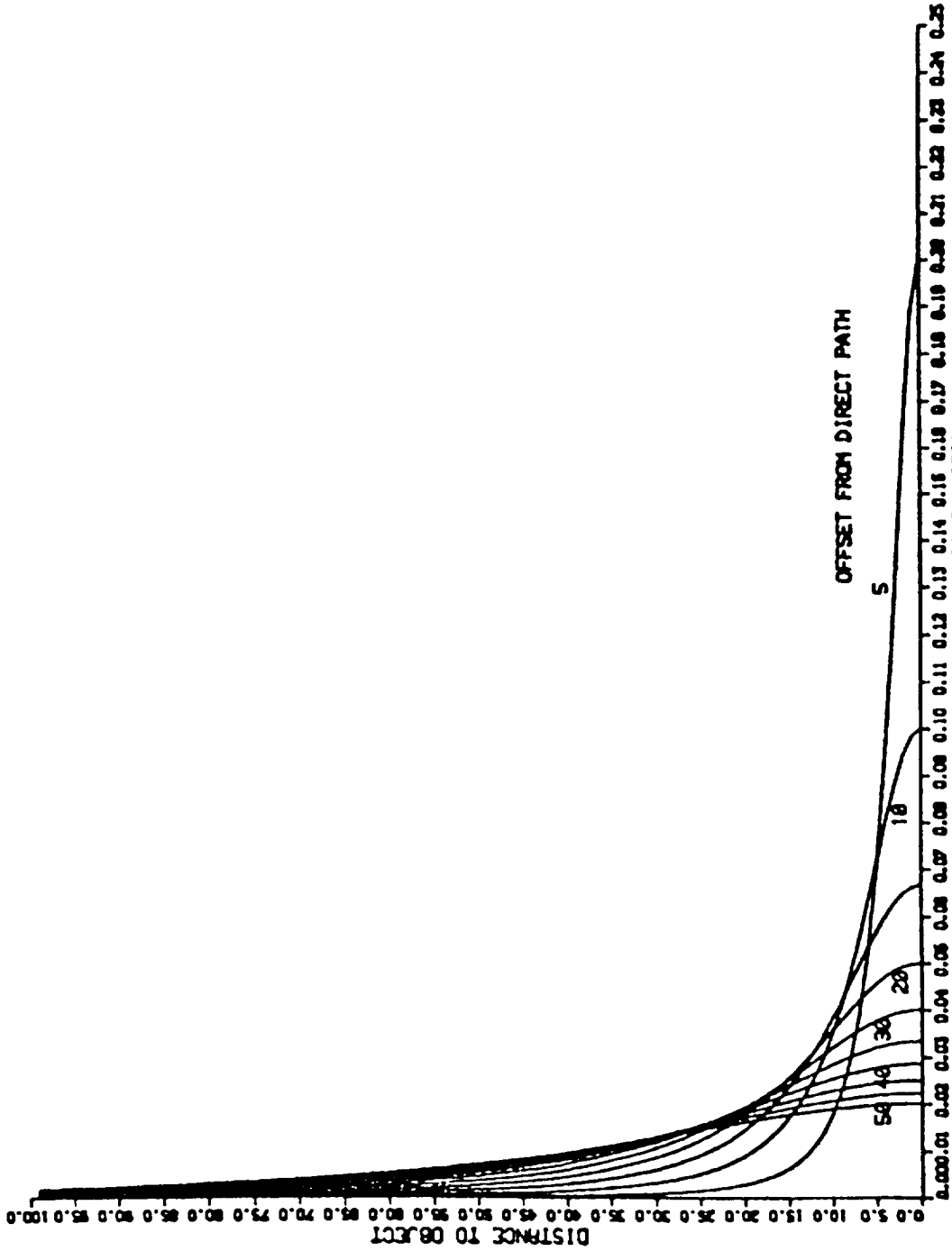

Figure 2-5.- Acceleration as a function of target offset.

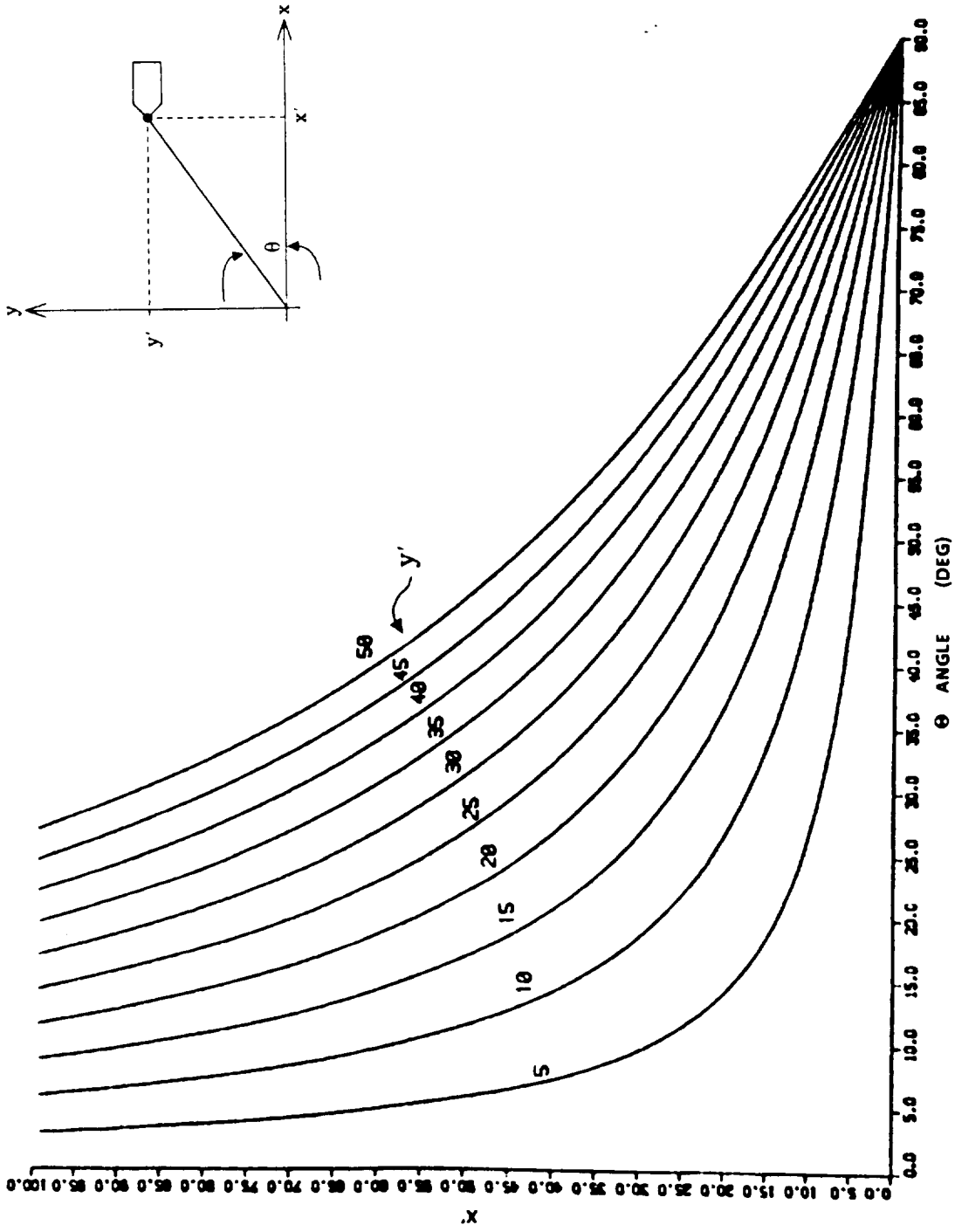

Figure 2-6.- Angle variations as a function of target offset.

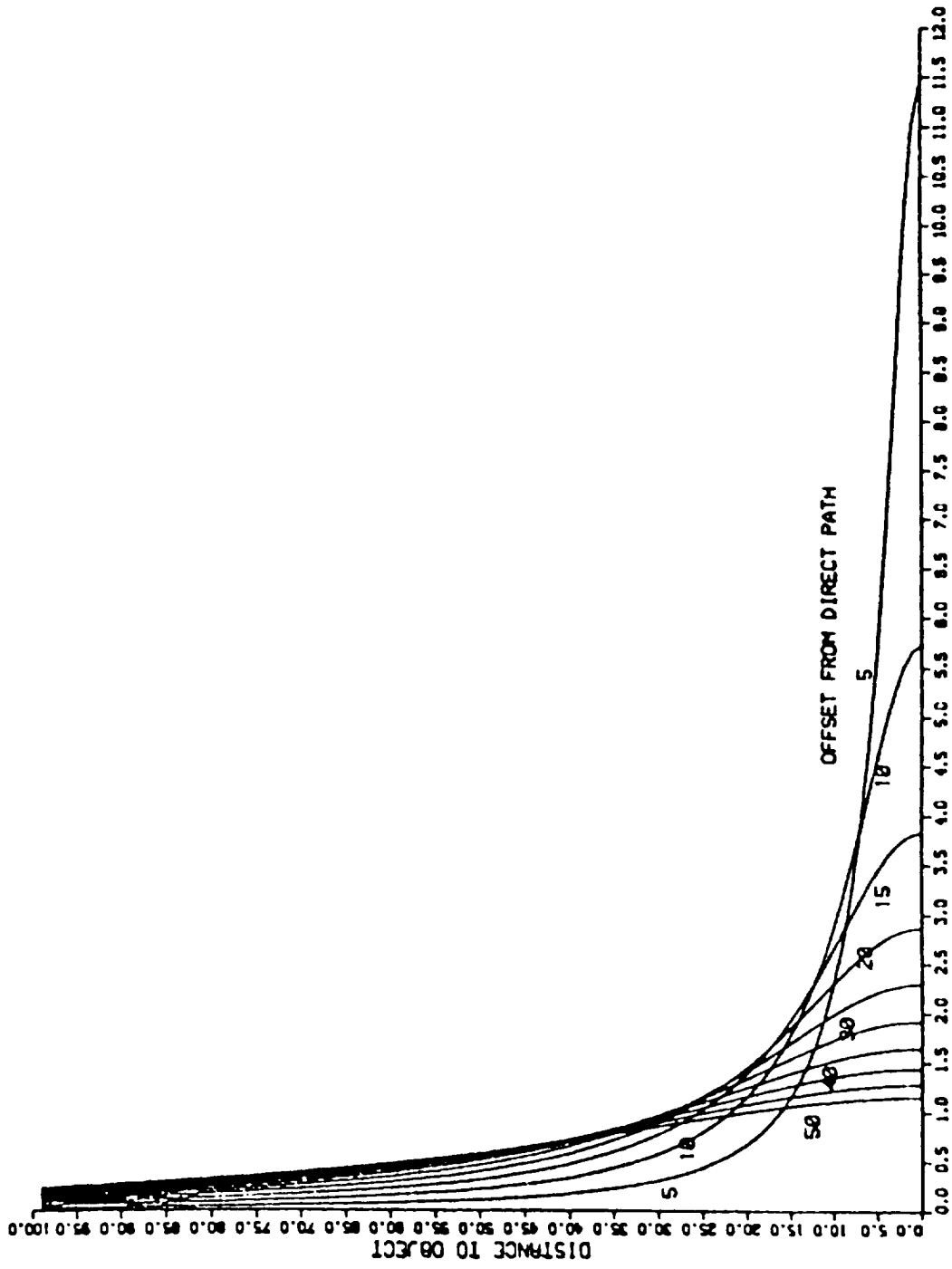

Figure 2-7.- Angle rate variations as a function of target offset.

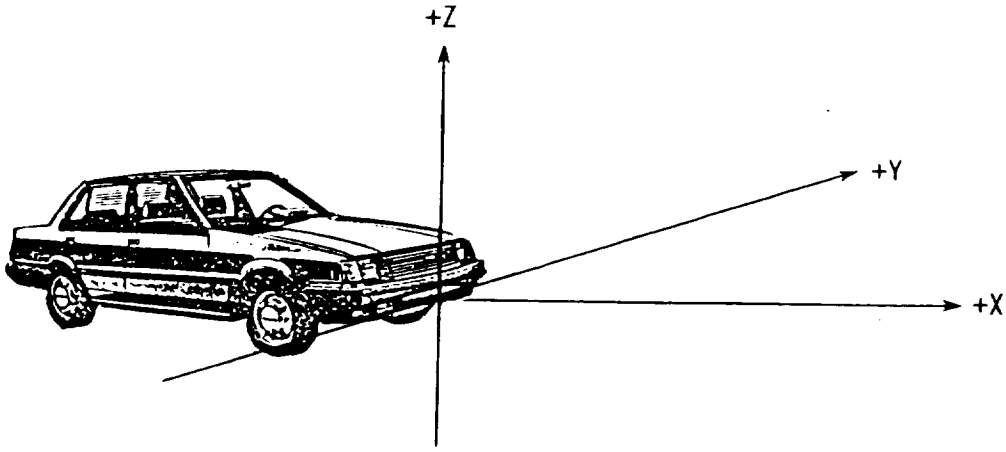

Figure 2-8.- Radar coverage diagram.

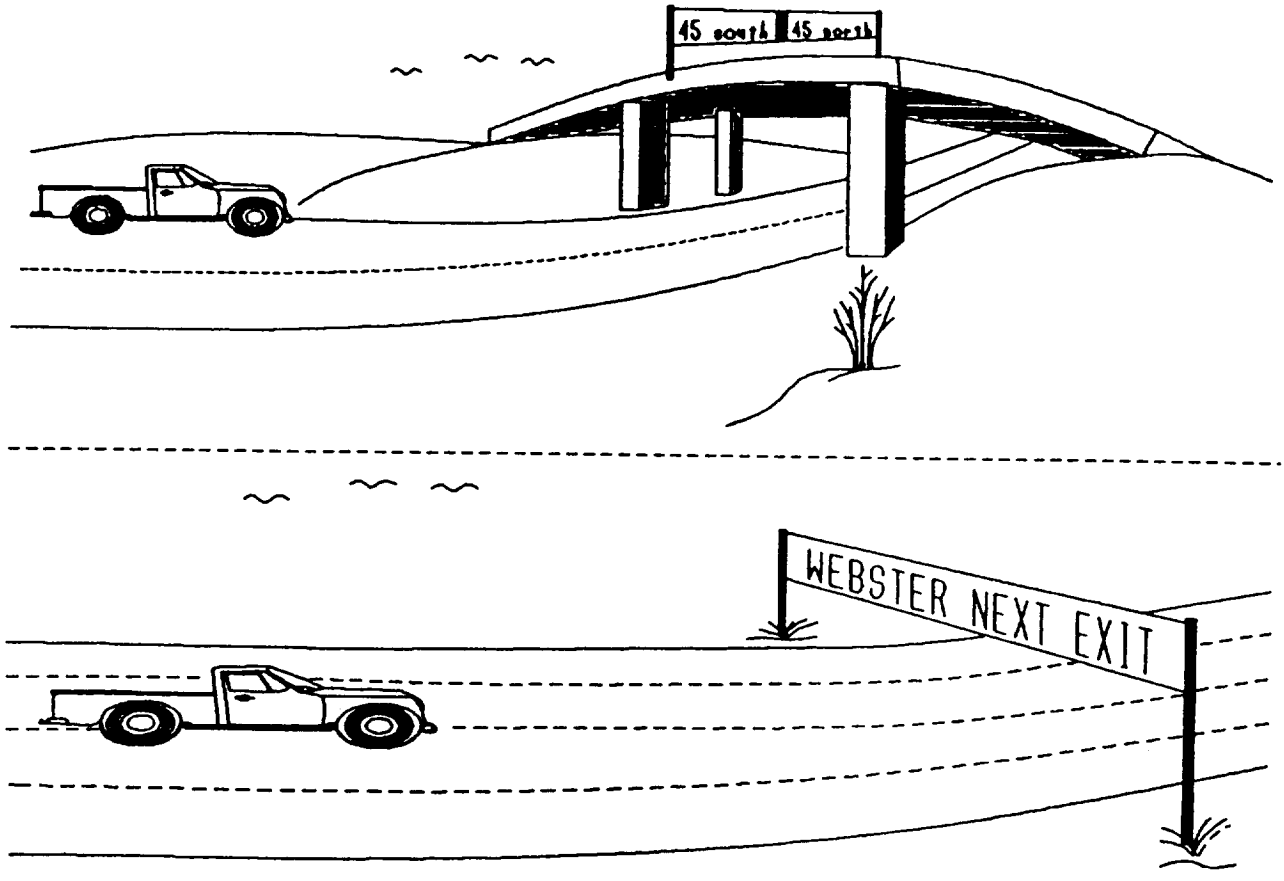

Figure 2-9.- Examples of overhead false targets.

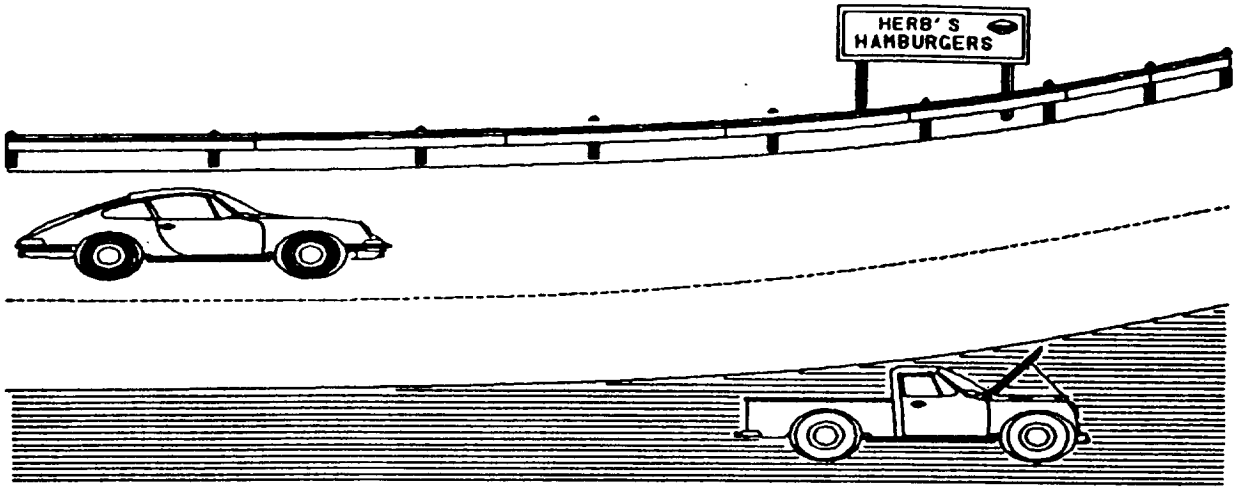

Figure 2-10.- Examples of roadside targets.

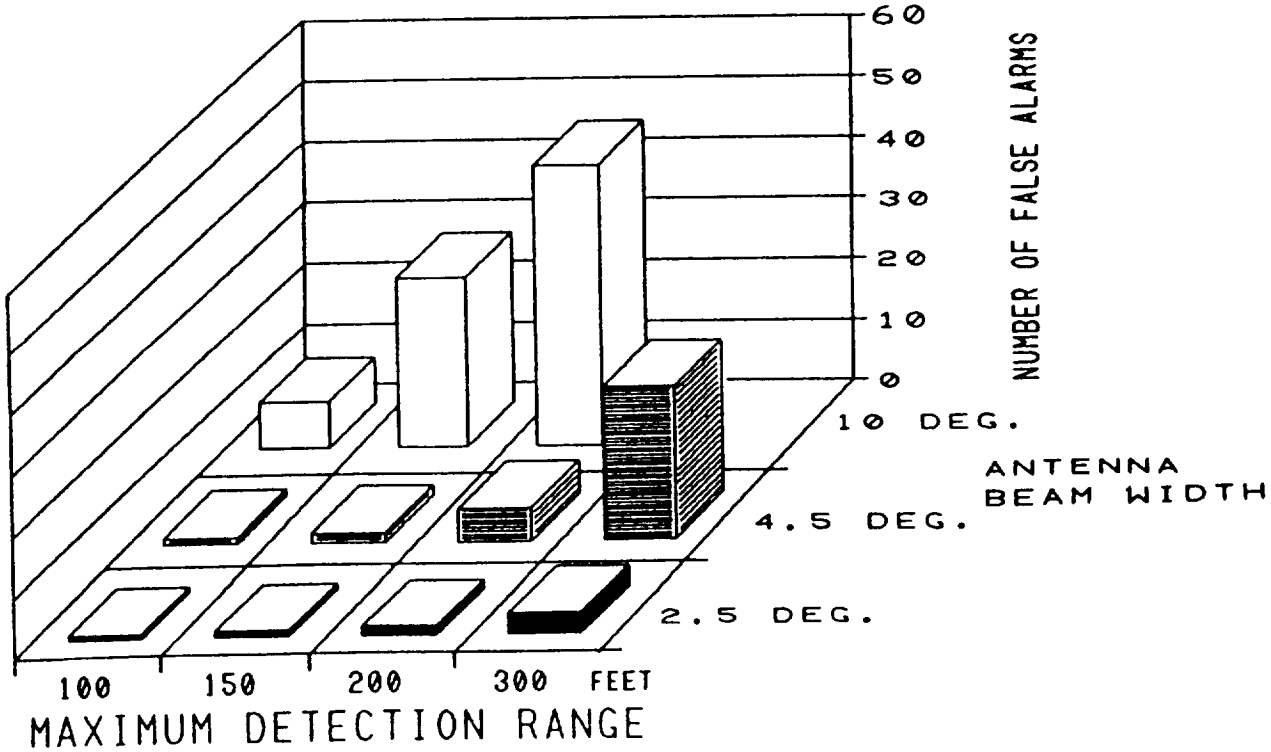

Figure 2-11.- False alarms as a function of beam width and maximum range.

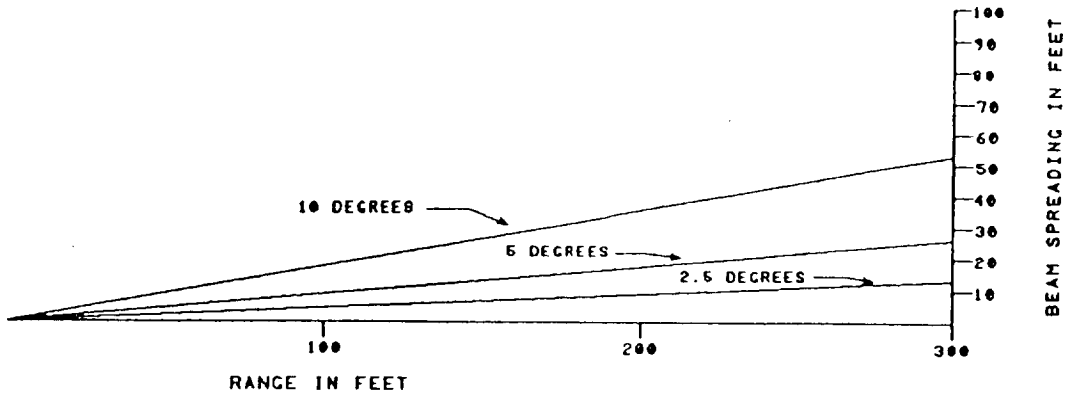

Figure 2-12.- Beam spreading as a function of distance and beam width.

REFERENCES

1. Ausherman, V. and K. Friedman, "Review of Collision Avoidance Cost-Benefit Analyses," Kinetic Research Technical Report, KR-TR-073, November 1980.

2. Grimes, D. M. and V. P. McGinn, "Automotive Radar: Practicality and Effectiveness," Society of Automotive Engineers (SAE) Government-Industry Conference, Washington, D.C., May 1984.

3. Tachibana, Akira, Norio Fujiki, Masao Sakata, Masami Kihoto, and Toshihisa Fuijiwara, "Stereo Radar System for Automobile Collision Avoidance," The Ninth Technical Conference on Experimental Safety Vehicles, November 1-4, 1982, Khoto, Japan.

4. Krage, Mark K., "Binaural Automobile Radar," Automotive Engineering and Exposition, February 24-28, 1975, (750089).

5. Martin, E. E. "Dual Polarized Radar Cross-Section Measurements of Vehicles and Roadway Obstacles at 16 GHz and 70 GHz," Eng. Exp. Station. Georgia Tech, November 1973.

APPENDIX

ASSESSMENT OF PARAMETRIC ACCURACIES REQUIRED OF AN AUTOMOTIVE COLLISION AVOIDANCE RADAR

by

Daniel F. O'Connell

PURPOSE AND SCOPE

This document presents an examination of the geometry and dynamic environment of traffic situations in order to evaluate the accuracies required of a radar system which would warn of impending collisions. The aim here is to establish generic requirements and not to evaluate particular systems. Each of the parameters measurable by a radar system (range, angle, and their derivatives) are discussed in terms of their possible uses in collision determination. The accuracies required to support these uses are generated. RF effects shall not be treated in this report.

INTRODUCTION AND BACKGROUND

The National Aeronautics and Space Administration, at the request of the Department of Transportation, is conducting a study in the application of radar systems for automotive collision avoidance. Past studies[1] have indicated that an effective system could significantly reduce the property loss and personal tragedy associated with automobile accidents. Several candidate systems have been designed and tested by different organizations,[2] but to date the reduction of false alarm occurrences remains a problem to be solved before a system may be deemed practical.

The designs and breadboards to be generated by this study will be geared toward solving this problem. Prior to developing these designs, the accuracies required of the various parameters it measures must be known, as these have a major impact on the system design. These accuracies may be determined by examining the dynamic environment in which the radar operates and establishing differences in the magnitudes of measured parameters (and the rate they are changing) for collision courses versus noncollision courses. The control algorithm which makes the collision/noncollision decision will be presented in a later report.

PRELIMINARY DEFINITIONS AND ASSUMPTIONS

"Range" and "angle" must be appropriately defined for discussion. These parameters shall be referenced to a vehicle-centered, vehicle-fixed coordinate system. The center of the coordinate system shall be taken to be the location of the radar transmitter if a single antenna system is under discussion and the middle of the front of the vehicle if multiple antennas are used. Unless otherwise stated, the latter location will be assumed. The X-dimension shall lie along the vehicle's velocity vector. Y is then perpendicular to the vehicle's motion.

Range in this system shall then refer to the root sum squared (RSS) distance of the target in question from the origin. Angle shall be defined as the arctangent of the Y-coordinate over the X-coordinate.

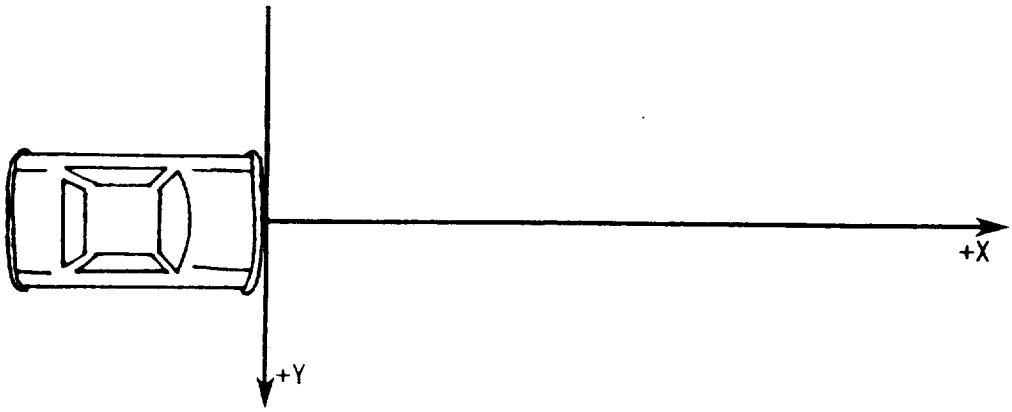

Figure 1.- Vehicle-centered, vehicle-fixed coordinate system.

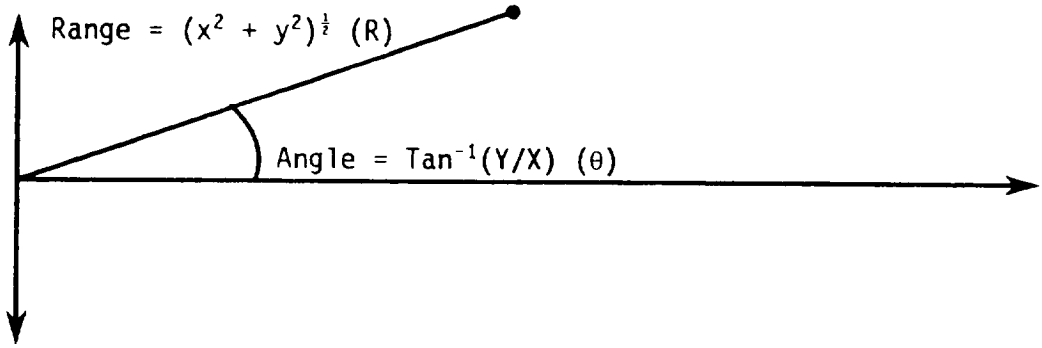

Figure 2.- Range and angle definitions.

Range rate and angle rate are the derivatives of the respective measurements. The following shall be assumed throughout this report:

- Measurements are made only in the forward direction.
- Radar detection range is 300 feet. Anything farther away is assumed not to be in the radar field-of-view.

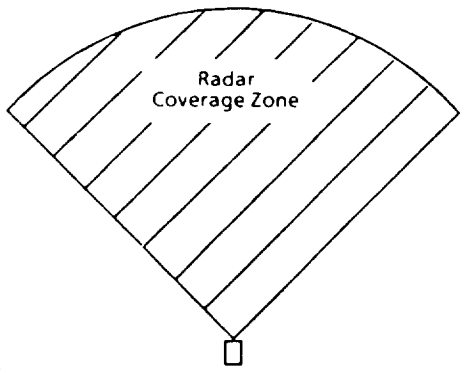

(Drawn approximately to scale)

- Angular coverage is ± 45° from direction of travel. Anything outside this region is not in the radar field-of-view.
- The range at which a decision to warn/not warn must be made is variable with the measured range rate.
- Range rate extremes are 176 fps (two cars approaching each other going 60 mph) and 5 fps (3.5 mph, no damage likely).
- Unless otherwise stated, targets are assumed to be idealized points.

ACCURACY DETERMINATION TASK

To generate the accuracy requirements for the proposed system, one must define the tasks the measurements will be required to support. As stated earlier, the primary task of the radar system is to warn of impending collisions, with special emphasis on reducing to the maximum extent possible the false alarm rate.

To accomplish this task, it will be necessary to determine not only if the target's range and velocity are such that the distance to the target is less than the required stopping distance, but also if the course it is on represents a collision trajectory. These two different tasks impose different requirements on the various parameters.

The first task involves establishing a "warning threshold" distance at which to sound an alarm, based on the measured distance and speed of the target. In many systems this task will be the major accuracy driver for the range and range rate measurements. The second task, determination of a collision trajectory, involves monitoring the behavior of the range and angle measurements to predict if the present course is an impending collision. This task will likely be the major driver for angle and angle rate accuracies.

This partioning is true in general, but there are system concepts in which collision prediction is the dominant driver of accuracy requirements for range or range rate, as well as angle. For completeness, these situations will be treated as well.

PARAMETERS

Range and Range Rate

The measured range to a target cannot in and of itself distinguish a collision trajectory from a noncollision trajectory. Range alone merely specifies that the target is somewhere on a circle with the measuring point at its center.

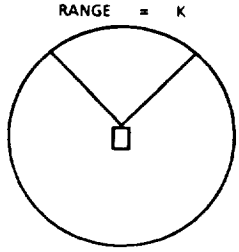

Of course, we are restricting our measurements to ± 45°, so a range would place the target somewhere on the sector depicted in the diagram.

Since the collision/noncollision decision is not heavily dependent on the range measurement, the accuracy requirements need not be overly strict. The use of the range measurement nominally will be to determine if the range to a target is less than some required threshold, in which case an alarm is to be sounded. For this reason, the range measurement should be at least accurate to the average length of a car. Therefore, a 1 σ magnitude of 15 feet is imposed.

It is possible that stricter requirements might need to be imposed for certain systems, however. If range rate is generated by differentiation of range measurements, then range rate accuracy requirements will drive the range accuracy. In this case, σ range is a function of σ range rate given by

$$\sigma_{\text{Range}} = \frac{\sigma_{\text{Range Rate}}}{2}$$

since two range measurements are subtracted to yield a range rate measurement.

Range rate has an important role in determining the warning threshold, since the distance required for an automobile to come to a stop (the reference for declaring a warning) is proportional to the square of the vehicle's velocity:[3]

$$\text{Distance to stop} = -\frac{v^2}{2\mu g}$$

where v = vehicle's speed, μ = coefficient of friction, g = acceleration of gravity.

Through this equation we can relate range rate errors to the error in warning threshold estimate. As with the range measurement, we would want no more error in the threshold than a car length, or 15 feet. Thus, the range rate measurement must be accurate to at least 15 fps, or 3.8 fps, 1 σ.

This is a relatively mild requirement. Range rate has potential uses other than determining warning threshold, however. Some potential system concepts use the difference in range rate measurements taken from two antennas a distance d apart to determine angle to a target, since the spacing D will cause the antennas to see different Doppler frequencies (proportional to range rate) as a function of the target angle. This situation is depicted below.

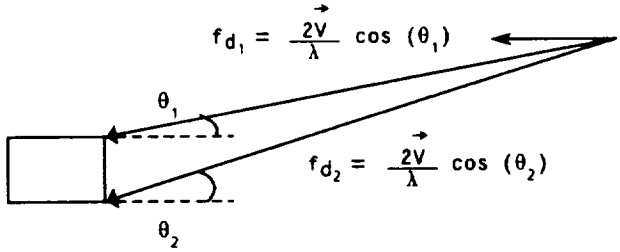

The effect on accuracy requirements is best described by evaluating a worst case example. Suppose we wish to evaluate the case of approaching an object just off to the side of the car from 300 feet away at a speed of 73.3 fps (50 mph). We will assume d = 5 feet (the typical width of a car). Then the velocity difference between the two antennas will be

$$V\ (\cos\ (\theta_1) - \cos\ (\theta_2))$$

$$= 73.3\ (1 - .99986)$$

$$\simeq .01 \text{ fps}$$

.01 fps is a very strict requirement. The worst case described is much stricter than the average case likely to be encountered; however, even as the scenario becomes more realistic, the requirement eases very little, if one wishes to make distinctions at a range of 300 feet. Two cars in opposite lanes (10-foot separation), each travelling 35 mph, would result in a range rate difference of only .05 fps, so an accuracy on the order of hundredths of a fps would still be required.

Angle and Angle Rate

Angle measurements and their behavior are quite necessary to the determination of a collision course. This report will not present the algorithm developed to make this determination, but typical situations will be examined to establish the strictest accuracy requirements.

Angle measurements have long been used on shipboard radar systems to indicate collisions. It is well known that a constant angle combined with a closing range indicates a collision course. This is true for straight line trajectories only, but quite a number of practical cases fall into this category. Any fixed object on or along a straight road section falls into this category. Any normal vehicle traffic along a straight road also falls into this category.

The angle accuracies required to support this determination may be arrived at by examining the change in angle behavior between an object directly in one's path and one just to the side of the vehicle, say 3 feet over. For the collision object, the angle measurement is zero and remains zero all throughout the approach. For the second case, the angle measurement starts at .573° and grows in magnitude, eventually reaching 90° as the car passes the object.

a. Angle = 0 throughout approach

b. Angle varies throughout approach

From this case it can be seen that the radar system should be accurate to at least .5°. However, the situation described is the worst case only for straight line trajectories. Many driving situations involve potential collision hazards approaching the radar vehicle along a curved trajectory. From an accuracy standpoint, the worst case would be as slight a curvature as possible, since this would result in the smallest angular changes. For this reason, a computer simulation was run involving a target object beginning at a distance of 500 feet in the opposite lane slowly curving into the radar vehicle's lane. The simulation was run twice, one for a collision case and once for a near miss of several feet. Equal velocities for radar vehicle and target were assumed. At 275 feet (stopping distance for a car going 60 mph under normal conditions), the angle measurements differed by .14°. Thus, to be able to distinguish these cases, accuracies to a tenth of a degree would be required.

It should be noted that at 300 feet, two objects need be separated by only .52 feet to have an angular separation of .1 degrees. Since a car is much wider than .52 feet, the specific point of the target that the radar tracks becomes important. But the phenonmenon is an RF effect to be investigated and really does not influence accuracy requirements.

SUMMARY AND COMMENTS

The arguments presented in this report were designed to arrive at accuracy requirements for a collision avoidance radar system based on an examination of the worst cases of normal driving conditions. The analysis herein is based solely on the geometry of the environment, as this was all that was required to determine the variations in magnitude that the radar parameters undergo.

It should be noted that cases can be envisioned which a radar system most likely could not solve. For instance, the situation depicted below, which is not entirely uncommon at construction sites:

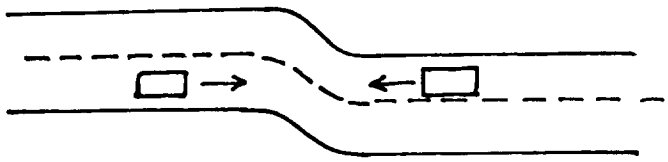

The difficulty here is that the vehicles do indeed follow a direct collision course until the very last moment, and the radar system has no way of knowing in advance that the driver intends to turn away at the last moment. Of course, it could be argued that a warning in this situation is not inappropriate, since a slight amount of driver inattention at the last moment can result in a collision. The point, however, is that situations of this sort are an odd extreme and are not likely to be encountered with any significant frequency. The design of the radar system should be geared towards the practical situations encountered in everyday traffic.

To summarize, if a radar system were designed around the requirements generated by this report, the following would be the accuracies required:

	Worst case error	Best case error
Range	.005 ft	15 ft
Range rate	.01 fps	3.8 fps
Angle	.1°	.1°

These requirements are intended to be a general guideline, dictated by the geometry of the environment. Actual requirements for a particular system will depend on how that system processes the various parameters.

The following plots present the results of the computer simulation referenced in the angle/angle rate section. Two sets of plots are presented, one set for a collision case and one set for a near miss case. On the trajectory plots, the radar vehicle path is indicated by the straight line from X = 0 to X = 500. The target path is depicted by the curved lines.

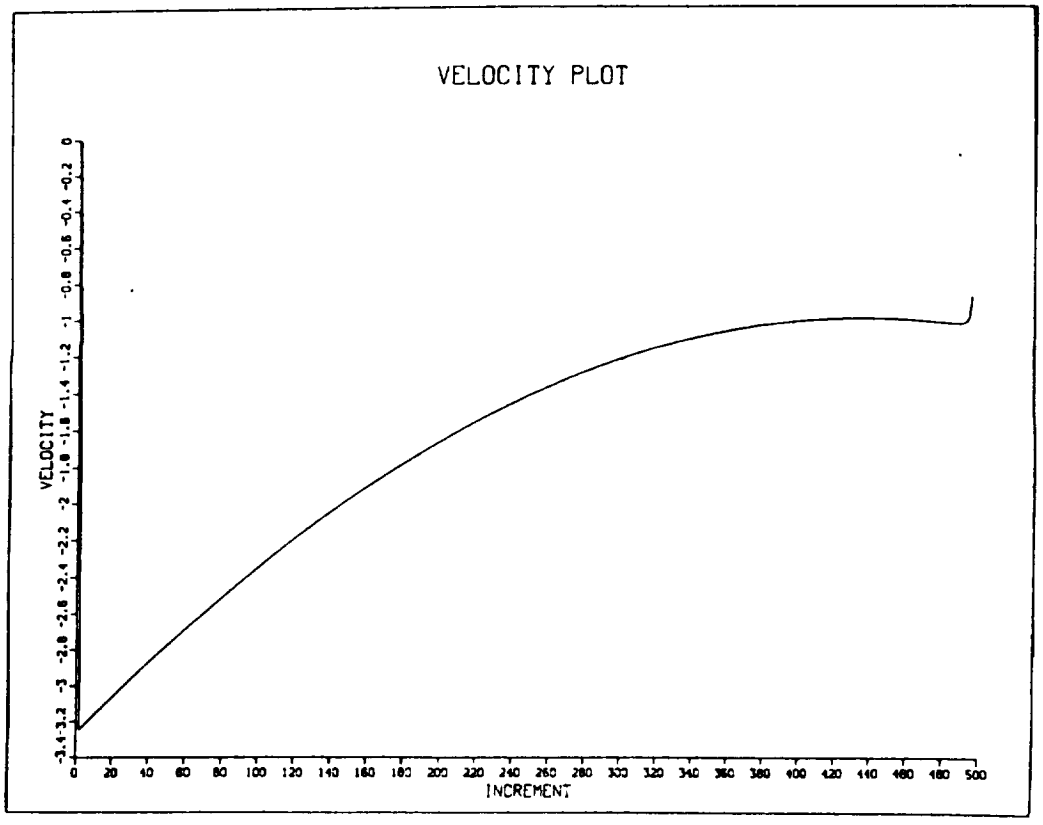

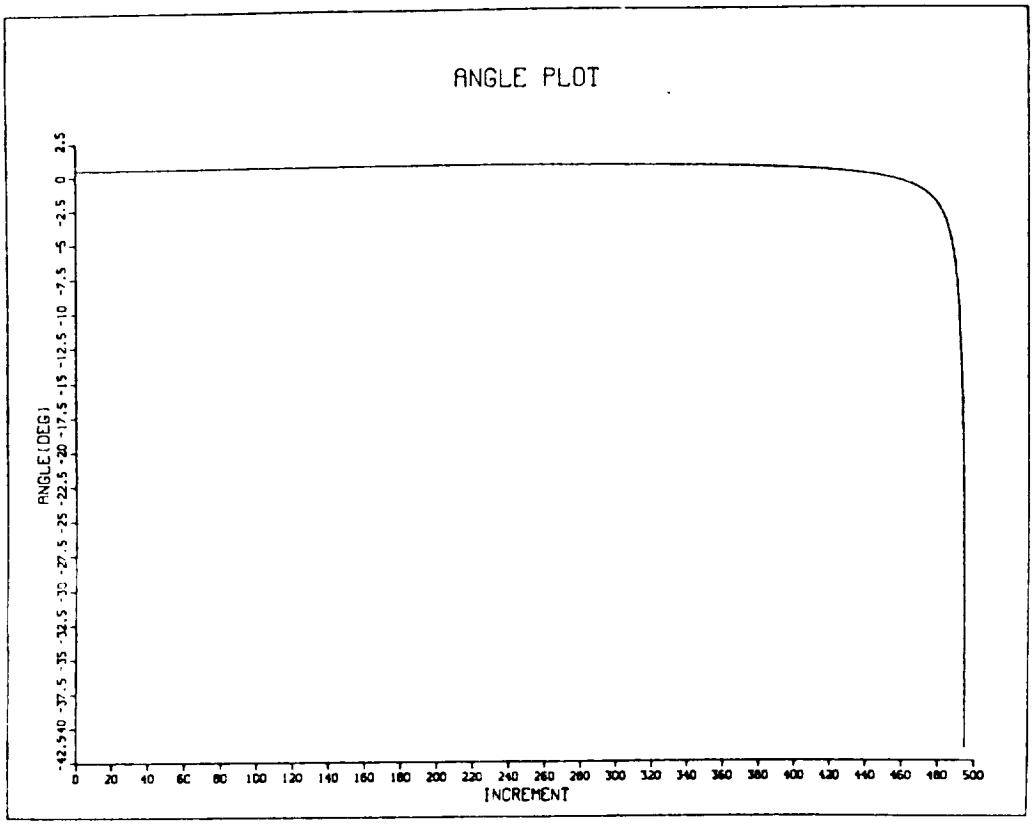
ANGLE PLOT
ANGLE(DEG)
2.5 0 -2.5 -5 -7.5 -10 -12.5 -15 -17.5 -20 -22.5 -25 -27.5 -30 -32.5 -35 -37.5 -42.5
0 20 40 60 80 100 120 140 160 180 200 220 240 260 280 300 320 340 360 380 400 420 440 460 480 500
INCREMENT

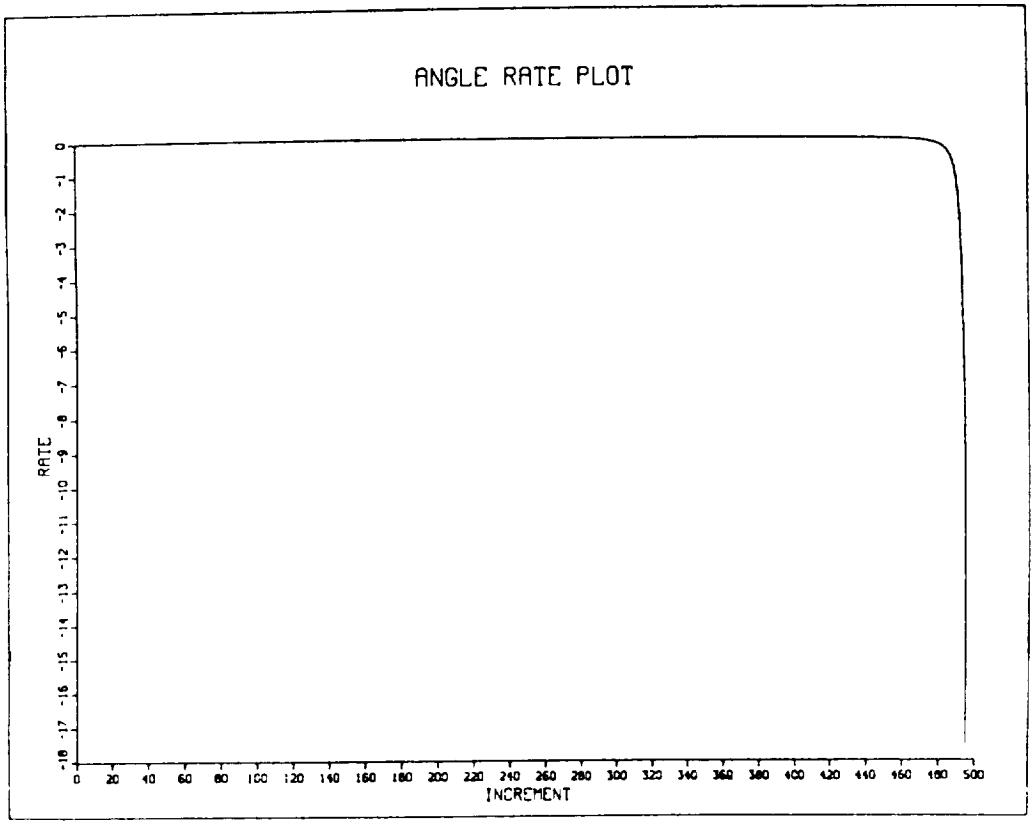
ANGLE RATE PLOT
RATE
0 -1 -2 -3 -4 -5 -6 -7 -8 -9 -10 -11 -12 -13 -14 -15 -16 -17 -18
0 20 40 60 80 100 120 140 160 180 200 220 240 260 280 300 320 340 360 380 400 420 440 460 480 500
INCREMENT

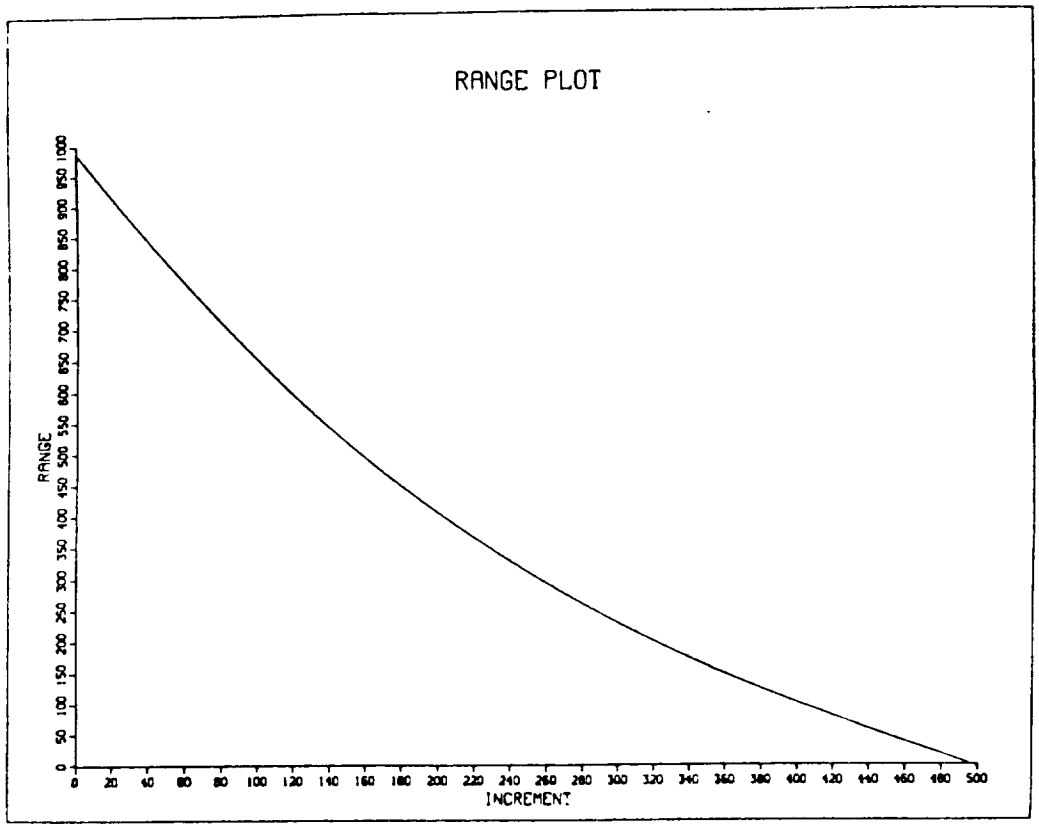
RANGE PLOT
RANGE
INCREMENT

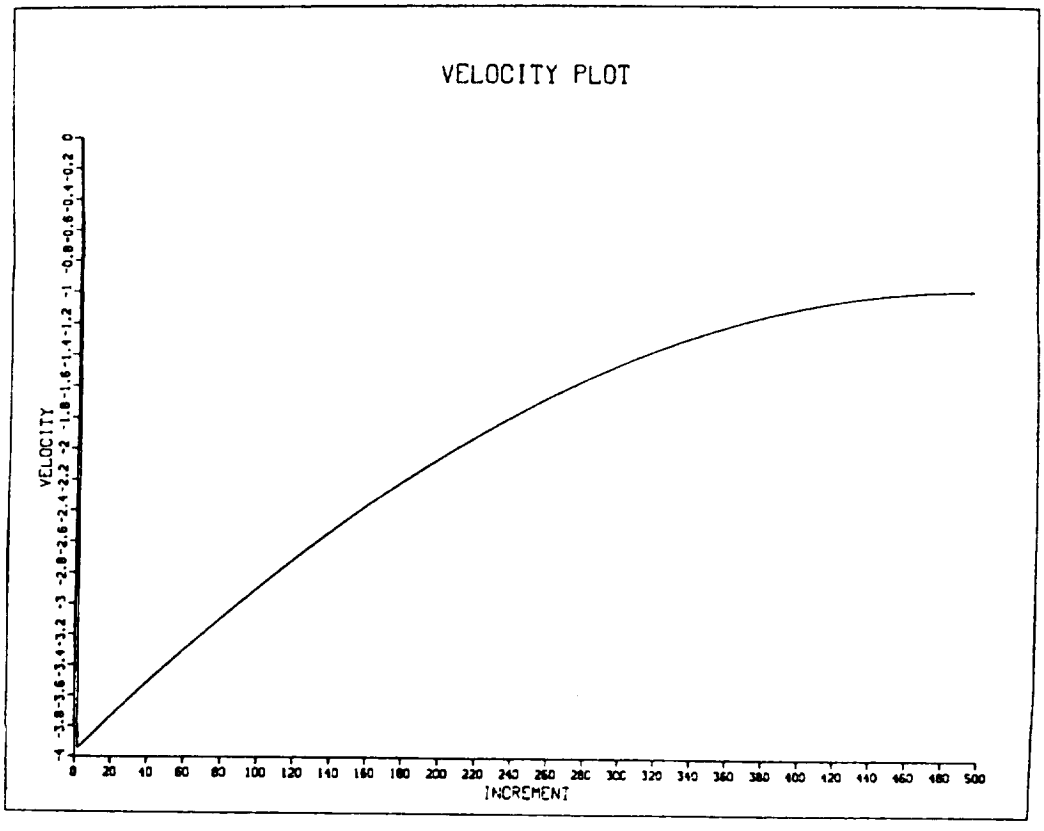
VELOCITY PLOT
VELOCITY
INCREMENT

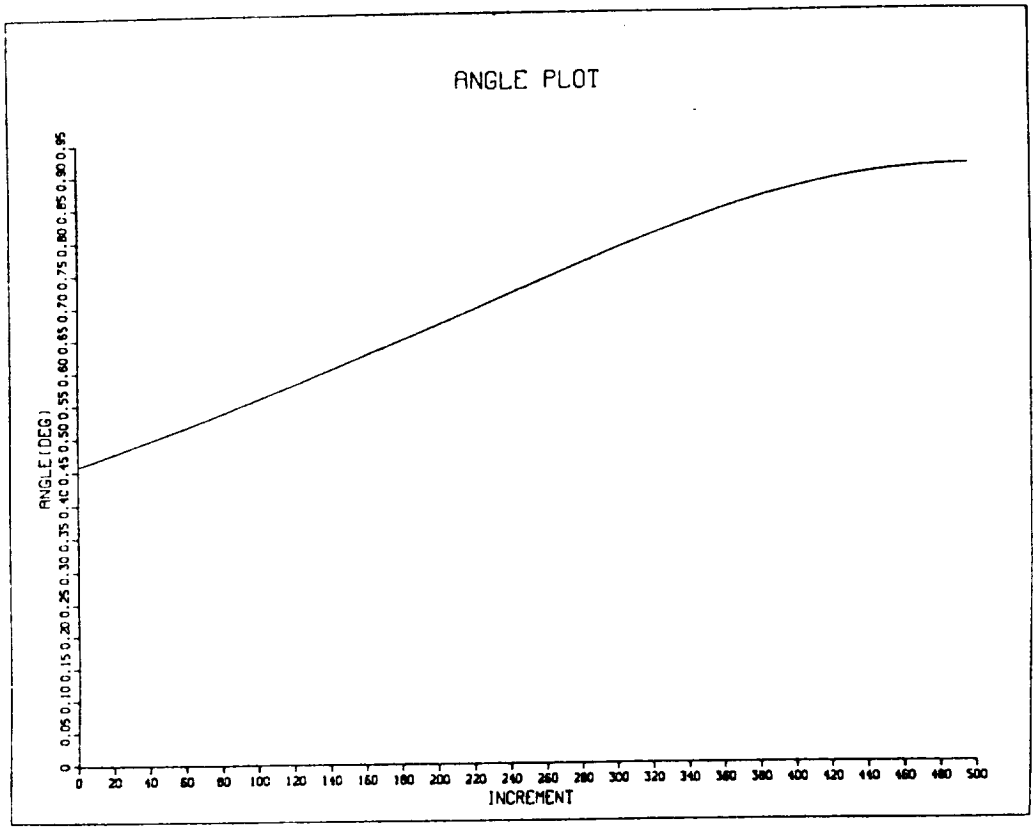
ANGLE PLOT
ANGLE(DEG)
INCREMENT

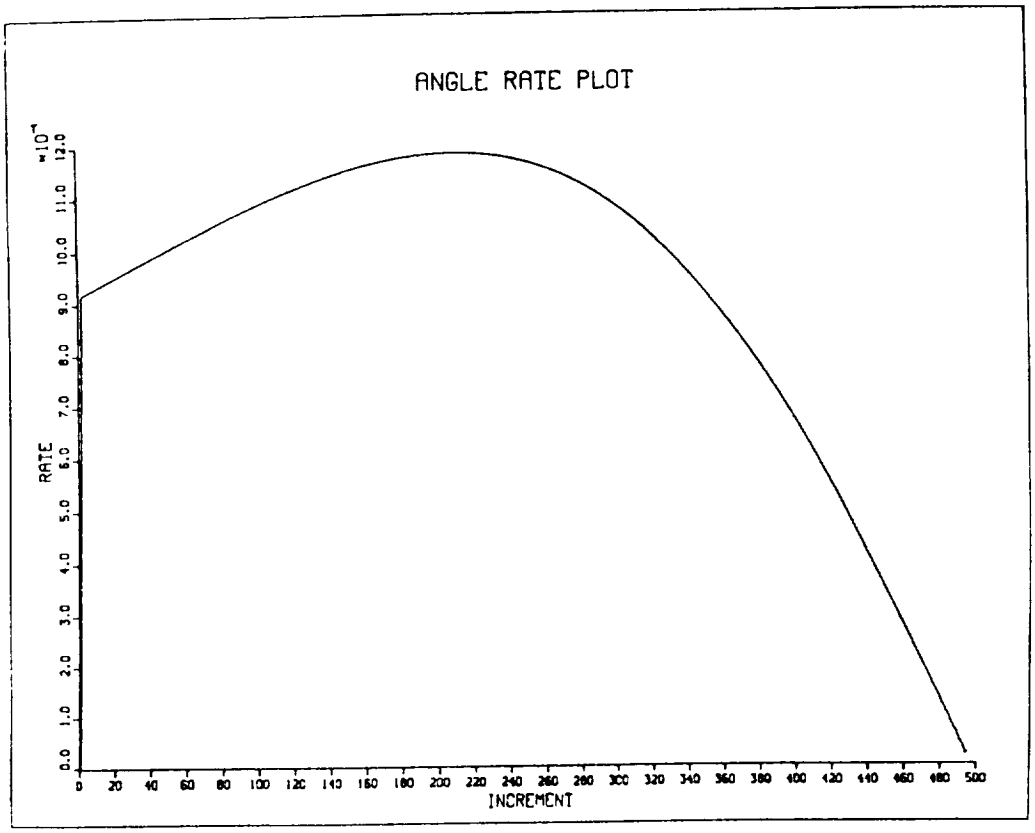
ANGLE RATE PLOT
RATE
INCREMENT

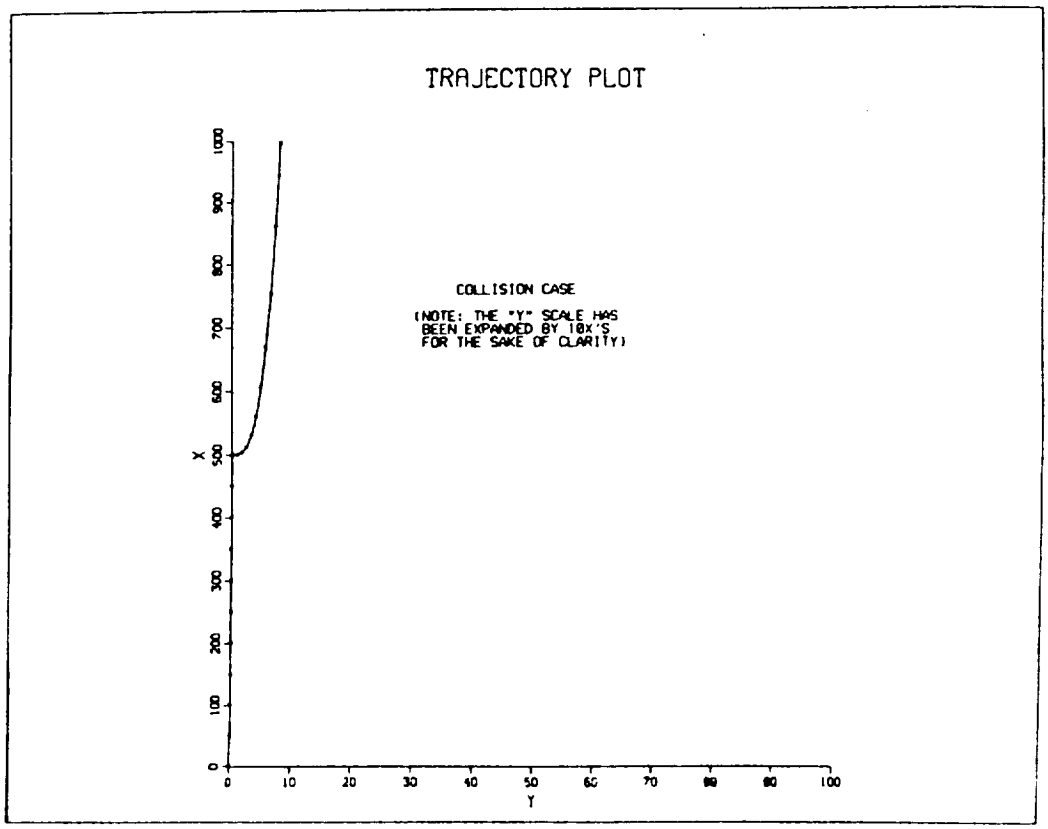

REFERENCES

1. "Some Automotive Radar System Considerations," T. D. Jones and D. M. Grimes, Second International Conference on Automotive Electronics, October 1979.

2. "Collision Avoidance System Cost - Benefit Analysis Technical Report," A. V. Kitadilkar, D. Redmond, and V. K. Aushorman, Kinetic Research, September 1981.

3. Fundamentals of Physics, D. Halliday and R. Resnick, Wicoy and Sons, 1970, p. 81.

SECTION 3
TRAFFIC ACCIDENT REPORT ANALYSES' CONCLUSIONS

INTRODUCTION

Traffic accident report data have been used in the past with some limited success for a variety of purposes relative to the design, development, and analysis of automotive collision avoidance radars:

a. General guidelines for system design have been formulated,[4,6,7,8,9,13] e.g., minimum range and maximum range of coverage, angular beam width of coverage, velocities of targets required to be accommodated, and sensitivity levels for range and angle. Generally only limited use of the accident data was made by each author. Not all parameters were derived using accident data. The impact of accident data on angle-tracking radars has been studied very little.

b. System features such as automatic application of braking versus warning as well as braking type (skid versus anti-skid) can be assessed against potential benefits.[4,6,7,8,9,10]

c. Once a system transfer function (radar sensor output plus output processing algorithm) is characterized, its potential effectiveness can be approximated.

d. After calculating the effect of implementing a radar in the environment described by the accident reports, figures describing potential numbers of lives saved, accidents avoided, accident severity reduced, and personal injury lessened can be generated.[4,6,7,8,9,10]

e. Finally, a dollar amount of potential savings to society can be developed based on lives saved, property damage lessened, etc.[3,4,7,8,10]

SYSTEM SPECIFICATIONS BASED ON TRAFFIC REPORTS

System specifications generated from traffic accident report analyses can be extremely important to developing an effective collision avoidance radar.

Attempts have been made to develop some of the radar system specifications from report analyses. It should be noted that these specifications are presently only starting points for future system development. Additional study is required. For example, a minimum range before detection of approximately 100 to 200 feet for simple radar has been developed based on cost-effectiveness because increasing detection range past 200 feet reduces accidents by only a few percent.[7] The greatest <u>total number</u> of accidents (40 percent) occurred on roads with 30-35 mph speed limits[2] while the three other categories (55, 40-50, 25 or less mph) each had approximately 16 percent. Assuming the drivers' speeds were somewhere near the posted speed limit, then radar operation versus combined driver and target object speed should be approximately equally sensitive (possibly peaked for 30-35 mph) across the range of car and collision object velocities. However, if reducing <u>fatal</u> accidents is the primary concern, then system operation should be optimized

for vehicle speeds in the 55 mph road class[1] (approximately 70 percent of all fatalities). An urban/rural set of sensitivities might be required for optimum radar operation. These velocity considerations allow a designer to place requirements on distance to detection and processing time, among other specifications.

Determination of required beam width, or angular coverage, is one of the more difficult tasks to perform using traffic accident data. Several authors have attempted to assess the effect of angular coverage on accident prevention/reduction. The beam width arrived at by previous authors determined by percentage accidents reduced, etc. has been generally on the order of several degrees.[4,8,9] However, 360 degree full coverage is the only coverage that will provide the absolute maximum accident prevention/reduction. Anything less is a compromise, even if necessitated by practical considerations. By necessity a coverage area less than 180 degrees, but greater than approximately 10 degrees, will most likely be used for a practical system. A preliminary review of impact angle indicates that approximately 80 percent of the accidents occur within ± 75 degrees.[2]

While beam widths on the order of several degrees may represent an effective compromise between hazardous targets detected versus false alarms generated in these simple radars, more beam width is needed. First, the traffic accident data bases do not generally contain very accurate accident impact angle information. Further, since data collection occurs after the accident, it is understandably difficult to accurately determine the precise angle of impact (e.g., within ± 2 degrees). Two important nationwide compilations of traffic accident statistics[1,2] only show angular breakdowns to within a 30 degree segment. This is shown in figures 3-1 and 3-2. It is felt that trying to predict the overall cost savings for radars with beam widths of, for example, 2.5 degrees compared to 4 degrees[9] is really very speculative and reads more accuracy into the data than exists. This is definitely true for nationwide statistics such as National Accident Sampling System (NASS) and Fatal Accident Reporting System (FARS) data which are based primarily on police accident reports.[1,2] The limitations of previous studies should be recognized when attempting to deduce the required beam width for the radar. For example, one study[4] used an algorithm for collision detection which was automatically disabled if the steering wheel was turned past some amount; thus, it did not consider preventing accidents on curved roads or when the radar-equipped vehicle was turning, precisely when more beam width is most needed. Merely widening the antenna beam width in such a limited radar system understandably would not offer much additional protection either. Thus, one might be led to conclude that additional beam width is not required, when in fact a better radar design and algorithm is needed. Take, for example, single vehicle fatal accidents (fig. 3-2). If accidents in the region ahead of the vehicle are considered, approximately 30 percent is the best savings in lives that could ever be achieved. If, on the other hand, you recognize that almost 70 percent of the fatalities occurred outside the ± 15 degree beam width ahead of the vehicle, then one concludes that more beam width (based on lives saved) should be designed into the radars as it becomes technically feasible. Additionally, the need for more sophisticated radars which contain angle-tracking means, multiple target capability, etc. should be obvious in view of the unsatisfactory results of simple radars.

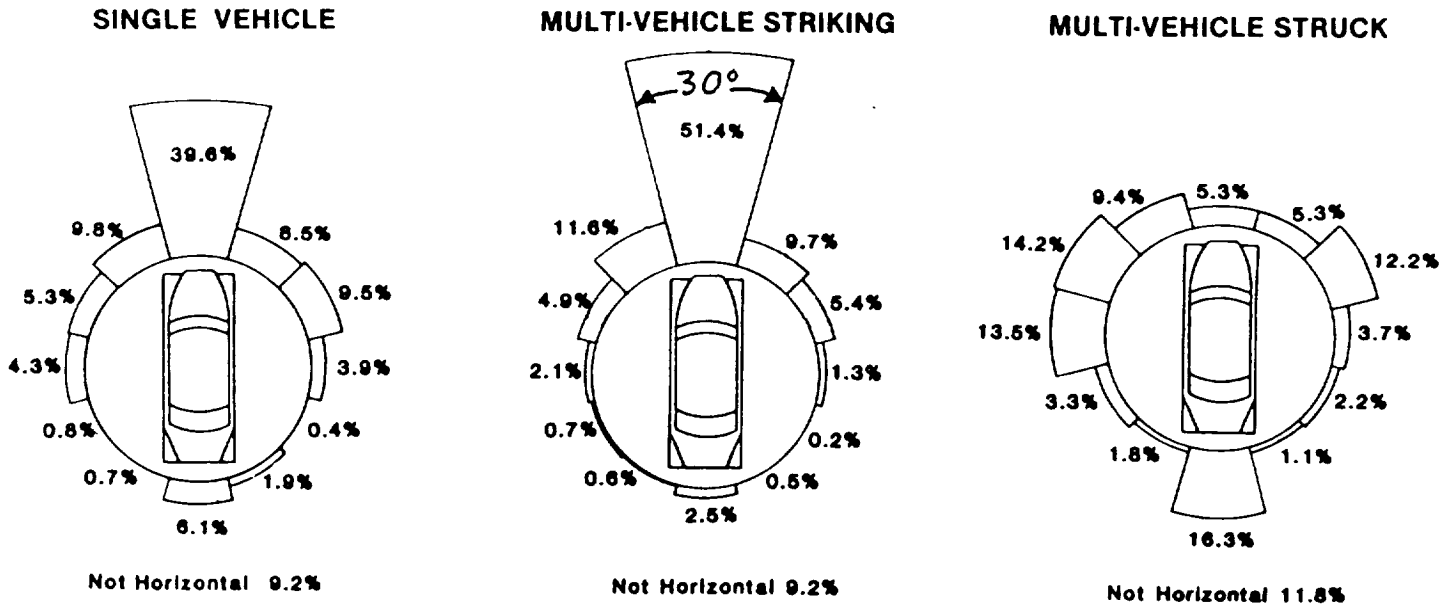

Figure 3-1.- Direction of force in passenger cars (reprinted from "National Accident Sampling System - 1982," DOT-HS-806-530, March 1984).

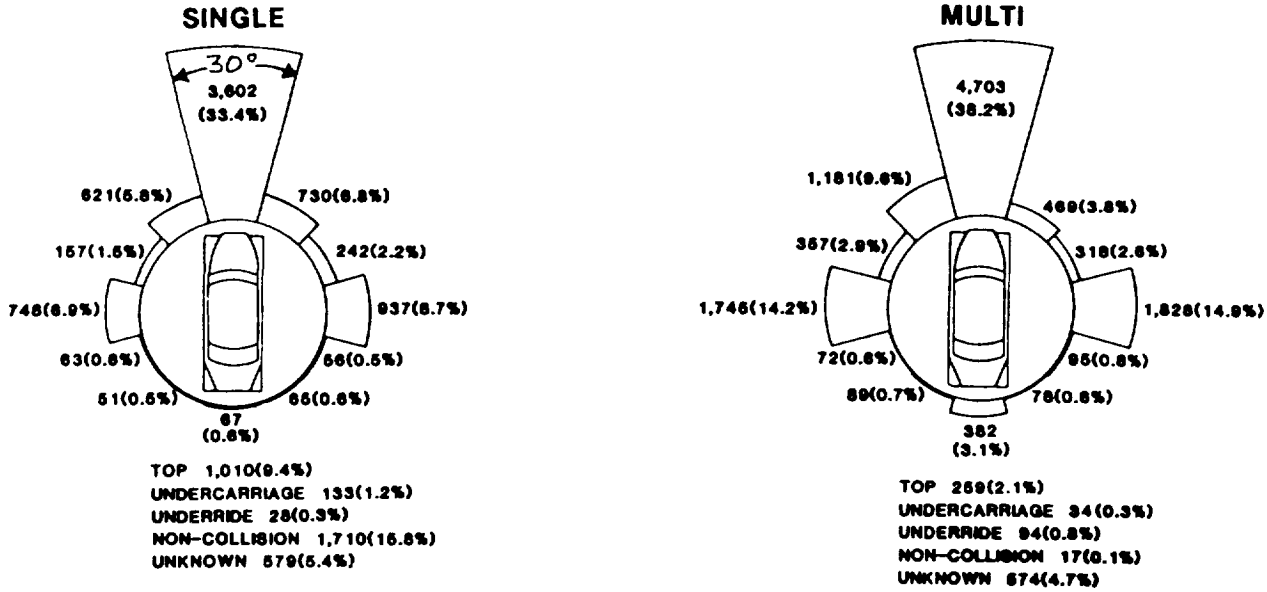

Figure 3-2.- Distribution of passenger car occupant fatalities by point of principal impact (reprinted from "Fatal Accident Reporting System - 1982," DOT-HS-806-566, May 1984).

The problem of beam width can also be approached heuristically. Suppose a radar has a beam width of approximately 2.5 degrees, which has been a commonly used value. At 300 feet only approximately 12 feet, or one lane, is being covered. At 150 feet only half of the lane ahead is covered. Conceivably an object could be in your lane at 150 feet, yet not be detected. Furthermore, it should be unsettling that objects approaching from any angle outside the lane (or fractions of lane) ahead would not be detected. A good driver is always alert to objects outside of this narrow region, for example, in curves, at intersections, and when cars are executing passes or otherwise changing lanes. It is only reasonable then that more than one lane should be observed by the radar. The radar would then perform complex surveillance and tracking functions of many objects, just as a driver does. Just imagine how dangerous it would be to drive with blinders on so that only about one lane of traffic straight ahead is all you could see. Two lanes of coverage at 150 feet requires approximately a 10 degree beam width. Twenty degrees would give about four lanes of coverage (1-1/2 lanes on each side of the lane you are presently in). Twenty degree coverage is probably a good initial goal for automotive radar, but it really is only a starting point.

REFERENCES

1. "Fatal Accident Reporting System - 1982," DOT-HS-806-566, May 1984.

2. "National Accident Sampling System - 1982," DOT-HS-806-530, March 1984.

3. "The Economic Cost to Society of Motor Vehicle Accidents," DOT-HS-806-342, January 1983.

4. "Collision Avoidance System Cost-Benefit Analysis," Volume I - Technical Report, Kinetic Research, DOT-HS-806-242, September 1981.

5. Duell, E. H., and H. J. Peters, "Collision Avoidance System for Automobiles," SAE Technical Paper 780263, 1978.

6. Tumbos, N. S. et al., "An Assessment of the Accident Avoidance and Severity Reduction Potential of Radar Warning, Radar Actuated, and Anti-Lock Braking Systems," SAE Paper 770266, 1977.

7. "Collision Avoidance Radar Braking Systems Investigation - Phase II Study - Summary Report," Bendix Research Labs, September 1976.

8. "Collision Avoidance Radar Braking Systems Investigation - Phase II Study - Technical Report," Bendix Research Labs, September 1976.

9. "Tri-Level Study of the Causes of Traffic Accidents: Interim Report II (Volume II: Radar and Anti-Lock Braking Payoff Assessment," Indiana University, DOT-HS-801-631, June 1975.

10. "Collision Avoidance Radar Braking Systems Investigation: Phase I Study," Bendix Research Labs, DOT-HS-801-253, October 1974.

11. "File Structure - Crash Avoidance Research Data File (CARDFILE)," DOT Memorandum, July 1985.

12. "Accident Type Analysis - Texas 1983 CARDFILE," DOT Memorandum, June 1985.

13. Grimes, D. M., and T. O Jones, "Automotive Radar: A Brief Review," Proceedings of the IEEE, Volume 62, Number 6, June 1974.

SECTION 4
RADIATION HEALTH HAZARDS

INTRODUCTION

In predicting the expected radiation levels for an automobile collision avoidance radar, several of the quantities of interest are peak transmitter power, duty cycle, antenna pattern, antenna physical configuration, and the number of effective simultaneous radiators. Since the spherical spreading loss is inversely proportional to the square of the distance from the radar, it will be impossible to achieve very high radiation levels because locating more than a limited number of automobiles in close proximity with each other is impossible. As the distance between an individual and a radar increases, the potential hazard diminishes. The purpose of this report is to present calculations which demonstrate that the radiation levels under worst case conditions will not be expected to exceed current United States (U.S.) safe levels of 5 mW/cm^2.[12]

BIOLOGICAL EFFECTS

Organs and tissues have a structure that is bathed in biological fluids. This structure is built of fixed molecules that often are electrically polarized, while the biological fluids contain ions of dissolved electrolytes and macromolecules. Under the influence of the electric fields from high frequency electromagnetic radiation, these polar molecules and ions experience electric forces whose magnitude is proportional to the product of the electric field intensity, E, and the charge on the ion or on the polar molecule.[10]

$$f = qE$$

where

f = force exerted on the ion or molecule
q = charge on the ion or polar molecule
E = vector electric field intensity (volts/meter)

These induced forces lead to current flow in the case of the dissolved ions and consequently to joule heating of the biological material. The rapid alternating electrical forces on the immobile structural molecules may cause them to vibrate or to rotate, which in turn leads to heat production. Additionally, the electric field-induced forces may change the spatial distribution of the polar molecules from a random orientation to an orientation aligned with the electric field.

The biological effects caused by radiation heating are called thermal effects; when a biological effect cannot be attributed to heating, it is called a nonthermal effect. Only thermal effects will be considered here. Thermal effects in the microwave region ($f > 1$ GHz) are presently associated with exposure levels greater than 10 mW/cm^2, while nonthermal effects are

generally associated with exposure levels less than 10 mW/cm^2. These exposure limits are called threshold limit values (TLV's).

These TLV's refer to the radio frequency (RF) and microwave radiation in the frequency range from 10 KHz to 300 GHz and represent conditions under which it is believed humans may be repeatedly exposed without adverse health effects. Table 4-1[10] presents TLV's which were selected to limit the average whole body specific absorption rate (SAR) to 0.4 W/kg in any 6-minute period (.1 hr).

TABLE 4-1.- RADIO FREQUENCY/MICROWAVE THRESHOLD LIMIT VALUES

Frequency	Power density (mW/cm^2)	Electric field strength squared (V^2/m^2)	Magnetic field strength squared (A^2/m^2)
10 kHz to 3 MHz	100	377,000	2.65
3 MHz to 30 MHz	$900/f^{2}$*	$3770 \times 900/f^{2}$*	$900/(37.7 \times f^{2}$*)
30 MHz to 100 MHz	1	3770	0.027
100 MHz to 1000 MHz	f*/100	3770 × f*/100	f*/37.7 × 100
1 GHz to 300 GHz	10	37,700	0.265

*f = frequency in MHz

EXPECTED POWER DENSITY LEVELS FROM THE ANTENNA

Power density levels in the vicinity of radiating sources are functions of several parameters such as effective radiated power, ERP, peak power, P_{peak}, average power, P_{avg}, antenna gain, $G(\theta)$, and others.

The gain of the antenna in the direction of the main lobe can be approximated by the following equation.

$$Imax = \frac{4\pi}{\theta_A \theta_B} \tag{4-1}$$

where

$Imax$ = maximum directive gain
θ_A = azimuth beam width (radians)
θ_B = elevation beam width (radians)

If these parameters are converted to degrees, the gain expression can be expressed as follows:

$$Imax = \frac{41253}{\theta_A \theta_B} \tag{4-2}$$

For the case of the prototype radar's standard gain horn antenna,

$$\text{Imax} = \frac{41253}{9.5 \times 10} = 414$$

$$\text{Imax (dB)} = 26.1$$

Regulations for the protection of workers and members of the public from the harmful effects of microwave radiation have been promulgated in numerous countries around the world. In the United States, the Occupational Safety and Health Administration (OSHA) established a maximum level of 10 mW/cm^2 incident electromagnetic power density for frequencies of 10 MHz to 100 GHz, inclusive, averaged over a 6-minute period. No distinction is made between pulsed and continuous radiation in the standard.[10] Since we are dealing with averaged power, for pulsed radars, the peak power, pulse repetition rate, and the pulse width must be known in order to determine if the radiation standards are met.

The power density at the aperture plane is determined from the physical dimensions of the prototype pyramidal horn antenna* and the average power transmitted. This calculation also assumes that the power is uniformly distributed across the aperture.

$$P_{avg} = P_{peak} \times PRR \times PW \tag{4-3}$$

where
P_{avg} = average power, watts
P_{peak} = peak power, watts
PRR = pulse repetition rate, pulses/sec
PW = pulse width, seconds

For the test radar the following power levels are calculated.

$$P_{avg} = \left(\frac{2 \text{ watts}}{\text{pulse}}\right)\left(\frac{100 \text{ K pulses}}{\text{sec}}\right)\left(20 \times 10^{-9} \text{sec}\right)$$
$$= 4 \text{ mW}$$

Now if the physical aperture and electrical aperture are assumed to be equal,

$$\text{area} = 3.5'' \times 4.0'' = 141 \text{ n}^2 \sim 90 \text{ cm}^2$$

*A pyramidal horn aperture was chosen because it represents the antenna structure used in data collection and because it is fairly representative of future possible antenna apertures.

The power density at the aperture plane is calculated as follows.

$$PD = \left(\frac{4\ mW}{90\ cm^2}\right) = .044\ mW/cm^2$$

This calculation indicates that the power density at the aperture place is on the order of five times the proposed Union of Soviet Socialist Republics (U.S.S.R.) level of .01 mW/cm^2.[11]

In order to calculate the power density at various field points the effective radiated power (ERP) is calculated for an equivalent isotropic source.

It is assumed for this case that the radiation efficiency of the antenna is 100 percent, i.e., all of the power, P_{avg}, is radiated.* The ERP will be determined for the antenna using the following equation.

$$ERP = Imax \times P_{avg} = 1656\ mW \tag{4-4}$$

The power density at various distances from the isotropic source (1656 mW in the direction of maximum gain) can now be obtained by applying the spherical spreading loss factor. One valid point for comparing power density for an antenna is the far field distance (FFD) given by the following formula.

$$FFD = \left(\frac{2D^2}{\lambda}\right) \tag{4-5}$$

where

λ = wavelength = .0125 m (f = 24 GHz)
D = aperture diameter E - plane = .1 m

$$FFD = \left(\frac{2\times 10^2}{1.25}\right) = 160\ cm$$

For the pyramidial horn antenna the ERP isotropic source will be located approximately 57 cm behind the physical aperture plane as shown in figure 4-1. The far field point location would be approximately one meter from the aperture plane. The power density at the far field point is calculated as follows.

$$PD = \frac{1656\ mW}{4\pi(160)^2} = 5.14 \times 10^{-3}\ mW/cm^2$$

*Actual efficiencies can run only as high as approximately 85 percent.

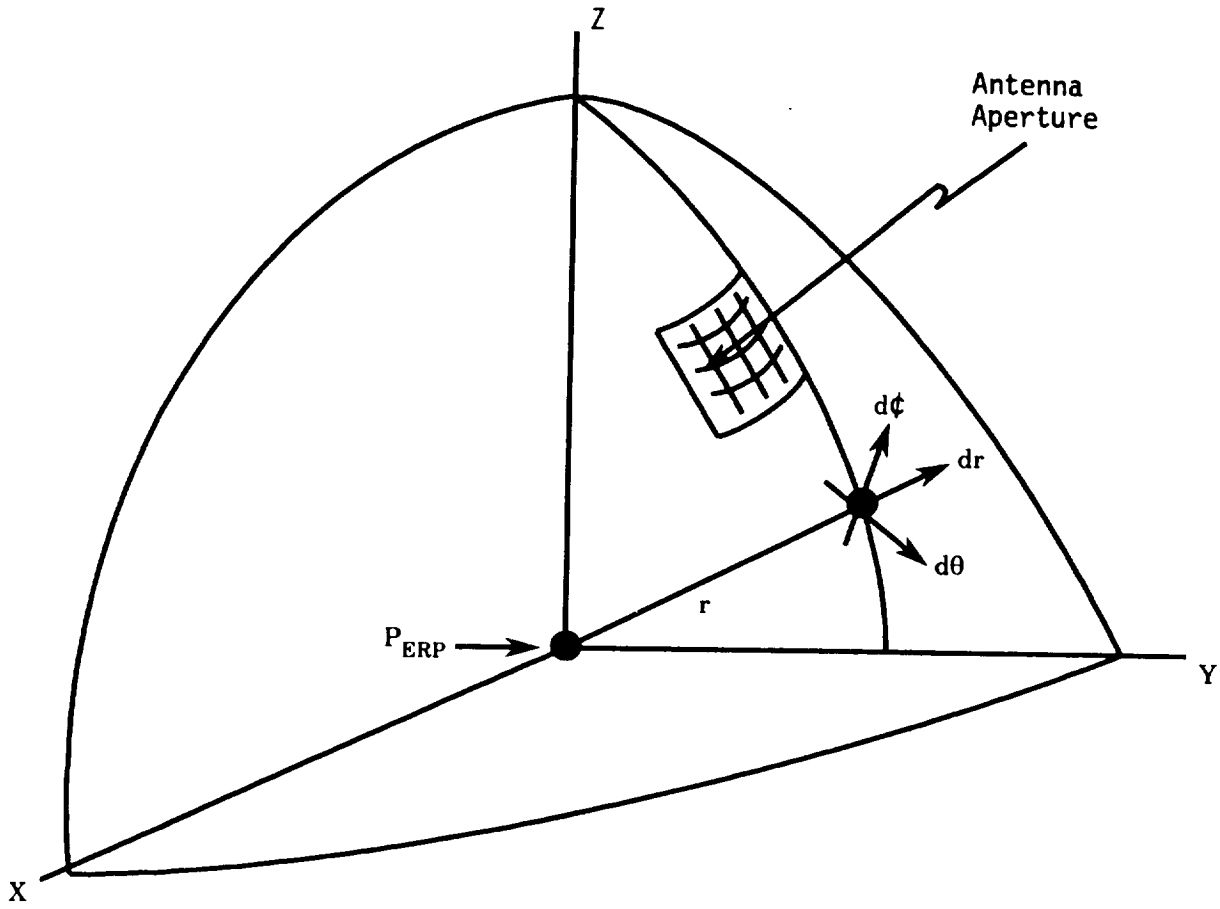

Figure 4-1.- Location of ERP sources.

It is clear from the previous calculation, providing system parameters remain fairly constant, that no adverse radiation safety problems will result from exposure to a single radiating source. This is also true if part of the human body is placed at zero inches from the antenna; in other words, right against the aperture. The power density at the aperture plane was shown to be on the order of .04 mW/cm^2. This does not answer the question of the effect of additive power from multiple sources which is the topic of the next section.

EFFECT OF MULTIPLE RADIATORS ON RADIATION HAZARD LEVELS

If a person is exposed simultaneously to radiation of several different frequencies or multiple sources at the same frequency, then in order to stay within the recommended exposure limits the sum of all the sources must fall below the allowed "safe" exposure level. A worst case condition is proposed as follows.

First, multiple radiators will be lined in a string by positioning the automobiles end-to-end in an infinite string, as shown in figure 4-2.

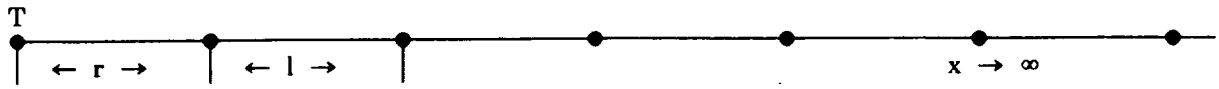

T = target being irradiated

r = distance from first radiator to target (cm)

l = spacing between radiators (cm)

Figure 4-2.- Multiple radiators in infinite string.

The power density at the target, T, is the sum of the power densities radiation from the individual radiators assuming no scattering loss. Phase coherence of waves in space is also assumed; this is the worst case. The total power density is computed using the following convergent power series.

$$PD_T = \frac{ERP}{4\pi} \sum_{i=0}^{\infty} \frac{1}{(r + li)^2} \tag{4-6}$$

where

PD_T = power density at target from sum of radiators

ERP = effective radiated power

r = distance from first car to target

l = spacing between radiators (constrained by physical length of automobile

The sum of the series in equation 4-6 is finite and bounded above. The upper bound given by equation 4-7 is derived in appendix A.

$$UB = \frac{ERP}{4\pi} \left(\frac{1}{r^2} + \frac{7}{4l^2} \right) \tag{4-7}$$

Next, the power density at the target, T, is determined for multiple infinite string radiators (simulation of a large traffic circle). The number of multiple string radiators is constrained by the physical width of the automobile on which the radar is mounted. It is assumed that the automobiles are arranged in an N-sided polygon. The polygon is approximated by the circle shown in figure 4-3. N is assigned as the number of infinite string radia-

tors that are co-located and irradiate a target located at the center of the N-sided polygon. The power density, PD, resulting from the multiple string radiator is given by

$$PD = N \times PD_T \tag{4-8}$$

As a direct result of the physical dimensions of the automobile limiting the number, N, of infinite string radiators for a given target distance, r, the limiting value of the target power density is zero (see appendix B).

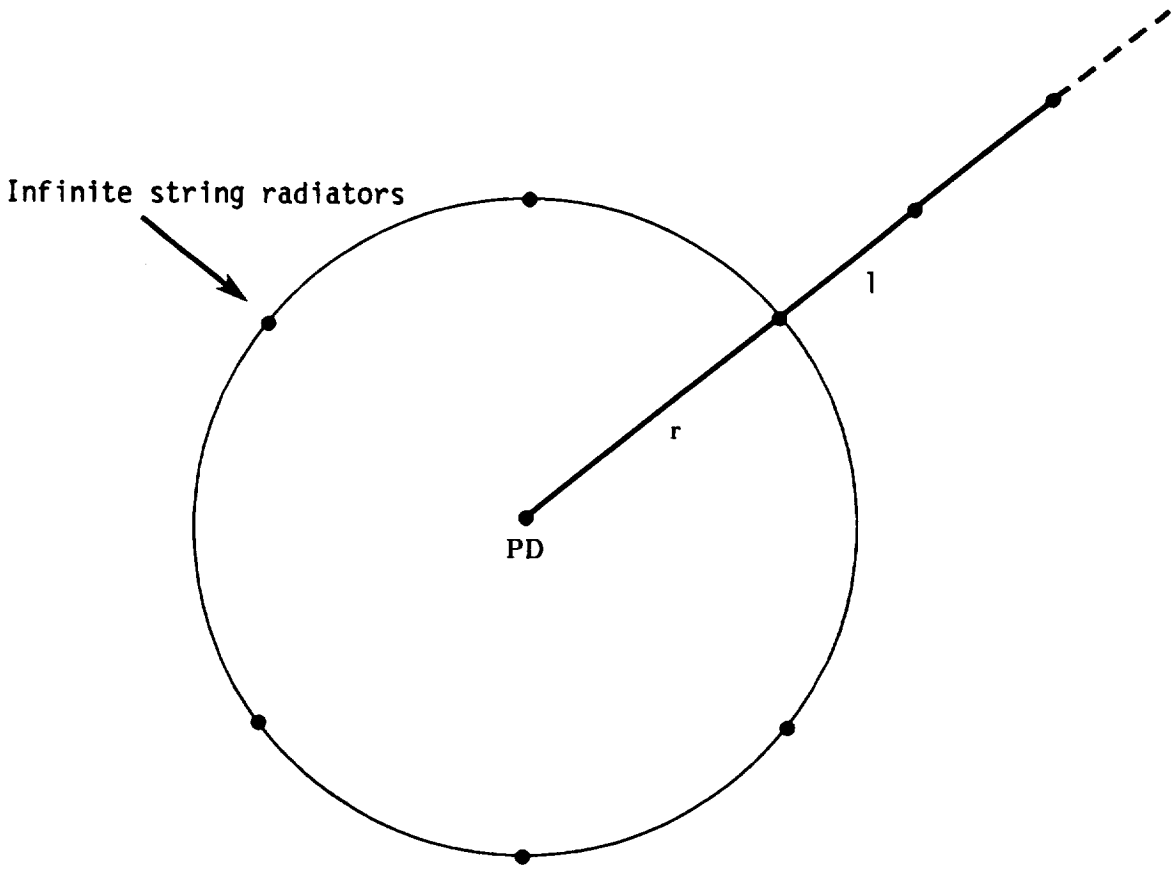

$PD = PD_T \times N$

PD = power density due to multiple infinite strings

PD_T = power density at target, T, due to one infinite string

N = number of infinite strings (integer value of $2\pi r/w$)

w = width of automobile

Figure 4-3.- Radiation geometry for multiple infinite strings.

An upper bound for target power density resulting from multiple string radiators is calculated as follows.

$$UB_{ms} = N \times UB \tag{4-9}$$

where

N = number of infinite string radiators

UB = upper bound single finite string radiator

UB_{ms} = upper bound multiple infinite string radiator

It should be noted that UB_{ms} is a simple upper bound and not a least upper bound. Therefore, the actual limiting value of the target power density for a fixed N will be somewhat less than the calculated upper bound.

A simple Fortran program (see appendix C) was written to generate the examples. Table 4-2 presents two examples for two N values.

TABLE 4-2.- EXAMPLES INTERSECTION MODEL

Fixed constants

P_{avg} = 4 mW

G_{max} = 26.6 dB

ERP = 1656 mW

i = 100

All values given in mW/cm^2

N	r (cm)	l (cm)	PD_T	PD	UB
18	609	609	5.84×10^{-4}	1.05×10^{-2}	1.6×10^{-1}
4	107	609	1.197×10^{-2}	4.8×10^{-2}	4.8×10^{-2}

The first example covers the case of long strings of cars coming together at an intersection. Next, consider a large parking lot filled with automobiles. The cars are arranged so that the maximum accumulation of power occurs at the geometric center of the parking lot. As in the previous example, it is assumed that there are no effects from shadowing or scattering and that the power from each source is additive at the center of the parking lot.

The power density at the center of the parking lot from a single radiator in the ith annular region is given by the following equation (fig. 4-4).

$$X_i = \frac{ERP}{4\pi (r + il)^2} \tag{4-10}$$

where

X_i = power density from single source in ith annular region

The number of cars in the ith annular region is given by the following equation.

$$N_i = \frac{2\pi (r + il)}{w} \tag{4-11}$$

where

w = width of the automobile

Multiplying equations 4-10 and 4-11 yields the total power density at the center of the parking lot resulting from all radiators located in the ith annular region.

$$PD_i = N_i X_i = \frac{ERP}{2w (r + il)} \tag{4-12}$$

Now the power density at the center of the parking lot filled with cars can be computed by summing equation 4-12 over n values if i, as given below.

$$PD = \frac{ERP}{2w} \sum_{i=0}^{n} \frac{1}{(r + il)} \tag{4-13}$$

A simple Fortran program (see appendix D) was written to calculate the power density at the center of a one mile diameter parking lot. Table 4-3 presents the results of this calculation.

TABLE 4-3.- EXAMPLE PARKING LOT MODEL

ERP	=	1656 mW	
l	=	20 feet (609.6 cm)	PD = 0.0885 watts/cm^2
r	=	3 feet (91.44 cm)	
w	=	6 feet (182.88 cm)	
n	=	132	

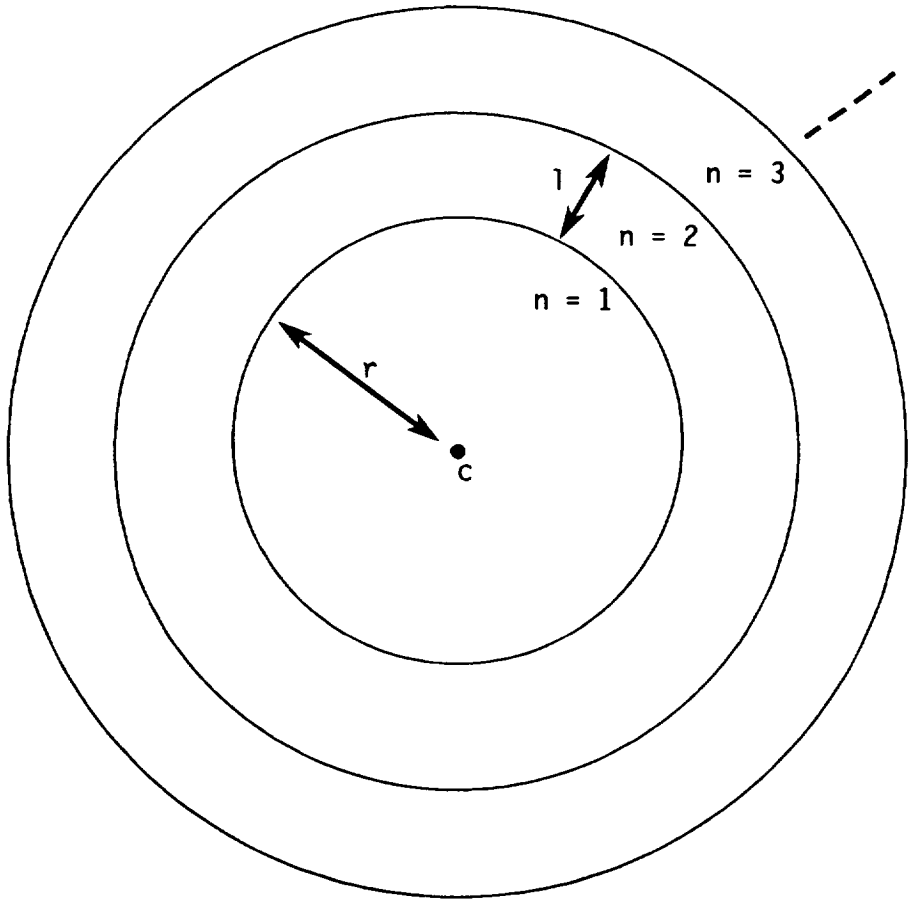

c = center of parking lot

r = distance to first annular region

l = width of annular region

n = number of annular regions

Figure 4.4.- Radiation geometry for circular parking lot.

CONCLUSIONS

Calculations to determine radiation hazards resulting from operating the radars indicate that no problems would result from radiation exposure. It must be emphasized that it will be necessary to make these calculations each time the radar spectral, power, or antenna characteristics are changed.

The results of this analysis also indicate for multiple string radiators simulating a traffic circle that the power density at the target is well below present American National Standards Institute (ANSI) standard. The second example simulating a large parking lot demonstrates that the power density levels do not exceed present safety standards.

REFERENCES

1. Merril I. Skolnik, Introduction to Radar Systems. New York, NY: McGraw-Hill, 1962.

2. K. R. Carver, "Notes on Microwave Antennas," Las Cruces, NM: January 1978.

3. Richard E. Wong, et al., "Collision Avoidance Radar Braking System Investigation: Phase 1 Study," Bendix Corporation, 1974. pp. 4.1, 4-11.

4. L. E. Wood, et at., "Analysis of Problems on the Application of Radar Sensors to Automotive Collision Prevention," DOT-HS-801-010, December 1973, pp. 3-15. TEA 6090. W66

5. Gene Proctor, NISOH Draft Report, "Recommended Standard on RF/Microwave Radiation," NISOH: 1979.

6. Mary Bernstein, BEMS Hears Evidence of Health Risk, Microwaves, and RF. August 1985.

7. Wilford Kaplan, Advanced Calculus, Reading Mass., 1952, pp. 371-460.

8. Sokolnikoff and Sokolnikoff, Higher Mathematics for Engineers and Physicists, New York, NY: McGraw-Hill, 1941, pp. 2-45.

9. Edward C. Jordan, Electromagnetic Waves and Radiating Systems, Englewood Cliffs, N.J., 1950.

10. Herman Cember, Introduction to Health Physics, New York, NY: Pergamon Press, 1985.

11. Michealson, S. M., "Human Exposure to Non-Ionizing Radiant Energy - Potential Hazards and Safety Standards," Proceedings, IEEE, April 1972, pp. 389-421.

12. American National Standard Safety Levels with Respect to Human Exposure to Radio Frequency Electromagnetic Fields, 300 KHz to 100 GHz, 1982.

APPENDIX A

CALCULATION OF AN UPPER BOUND

FOR EQUATION 4-7

$$S = PD_T = \frac{ERP}{4\pi} \sum_{i=0}^{\infty} \frac{1}{(r + 1i)^2} \tag{A-1}$$

$$= \frac{ERP}{4\pi} \left[\frac{1}{r^2} + \sum_{i=1}^{\infty} \frac{1}{(r + 1i)^2} \right]$$

$$\leq \frac{ERP}{4\pi} \left[\frac{1}{r^2} + \frac{1}{1^2} \sum_{i=1}^{\infty} \frac{1}{i^2} \right] \tag{A-2}$$

Now let S = Sn + Rn

where

$$Sn = n^{th} \text{ partial sum}$$

$$Rn = \text{remainder} = \sum_{n+1}^{\infty} f(i)$$

This remainder is calculated as follows.[7] Using the integral test for infinite series

$$0 < |Rn| = \sum_{m=n+1}^{\infty} \frac{1}{m^P} < \int_n^{\infty} \frac{1}{x^P} dx \tag{A-3}$$

Let p = 2

$$|Rn| < \int_n^{\infty} \frac{1}{x^2} dx = \frac{1}{n} \tag{A-4}$$

From this result, we can calculate an upper bound for the sum S, i.e., for n = 2,

$$S_{UB} < \frac{ERP}{4\pi} \left[\frac{1}{r^2} + \frac{1}{1^2} \left(1 + \frac{1}{4} + \frac{1}{2} \right) \right] \tag{A-5}$$

$$< \frac{ERP}{4\pi} \left[\frac{1}{r^2} + \frac{7}{41^2} \right]$$

APPENDIX B

POWER DENSITY OF THE INFINITE STRING

The power density of the infinite string is inversely proportional to r^2 as indicated by the following equation

$$PD_T = f\left(\frac{1}{r^2}\right) \tag{B-1}$$

The number of infinite strings N is directly proportional to r. Since the power density at the target resulting from the multiple string radiators is N times PD_T, the PD_{ms} becomes a function of 1/r. Now if we let r get large without bound, PD_{ms} diminishes to zero, i.e.,

$$\lim_{r \to \infty} PD_{ms} \to 0 \tag{B-2}$$

APPENDIX C

PROGRAM COMPUTE

```
      program compute
      pi=3.14159265
      write(*,100)
  100 format( ' Input length of series to compute: ', )
      write(*,150)
  150 format( ' format: I3  ')
      read(*,110)  n
  110 format(i3)
      write(*,120)
  120 format( ' Input (p)ower, (r)adius, and (l)ength : ')
      write(*,130)
  130 format( ' format:  2F6.3,I3     ')
      read(*,140) p,r,l
  140 format(2f6.3,i3)
      write(*,160) p,r,l
160   format(///,' input power = 'f10.5,/,' input radius = ',
     + f10.5,/,' input length = ',i5,///)
      sum=1.0/(r*r)
      do 10 i=1,n
         sum=sum + 1.0/(r + 1*i)**2
10    continue
      write(*,200) p*sum/(4.0*pi)
  200 format(///,' And the sum of the series is ...',e15.5,/////)
      stop
      end
```

APPENDIX D

PROGRAM POWER

```
      program power
      real l,w
      pi=3.14159265
      write(*,100)
  100 format(   ' Input length of series to compute: ',\)
      write(*,150)
  150 format(   '  format: I3   ')
      read(*,110) n
  110 format(i3)
      write(*,120)
  120 format( ' Input (p)ower, (r)adius, and (l)engtn : ')
      write(*,130)
  130 format( '  format: 3F10.3       ')
      read(*,140) p,r,l
  140 format(3f10.3)
      write(*,160) p,r,l
160   format(///,' input power = ',f10.5,/,' input radius = ',
     + f10.5,/,' input length = ',f10.5,///)
      sum=1.0/r
      w=182.88
      do 10 i=1,n
         sum=sum + 1.0/(r + l*i)
10    continue
      write(*,200) n,p*sum/(2.0*w)
  200 format(///,' Power density for n = ',i5,' is ',e15.5,/////)
      stop
      end
```

SECTION 5
MODELING AND ACCURACY CONSIDERATIONS

INTRODUCTION

This document provides details of a decision logic in support of the development of collision avoidance radar technology; however, until the hardware and software system is in place to permit qualification of the system performance on actual candidate collision target objects, these developments must necessarily be taken as preliminary. Included herein are the decision logic objectives, preliminary collision avoidance trajectory models, and the associated collision avoidance decision logic developed over the previous several months.

DECISION LOGIC OBJECTIVES

The modeling objectives are summarized as follows:

Support the development of a collision avoidance radar system via effective determination of

a. Underlying governing models including critical model variable characteristics (e.g., determination of deterministic and stochastic nature of the variables involved in the model decision logic, their distributional characteristics, model sensitivities, etc.)

b. Expected model performance characteristics relative to

    1. A wide variety of accident configurations

    2. Differing models/variables accuracies

More specifically, the above support decision logic objectives are summarized as follows:

a. Determine underlying mathematical models governing

    1. The minimum stopping distance of the sensing vehicle and the target vehicle or object

    2. The critical crash threshold (e.g., the minimum braking/warning distance, velocity combinations, distances, directions, differing angular approaches, and/or derivatives of the same) required for collision avoidance determination

b. Determine the influence of the stochastic variables comprising the underlying models with particular considerations for the distributional characteristics of

    1. The target cross-sectional backscatter

    2. The estimated range between the sensing and target vehicles (objects)

3. The estimated received power

4. The angle between the sensing vehicle and target

5. Others (e.g., the forward and backscatter interference resulting, for example, from inclement weather)

The materials herein initiate, at best, necessary front-end model development in support of these objectives; critical limitations of these developments and the challenge for future developments are in the area of the extendability of models (no small task in view of the large variety of target types to be confronted).

EQUATIONS RELATING APPROACH TO TARGET

Linear motion only is considered. Accelerations considered are in the direction of motion only. No transverse accelerations are considered.

Key to the decision logic development is an understanding of the minimum distance required for a vehicle to stop once braking occurs (in particular, this will be needed to determine an alarm threshold for when to sound a warning). Consequently, it is well-known that the minimum distance for a vehicle to come to a complete stop is given by

$$X = V_0^2/2\,g\mu_s$$

where V_0 is the velocity of the vehicle at the time the braking occurred, g (= 32 ft/sec^2) is the acceleration due to gravity, and μ_s is the coefficient of friction. It should be mentioned that μ_s should be the coefficient of static friction provided

a. There is no sliding between the tires and road.

b. Rolling friction is negligible.

c. The maximum force of static friction operates because the problem seeks the shortest distance for stopping.

d. The correct braking technique required is to keep the car just on the verge of skidding.

In case the surface is smooth and the brakes are applied fully, sliding may occur. In this case, the coefficient of sliding friction, μ, should replace that of static friction and, as a result, the distance required to stop is seen to increase since, typically, $\mu_s > \mu$.

To structure the situation of an approach by the sensing vehicle upon a target, consider the situation whereby two vehicles are approaching one another at differing speeds and at time-dependent (i.e., changing) bearings relative to one another. The emphasis in the remainder of this report is on the

derivation of the decision logic for collision avoidance. Reference throughout is to figure 5-1 which depicts the geometry of the situation.

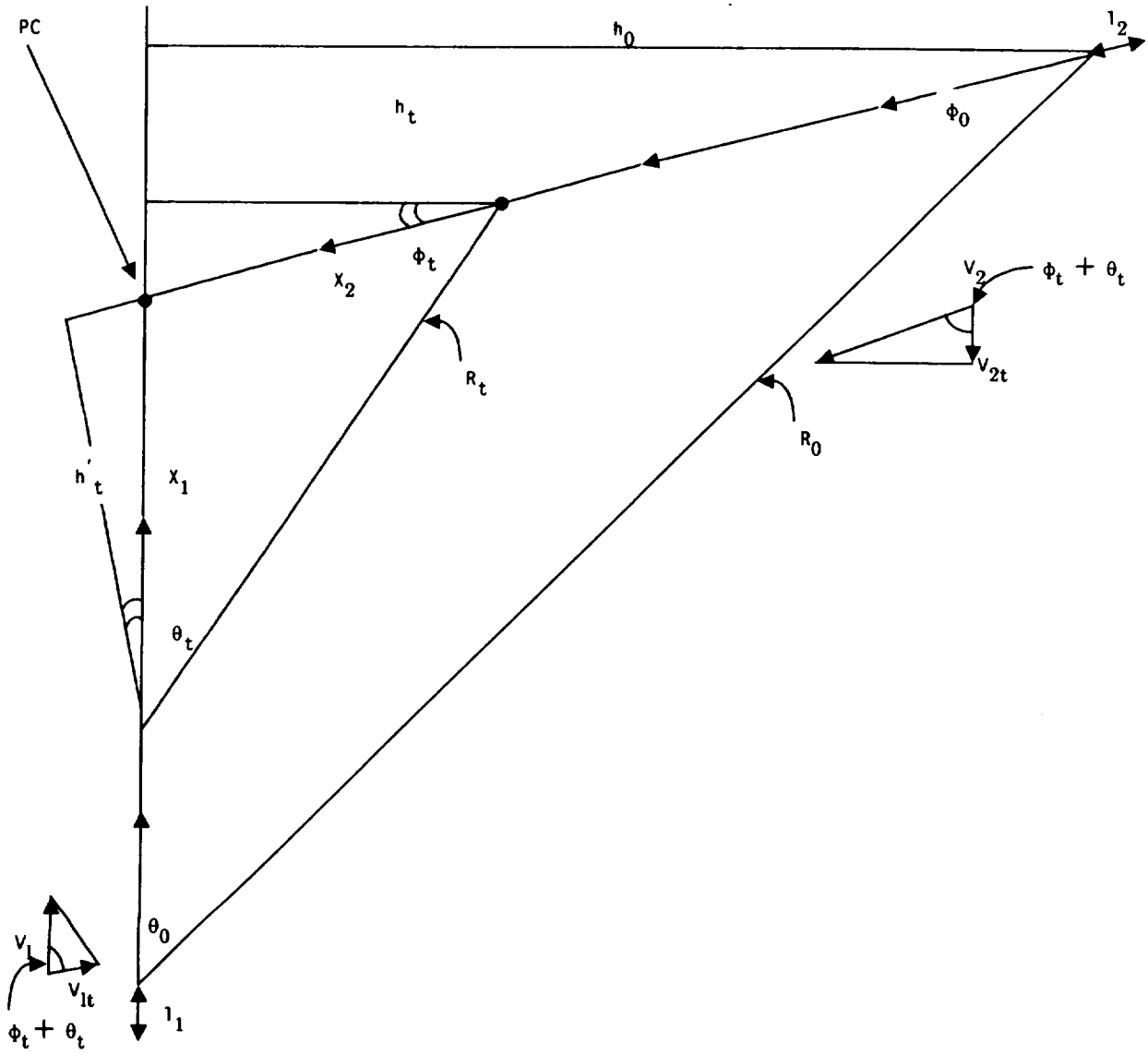

Figure 5-1.- Collision course geometry.

a. Earth fixed reference frame is used.

b. The notation utilized in figure 5-1 is as follows:

l_1 = length of vehicle #1

l_2 = length of vehicle #2

R_0 = range between vehicles at time t_0

R_t = range between vehicles at time t

θ_0 = bearing of vehicle #2 from #1 at time t_0

θ_t = bearing of vehicle #2 from #1 at time t

Φ_0 = bearing of vehicle #1 from #2 at time t_0

Φ_t = bearing of vehicle #1 from #2 at time t

h_0 = offset of vehicle #2 from path of #1 at t_0

h_t = offset of vehicle #2 from path of #1 at t

h'_t = offset of vehicle #1 from path of #2 at t

V_1, V_2 = ground velocities of vehicles #1 and #2, respectively (also functions of t in the forthcoming dicussion)

V_{1t} = component of velocity of vehicle #1 parallel to the path of vehicle #2 at time t

V_{2t} = component of velocity of vehicle #2 parallel to the path of vehicle #1 at time t

X_1 = distance of vehicle #1 from potential collision point

X_2 = distance of vehicle #2 from potential collision point

PC = potential collision point (in general, the vehicles may pass through this point at differing times and without colliding

From the above notation, a key relationship is that of the quantity $dR_t/dt = \dot{R}_t$ which is seen to result in the following (using $R_t = h_t/\sin\theta_t = h_t \csc\theta_t$):

$$\dot{R}_t = dR_t/dt = \left(dR_t/d\theta_t\right)\left(d\theta_t/dt\right) + \left(dR_t/dh_t\right)\left(dh_t/dt\right)$$

$$= -h_t \csc\theta_t \cot\theta_t \dot{\theta}_t + \dot{h}_t \csc\theta_t$$

or

$$\dot{R}_t = -R_t\left(\dot{\theta}_t \cot\theta_t - \dot{h}'_t/h_t\right) \qquad (5\text{-}1)$$

Equation 5-1 is of interest in a theoretical sense only. It is not used in the estmation of $\dot{R}_t$ since $\dot{R}_t$ is completed using successive range measurements.

FURTHER DECISION LOGIC DETAILS

The minimum stopping distance between vehicle #1 and vehicle #2 prior to collision, assuming both drivers brake simultaneously, is given by*

$$R_M = V_1^2/2g\mu_1 + \alpha v_2^2 \cos^2\left(\phi_t + \theta_t\right)/2g\mu_2 + V_1/\tau_1\Big) +$$

$$V_2 \tau_2 \cos\left(\phi_t + \theta_t\right) + \tau\left[V_1 + V_2\cos\left(\phi_t + \theta_t\right)\right] \qquad (5\text{-}2)$$

where

τ_1 = driver reaction time plus mechanical braking time of vehicle #1

τ_2 = driver reaction time plus mechanical braking time of vehicle #2

τ = radar system delay time (i.e., time delay due to radar circuitry plus system computing time

V_1 = the velocity of vehicle #1 at time braking occurs

V_2 = the velocity of vehicle #2 at time braking occurs

and

$$\alpha = \text{the sign of} \cos\left(\varnothing_t + \theta_t\right)\left(\text{i.e., } \alpha = -1 \text{ or } +1\right)$$

e.g., $\alpha = +1$ for oblique intersecting paths, and

$\alpha = -1$ for acute intersecting paths

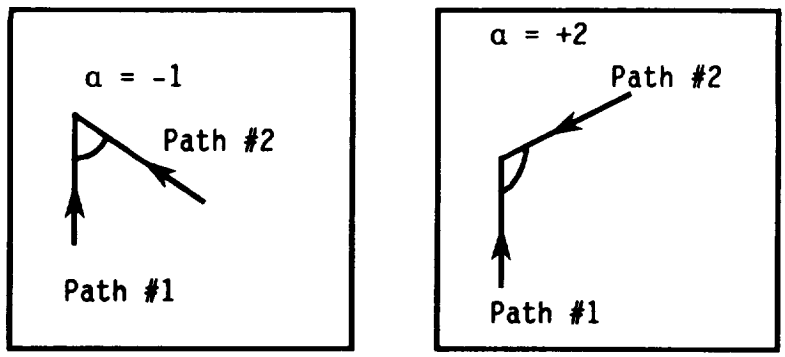

*See the section on further discussion of the "alarm" threshold for a detailed discussion of the meaning of R_M.

If braking is not simultaneous, e.g., vehicle #2 brakes Δ seconds after vehicle #1, then R_M would be altered by the add on amount C_2 where

$$C_2 = \left(V_2\Delta + a_2\Delta^2/2\right)\cos\left(\varnothing_t + \theta_t\right)$$

where a_2 is the acceleration (deceleration) of vehicle #2 (also not that $\varnothing_t$ and θ_t in equation 5-1 would be replaced with $\varnothing_{t+\Delta}$ and $\theta_{t+\Delta}$ respectively). Similarly, if vehicle #1 brakes Δ seconds after vehicle #2, then R_M in equation 5-1 would be altered by the add on amount C_1 where

$$C_1 = V_1\Delta + a_1\Delta^2/2$$

and where a_1 is the acceleration (deceleration) of vehicle #1. Note also that a_1, a_2, V_1, and V_2 in C_1 and C_2 may vary with time. Whether a hardware and software system can be structured with enough sensitivity to incorporate in adjustments for accelerations (decelerations) as discussed above is, yet, another matter; indeed, a slight increase in the frequency of monitoring the velocities of the two vehicles may prove to be more accurate than attempting to incorporate in the various accelerations (decelerations).

From the radar time delay equation,

$$R = ct_R/2$$

where

t_R = time delay between transmitted and received signal

R = the radar target range

c = the propagation velocity

the distance R_t at time t may be estimated (detailed below). From this and the use of the radar range equation

$$P_r = \left(P_t G^2\lambda^2\sigma\right)/\left(64\pi^3 R^4\right)$$

the backscatter cross-section, σ, may also be estimated (which is key to assessing the decision logic performance on differing target types). In the above, P_t is the power transmitted from the radar, P_r is the power received back to the antenna from the target, G is the antenna gain, and λ is the

wavelength of the transmitted signal. With these, the following decision logic is conceivable:

SEQUENCE I

1. Pulse is transmitted from radar with known power P_t and velocity c
2. Clock time $\hat{t}_i$ of transmission is sent to microprocessor
3. Signal echo off target object with power $\hat{P}_r$ is received back at antenna
4. Clock time $\hat{t}_f$ of reception sent to microprocessor
5. The boresight angle $\hat{\theta}_{t_f}$ to the target is sent to microprocessor*

SEQUENCE II

1. Microprocessor computes:
   a. $\hat{R} = (\hat{t}_f - \hat{t}_i)\ c/2$
   b. $\hat{\sigma}$ from $\hat{R}$ and $\hat{P}_r$ (or from table look-up)
   c. Offset distance $\hat{h}_{t_f}$ (computed from relationship) $\hat{h}_{t_f} = \hat{R}_{t_f} \sin\hat{\theta}_{t_f}$
2. $\left(R, P_r, \sigma, t_f, \theta_{t_f}, h_{t_f}\right)$ is stored temporarily in microprocessor

SEQUENCE III

1. Sequences I and II are repeated to obtain $\left(\hat{R}', \hat{P}_r', \hat{\sigma}', \hat{t}_f', \hat{\theta}_{t_f}', \hat{h}_{t_f}'\right)$ at a later time t_f'.
2. Microprocessor computes:
   a. $\hat{\dot{R}} = \left(\hat{R}' - \hat{R}\right) / \left(\hat{t}_f' - \hat{t}_f\right)$
   b. $\hat{\dot{h}} = \left(\hat{h}_{t_f}' - \hat{h}_{t_f}\right) / \left(\hat{t}_f' - \hat{t}_f\right)$
   c. $\hat{\dot{\theta}} = \left(\hat{\theta}_{t_f}' - \hat{\theta}_{t_f}\right) / \left(\hat{t}_f' - \hat{t}_f\right)$

3. Decision logic (discussed below is exercised based on table look-up for

$$\left(\hat{\dot{R}}, \hat{\dot{h}}, \hat{\theta}_{t_f}, \hat{\dot{\theta}}\right)$$

computed from a pre-selected moving window.

With the above, then, a possible decision logic is given below (reference the notation detailed in the previous sections):

1. If $\hat{\dot{R}} \geq 0$, the system remains passive.

2. If $\hat{\dot{R}} < 0$, the following is done:

   a. If $(\hat{\dot{\theta}}, \hat{\theta}) \notin I_0$, for a to be determined region I_0 in 2-space, the system remains passive.

   b. If $(\hat{\dot{\theta}}, \hat{\theta}) \in I_0$, then the following is checked:

      If $\hat{R}_P < R_M$, a warning is sounded; otherwise, the system remains passive.

   NOTE: $\hat{R}_P = \hat{R}_t \cos\theta_t$

DISCUSSION OF INTERVAL I_0

From a fixed point $t = t_0$ in time, let

t_{1I} = time required for front-end of vehicle #1 to reach the potential collision point, PC.

t_{1F} = time required for rear-end of vehicle #1 to reach PC.

t_{2I} = time required for front-end of vehicle #2 to reach PC.

t_{2F} = time required for rear-end of vehicle #2 to reach PC.

*Variables with a "hat" (e.g., $\hat{\theta}$) are computed from radar sampled values as opposed to error-free, theoretical values.

then under constant velocities V_1 and V_2, both assumed to be positive,

$$t_{1I} = X_1/V_1,\ t_{1F} = \left(X_1 + 1_1\right)/V_1$$

$$t_{2I} = X_2/V_2,\ t_{2F} = \left(X_2 + 1_2\right)/V_2$$

Consequently, the logic concerning the interval I_0 discussed above is detailed as follows:

$$\text{If } [X_1/V_1 \leq X_2/V_2 \leq (X_1 + 1_1)/V_1] \text{ or}$$

$$\text{if } [X_1/V_1 \leq (X_2 + 1_2)/V_2 \leq (X_1 + 1_1)/V_1]$$

then the system checks against a threshold R_M (discussed in the next section) to see if the following is satisfied:

$$\hat{\hat{R}}_P < R_M$$

If so, the system sounds a warning; otherwise, it remains passive. It should be particularly noted that the above logic assumes V_2 is positive; if $V_2 = 0$, then we need only check to see if $h_t > 0$ in which case the object is stationary and no warning is necessary. Consequently, the above details the specifics of the interval I_0. It should be noted that, expectedly, I_0 would be dependent on $\hat{\theta}_t$ and $\dot{\hat{\theta}}_t$; one can, indeed, re-express the above inequalities as functions of these latter two entities, but it is not necessary since the logic should work just as well using the above checks.

FURTHER DISCUSSION OF THE "ALARM" THRESHOLD

A key entity in the decision logic laid down above involves the entity R_M. To further clarify this aspect of the decision logic, note that R_M is as follows:

$$R_M = R_{M_1} + R_{M_2}$$

where

$$R_{M_1} = V_1^2/2g\mu_1 + V_1\left(\tau_1 + \tau\right)$$

and

$$R_{M_2} = \propto V_2^2\cos^2\left(\varnothing_t + \theta_t\right)/\,2g\mu_2 + V_2\cos\left(\varnothing_t + \theta_t\right)\left(\tau_2 + \tau\right)$$

Consequently,

R_{M_1} = the minimum distance required for vehicle #1 to come to a stop

R_{M_2} = the minimum distance, parallel to the path of vehicle #1, required for vehicle #2 to come to a stop

Hence, the comparison of $\hat{R}_P$ with R_M, i.e., the check for $\hat{R}_P < R_M$ is equivalent to the condition that $d < 0$ where d is the quantity indicated in the figure below. Equivalently, $\hat{R}_P = R_{M_1} + R_{M_2}$ when $d = 0$ (refer to the figure below).

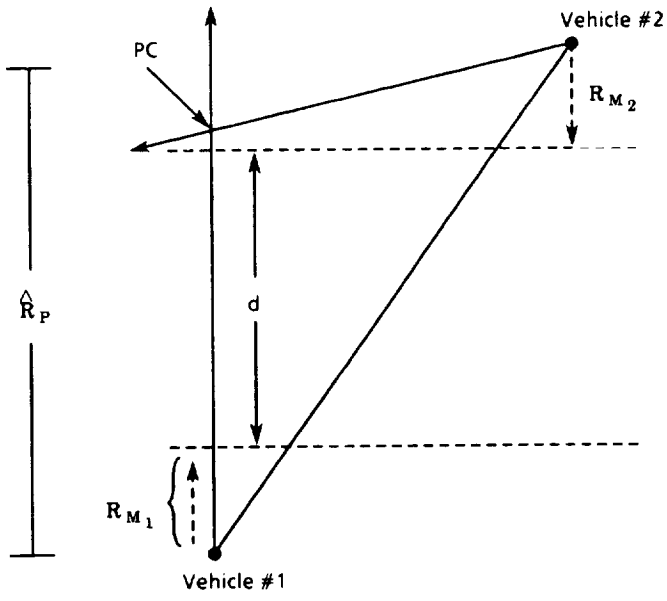

Figure 5-2.- Forces acting on a decelerating (accelerating) vehicle.

ESTIMATION OF PARAMETERS NOT DIRECTLY MEASURABLE

The decision logic assumes knowledge of certain quantities some of which are not directly measurable by the radar system. Consider the re-annotated version of figure 5-1 as shown below. Here A and B are the respective positions of vehicle #1 at times t - Δt and t, while C and D indicate the corresponding positions of vehicle #2. The interval Δt represents the time lapse between successive radar pulses. The relevant entities directly obtainable from the radar system are θ_t, $\theta_{t-\Delta t}$, $R_{t-\Delta t}$, and R_t. Also known is the velocity, V_1, of vehicle #1. The quantities not directly measurable are X_1, X_2, and V_2.

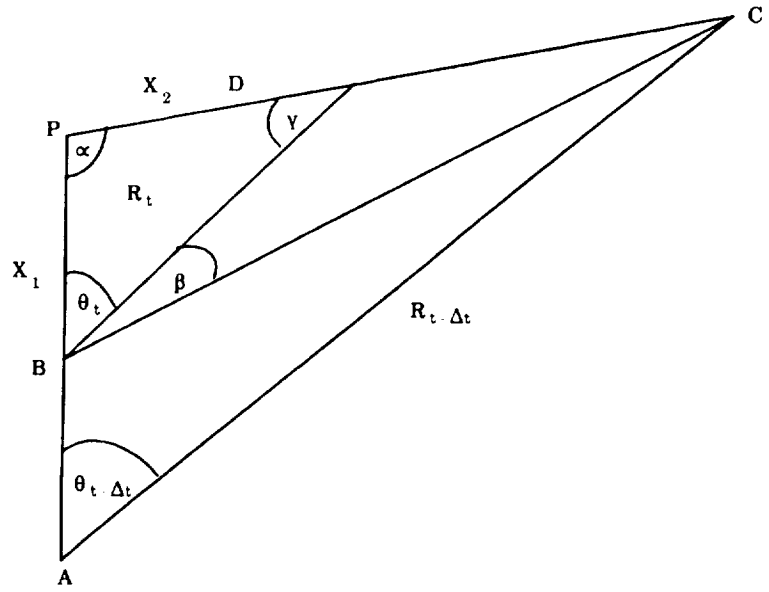

To obtain these quantities, we proceed as follows:

1. $\overline{AB}$ can be found from V_1, since $\overline{AB} = V_1 \Delta t$.

2. The lengths of two sides ($\overline{AB}$ and $R_{t-\Delta t}$) and the included angle $\theta_{t-\Delta t}$ of triangle ABC are known, hence all angles and side lengths of this triangle can be calculated using the law of cosines and the law of sines.

3. The angle β can now be calculated as a difference from a straight angle of θ_t and $\angle ABC$; i.e., $\beta = \pi - \theta_t - \angle ABC$.

4. Since $\overline{BC}$ is known from #2 above, we now know two sides (R_t and $\overline{BC}$) and an included angle (β) of triangle BCD; hence all angles and side lengths of this triangle can be calculated.

5. Since $\overline{DC}$ is now known, we may compute $V_2 = \overline{DC} / \Delta_t$.

6. The angle γ can now be calculated as a difference from a straight angle of $\angle BDC$ which is now known; i.e., $\gamma = \pi - \angle BDC$.

7. We may now calculate $\alpha = \pi - \theta t - \gamma$.

8. Since all three angles and a side (R_t) of triangle BPD are now known, we may now use the law of sines to find

$$X_1 = R_t \sin \gamma / \sin \alpha$$

and

$$X_2 = R_t \sin \theta_t / \sin \alpha$$

NOTE: To recall the law of sines and the law of consines, note the following:

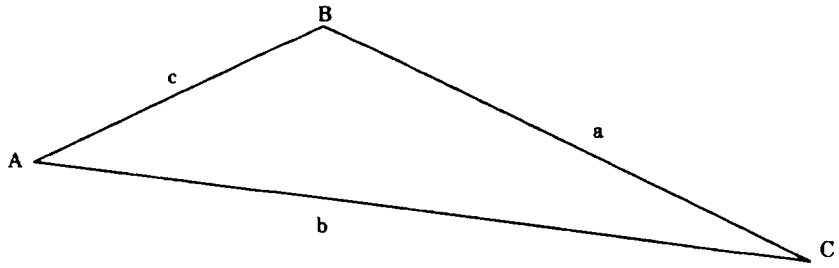

Law of cosines: $\cos (A) = (c^2 + b^2 - a^2) / 2bc$

Law of sines: $(\sin (A)) / a = (\sin (B)) / b = (\sin (C)) / c$

SUMMARY

Most variables involved in the decision logic are stochastic (e.g., the range, range rate, cross-sectional back-scatter, received power, etc.) and will necessarily need to be sufficiently understood in terms of their distributional characteristics to permit a performance evaluation of the radar system. As a part of future testing, true values for the estimated quantities can be compared against the estimated values to permit variance and bias estimation (i.e., accuracy assessments) of the estimated quantities that go into the decision logic. In particular, key aspects of future developments should include assessments of such things as the following:

1. Likelihood of occurrence of specific target types

2. Shape, duration, and phase of the echo from anticipated targets

3. Variation in echo as a function of radar settings (e.g., differing G, P_t, λ, and c)

4. Variation in echo with change in viewing angle

SECTION 6
WEATHER EFFECTS ON RADAR PERFORMANCE

INDEX OF REFRACTION FOR AIR

Variations in propagation velocity cause radar to incorrectly estimate range and range rate because these measurements are derived using propagation velocity.

The speed of a radar beam propagating through air, or atmosphere, is less than in free space. This effect is frequency independent below 100 GHz. The resulting velocity (v) is given by

$$v = \frac{c}{n} \tag{6-1}$$

where c = velocity of light in vacua
n = refractive index of medium for propagation

The refractive index (n) for air is a function of temperature (T, °K), pressure (P, millibars), and partial pressure of water vapor (e, millibars).

The refractive index (n) is calculated[1,2] using

$$n = \frac{77.6}{T}\left(P + \frac{4810 \times e}{T}\right)10^{-6} + 1 \tag{6-2}$$

The equation for partial water vapor pressure (e) is[2]

$$e = 6.11\left[10^{\left(\frac{7.5 \times DPT}{DPT + 237.3}\right)}\right] \tag{6-3}$$

where DPT = dew point temperature (°C)

Relative humidity (RH,%) can also be used to calculate partial water vapor pressure (e)[2]

$$e = \frac{RH \times e_s}{100} \tag{6-4}$$

where saturation pressure (e_s) is found from equation 6-3 when DPT = air temperature.

An estimated range of values expected to be encountered in the local atmospheric environment around an automotive crash avoidance radar is given in table 6-1.

TABLE 6-1.- EXTREME VALUES OF CLIMATE PARAMETERS

Parameter	Value	Condition
Pmin	600 mb	12,000 ft w/depression overhead
Pmax	1050 mb	sea level w/high pressure front overhead
Tmin	-40°C (= -40°F = 233°K)	deep winter, northern U.S.A.
Tmax	+79°C (= +175°F = 352°K)	hot summer; at road surface, U.S.A.
e min	0.0 mb	relative humidity = 0%
e max	456 mb	relative humidity = 100%, T = +79°C

Table 6-2 shows extreme values of n as calculated from equation 6-2 using the range of values from table 6-1.

TABLE 6-2.- RANGE OF VALUES FOR REFRACTIVE INDEX (n)

1/n	Refractive index (n)	Parameter conditions (P, T, e)
.999868	1.000132 (min.)	P = 600 mb, T = 352°K, (minimum n) e = 0.0 mb (relative humidity = 0%)
.999681	1.000319 (avg.)	P = 1013 mb, T = 288°K, e = 10 mb (standard atmosphere at sea level, average value for n)
.998398	1.001605 (max.)	P = 1050 mb, T = 352°K, e = 456 mb (100% relative humidity) (maximum n)

Using the values of n from table 6-2, variations in propagation velocity can be calculated. A correction factor can be used to calculate the deviation from free space values. The correction factor is 1/n. To use this factor to find actual distance to an object, one multiplies the distance found as determined by a radar calibrated to free space by the correction factor. The actual distance will be less than that measured using free space values, which means the radar will tend to overestimate range to a target. Table 6-3 shows the errors of range measurement.

TABLE 6-3.- RANGE MEASUREMENT DEVIATIONS DUE TO ATMOSPHERIC PROPAGATION VELOCITY
(Range = 1000 feet)

1/n	Range error	Condition
.999868	0.132 feet over estimated range	Maximum expected velocity of propagation
.999681	0.319 feet over estimated range	Propagation through standard atmosphere
.998398	1.602 feet over estimated range	Slowest expected velocity of propagation

The variation in range measurement error = 1.47 feet.

For a radar calibrated at standard atmosphere, the range of distance measurement errors (for a target at 1000 feet range) will vary from -0.187 feet (for 1/n = .999868) to + 1.283 feet (for 1/n = .998398).

Several conclusions can be reached from this analysis: (1) On the average a 0.3 foot bias error (at 1000 feet) in distance measurement will be encountered if free space propagation values are not corrected for refraction effects in a standard atmosphere; (2) A range measurement variation of approximately 1.5 feet (at R = 1000 feet) will be encountered as the refractive index of air (n) varies with climate conditions and altitude; and (3) In light of the accuracies contemplated for crash avoidance radars (approximately several feet) these distance errors should not have serious impact on radar performance.

MODULATION EFFECTS

The amount and severity of interference generated in a radar due to rain, snow, hail, sandstorm, and fog is dependent on (among other things) the modulation method used. For example, pulse radars offer better interference suppression potential over FM-CW and other CW-type radars.[4,7,8] Interference suppression is obtained in pulse radars by effectively gating-out rain returns earlier or later than the region of interest around a target's return pulse. Thus, only rain clutter in a volume around the target will disrupt detection. CW systems generally cannot implement interference suppression methods as easily or effectively due to receiver designs which are usually always "on."

ANTENNA POLARIZATION CONSIDERATIONS

By transmission and reception of circularly polarized waves of the same sense, precipitation backscatter, or clutter, can be reduced. This is due to the fact that smooth, round objects reverse the polarization sense. A representative figure for improvement of target signal to precipitation signal is approximately 15 to 20 dB for wet snowflakes to dense rainfall.[1]

Other approximately spherical, interfering particles such as dust and sand should exhibit similar signal suppression. Coincidentally, the signal returns from automobiles are reduced typically 3 to 5 dB.[1] This is due to polarization mismatch of transmitted to received signal.

GASEOUS ATTENUATION

Microwaves experience attenuation when propagated through atmospheric gases. Backscatter from gases can generally be neglected (unlike in the case of precipitation). Gaseous attenuation is a function of carrier frequency, altitude, and time of year.[1] Figure 6-1 shows the extreme values (maximum and minimum) expected in the continental United States. K-band (24 GHz), a commonly used frequency, experiences at worst .05 dB/200 m (which is the amount incurred in a two-way trip out to 100 m and back). This is definitely negligible. However, for frequencies near 60 GHz and then again near 200 GHz, the attenuation increases to an expected maximum of approximately 6 dB/200 m. For a radar system with adequate signal margin this can be tolerated. If system operation is marginal, then gaseous attenuation could reduce system effectiveness. One can conclude from the gaseous attenuation spectrum that the 55-65 GHz, 175-225 GHz, and 300-400 GHz region requires additional signal margin to be designed into the system.

RAIN INTERFERENCE

The effect of rain on radar performance has been studied extensively.[1,4,5,6,7,9,10,11] Figure 6-2 shows the attenuation effect of various rainfalls versus frequency. A radar is compensated for simple rain attenuation by adding appropriate margin into the system design. For example, at 24 GHz add approximately 3 dB to offset the maximum two-way loss for a target at 100 m. Below 24 GHz this attenuation need not be considered. Above 24 GHz one adds proportionately more margin. For example, 9 dB should be added at 100 GHz to maintain adequate target signal return for a target distance of 100 m. Of course, decreased distance requires less margin addition to system design.

The more challenging problem presented by rain interference centers around maintaining radar operation in rain clutter, or backscatter. Rain backscatter has the potential to obscure detection of actual hazard targets.[4]

The ratio of rain clutter power (Pr) to target cross-section power (P_{target}) for CW radar[10] is

(CW radar)

$$\frac{Pr}{P_{target}} = \frac{2\eta R^3}{\sigma} \qquad (6\text{-}5)$$

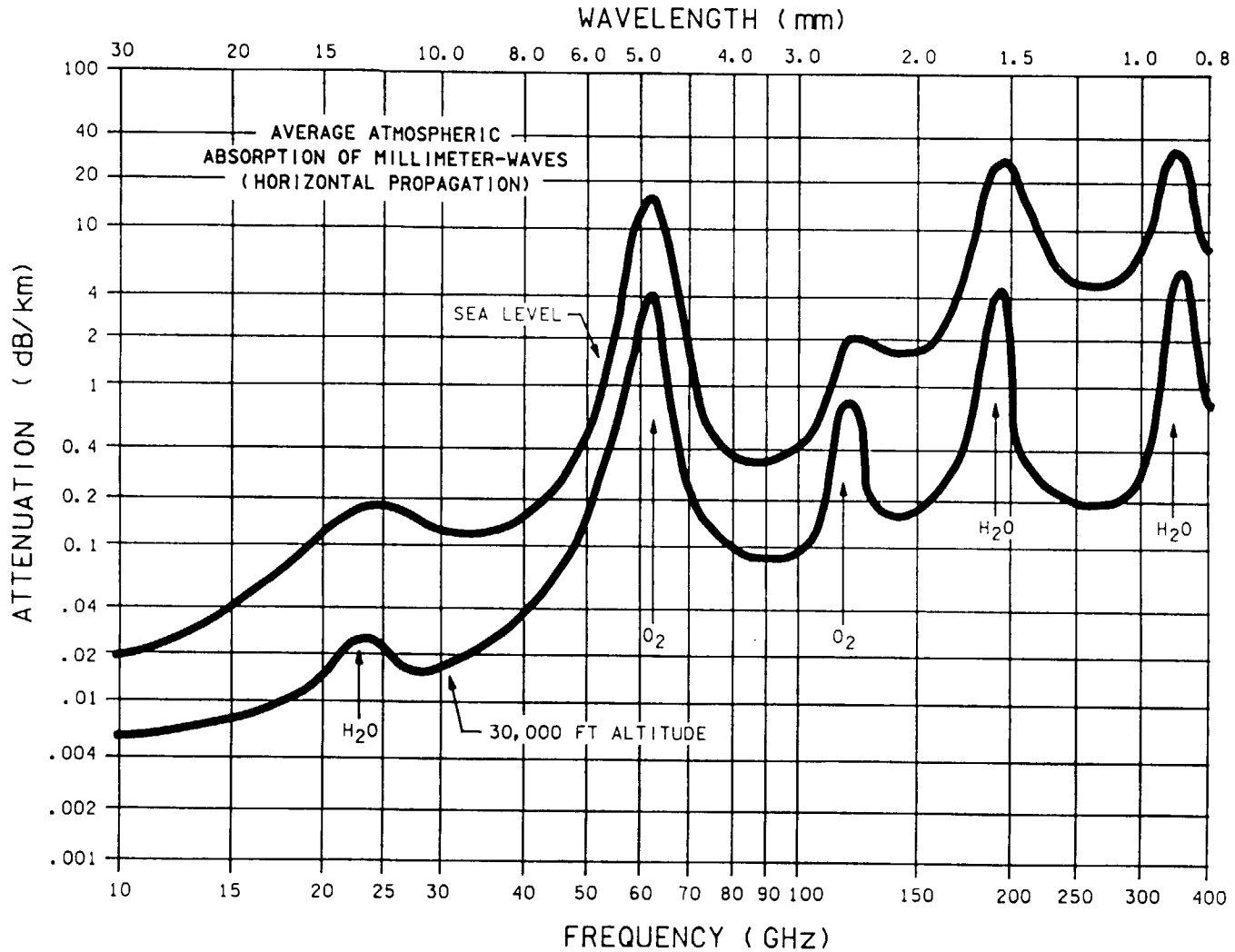

Figure 6-1.- Atmospheric attenuation of millimeter waves.

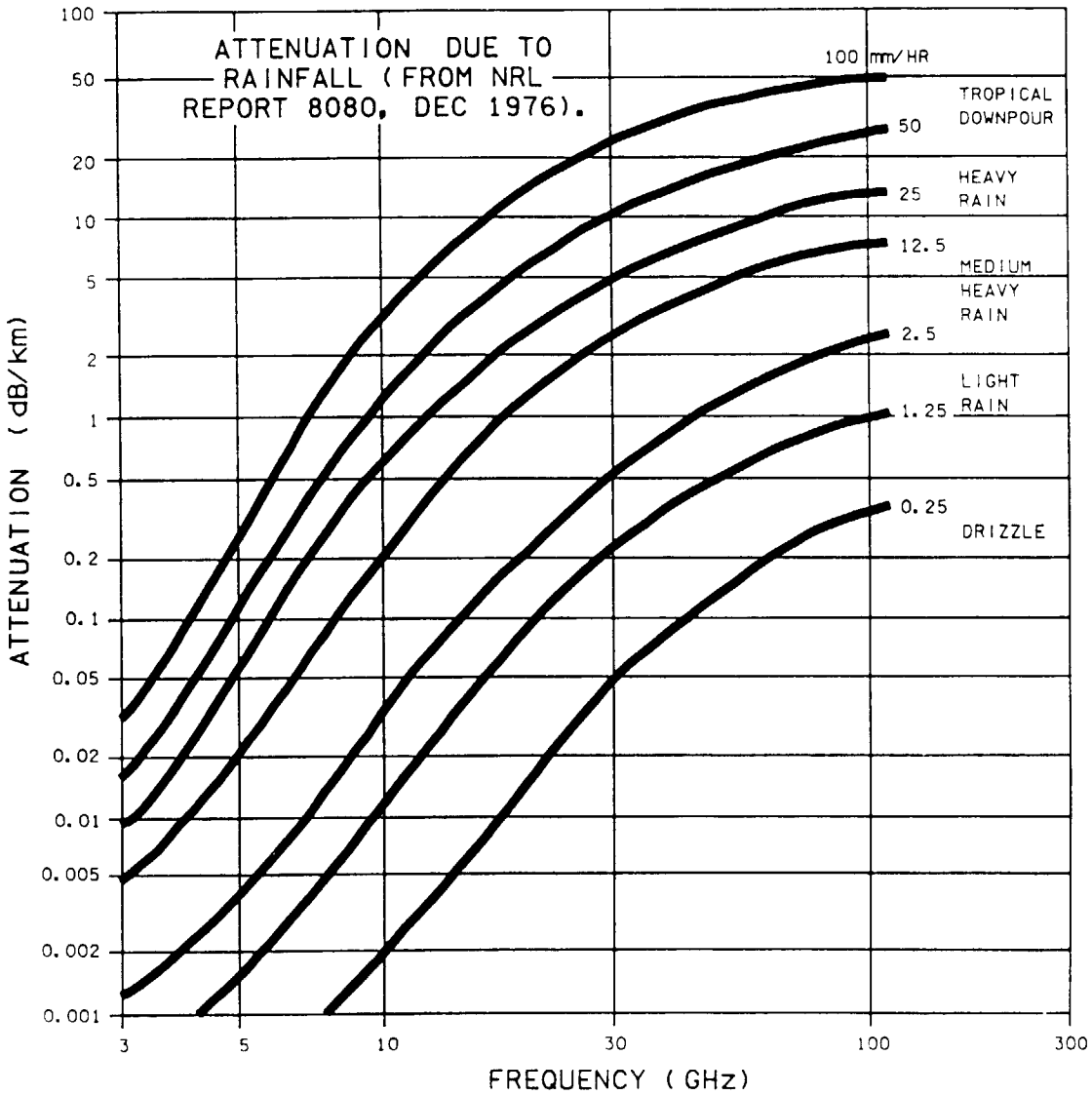

Figure 6-2.- Rainfall attenuation.

The time averaged gated rain return ($\overline{P}$ rain) during a pulse for pulse radar[1] is

(Pulse radar)
$$\overline{P}_{rain} = \frac{P_t A_e C \tau \eta}{32 R^2} \qquad (6\text{-}6)$$

where η = frequency and rainfall dependent rain reflectivity
R = distance to target
σ = frequency dependent radar cross-section (RCS)
A_e = effective antenna aperture
c = speed of propagation
τ = pulse width
P_t = peak transmitter power

Return power from a target depends on whether a radar and target are operated in their near fields or far fields. Due to the size of automotive environment radar targets, near field operation will probably occur over much of the target's range. The reflecting area of rain in the near-field appears less than in the far field;[5] therefore, far field calculations should give worst case values.

The average power during the pulse from an ideal target (P_{target}) of radar cross-section σ at range R for a pulse radar[1] is

$$P_{target} = \frac{P_t \sigma A_e^2}{4\pi R^4} \qquad (5\text{-}7)$$

This assumes no rain attenuation experienced in the wave traveling to the target and back. Attenuation values given previously can be included if desired.

The ratio of rain clutter power to power from an ideal target is calculated to be

$$\frac{\overline{P}_{rain}}{P_{target}} = \frac{\pi C \tau \eta R^2}{8 \sigma A_e} \qquad (6\text{-}8)$$

Backscatter cross-section (η) is found[5] from figure 6-3. As an example, for a rainfall of 5 mm/hr ($\eta = 3.10^5$), pulse width of 20 ns ($C\tau$ = 6 m), R = 100 m, A_e = 0.06 m^2, cross-section (σ) of 10 m^2, and λ = 1.25 (24 GHz), a ratio of unity occurs. If rain interference cancellation by circular polarization of the antenna is added to this, a signal-to-clutter noise ratio increase of 15 to 20 dB will occur[1] which should allow system operation.

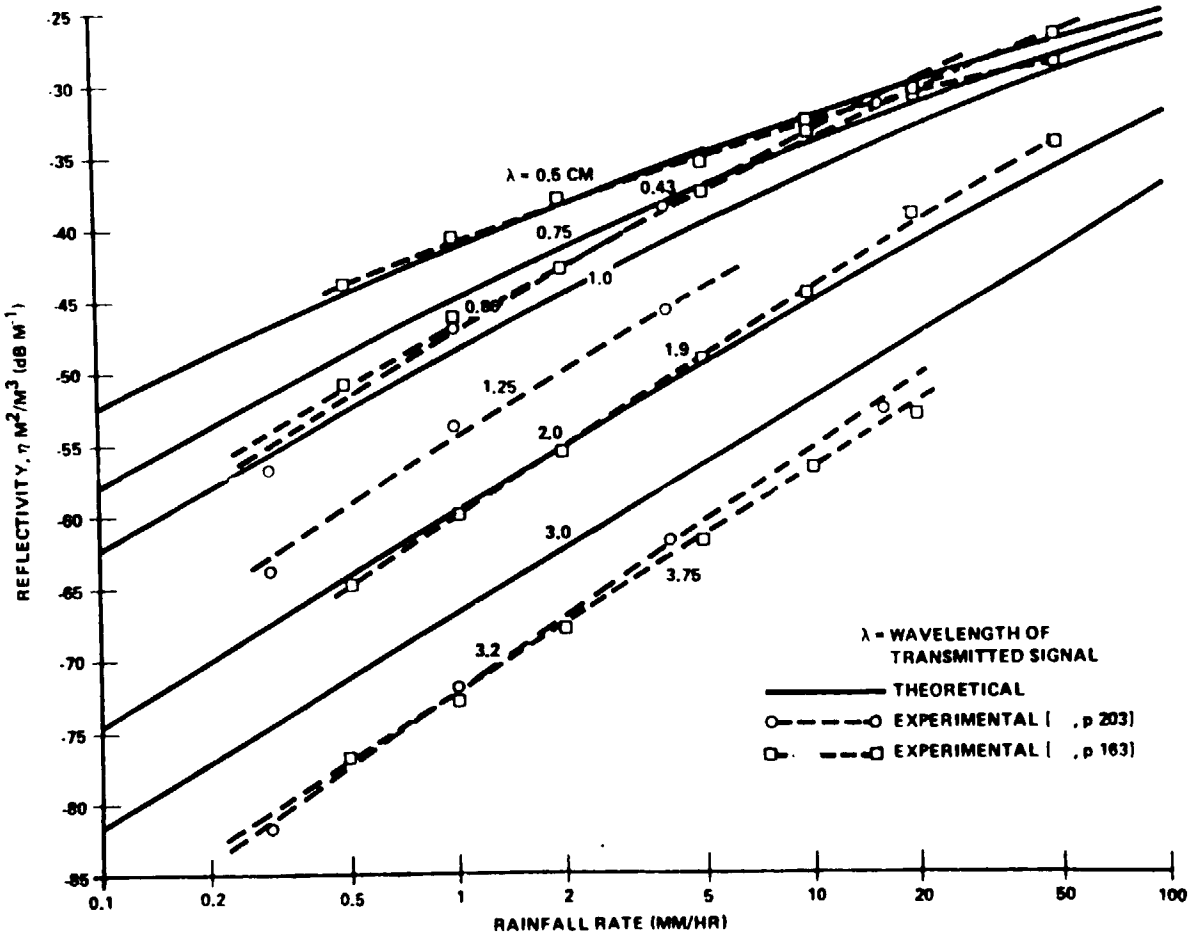

Figure 6-3.- Specific radar reflectivity of rain as a function of rainfall rate. (Reproduced from reference 5)

Tests conducted at 50 GHz[11] using FM-CW radar indicate that rain attenuation is probably of no consequence, whereas rain backscatter must be considered in system design. In addition, the effect of water adhesion to the radome was shown to cause measurable loss of sensitivity (approximately 10 dB attenuation for a 0.5 mm thin film of water). Pattern distortion due to reflecting materials on the radome (e.g., water) can be expected to have some effect on radar performance. However, careful selection of radome materials and shape should be adequate to control problems encountered.

The general guidelines apparent in equation 6-8 are (1) narrower pulse width radar can better exclude rain clutter; (2) the closer the range the better will be the target power-to-rain clutter power ratio; and (3) bigger targets are easier to detect in rain clutter, and bigger antenna areas (smaller beam widths) offer better performance. In addition, (4) higher frequencies could suffer more from rain interference. However, the increased radar cross-section as a function of frequency will tend to somewhat negate the effect of increased rain clutter. Other observations to be made are that (5) increasing the transmitter power (once rain clutter is detected in the receiver) does nothing to improve the situation and (6) similarly, improving receiver sensitivity will not decrease the clutter-to-target ratio.

FOG INTERFERENCE

Fog interferes with radar operation by absorbing, or attenuating, power as a radar pulse propagates through it. Table 6-4 shows typical values for 24 GHz and 10 GHz[1] and extrapolated values for 100 GHz.

TABLE 6-4.- ATTENUATION BY FOG OR CLOUDS

Fog visibility	Attenuation dB/100 m		
	10 GHz	24 GHz	100 GHz (extrapolated)
30 m 0°C	0.020	0.125	1.25
30 m 25°C	0.008	0.050	0.50
90 m 0°C	0.004	0.025	0.25
90 m 25°C	0.0016	0.01	0.1

The values in table 6-4 are more conservative than those published previously.[6] Even so, losses not to exceed approximately 1 dB can be considered *negligible*.

C-2

SNOW INTERFERENCE

Snow may cause backscatter interference to radars. However, the effect is approximately one-fifth of the value for water (rain).[17] Since snowfall rates are generally less than rainfall rates, the effect of snowfall should be much less compared to rain interference. A possible problem might arise if considerable snow, ice, or slush accumulation occurs over the antenna face. However, tests conducted on an automotive radar at 50 GHz[11] showed that no significant effect (less than 1 dB attenuation) for attenuation due to snowfall or snowfall accumulation (up to 20 mm on radome) was noted. Additionally, snow backscatter caused no significant degradation in radar performance. Ice up to 30 mm on the radome showed similar, negligible (less than 0.5 dB attenuation) effect. The difference in relative dielectric constant of water (> 60) compared with ice/snow (1-3) account for the variation in radar performance for rain, snow, hail, and ice. If the snow/ice should begin to melt forming a layer of water, then degraded performance might be encountered (see section on rainfall interference).

HAIL INTERFERENCE

Attenuation due to hail is of the same order or less than equivalent rainfall rates. Completely frozen hail particles create considerably less (approximately 1/100) attenuation and backscatter than particles with water present. However, when 10-20 percent melted mass is present, hail attenuation/backscatter becomes of the same order of magnitude as rain.[1] The cause of this change is that the dielectric constant of water is approximately 20 times (or more) greater than ice. Particles with higher dielectric constants scatter more energy. In addition, the loss tangent, tan (δ), of water is also much greater. At 10 GHz, tan (δ) of water is approximately 0.55 compared with tan (δ) of ice which is approximately 0.0008. This causes greater absorption of energy for water.

SANDSTORM/DUSTSTORM INTERFERENCE

Analysis of the effects of sandstorm and duststorm (or any other particulate scattering) would proceed as previous authors have done for analyzing rainfall effects.[1] One calculates the average scattering cross-section per scatterer, the density of scatters per unit volume, and then arrives at the reflectivity.

The reflectivity of particles varies with $|K|^2$. $|K|^2$ is determined by the dielectric constant of the scatterer. $|K|^2$ for water is approximately 0.93 at 10°C at X-band. $|K|^2$ for ice = 0.197 over all temperatures and centimeter wavelengths.[1] $|K|^2$ for sand and dust (assuming quartz, silica, and other oxides are major constituent elements) should be approximately equivalent to ice, possibly slightly larger. In addition, the particle size should average less than rain and ice thereby further reducing the scattering and attenuating cross-section. An increase in scatterers per unit volume could cause higher attenuation and backscattering. It is felt that sandstorm and duststorm interference should be orders of magnitude less than rainfall.

REFERENCES

1. Skolnick, M. I., "Radar Handbook," McGraw-Hill Book Company, 1970.

2. Robel, M. C., "Prediction of Atmospheric Refraction Angular Error by a Computer Raytrace Program with Application to the Space Shuttle MSBLS," LEC-16619, December 1979.

3. Jessop, G. R., "VHF/UHF Manual," Radio Society of Great Britain, 1983.

4. "Collision Avoidance Radar Braking Systems Investigation - Phase I Study," DOT-HS-801-253, Bendix Corporation, October 1974.

5. "Collision Avoidance Radar Braking Systems Investigation - Phase II Study," DOT-HS-802-020, Bendix Corporation, September 1976.

6. "Collision Avoidance System Cost-Benefit Analysis," - Volume I, DOT-HS-806-242, Kinetic Research, September 1981.

7. "Collision Avoidance System Cost-Benefit Analysis," - Volume III, DOT-HS-806-244, Kinetic Research, September 1981.

8. "Analysis of Problems on the Application of Radar Sensors to Automotive Collision Prevention," DOT-HS-801-011, Institute for Telecommunications Sciences, December 1973.

9. "Analysis of Problems in the Application of Radar Sensors to Automotive Collision Prevention," DOT-HS-801-453, Institute of Telecommunications Sciences, March 1975.

10. Grimes, D. M. and Jones, T. O., "Automotive Radar: A Brief Review," Proceedings of the IEEE, Volume 62, Number 6, June 1974.

11. Takenhana, T., et al., "Automotive Radar Using m.m. Wave," I. Mech. E., C178/81, 1981.

SECTION 7
DATA COLLECTION RADAR SYSTEM (RF/IF)

INTRODUCTION

This section provides a technical discussion of the data collection radar, or test bed radar, used during Phase I. System components described in this section are the transmitter and receiver RF and IF hardware. Considerations on system design are also presented. This radar was designed and fabricated by NASA-JSC personnel and NASA-JSC support contractor personnel.

PURPOSE OF DATA COLLECTION RADAR

A data collection radar was required to provide data not obtainable elsewhere on target return signal behavior and facilitate verification of radar hardware techniques which could be useful in later development stages of this project.

PRELIMINARY SYSTEM REQUIREMENTS FOR DATA COLLECTION RADAR

A set of preliminary system requirements was generated based primarily on considerations of the automotive target environment, limitations on antenna size, previous researchers work in this area, component availability, weather interference effects on radar performance, and ready availability of certain antenna testing and component testing equipment. Table 7-1 shows these requirements.

Carrier Frequency

Selection criteria for the requirements will now be given. Initially, 24 GHz was chosen for several reasons. First, it has been proved effective in the automotive environment. For example, 24 GHz police speed radars are offered by most of the major vendors.[1,2,3,4] These radars have demonstrated useful velocity measurement over the range of vehicle speeds from approximately 10 through 100 mph. In addition, previous researchers have used K-band (24 GHz) for the development of simpler collision avoidance radars. However, Nissan of Japan appears to be the only automotive radar researcher heretofore attempting to significantly develop a system which extracts information useful in determining angle rate data using K-band radar.[5] However, only limited experimental results were available for review during this Phase I effort. Thus, it is felt that while K-band <u>is</u> appropriate for range and range rate determination, angle and angle rate capability in this general application has <u>not yet</u> been proved for automotive radar application. Incidentally, no other frequency has been yet proved to our knowledge.

Secondly, K-band microwave hardware and test equipment are relatively easy to obtain and are moderately priced. Because of the limited use of components built for higher millimeter-wave frequencies, their costs still reflect the

TABLE 7-1.- PRELIMINARY DATA COLLECTION RADAR SYSTEM REQUIREMENTS

System parameter	Requirement
Carrier frequency	24 GHz
Modulation type	Pulsed - on/off keyed
Pulse width	20 ns
Pulse repetition frequency	100 KHz (rough order of magnitude)
Peak transmitter power	2 W
Receiver	2 channels
Reference channel	Ranging within several feet
Angle channel	Target angle indication within TBD* degrees
Receiver dynamic range	65 dB minimum
Receiver noise figure	9-10 dB maximum
Amplitude tracking	± 1 dB or TBD
Angle channel nulling	30 dB minimum
IF bandwidth	120 MHz
Detected video bandwidth	60 MHz

*TBD = To be determined

low volume nature of production. On the other hand, the microwave component industry is currently growing and expanding due to Department of Defense (DoD) activities and satellite applications with more low cost, high volume suppliers appearing every year. In addition, components capabilities are also increasing each year. The current limited production capability of the industry should not deter researchers from investigating the higher millimeter-wave frequency bands. At present, K-band components are the most readily available within the millimeter-wave bands.

Modulation Type

Pulsed (on/off keyed transmitter) modulation was chosen basen on several important considerations. Lack of isolation is a problem that continuous wave radars must always contend with. Pulse radars do not generally suffer from this. The on/off nature of the transmitter assures there will be quiet, or isolated, periods during which the receiver can operate at maximum gain and sensitivity. The only exception to this might be if a continuously running (coherent) transmitter were on/off keyed using series RF switches (e.g., pin diode switches). High isolation switches would be required.

Pulse radars offer very good range information. For example, by counting the time interval from the edge of the transmitted pulse to the target return pulse edge, a precise indication of range to the target can be derived. The accuracy achieved is determined by signal-to-noise (S/N) ratio, leading edge risetime, detector circuitry, target noise, etc. In addition, extended length targets can be detected fairly easily during signal processing of the return signal by observing the length of the target return pulse.

Immunity to rain backscatter is another advantage of pulse radar (see section on weather effects). Rain clutter is suppressed by using narrow pulse widths with a receiver that employs some type of gating, detection scheme (e.g., range bins), digitally or analogically generated.

Pulse Width

A pulse width requirement of 20 ns is based on several considerations. First, an average car is approximately 20 feet long. If equal reflections are received along each point of the 20-foot length, a reflected pulse of 60 ns (approximately three car lengths) will be received. On the other hand, a flat metal sign (e.g., boulevard stop sign or speed limit sign) has essentially no depth. It will generate a 20 ns reflected pulse. A receiver bandwidth of approximately 33 to 100 MHz respectively will be required (α = 2, see IF/video bandwidth section) for these pulse widths. If, however, longer pulse widths are used, the target resolution will suffer. Conversely, shorter pulse lengths require proportionately wider receiver bandwidths. In addition, narrower pulse widths require proportionately higher transmitter power to maintain similar sensitivity to the 20 ns pulse width.

Pulse Repetition Frequency (PRF)

The choice of PRF is based on the motion or speed of target, distance to the farthest target which will come into view, and receiver signal processing. Targets that change position quickly require higher PRF's. A target's change in position in effect modulates the return pulses, e.g., in amplitude for different angles from the radar boresight. By using the highest possible PRF, a radar has a chance at following these target return pulse modulations. If too slow a PRF is used, pulse-to-pulse fluctuations can occur which will disrupt the tracking process. However, in simple radars (constant pulsewidth, constant PRF) an upper limit for the PRF is ultimately determined by the farthest possible target which the radar will see. For example, for a farthest possible target at 5,000 feet (approximately 5,000 ns delay each

way) a PRF of 100 KHz is required. If a target at greater than 5,000 feet should return enough power to be detected in the receiver, it would appear just after the next transmitted pulse. This situation is termed range ambiguity. Reducing the PRF is the simplest way to alleviate it. Varying the PRF and employing target signal processing is another more complicated method, but it would allow higher PRF's if they become necessary.

Radar System Performance Calculations

Link margin calculations are usually employed when determining the effect of radar system component performances on the total system performance. Equation 7-1 shows the basic radar range equation used in radar system design.[6] Assumptions made when using equation 7-1 are (1) monostatic antenna, (2) near-ideal propagation conditions, and (3) single pulse detection (no averaging). It nevertheless provides a sound basis for initial system design.

$$\text{Rmax} = 4{,}416 \left[\frac{P_t G^2 \sigma}{f^2 T S/N B L} \right]^{\frac{1}{4}} \tag{7-1}$$

where

P_t = peak transmitter power (kW)
Rmax = range (thousands of feet)
f = frequency (MHz)
T = system noise temperature (degrees Kelvin)
S/N = required signal-to-noise ratio (ratio)
B = effective receiver bandwidth (kHz)
G = antenna gain (ratio over isotropic)
σ = target radar cross-section (m^2)
L = miscellaneous loss factor (ratio)

Equation 7-1 can be used several ways. It could be used to find the transmitter power required given a certain set of remaining parameters, or an investigation into the effect of varying system characteristics (e.g., change in noise figure, etc.) can be performed.

Table 7-2 shows calculations used during the design of the data collection radar. These were used to predict system performance under a variety of conditions. Transmitter power, antenna gain, range, cross-section, receiver bandwidth, and miscellaneous losses were considered for their effect on system response as measured by the predicted S/N ratio. Equation 7-2 shows the radar range equation rewritten to solve for S/N.

$$S/N = 3.803 \times 10^{14} \left[\frac{P_t G^2 \sigma}{R^4 f^2 T B L} \right] \tag{7-2}$$

TABLE 7-2.- EFFECT OF RADAR PARAMETER VARIATIONS ON S/N PERFORMANCE

Radar parameter (units)	Radar factor values for various configurations				
	Initial system		Actual data collection radar (end of Phase-1 system)		
	Ideal	Ideal	Actual	Actual	Actual
Pt (KW)	.002 (2 W)	.002	.0002 (200 mW)	.0002	.0002
G (ratio)	50 (17 dB) W/G array	50	50	295 (24.7 dB) standard gain	295
σ (m^2)	10 (car)	1 (man)	10	1	10
R (10^3 ft)	.300 (300 ft)	.150 (150 ft)	.300	.150	.300
F (MHz)	24,000 (24 GHz)	24,000	24,000	24,000	24,000
T(°K)	1540 (8 dB NF)	1540	1540	1540	1540
B (kHz)	75,000 (75 MHz)	75,000	350,000 (350 MHz)	130,000 (130 MHz)	130,000
L (ratio)	1.25 (1 dB)	1.25	2 (3 dB)	1.25	1.25
S/N (ratio)	28 (14 dB)	45 (17 dB)	.4 (-4 dB)	91 (20 dB)	57 (18 dB)

NOTE: These are the specifications for the radar actually used during Phase 1 to collect radar data presented in later sections of this report.

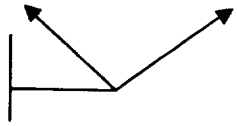

Reflected in table 7-2 is a chronological development of the Phase 1 data collection radar. Initial calculations showed that a S/N ratio of 14 dB should be obtained using 2 watts transmitter power, 17 dB (slotted waveguide) antenna, 10 m^2 target (average car) at 300 feet, 75 MHz receiver bandwidth, and approximately 9 dB overall system noise figure. A 1 m^2 (man) target at 150 feet should generate a S/N ratio of approximately 17 dB in this radar system.

These system design goals are not realistic, but within the time/budget constraints of the Phase I program, system adjustments and substitutions were required to obtain a usable system. Transmitter peak power of 200 mW as opposed to 2 W had to be used. The original antenna had a VSWR of approximately 2:1 to 4:1 depending on the port measured. The log-IF amplifiers were specified at 100-200 MHz bandwidth, but actually had in excess of 350 MHz bandwidth. Filters were constructed and added at the IF input and detected video output. Standard gain horns (24.7 dB nominal gain) were used as a functional replacement for the slotted waveguide array antenna. These changes resulted in a usable data collection radar system. The slotted waveguide array antenna was used during preliminary system testing, but could not provide sufficient gain for useful data collection. To alleviate this problem, standard gain horns were used during data collection. The standard gain horns do not provide a wide enough horizontal coverage area. In addition, their vertical beam width is too wide.

Receiver Dynamic Range

Required receiver dynamic range is determined by considering the various radar cross-sections to be tracked and the distance over which they must be tracked. Adverse propagation conditions will eventually need to be considered, but could be neglected during Phase I system design because Phase I testing did not include inclement weather testing and because it is felt that weather attenuation effects for K-band (24 GHz) radar used for distances out to 300-500 feet are not significant (see weather effects section). In addition, the angle channel required some additional dynamic range to be added to allow useful operation over the range of target cross-sections.

Tests were performed on a limited set of targets. Target RCS span of 1 to 100 m^2 was chosen for calculation purposes. The useful target ranges (minimum to maximum) were set at 50 to 300 feet, respectively. Approximately 15 dB were added for angle channel variation. The power received from a target varies as the quartic (4th power) of range. Receiver power varies linearly with RCS (refer to equation 7-1). An additional amount of receiver dynamic range is required to track targets through the angle channel lobes. The total receiver dynamic range is estimated by equation 7-3.

$$dBdyn = 10 \log \left(\frac{R^4 max}{R^4 min} \right) + 10 \log \left(\frac{\sigma max}{\sigma min} \right) + KdB \qquad (7\text{-}3)$$

where dBdyn = receiver dynamic range (dB)
Rmax = maximum target range (feet)
Rmin = minimum target range (feet)
σmax = largest target RCS (m^2)
σmin = smallest target RCS (m^2)
KdB = angle channel requirement (dB)

Results of equation 7-3 and values used to calculate it are shown in table 7-3.

TABLE 7-3.- RECEIVER DYNAMIC RANGE VALUES

Variable	Value	Contribution
Rmax	300 ft	31 dB
Rmin	50 ft	
σ max	100 m^2	20 dB
σ min	1 m^2	
KdB	14 dB	14 dB
Total dynamic range		65 dB

Receiver Noise Figure

Based on components appropriate for this application, a 9-10 dB worst case noise figure was expected. Exotic and costly receiver techniques such as cooled paramps are not cost effective nor reliable enough for this use. Standard waveguides, coaxial components, microwave mixers, and moderate cost IF amplifiers were employed. Figure 7-1 shows noise component distribution.

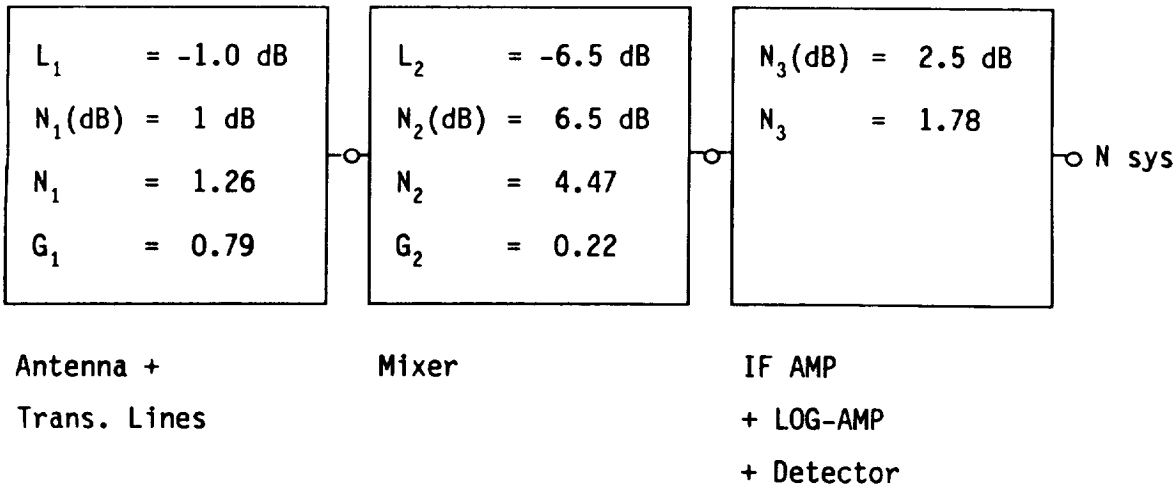

Figure 7-1.- Noise component distribution.

The equation for calculating cascaded system noise factor is

$$N\,sys = N_1 + \frac{N_2 - 1}{G_1} + \frac{N_3 - 1}{G_1 G_2} \qquad (7\text{-}4)$$

Using the estimated values given in figure 7-1, an overall noise figure of 10 dB was estimated.

IF/Video Bandwidths

The IF bandwidth requirement is set primarily by transmitted pulse width. IF bandwidth is found from[6]

$$Bopt = \frac{\alpha}{\tau} \qquad (7\text{-}5)$$

where Bopt = optimum receiver bandwidth

α = bandwidth constant (1.0 - 2.0)

τ = transmitted pulse width

For a 20 ns pulse and letting α be 1.2, a commonly used value, an optimum bandwidth (Bopt) of 60 MHz is found. This is optimum in that it should maximize the signal-to-noise ratio. It does not optimize suppression of pulse distortion nor does it allow for any IF center frequency drifting due to oscillator drift caused by thermal effects. A compromise IF bandwidth of 120 MHz (α = 2) was chosen for implementiation. The required video bandwidth is one-half of the IF bandwidth due to spectral folding arising from detection.

RF/IF System

A radar was assembled using the previously discussed system characteristics (fig. 7-2). The radar is a two-channel, phase monopulse system. The angle channel compromises antennas A and B which are vectorially differenced in a microwave hybrid. Its output is down-converted by a coaxial K-band mixer. This output is amplified by an IF preamplifier whose gain is 16 dB. A Chebyshev bandpass filter is used after the preamplifier (1) to set the noise bandwidth presented to the succeeding log-IF amplifier and (2) to eliminate out-of-band interference from external and internal sources (e.g., pulse modulator bleed-through and radars operating in adjacent frequency bands). The appendix of this section includes a report of the Chebyshev filters. After filtering, the return signal is applied to a log-IF amplifier. The output of the log-IF amplifier is a direct current (dc) pulse which is the logarithm of the input pulse envelope. This technique allows compressing an 80 dB, or

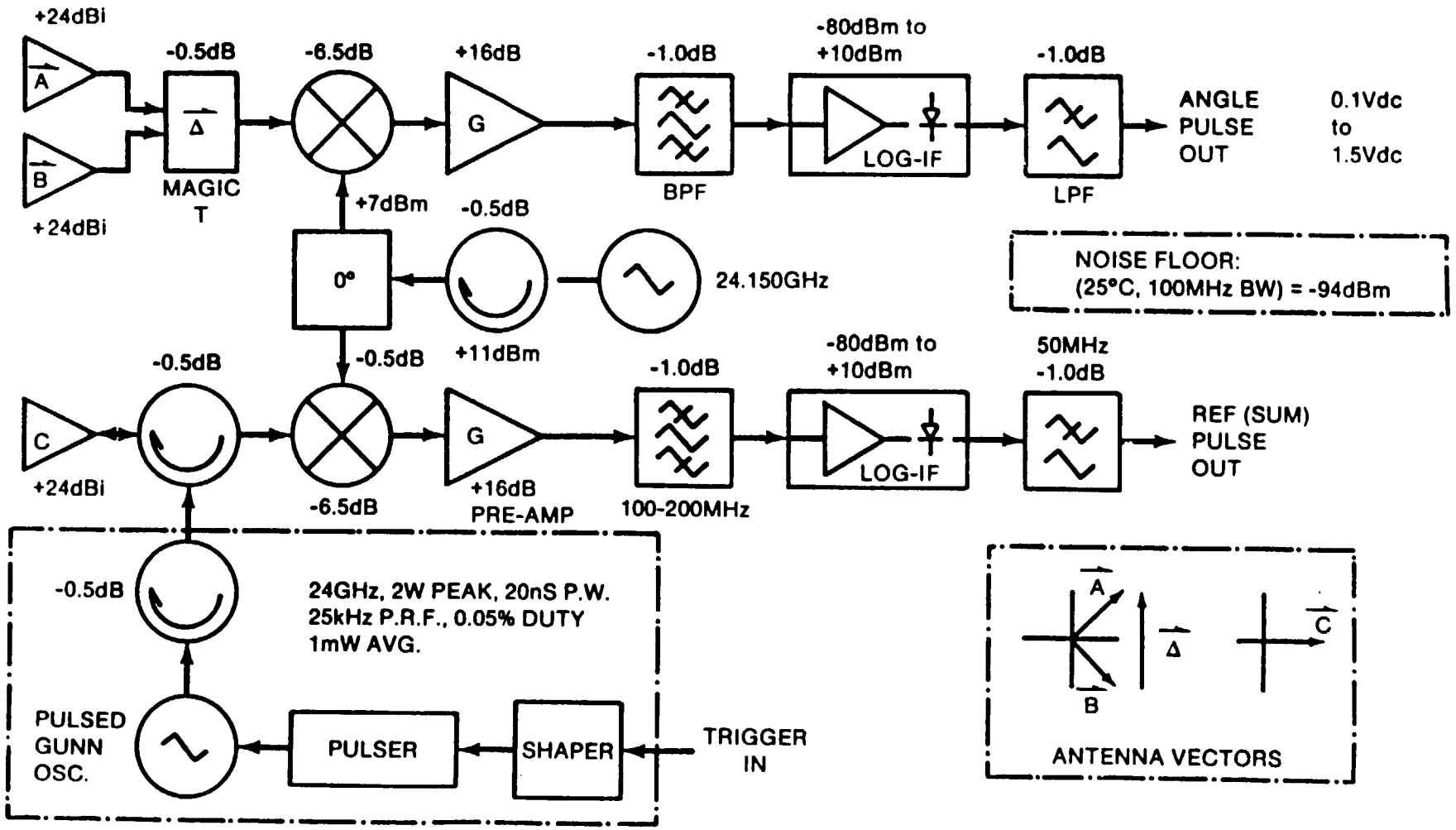

Figure 7-2.- RF/IF block diagram - test bed radar.

100 million-to-one power ratio, into a 0 to 1.5 V range. Logarithmic amplification and detection obviates the need for automatic gain control circuits. Pulse-to-pulse variations of 80 dB are instanteously accommodated. Finite fall-time of the detected pulse output is one limitation of this technique. A typical fall-time is approximately 3 pulse widths. However, strong pulses adjacent to each other can be detected sooner. Since detection is performed noncoherently, no phase balance between channels is required. Time delay variations versus input power appeared to be less than 1 ns for a 30 dB change in input power which is the maximum power difference expected between the two receiver channels.

Direct current coupled Chebyshev lowpass filters were used on the detected video output from the log-IF amplifiers. Table 7-4 shows the specifications for the lowpass filters used. Figures 7-3 and 7-4 show additional detail needed for completeness of system documentation.

TABLE 7-4.- CHEBYSCHEV LOWPASS FILTER SPECIFICATIONS

dc - 60 MHz (actual)

5-element, PI configuration

1 dB ripple (actual)

≥ 50 dB out-of-band rejection (through 1 GHz)

50 to 100 ohm characteristic impedence (actual)

SMA connectors

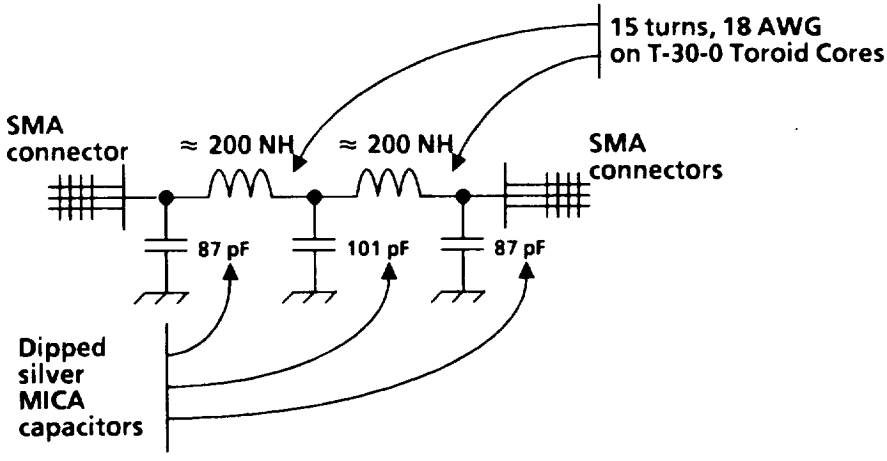

Figure 7-3.- Lowpass filter schematic/construction diagram.

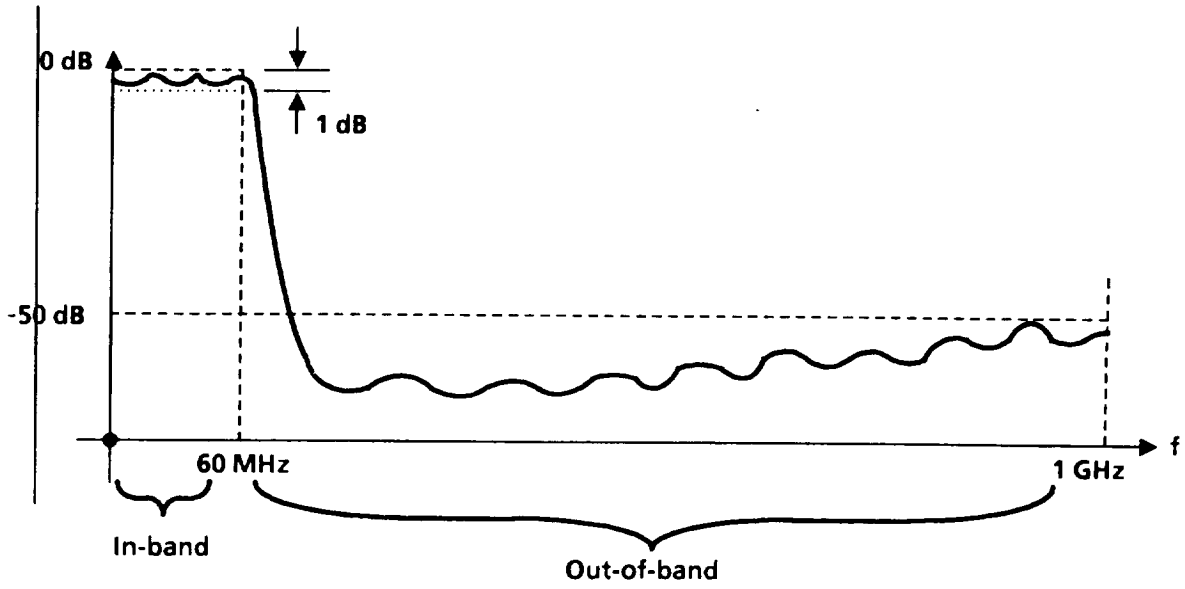

Figure 7-4.- Typical lowpass filter measured response.

Operation of the receiver reference channel parallels the previously described angle channel with the exception that only a single wide beam width antenna is used. Because of this no microwave hybrid is needed. However, the transmitter antenna is diplexed with the reference channel receiver antenna.

An on/off pulse transmitter is used. A trigger pulse is generated by the timing and sampler board. It is fed to a shaper circuit which buffers it for use with a high current pulser. The pulser generates an adjustable high current pulse which is the only power applied to the microwave Gunn diode. The current and duration of the dc pulse determines the RF pulse power and pulse width. The microwave generating components comprise an iris coupled waveguide cavity, a Gunn diode, and the dc pulse bias network. A low-power (10 mW) CW Gunn diode is used in a low-duty cycle (.001) pulsed mode. CW Gunn diodes can produce significantly more peak power when operated in this manner. Peak power of 200 mW was achieved in this application. Because of the low average power dissipated, virtually no heating of the cavity occurred. Peak power of 2 W was intended for this radar; however, the 2 W diodes were not used because they did not arrive until the end of Phase I. There is nothing exotic in the construction of the 2 W diodes although they are special order items (Microwave Associates - M/A COM, Burlington, Mass.). When produced in quantities similar to the lower power diodes they should cost approximately the same ($10 - $20 in quantities of 100 or more).

REFERENCES

1. Kustom Electronics, Inc., Lenexa, Kansas.

2. Decatur Electronics, Decatur, Illinois.

3. Federal Signal Corporation, Signal Division, University Park, Illinois.

4. M.P.H. Industries, Inc., Chanute, Kansas.

5. Tachibana, A., et al., "Stereo Radar System for Automobile Collision Avoidance," Nissan Motor Co., Ltd., Ninth International Technical Conference on Experimental Safety Vehicles, Kyoto, Japan, November 1-4. 1982.

6. Skolnick, M. I., Radar Handbook, McGraw-Hill Book Co., 1970.

APPENDIX

BANDPASS FILTERS DESIGN AND CONSTRUCTION REPORT

by

Christopher L. Lichtenberg

INTRODUCTION

This report describes the design, analysis, construction, and testing of bandpass filters presently used in the collision avoidance radar intermediate frequency circuitry. These filters are required to (1) reject out-of-band interference caused by other microwave sources adjacent to the radar frequency used in this radar, (2) suppress pulse modulation bleed-through which exists from dc to 100 MHz, and (3) to set the noise bandwidth presented to the logarithmic-IF (LOG-IF) amplifiers which amplify and detect the target return signals. These filters are installed between the pre-amplifiers and the LOG-IF amplifiers (fig. 1).

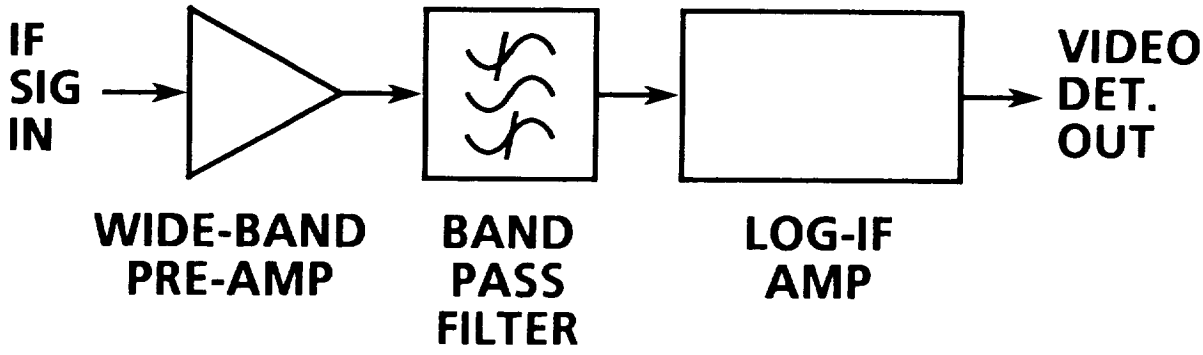

Figure 1.- IF component arrangement.

DESIGN SPECIFICATIONS

The required bandwidth is set by the pulse width (PW) of the transmitter. A pulse width of 20 ns is used. The best signal-to-noise ratio and least pulse distortion occur when the IF bandwidth is chosen between 1/PW and 2/PW. To achieve low pulse distortion and to allow for oscillator frequency drifting due to temperature changes, 2/PW was chosen as a filter design goal. Because of nonideal filter shape at band edges due to gradual roll-off, the effective detected noise bandwidth will be slightly higher (approximately 2 dB). The design goal for filter bandwidth was 100 MHz. A filter center frequency of 150 MHz is required by the LOG-IF used. The structure of the filter was chosen as 6-element PI configuration which represents a compromise between ideal filter response and a structure which is easy to build and align. A Chebyshev 0.1 dB ripple filter design was used. This filter design offers good out-of-band rejection, sharp roll-off, controllable in-band loss, and ease of alignment.

PROCEDURE

First, a Chebyshev lowpass prototype is chosen. Then a transformation is performed which (1) changes the structure from lowpass to bandpass, (2) sets the center frequency and ripple bandwidth, and (3) changes the impedance to 50 ohms. Finally, a filter schematic with component values can be constructed. The above steps are listed in the following section.

DESIGN TABLES

Bandpass Filter: 6-Element Chebyshev

1. Design Goals
   a. Center frequency = 150 MHz
   b. Ripple bandwidth = 100 MHz
   c. 6 elements = > 6-pole response
   d. In-band ripple = 0.1 dB
   e. Maximum insertion loss < 1 dB
   f. Out-of-band attenuation > 50 dB

2. Lowpass Prototype Structure
   a. 3 elements
   b. 0.1 dB ripple
   c. Pi-configuration
   d. Fc = 1 radian
   e. Zin = 1 ohm
   f. Clp = 1.0316 F
   g. Lls = 1.1474 H

3. Transformed Values

$L_2 = ((L_{LP})(Z))/(B)$ - - - - - - - - - - - - EQ. 1

$L_1 = ((B)(Z))/((w_0^2)(C_{LP}))$ - - - - - - - - - EQ. 2

$C_2 = (B)/((w_0^2)(C_{LP}))$ - - - - - - - - - - - EQ. 3

$C_1 = (C_{LP})/((B)(Z))$ - - - - - - - - - - - - EQ. 4

Where B = radian bandwidth of transformed filter

w_0 = transformed radian center frequency

Z = desired filter impedance

B = 6.2832×10^8 (100 MHz)

Z = 50 ohms

w_0 = 9.4248×10^8 (150 MHz)

w_0^2 = 8.8826×10^{17}

C_{LP} = 1.0316 Fd

L_{LS} = 1.1474 H

4. Calculated Values for Transformed Bandpass Filter

L_2 = 91.307 nH

L_1 = 34.285 nH

C_2 = 12.330 pF

C_1 = 32.837 pF

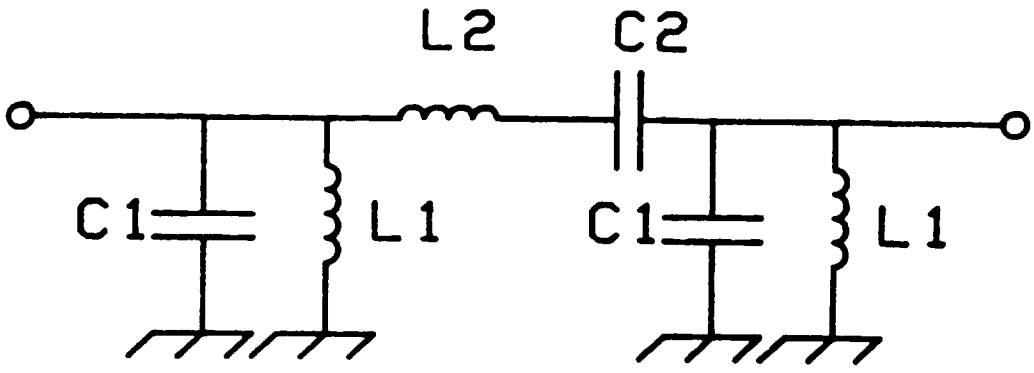

Figure 2.- Filter schematic.

IDEAL (CALCULATED) FILTER RESPONSE

After a candidate filter schematic is generated, it is good modern engineering practice to verify the design by computer analysis. To this end a computer file was written and results of its analysis were plotted. A sophisticated microwave and RF computer-aided design (CAD) program, SUPER COMPACT PC, was used for this analysis. Results verify that correct component values were calculated, and the frequency response plots act as a guide or baseline for comparison with actual measured response of the constructed filters. Results of this analysis show that this filter design meets all of the design goals. (Computer file and plots are included at the end of this section.)

SUPER COMPACT PC 10/23/85 10:07:28 File: BPASS3

```
*CHEBYSHEV BANDPASS FILT., 0.1DB RIP., 100MHZ RIP BW, Fc=150MHZ
* 6-ELEMENT, PI-CONFIGURATION, Z=50 OHM, DESIGNED FROM LOWPASS PROTOTYPE
 LAD
  CAP   1   0 C=32.837PF
  IND   1   0 L=34.285NH
  CAP   1   2 C=12.330PF
  IND   2   3 L=91.307NH
  IND   3   0 L=34.285NH
  CAP   3   0 C=32.837PF
  A: 2POR 1 3
 END
 FREQ
* USE FIRST FREQ'S FOR IN-BAND RESPONSE
   STEP       100MHZ 220MHZ 2MHZ
*  STEP       10MHZ 1000MHZ 10MHZ
 END
 OUT
  PRI A S
 END
```

Computer Analysis Program

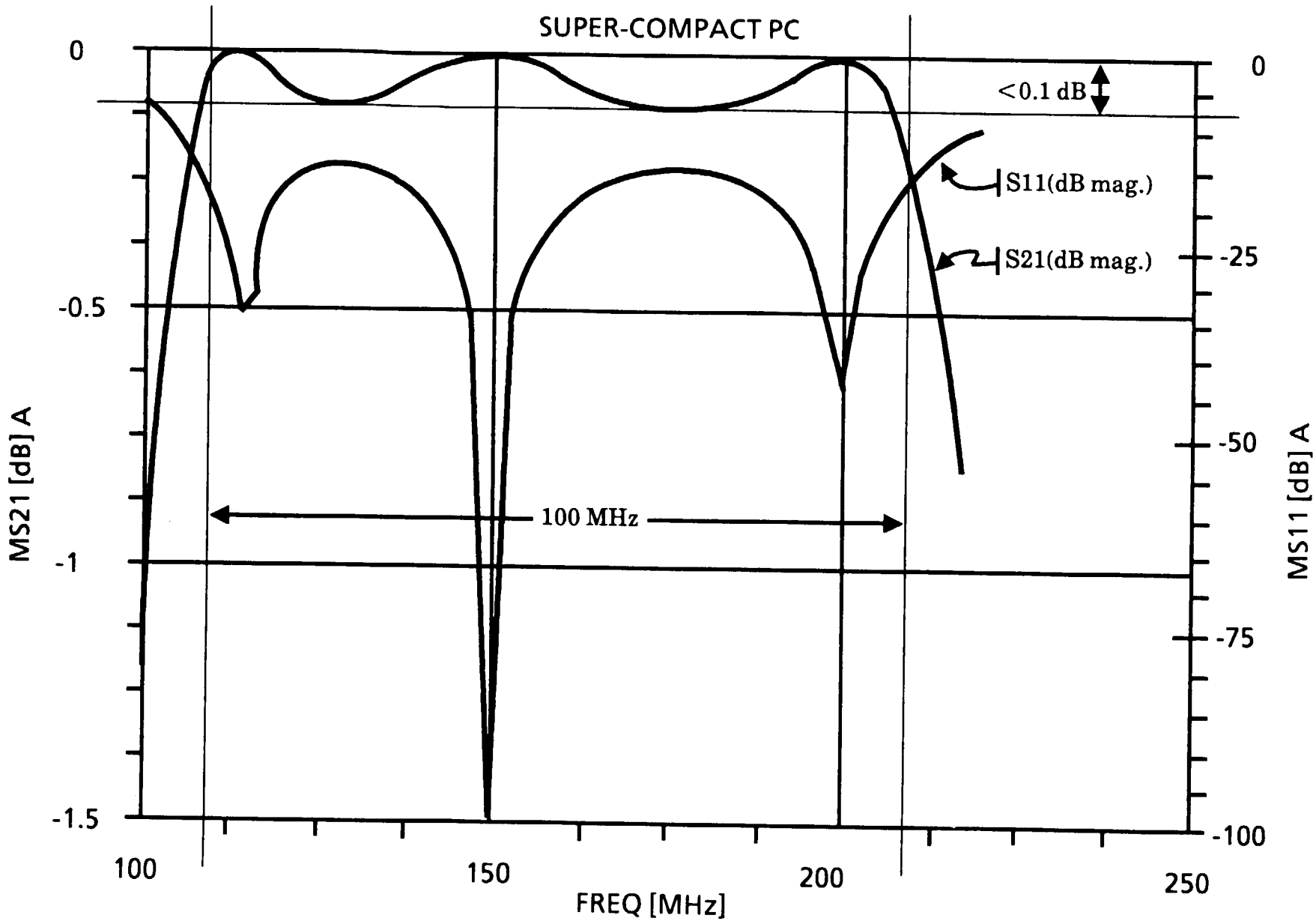
SUPER-COMPACT PC
0
-0.5
-1
-1.5
MS21 [dB] A
0
-25
-50
-75
-100
MS11 [dB] A
< 0.1 dB
S11(dB mag.)
S21(dB mag.)
100 MHz
100
150
200
250
FREQ [MHz]

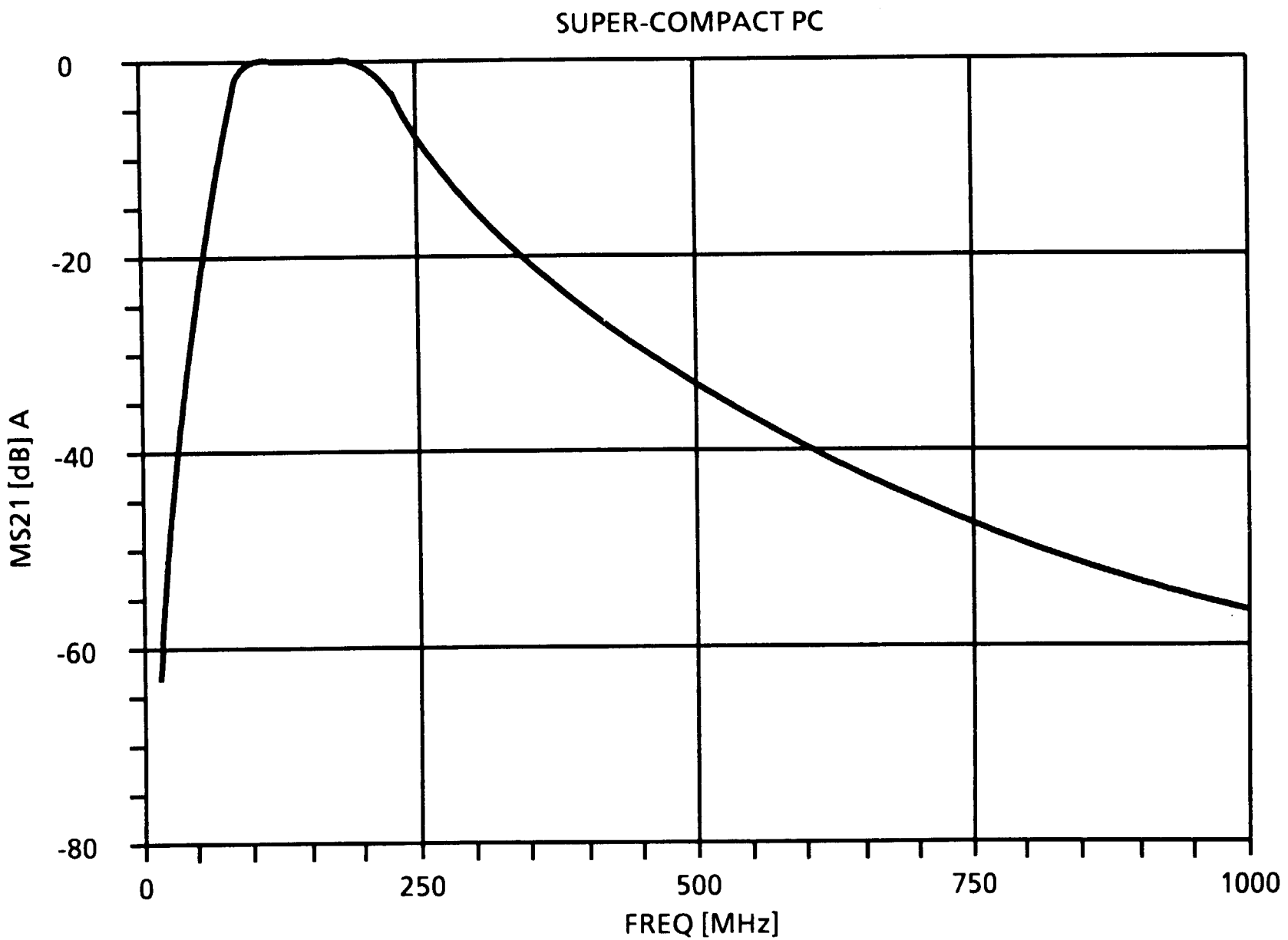
SUPER-COMPACT PC
0
-20
-40
-60
-80
MS21 [dB] A
0
250
500
750
1000
FREQ [MHz]

MEASURED RESPONSE

Two filters were constructed, tuned, then tested using a scalar network analyzer. Results of the measurements are plotted and shown at the end of this section. The maximum insertion (in-band) loss was less than 0.5 dB. The ripple bandwidths were on the order of 85 MHz while the 3 dB bandwidths were approximately 130 MHz. Thus, the design goal of 100 MHz is determined to be met adequately. A maximum ripple of approximately 0.3 dB is also allowable for this application. Out-of-band attenuation follows the theoretical values closely. The following plots show return loss (S11) and transmission loss (S21) versus frequency for each of the two filters.

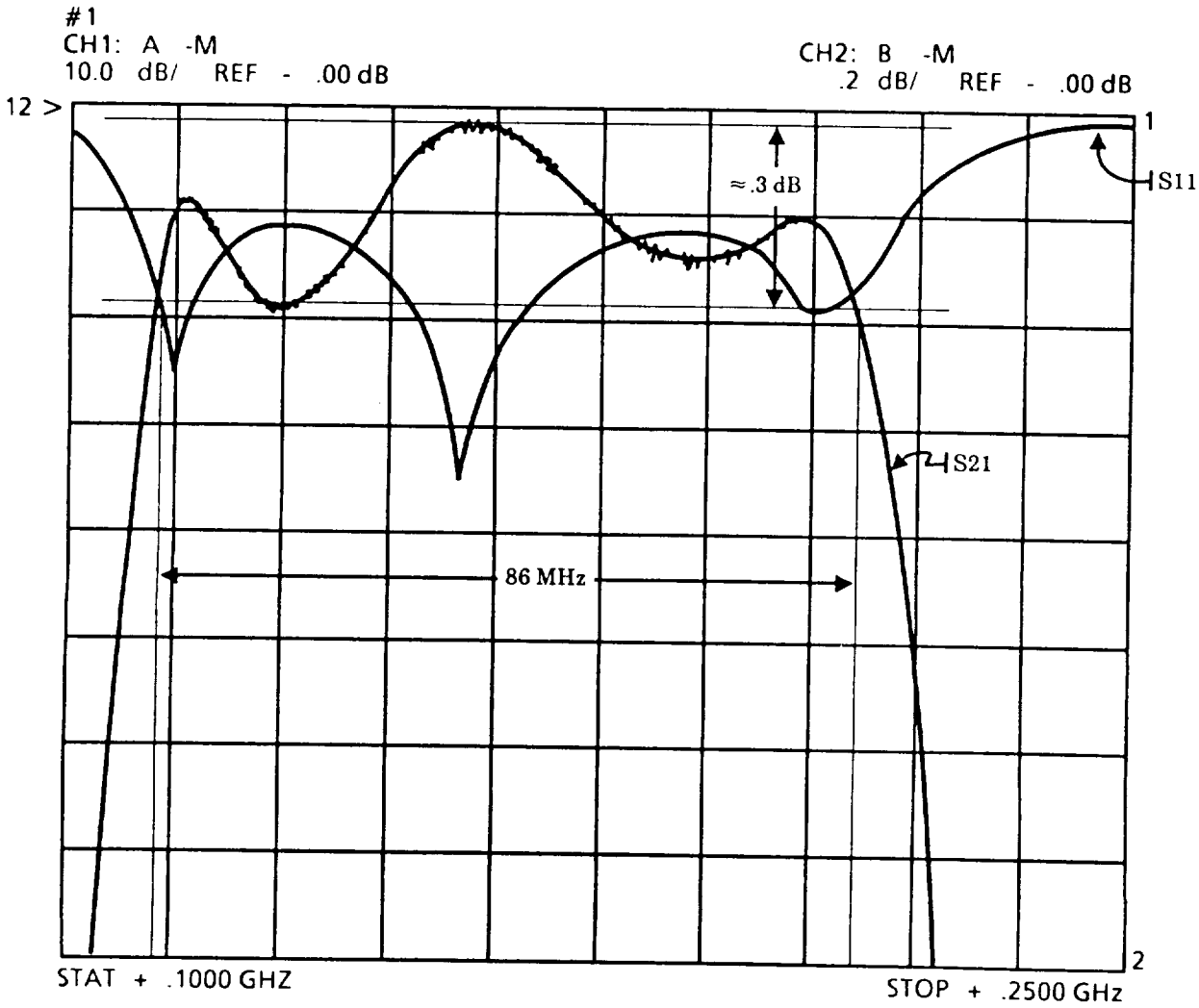

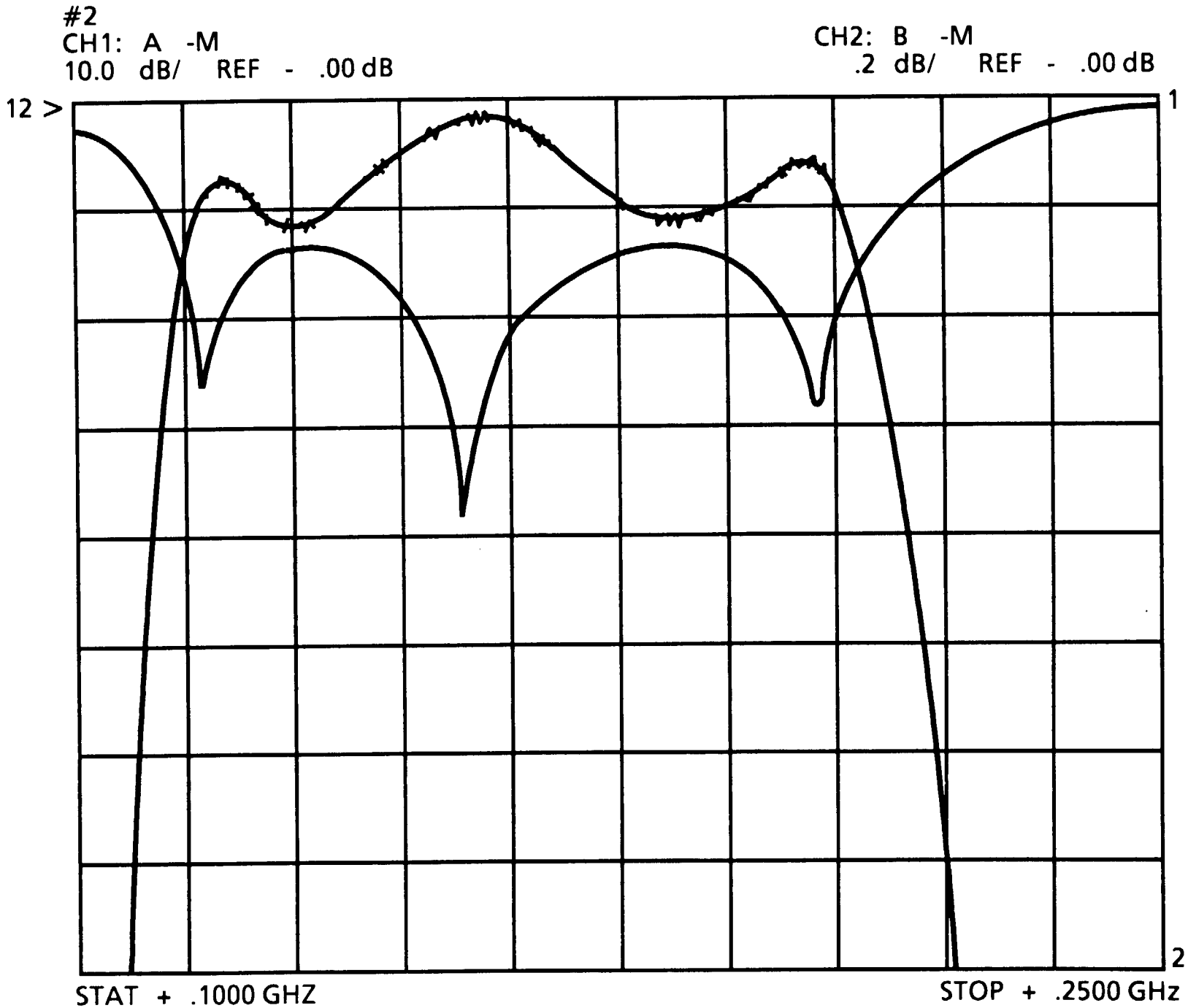
#2
CH1: A -M
10.0 dB/ REF - .00 dB
CH2: B -M
.2 dB/ REF - .00 dB
12 >
1
2
STAT + .1000 GHZ
STOP + .2500 GHz

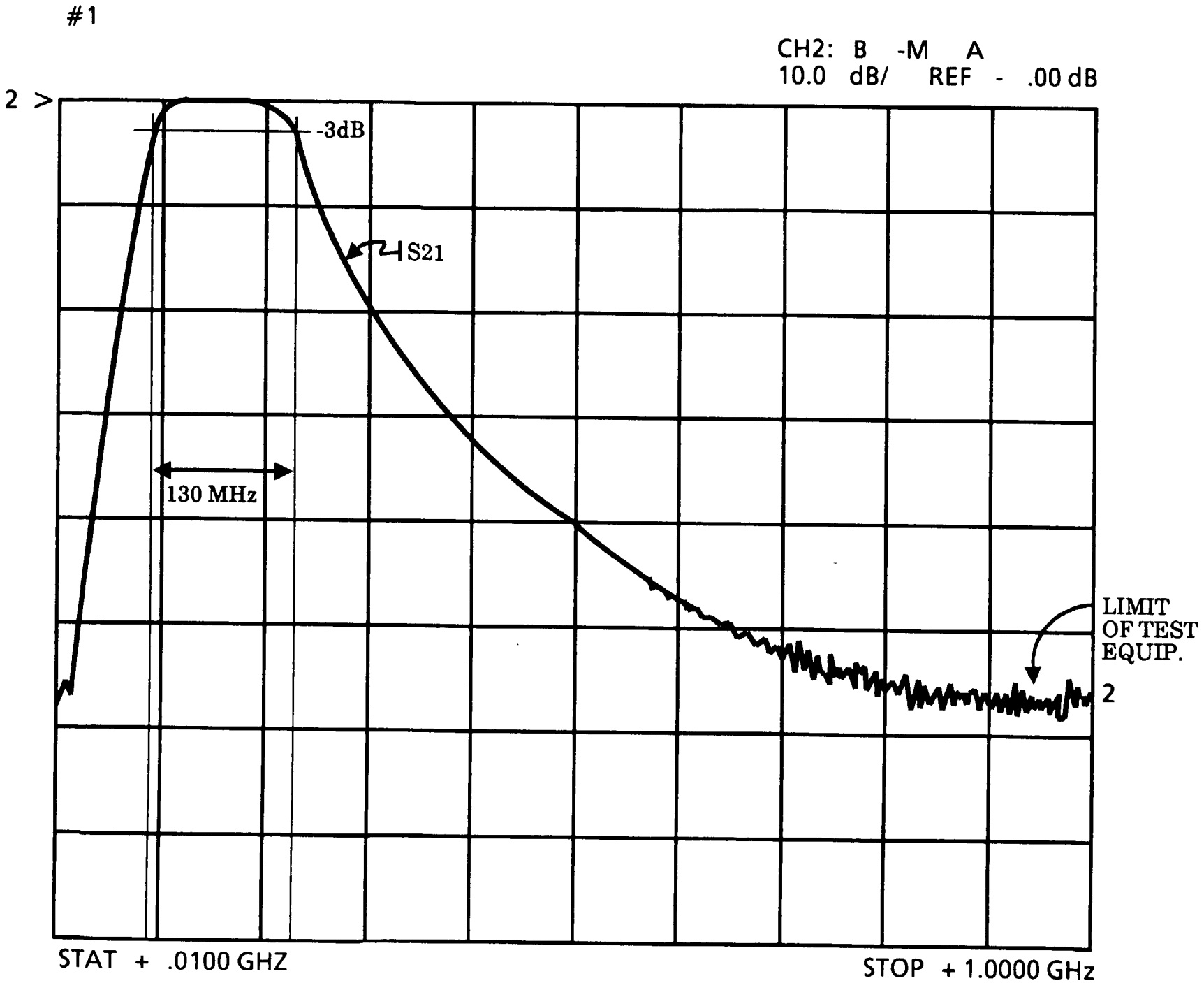
#1
CH2: B -M A
10.0 dB/ REF - .00 dB
2 >
-3dB
S21
130 MHz
LIMIT
OF TEST
EQUIP.
2
STAT + .0100 GHZ
STOP + 1.0000 GHz

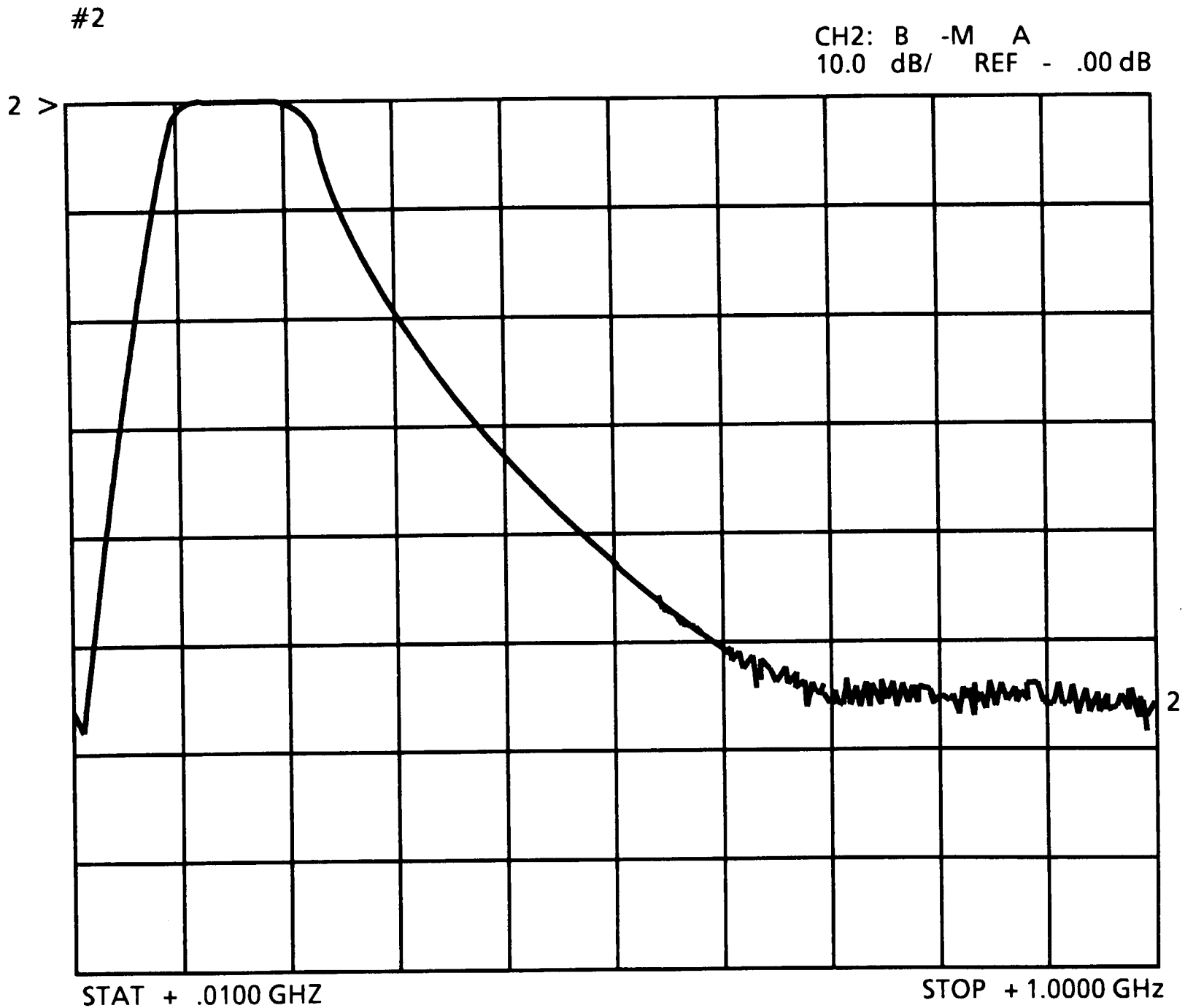
#2
CH2: B -M A
10.0 dB/ REF - .00 dB
2 >
2
STAT + .0100 GHZ
STOP + 1.0000 GHz

CONSTRUCTION

Standard, modern lumped element RF engineering techniques were used to realize these filters. C1 is two chip capacitors soldered in parallel. L1 is a hand-wound inductor of four turns of 18 A.W.G. magnet wire. The diameter is 0.15 inches and the length is 0.15 inches. L2 is also a hand-wound inductor of eight turns of 18 A.W.G. magnet wire measuring 0.25 inches by 0.15 inches diameter. C2 is a commercially available variable capacitor (3 pf to 23 pf). A figure is included at the end of this section showing additional construction details.

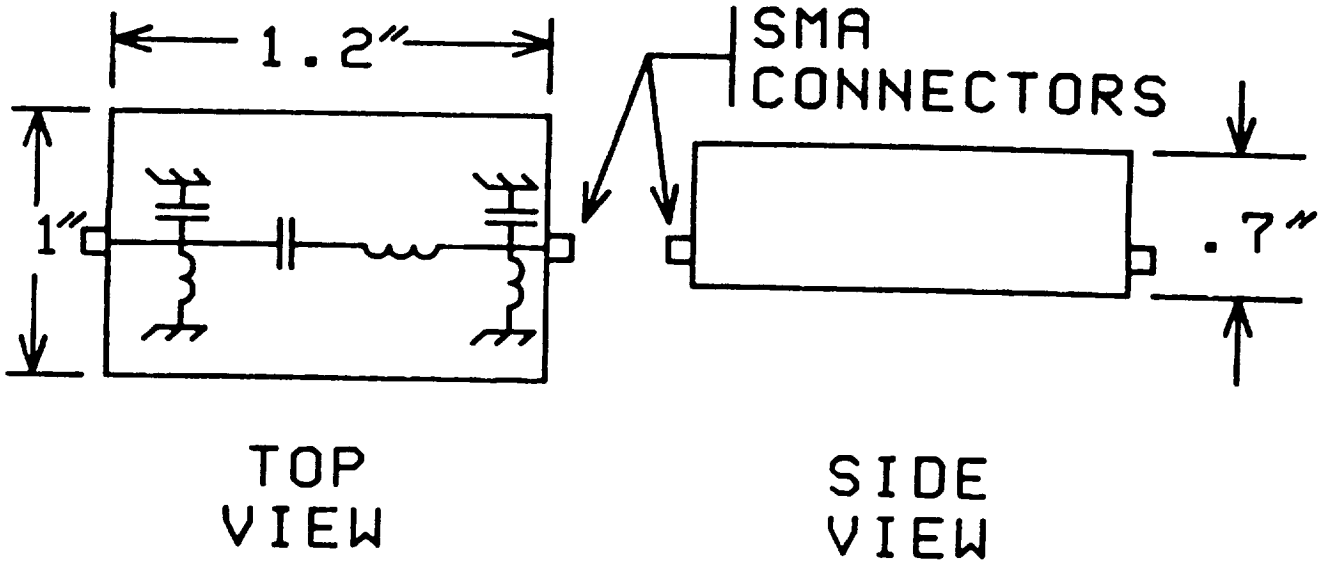

Figure 3.- Filter packaging details.

SECTION 8
PREDICTED RESPONSE FOR DATA COLLECTION RADAR

INTRODUCTION

This section presents the predicted IF response of the data collection radar. Details of the antenna placement, spacing, and relationships are discussed. Predicted patterns are given for the antennas used during Phase 1. The originally intended antenna array had a much wider azimuth beam width and lower gain. Standard gain horns were used as functional replacements because of their higher gain. The normalized angle channel response (fig. 8-10) is not now significantly different except the peaks are slightly closer spaced (compare with fig. 8-11) than the slotted waveguide array. Operation, function, and purpose for the important microwave and IF components are discussed.

RADAR CONFIGURATION AND RESPONSE

Block diagrams showing pertinent radar RF/IF component detail as well as antenna information are given below.

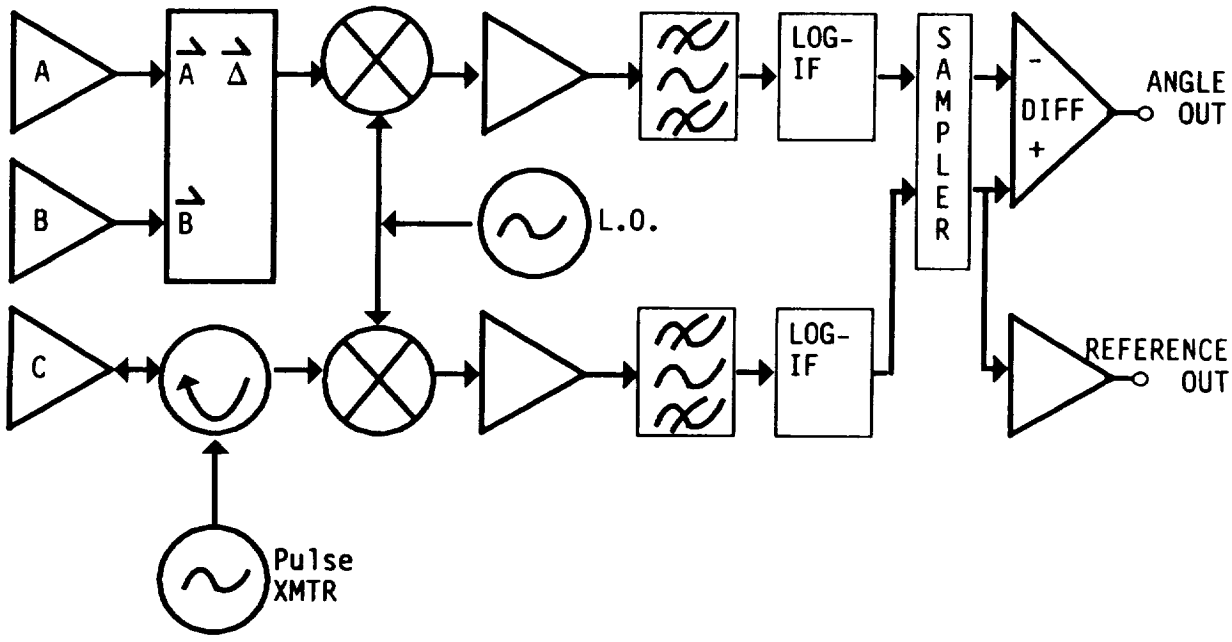

Figure 8-1.- Radar block diagram.

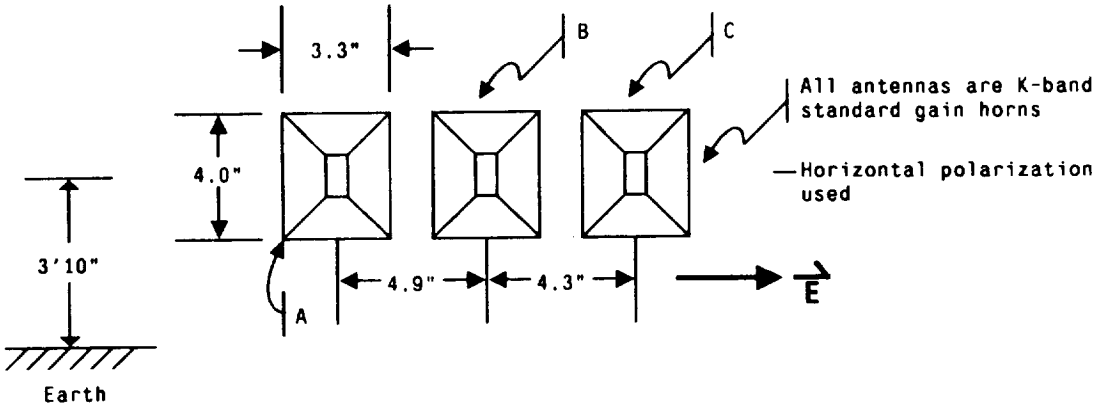

Figure 8-2.- Front view - looking into antennas.

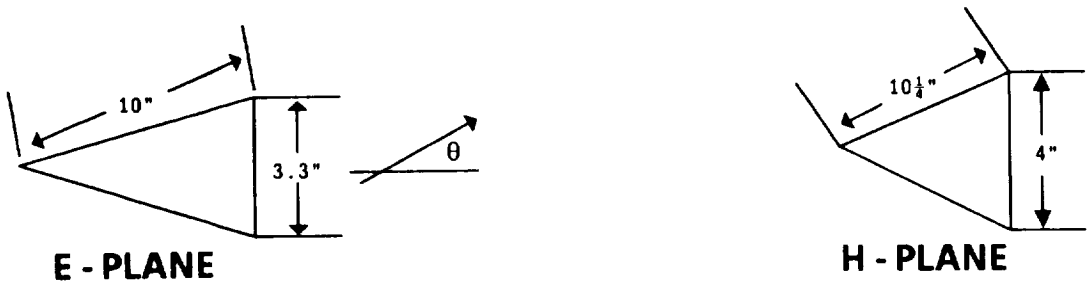

Figure 8-3.- Sectoral horn dimensions.

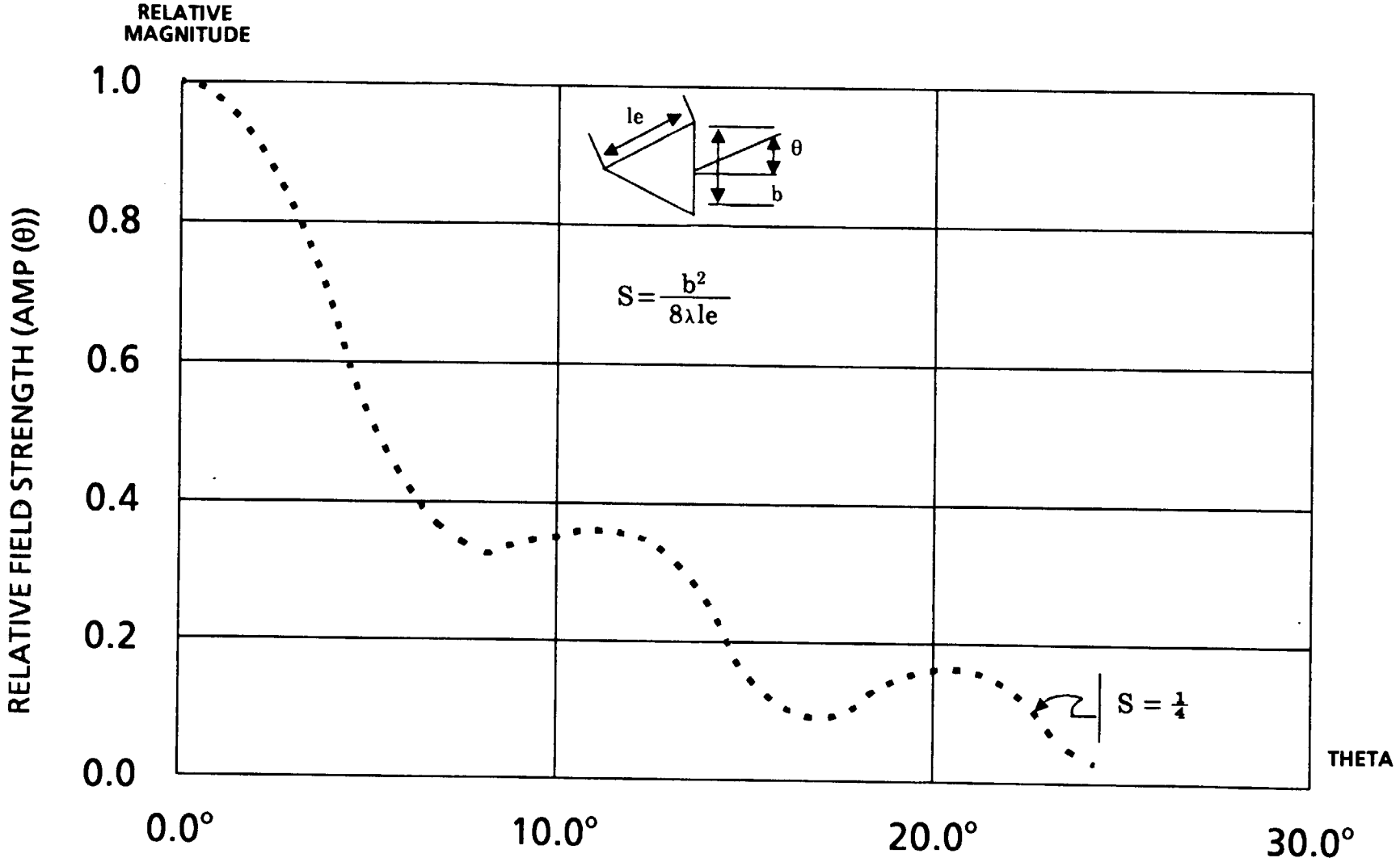

Figure 8-4.- Universal radiation pattern of horn flared in the E-plane (sectoral or pyramidal) (after Jasik, *Antenna Engineering Handbook*).

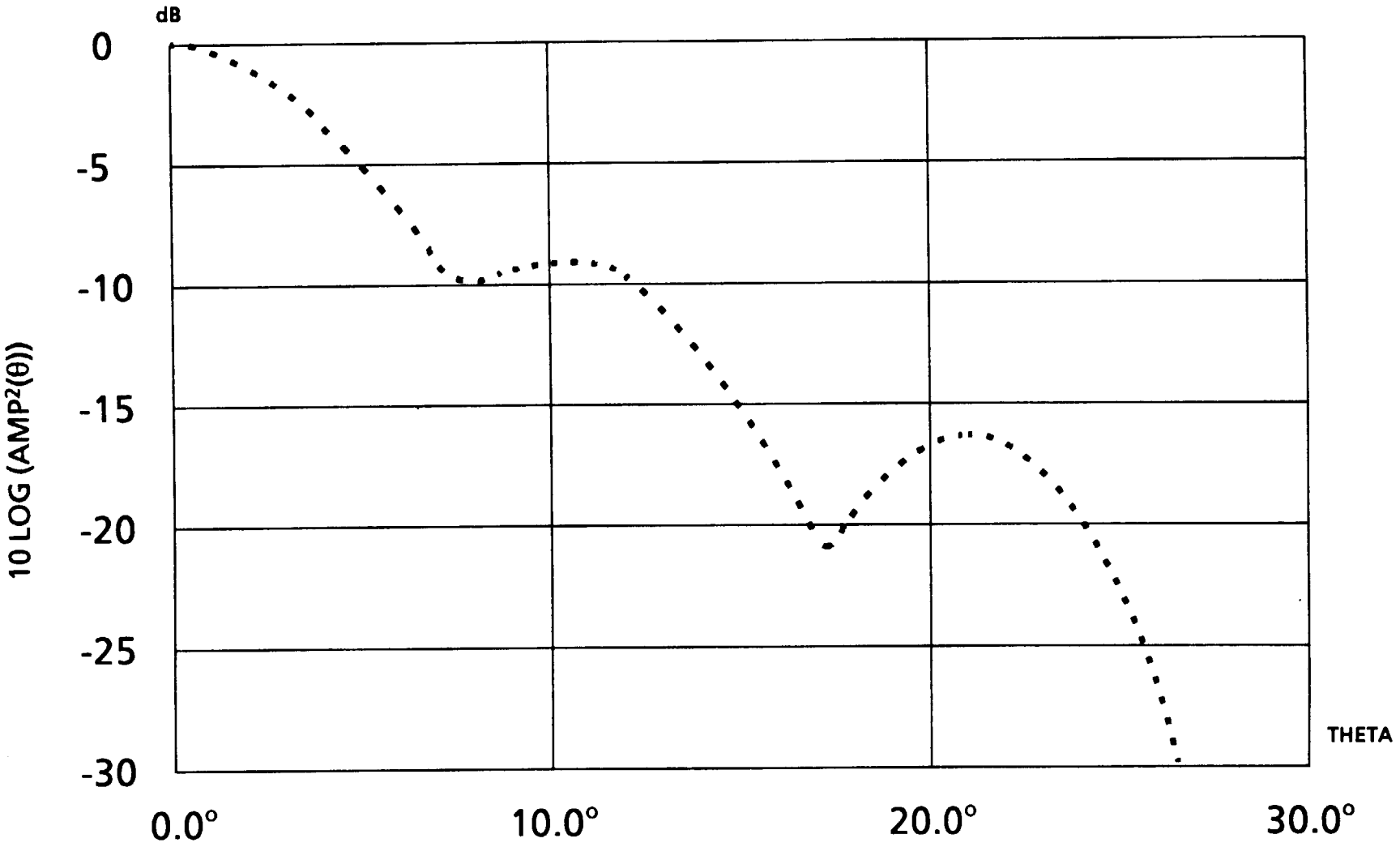

Figure 8-5.- E-plane power radiation (one-way) of horn.

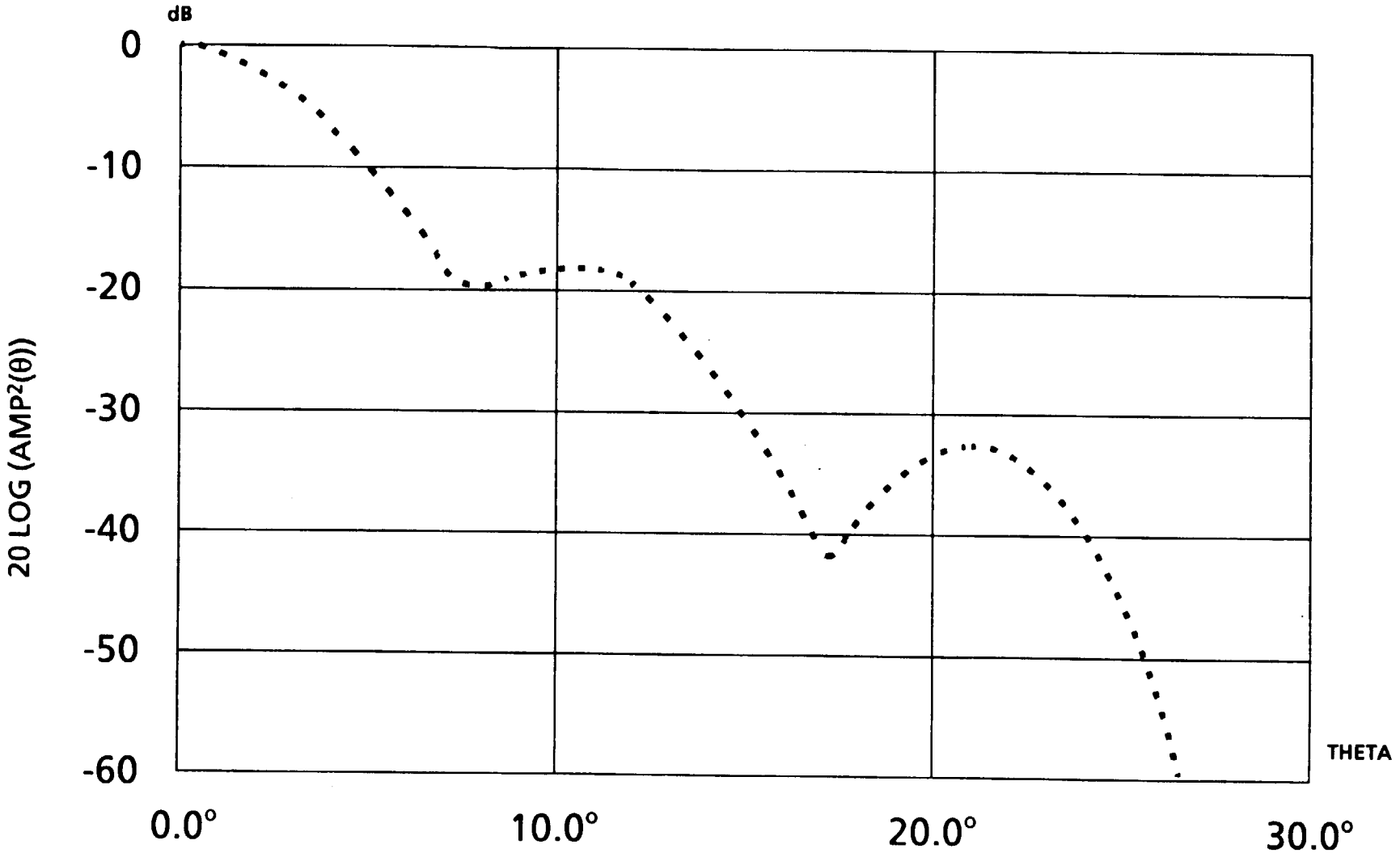

Figure 8-6.- Relative power [$Amp^2(\theta)$] vs. θ for reference channel.

Figure 8-5 shows predicted radiation from a standard gain horn (at 24 GHz) in the E-plane. One-way power is shown. The vertical beam width for these standard gain horns is approximately 8-10 degrees.

Figure 8-6 shows relative power versus angle for the reference channel. This curve includes two-way gain. Suppose a certain target gives a return of -40 dBm on boresight (zero degrees); from figure 8-6 it can be seen that approximately -58 dBm signal level will be received if the target moves to ± 10° from boresight. This curve can be used to visualize how the received signal level will fluctuate as a target of constant radar cross-section at a constant range changes angle with respect to the radar. The angle channel ($\vec{\Delta}$) response will now be derived. Angle antenna arrangement for an incoming plane is shown in figure 8-7.

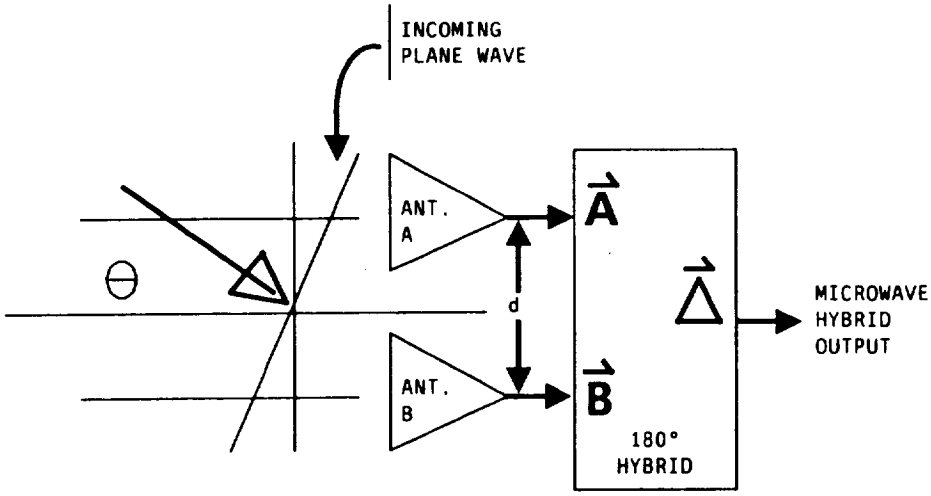

Figure 8-7.- Angle channel orientation (azimuth plane).

Since both antennas are co-aligned, their amplitude versus angle responses are the same. The signal amplitude reaching each antenna will be similar. However, a phase shift exists due to the slanted wavefront. In addition, the amplitude response will decrease as θ moves away from zero degrees. This pattern response was shown for a single antenna in figure 8-6. In the 180 degree microwave hybrid, vector signal differencing takes place.

The relative phase shift between antenna A and antenna B is given by

$$\Psi[\text{radians}] = \frac{2\pi d}{\lambda} \sin\theta \qquad (8\text{-}1)$$

where d = distance between antenna phase centers

λ = wavelength of radiation

θ = angle from boresight (zero degrees)

The output of the 180 degree microwave hybrid difference port is

$$\vec{\Delta} = \vec{A} - \vec{B} \tag{8-2}$$

where $\vec{A}$ = signal from antenna A

$\vec{B}$ = signal from antenna B

Noncoherent (envelope) detection is used in the angle channel. Therefore, the phase shift of $\vec{\Delta}$ is not important. Amplitide is the parameter of interest. This is given by the absolute value of $\vec{\Delta}$ which is

$$|\vec{\Delta}| = |\vec{A} - \vec{B}| \tag{8-3}$$

Antenna signals $\vec{A}$ and $\vec{B}$ are given in phasor notation by

$$\vec{A} = \mathrm{Amp}^2(\theta)\, e^{+j\Psi/2} \tag{8-4}$$

$$\vec{B} = \mathrm{Amp}^2(\theta)\, e^{-j\Psi/2} \tag{8-5}$$

where $\mathrm{Amp}^2(\theta)$ = two-way relative field strength pattern (fig. 8-6). Proceeding from equation 8-3 we find

$$|\vec{\Delta}| = \left| \mathrm{Amp}^2(\theta)\, e^{+j\Psi/2} - \mathrm{Amp}^2(\theta)\, e^{-j\Psi\ \mathrm{psi}/2} \right| \rightarrow \tag{8-6}$$

$$|\vec{\Delta}| = \mathrm{Amp}^2(\theta) \left| e^{+j\Psi\ \mathrm{psi}/2} - e^{-j\Psi/2} \right| \rightarrow \tag{8-7}$$

$$|\vec{\Delta}| = \mathrm{Amp}^2(\theta) \left| 2j \sin\left(\frac{\Psi}{2}\right) \right| \rightarrow \tag{8-8}$$

$$|\vec{\Delta}| = 2\,\mathrm{Amp}^2(\theta) \left| \sin\left(\frac{\Psi}{2}\right) \right| \tag{8-9}$$

The influence of the term $\left| \sin\left(\frac{\Psi}{2}\right) \right|$ is shown plotted in figure 8-8.

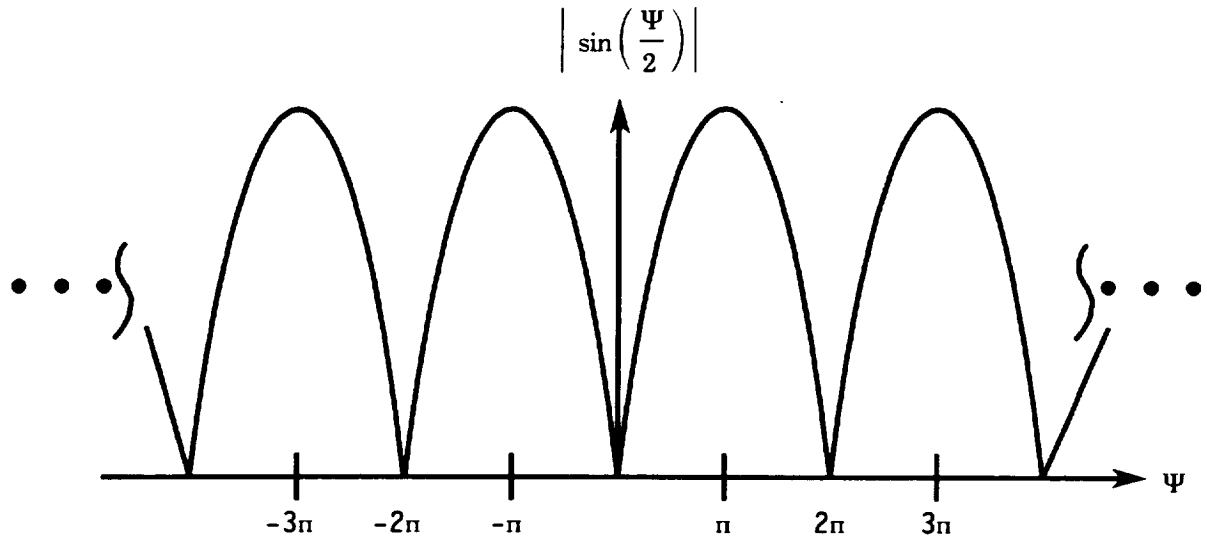

Figure 8-8. $\left|\sin\left(\frac{\Psi}{2}\right)\right|$ versus Ψ.

Substituting for Ψ_{psi} in equation 8-9 leads to

$$|\vec{\Delta}| = 2\,Amp^2(\theta)\left|\sin\left[\frac{\pi d}{\lambda}\sin(\theta)\right]\right| \qquad (8\text{-}10)$$

The graph of equation 8-10 in decibel power form is shown in figure 8-9. After passing through the receiver IF circuitry, both the reference channel and angle channel signals are logarithmically envelope detected. These logarithmic signals are processed in a difference (normalizing) amplifier which also compensates for any amplitude imbalances between the channels. This is required because (1) the angle channel peak signal will be 3 dB higher than the reference channel due to the two antenna array used in the angle channel and (2) the circulators, mixers, pre-amplifiers, filters, and sampler channels each have a fixed (unknown) amplitude imbalance between channels which can be nulled out by amplitude trimmers in a difference amplifier.

The output of the normalized angle channel, which can now be analog-to-digital converted, is given by

$$\text{Normalized angle channel voltage} = K \cdot \log\left(\frac{Ref}{Angle}\right) \qquad (8\text{-}11)$$

where K = gain constant (adjustable)

Ref = reference channel voltage

Angle = angle channel voltage

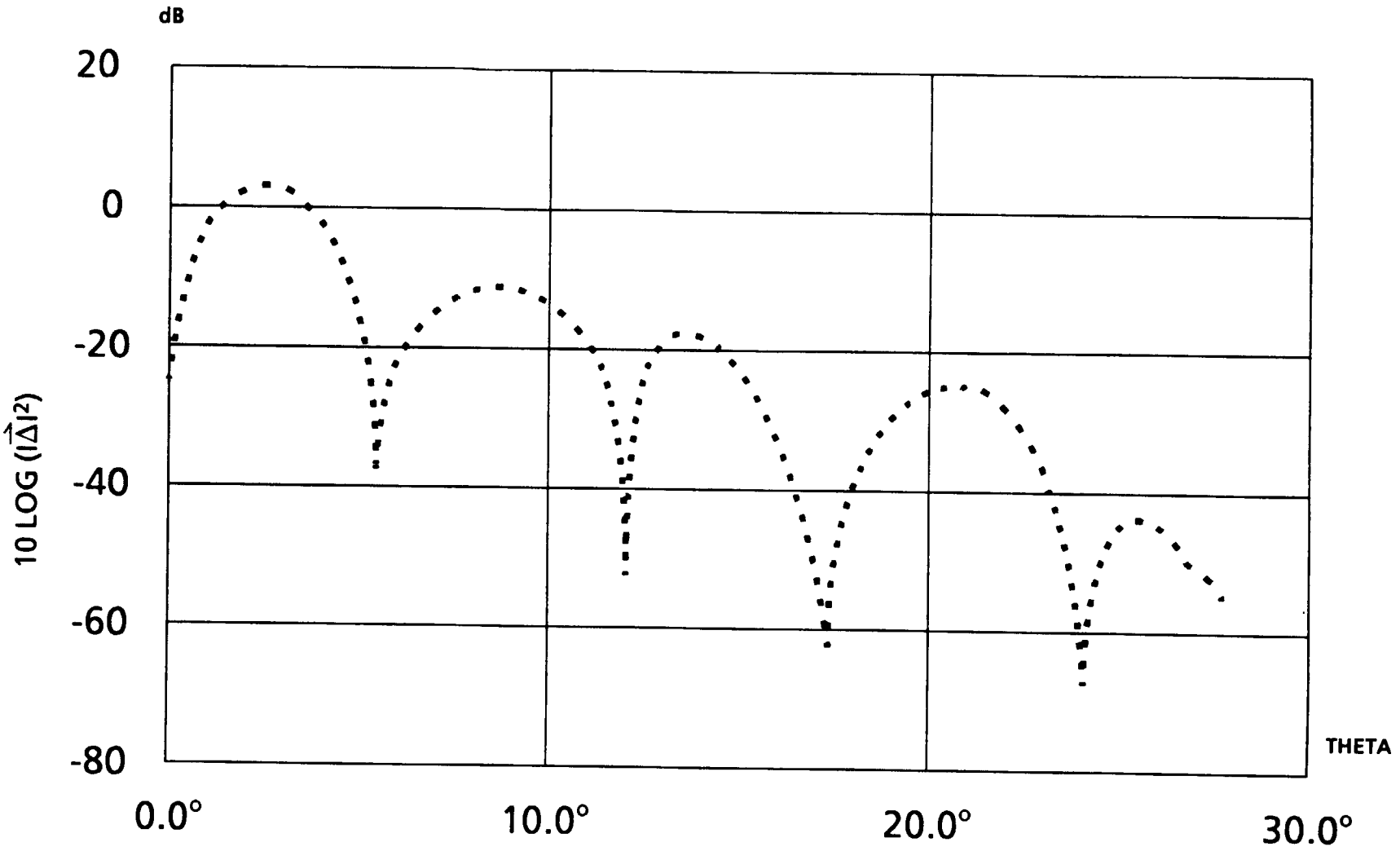

Figure 8-9.- Power amplitude output of difference channel.

The logarithmic detection transfer function is also reflected in equation 8-11. Amplitude trimmer adjustment is made so that both the reference and angle channel signal achieve the same peak values as θ is changed. Thus, the normalized angle voltage will dip to zero, but never below, since the reference channel signal is adjusted so that it is always greater than or equal to the peak angle channel voltage (equation 8-12).

$$\text{Reference channel signal} \geq \text{angle channel signal} \tag{8-12}$$

The purpose of the logarithmic amplifier/detectors, gain trimmers, and difference amplifier is to produce an angle channel voltage which is independent of the target's radar cross-section, the power transmitted, the range to the target, the amplitude pattern of the antennas used, and the wavelength of operation. This can be seen from the following. The total reference channel signal is given by

$$\text{Reference channel voltage} = K_2 \sqrt{Pr}\ \text{Amp}^2(\theta) \tag{8-13}$$

Where K_2 = adjustable gain constant (e.g., $K_2 = 2$)

$\sqrt{Pr}$ = voltage due to power received (found from radar range equation)

$\text{Amp}^2(\theta)$ = amplitude versus angle field strength pattern factor (two-way)

The total angle channel signal is

$$\text{Angle channel} = \sqrt{Pr}\, 2\, \text{Amp}^2(\theta) \left| \sin\left[\frac{\pi d}{\lambda} \sin(\theta)\right] \right| \tag{8-14}$$

Substituting into equation 8-11 yields

$$\text{Normalized angle voltage} = K \log \left\{ \left| \sin\left[\frac{\pi d}{\lambda} \sin(\theta)\right] \right|^{-1} \right\} \tag{8-15}$$

Equation 8-15 results are shown plotted in figure 8-10. Figure 8-11 shows the expected pattern for the original slotted waveguide array antenna which was not used for data collection. Achieving these response curves in practice requires an adequate signal-to-noise ratio existing in each channel, otherwise the amplitude will be limited and additional noise will be introduced.

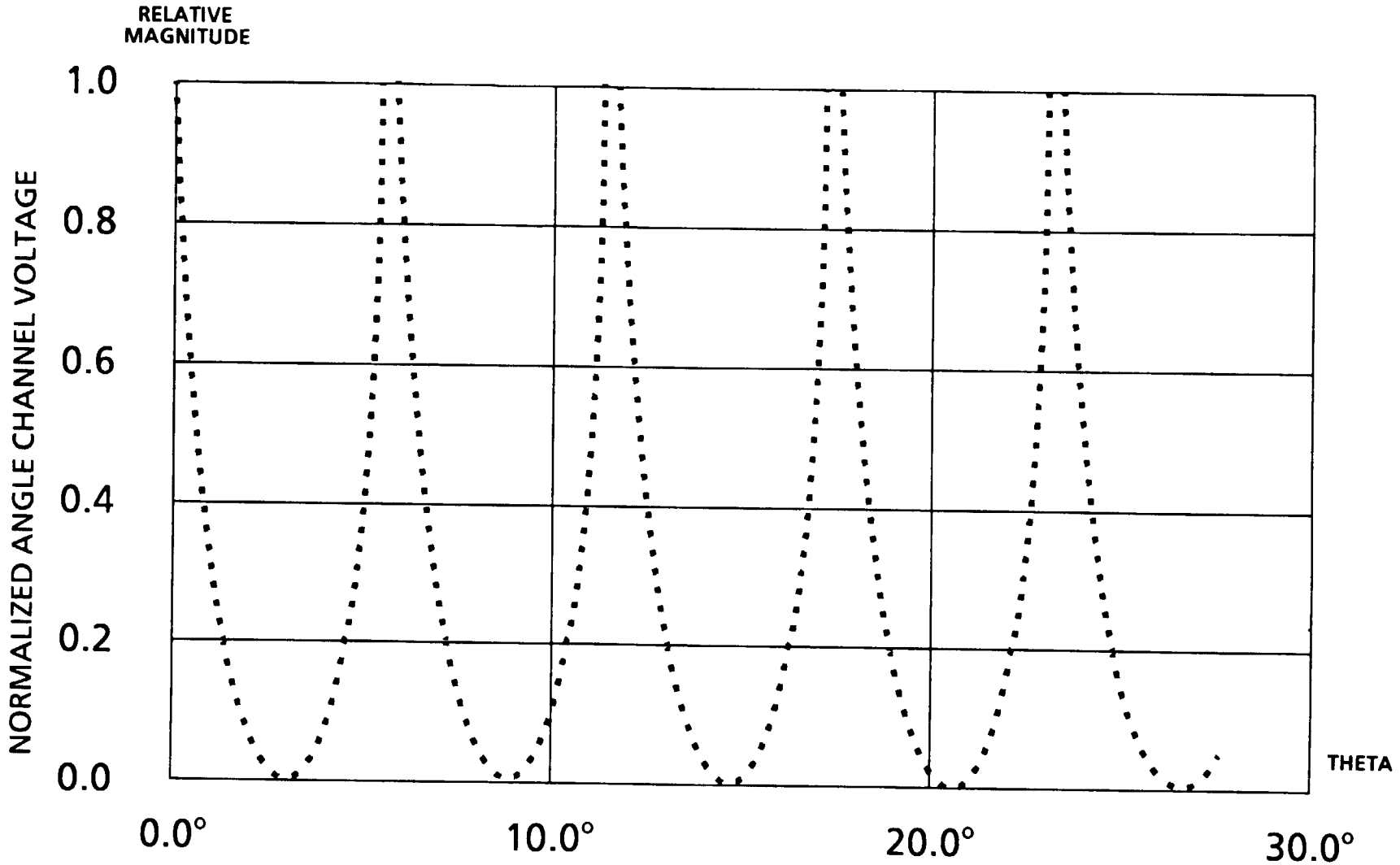

Figure 8-10.- Normalized angle channel response (standard gain antennas).

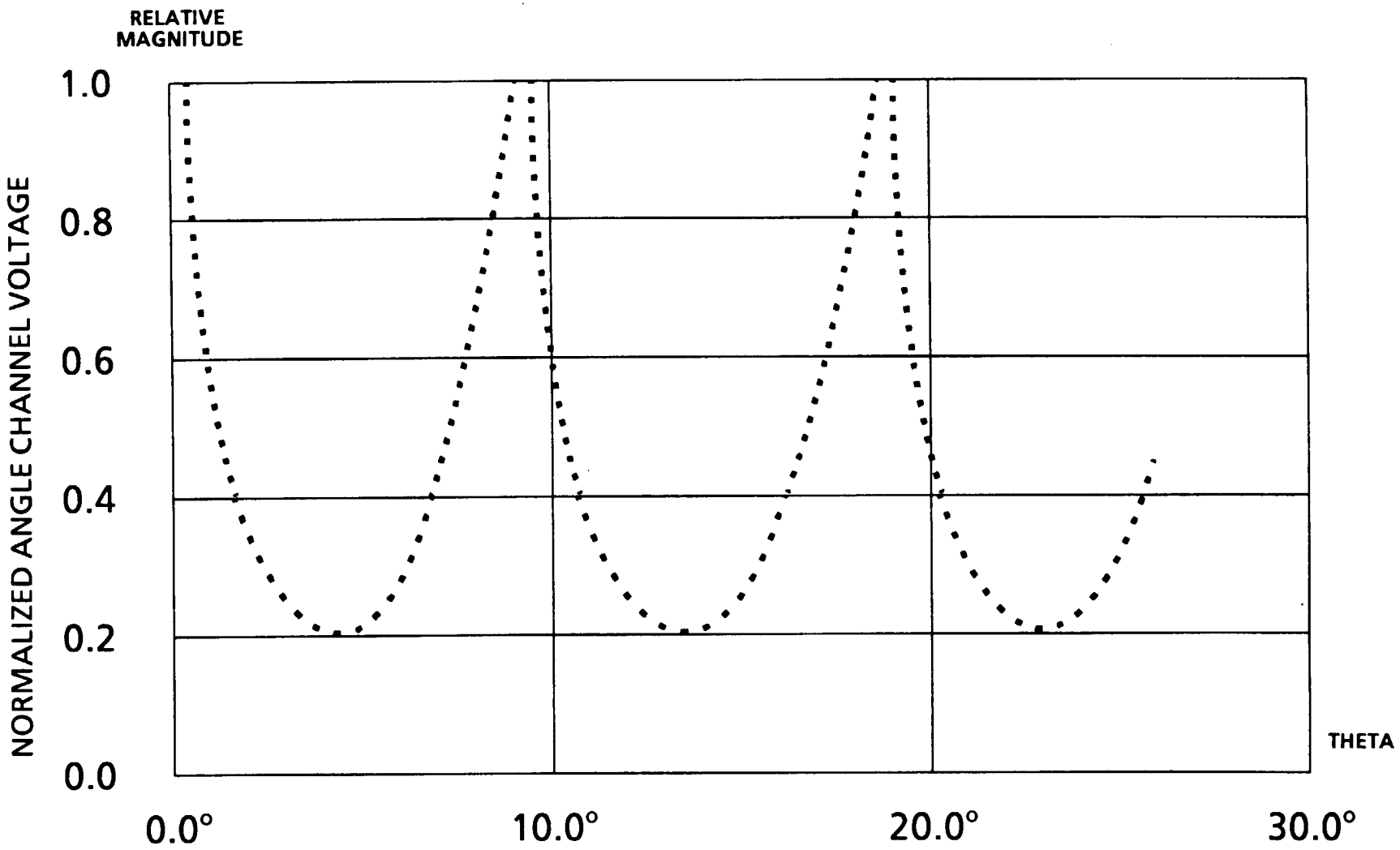

Figure 8-11.- Normalized angle channel response (original slotted waveguide antenna).

ANTENNA PLOTS GENERATING PROGRAM AND DATA

The data shown in figure 8-4 is a reconstructed plot of data points taken from a curve in the *Antenna Engineering Handbook* by Jasik. The data are given is table 8-1. Sixty-one points were used. Figure 8-5 is the same curve, only the Y-axis has been put into decibel power units [10 log (y^2)]. In addition, the X-axis was plotted in linear degree scale as opposed to the non-linear scale used by Jasik. The plot of figure 8-6 is the same as figure 8-5 except that to represent two-way power the verticle scale dB values were doubled. Equations 8-10 and 8-15 were solved using a computer program which is given in table 8-2. The computer program was used to generate the data files for the plots used in figures 8-4, 8-5, 8-6, 8-9, 8-10, and 8-11. In equation 8-15, d = 4.9 inches for the standard gain horn array whereas d = 3.0 inches for the slotted waveguide array. The value used for K was 1.0. Lambda (λ) was 0.49 inches.

TABLE 8-1.- DATA USED TO GENERATE PLOTS

X	Y	X	Y	X	Y
0.00	1.000	1.05	.330	2.10	.108
0.05	.996	1.10	.338	2.15	.120
0.10	.980	1.15	.340	2.20	.132
0.15	.960	1.20	.346	2.25	.144
0.20	.936	1.25	.348	2.30	.152
0.25	.908	1.30	.348	2.35	.156
0.30	.868	1.35	.346	2.40	.160
0.35	.820	1.40	.338	2.45	.160
0.40	.760	1.45	.328	2.50	.156
0.45	.710	1.50	.308	2.55	.146
0.50	.660	1.55	.280	2.60	.136
0.55	.610	1.60	.260	2.65	.124
0.60	.560	1.65	.230	2.70	.108
0.65	.500	1.70	.200	2.75	.092
0.70	.450	1.75	.176	2.80	.080
0.75	.416	1.80	.152	2.85	.066
0.80	.380	1.85	.128	2.90	.054
0.85	.356	1.90	.110	2.95	.040
0.90	.332	1.95	.098	3.00	.034
0.95	.326	2.00	.090		
1.00	.324	2.05	.096		

NOTES: (1) $X = \frac{b}{\lambda} \sin(\theta)$

(2) Y = Relative field strength

(3) b = 3.3

(4) λ = .49

TABLE 8-2.- COMPUTER PROGRAM #1 - DATA FILE GENERATION

```
5  REM REVISION 4-17-86 8:30
10 OPEN"I",20,"A:STDGAIN.DAT"
20 OPEN"O",1,"A:PLOT1.DAT"
30 OPEN"O",2,"A:PLOT2.DAT"
40 OPEN"O",3,"A:PLOT3.DAT"
50 OPEN"O",4,"A:PLOT4.DAT"
60 OPEN"O",5,"A:PLOT5.DAT"
70 OPEN"O",6,"A:PLOT6.DAT"
80 RTD=180/3.14159
90 LAMBDA=.49
100 B=3.3
110 K=1
120 INPUT#20,X,Y
130 REM SIN(THETA)=Z
140 Z=X*LAMBDA/B
150 THETAR=ATN(Z/SQR(1-Z*Z))
160 THETAD=THETAR*RTD
170 PRINT#1,THETAD,Y
180 AMPDB=10*LOG(Y*Y)/LOG(10)
190 PRINT#2,THETAD,AMPDB
200 AMPDB2=AMPDB+AMPDB
210 PRINT#3,THETAD,AMPDB2
220 D1=4.9
230 C1=3.14159*D1/LAMBDA
235 IF Z=0 THEN Z=.001
240 F1=ABS(SIN(C1*Z))
250 DIFF=2*Y*Y*F1
255 DIFFDB=10*LOG(DIFF*DIFF)/LOG(10)
260 PRINT#4,THETAD,DIFFDB
270 ANG1=K*LOG(1/F1)/LOG(10)
280 IF ANG1>1 THEN ANG1=1
290 PRINT#5,THETAD,ANG1
300 D2=3
310 C2=3.14159*D2/LAMBDA
315 IF Z=0 THEN Z=.001
320 F2=ABS(SIN(C2*Z))
330 ANG2=K*LOG(1/F2)/LOG(10)
340 IF ANG2>1 THEN ANG2=1
350 PRINT#6,THETAD,ANG2
355 IF X=3 THEN STOP
360 GOTO 120
```

SECTION 9
DATA ACQUISITION SYSTEM

INTRODUCTION

The ground rules used in developing the data acquisition system centered around the following:

1. Minimum development time by procuring off-the-shelf items as much as possible.

2. No real time data processing, i.e., radar data will be recorded to be reduced after the test.

The availability of compatible items dictated to a significant extent the capability of the system, e.g., the analog-to-digital (A/D) converter conversion delay and the time expander bandwidth.

HARDWARE DESCRIPTION

Figure 9-1 shows the block diagram of the data acquisition system used in the radar development program. Part a of the figure shows the portable portion of the system that was installed in the van carrying the radar. Part b shows

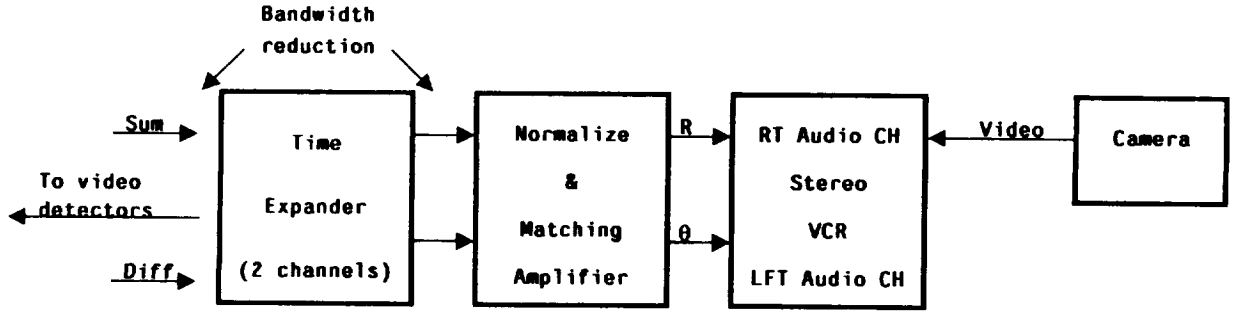

(a) Portable portion of system

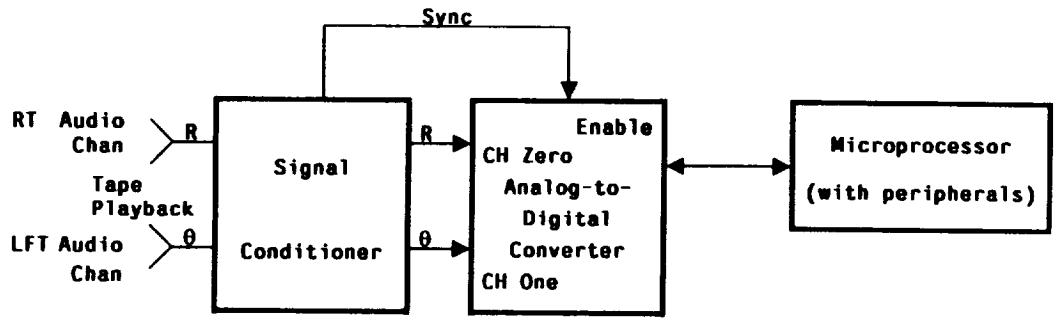

(b) Laboratory portion of system

Figure 9-1.- Data acquisition system.

the laboratory portion of the system that was utilized after the test to acquire the radar data from a tape.

The data flow starts with the signals carried in from the radar video detectors. The incoming two channels are the sum or range channel of the radar and the difference or angle channel of the radar. Each of these channels is input to a channel of the time expander subsystem where the system bandwidth is reduced to roughly 10 kHz. The integrity of these separate channels is maintained through the expansion process and then into the normalizing amplifier. This amplifier conditions the sum channel to be compatible with the audio input of the video cassette recorder (VCR) and outputs the sum channel to the VCR. From this point in the flow the sum channel is also called the range, R, channel since this is the channel used for threshold detection and time delay measurements. The difference channel input is processed through the normalizing amplifier by comparing and subtracting its value from the magnitude of the sum channel. This subtraction normalizes this channel to be independent of target size and target range so that the amplitude of the output is a function of target angle. Hence, after conditioning to be compatible with the VCR, the channel is the angle, θ, channel.

During testing the radar range and angle information are recorded on the two channels of the stereo audio system. Simultaneously the test scene is recorded on the video portions of the VCR tape. This video scene information is essential in documenting the radar data to the actual test.

After completion of tests the VCR is brought into the laboratory and played back into the signal conditioner in figure 9-1 (b). This conditioner converts the signal level to be compatible with the A/D converter 0 to 5 volt level. The signal conditioner unit also generates a trigger or sync that initiates the action of the A/D converter. This sync occurs every 88 ms.

The A/D converter is a multichannel system of which only the first two A/D channels are used. The converter is set to accept unipolar signals from 0 to 5 volts. The converter operates with 12 bits of precision and a conversion rate of 27 kHz. Output from the A/D is taken by the computer by a direct memory access (DMA) port.

The computer is a 16-bit IBM-PC-XT compatible co-processor and peripheral support. Data taken via this system are processed to an end product (e.g., plots) or written to disk file for accessing and processing later.

Table 9-1 shows values of some of the overall system parameters. As was stated, the time magnification factor is 4000, meaning that instead of a 2 ns delay to measure 1 foot of range, there is an 8 μs delay. For an environment with four or fewer targets, the system update rate is once every 88 ms (or 11.36 updates per second). For 5 to 20 targets this will increase to 176 ms. Final transmitted pulse width was 55 ns, increased from 20 ns. This was required due to sampler/digitizer deficiencies.

As is shown in table 9-1, a two-channel A/D converter is used to sample range and angle sequentially. There is a 37 μs interval between samples. The maximum range is 508.75 feet with a resolution of 9.25 feet. Angular resolution was measured to be something less than 0.25 degrees for a static point target with no multipath.

TABLE 9-1.- PERTINENT CAR SYSTEM PARAMETERS

Radar system (Used to collect experimental data only)

Time magnification:	4000
Effective date rate:	11.36 updates/second (≤ 4 targets)
Transmitter pulse width:	55 ns

Data acquisition system

A/D converter:	two channel - sampled sequentially
Channel information:	zero = range; one = angle
Conversion time/channel:	37 μs
Maximum range:	508.75 feet
Range resolution:	9.25 feet (1)
Angular resolution:	< 0.25 deg meas (2)

(1) 74 μs between samples divided by 8 μs/foot

(2) For a static point target with no multipath

Time Expander Board

The purpose of this board is to slow down or time magnify the radar echo signals so that they can be processed at a slower rate. This is done basically by saving single samples from consecutive, transmit/echo intervals, each sample delayed slightly in time from the previous sample, to build a slowed-down version of the transmit/echo interval. For the case of this radar, the time magnification was 4000.

Figure 9-2 is a block diagram of the sampling board. The heart of the subsystem is a circuit board from a Tektronix 1502 time domain reflectometer. However, because of difference and additional requirements, modifications had to be made.

The 250 kHz oscillator shown in the figure is the master timing clock of the radar. Its output, which is delayed to the modulator to allow time to start the sampling system, is the trigger to the radar for a transmission. It also triggers the fast ramp generator once for every transmit pulse.

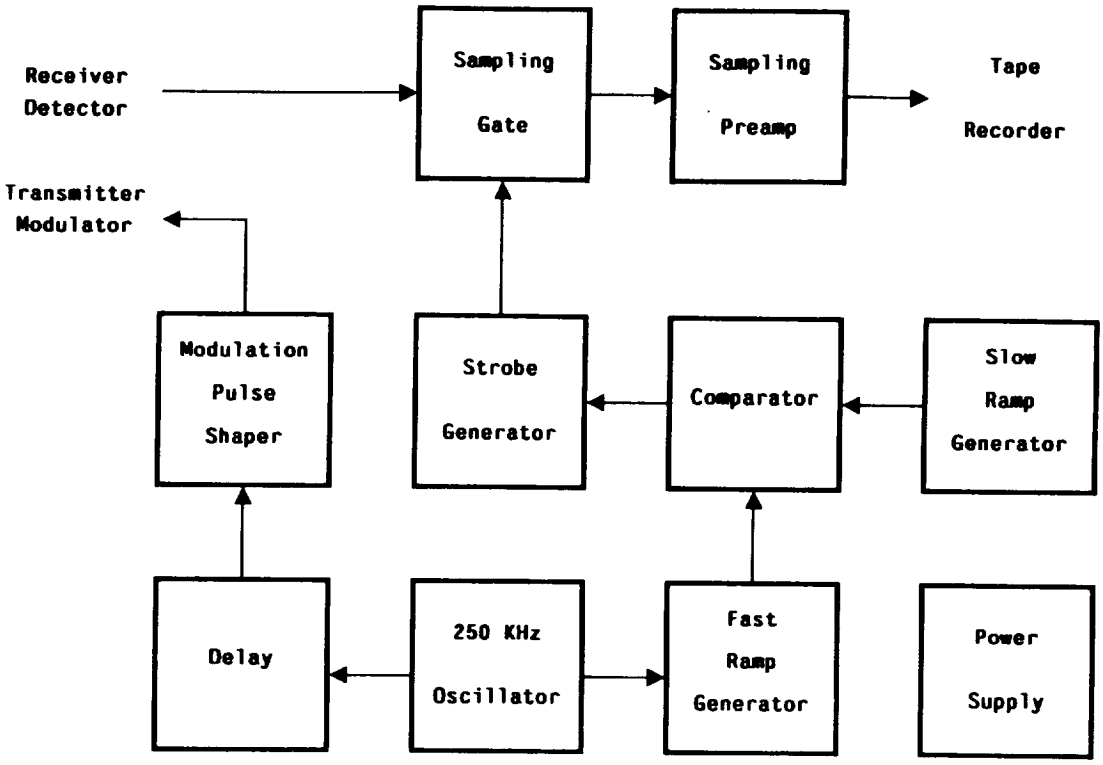

Figure 9-2.- Block diagram of time expander system.

The output of the fast ramp is compared to a ramp that is running much, much slower. When the two voltages are equal, the strobe generator is activated and it generates a pulse that is less than a ns in width. This pulse activates the sampling gate so that the voltage present from the receiver detector during this short pulse width is captured and held as an output until the next strobe generator output. This captured voltage is conditioned and sent to one of the channels of the VCR audio inputs. Though not shown on figure 9-2, there are two sampling gate channels: one for the radar reference channel and one for the radar difference channel.

The time delay between samples at the sampling gate output is the period of the 250 KHz oscillator plus a small fraction of time, t. Hence, in order to cover all of the radar transmit/echo interval, many, many transmit intervals must pass. A different way of saying this is that the sampling gate output will take a long time to show samples at the end of the transmit/echo interval. Or, time expansion has taken place.

The prices of time expansion, of course, are reduced throughput data rate, desired in this application, and loss of ability to correctly resolve velocities, a penalty in this case if pushed to an extreme.

Video Cassette Recorder

The VCR used in this project was the Panasonic PV-9000/PV-A860 portable stereo recorder. It was run as a portable unit as needed, but often was run with normal ac voltage as the prime power. Video was provided to the recorder by a JVC GX-N70U color video camera.

Modifications were made to the electronics in the audio channels of the VCR. These changes were made to disable the automatic gain control (AGC) circuitry to enable a linear transfer function for voltage through the system. This was necessary since angular position was to be determined from absolute voltage in the angle channel. The modifications installed were done such that they could be switched out and the VCR audio channels operated normally. Appendix A discusses the modifications made to the VCR.

A/D Converter Unit

The A/D converter used was a Data Translation DT 2801-A, 12-bit converter. The voltage levels were from 0 to 5 volts, positive. The conversion delay was set to the minimum of 37 μs which yields a throughput of roughly 27 kHz.

Two channels were active with the first channel sampling the sum or range channel and the second being the difference or angle channel. With each sample being separated by 37 μs, range is sampled every 74 μs, with angle being measured in the interval between range samples.

Computer

The computer required was an IBM PC or compatible. The computer dedicated in this application was the AT&T 6300 PC. The main reason for the AT&T over an IBM XT was speed. The AT&T benchmarked roughly twice as fast as the IBM for the software being run. This was an important factor in the number of targets that could be handled.

Peripheral and extra hardware in the computer included a color cathode ray tube (CRT), graphics board, math co-processor, printer, and plotter. The Data Translation DT-2801A A/D board plugged into a standard slot in the AT&T and was powered by the computer. A cable extended the A/D inputs out to a terminal board.

The computer operating system was MS DOS and the software package used in the program was an engineering package called ASYST. Included in ASYST are IO drivers to call and exercise the plotter and to initiate and handle the A/D converter. This hardware/software compatibility was intentional and shortened the overall development time.

SOFTWARE DESCRIPTION

The software of choice in the CAR was a scientific software package called ASYST distributed by Macmillan Software Company, New York, N.Y. This software set was chosen because of its capabilities in mathematics, ease of use

in graphics (e.g., plots) and, most importantly, its inclusion of subroutines to handle inputs through the A/D converter system up to its rated 27 kHz throughput. ASYST runs on an IBM PC or equivalent and requires a math co-processor and a graphics board. It was used in the CAR program in an AT&T 6300 PC.

The software areas involved with completion of the first phase of the CAR program are discussed in the remainder of this section. These areas include real time data acquisition software, target identification, and systems calibration and tests.

A/D Sample Rate Tests

In testing the A/D converter to prove the 27 kHz throughput capability, a program called CSPEC.CAR was developed. This program takes in a time sample of the signal present on channel zero of the converter and, using the math capabilities of the ASYST software, converts this voltage versus time history into the frequency spectrum of this input signal. The listing of the ASYST program to do this is shown in table 9-2.

ASYST uses word definitions, or macros, to denote functional lines of code. A defined word extends from: "word name" to a semicolon. In the code of table 9-2, the defined words are INFREQ, DMAP, and FPLOT. To get the signal spectrum, INFREQ and FPLOT need to be run and, as is noted in the last two lines, function keys F9 and F8 are programmed to execute these words.

Assuming that some time-varying voltage is being applied to channel zero of the A/D converter, pressing function F9 will initiate execution of INFREQ. This macro orders the A/D converter to take in 512 samples of channel zero, one sample every 37 μs and store them in the array INSPEC. INSPEC is then scaled from 0 to 10 volts, the magnitude of the fast fourier transform (FFT) calculated over the INSPEC array and this result stored in the array FARRAY. The dc term in the FARRAY is then set to zero.

If function key F8 is then depressed, the macro FPLOT will execute. This plots the FFT of the input as stored in FARRAY as a function of the array FRAX. FRAX contains numbers, in ascending order, that scales the abscissa to frequency. Thus, with FRAX plotted as the independent variable and FARRAY as the dependent variable, the spectral content of the input is plotted with appropriate labels.

Figure 9-3 is an example of this program. It shows the spectral content of a 6 kHz sine wave amplitude modulated by a 1 kHz sinewave. The plus and minus sidebands located 1 kHz from the 6 kHz carrier are as expected. Figure 9-4 shows the same 6 kHz carrier, but modulated this time by a 1 kHz square wave. More spectral components are present and some spectral folding can be surmized. These frequencies were used only to test capability of the A/D converter.

It should be noted, that even though the plot axes are scaled to 20 kHz by the plot routine, data points are plotted only to 13.5 kHz. This is the Nyquist rate for the A/D converter throughput rate of 27 kHz.

TABLE 9-2.- PROGRAM LISTING OF CSPEC.CAR PROGRAM TO DEMONSTRATE A/D CONVERTER THROUGHPUT RATE

```
DIM[ 512 ] DMA.ARRAY INSPEC
REAL DIM[ 256 ] ARRAY FRAX
REAL DIM[ 512 ] ARRAY FARRAY
FRAX []RAMP
FRAX 13.5 * 256. /
FRAX :=
0 0 A/D.TEMPLATE ONE.ONLY
0 A/D.GAIN
.037 CONVERSION.DELAY
EXT.TRIG
A/D.INIT
: INFREQ
0 INSPEC :=
INSPEC DMA.TEMPLATE.BUFFER
A/D.INIT
ONE.ONLY A/D.IN>ARRAY(DMA)
INSPEC
0 10 A/D.SCALE
FFT ZMAG
FARRAY :=
FARRAY
0. SWAP
[ 1 ] :=
;
: DMAP
INSPEC
0 10 A/D.SCALE
Y.AUTO.PLOT
;
: DPLOT
FARRAY
SUB[ 2 , 256 , 1 ]
Y.AUTO.PLOT
;
: FPLOT
FRAX
FARRAY
SUB[ 1 , 256 , 1 ]
XY.AUTO.PLOT
NORMAL.COORDS
.017 .090 CHAR.SIZE
.4 .075 POSITION
" FREQUENCY (KHz) " LABEL
.4 .975 POSITION
" IBM/DT SPECTRUM ANALYZER " LABEL
270 LABEL.DIR
.035 .7 POSITION
" MAGNITUDE " LABEL
;
F9 FUNCTION.KEY.DOES INFREQ
F8 FUNCTION.KEY.DOES FPLOT


ASYST Version 1.5
Page 1    c:cspec.car    03/13/86
```

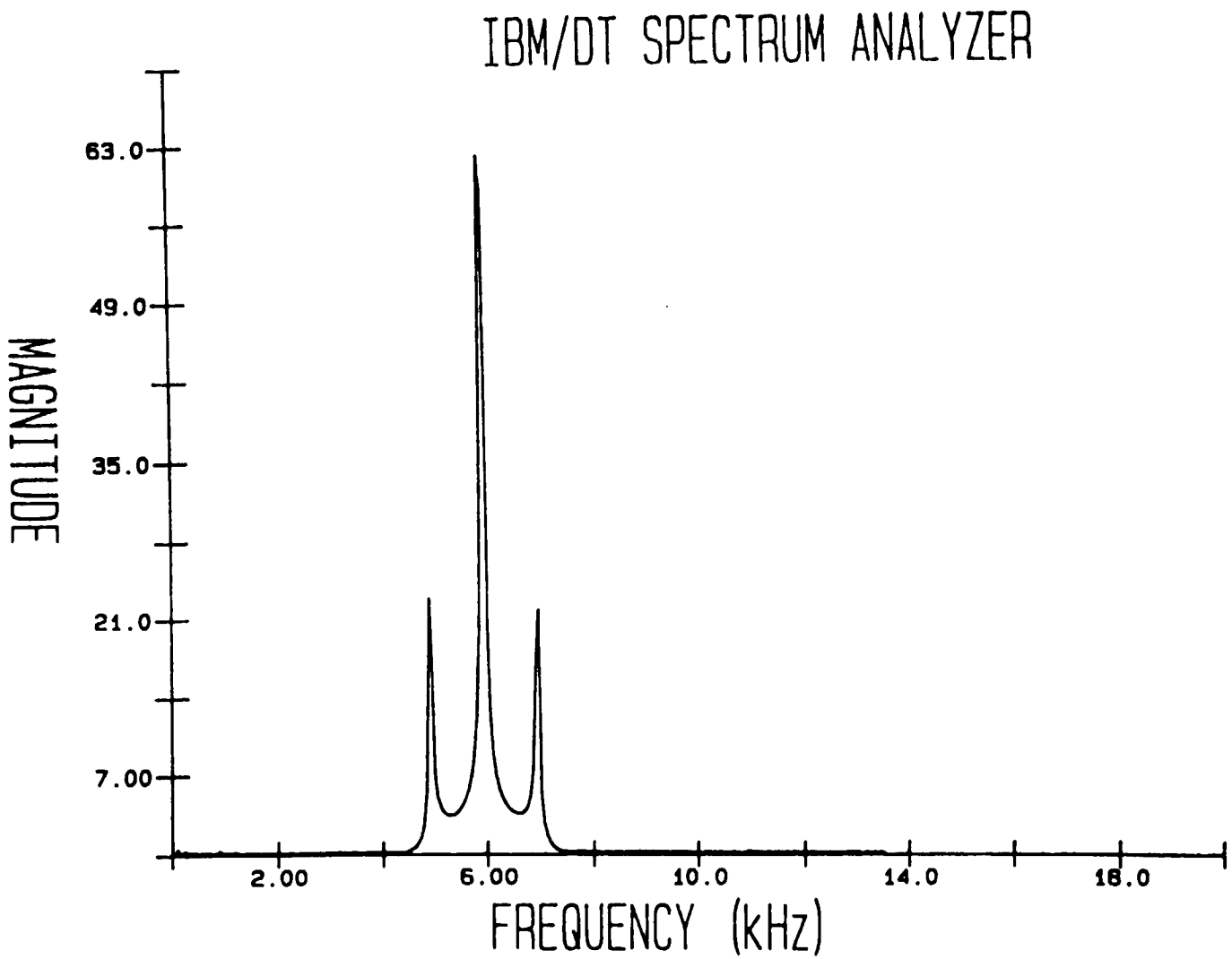

Figure 9-3.- Example plot from CSPEC.CAR program.

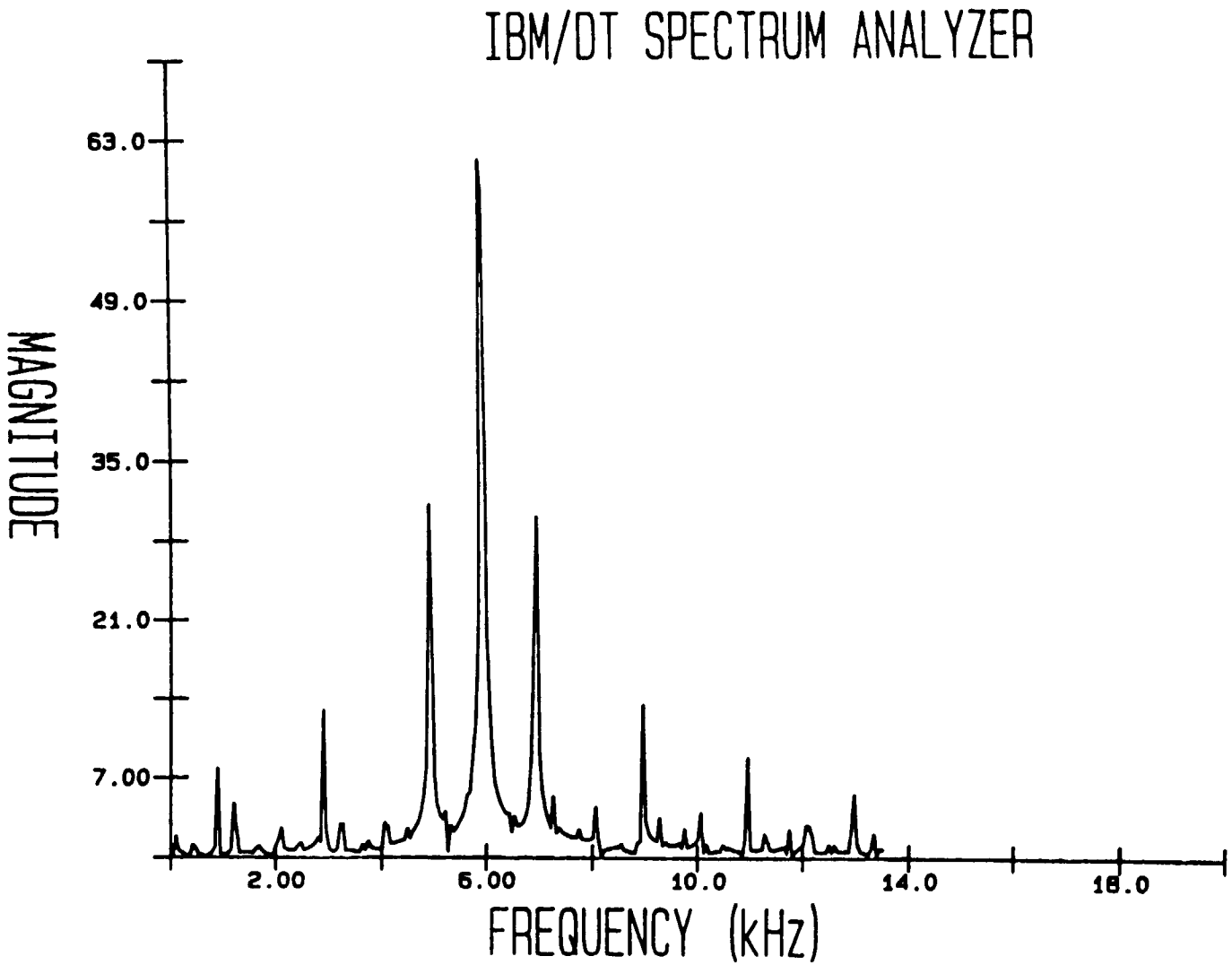

Figure 9-4.- Square wave modulated carrier as per CSPEC.CAR.

Real Time Processing Software

It was understood at the beginning of the program that it would not be possible to process the CAR radar data and make decisions on that data set in real time. This is due to the complexity and unique requirements for signal processing which can be handled easier using slower off-line processing techniques. The best that could be done for the amount of time available to develop the overall system was to record the data to be played back later. While this allows data reduction to be done after the test completion, there is still a real time interface required to digitize the audio channels as the data tape is being played back. That piece of software and the hardware limits are the topic of discussion here.

The final configuration of the processing used two channels of the A/D converter sampling alternately between the range and angle channels of the radar. A total of 112 samples are taken with odd numbered samples being range. The first range sample is taken at the same time the transmitter is triggered to transmit so that this sample became a "clock tick" to keep track of time rather than a "zero range" reading. Range samples were taken every 74 μs thereafter until the 112 sample array was full. Sample number 111 represented the last range sample. This range bin correlates to a range of 508.75 feet. The range interval covered by the radar then was from 0 (theoretically) to 508.75 feet.

Angle measurements were data conversions stored in the even numbered array positions, e.g., 2, 4, 6,..., n, etc. The angle value associated with range bin 111, the maximum range, was in bin 112. This approach was used because the target detection criteria was whenever the signal level in the range channel exceeded a minimum threshold a detect would be declared and that point in time (called a "range bin") would be saved as a target. The 37 μs delay between the detection in the range channel and the A/D conversion in the angle channel would allow extra time for the angle channel voltage to reach its proper level, i.e., measured angle is proportional to absolute angle channel voltage.

Figure 9-5 shows the correlation of range and angle samples from the A/D converter. A total of 112 samples are taken, but in the figure they are divided into the odd numbered, representing range, and the even numbered for angle. In the example, enough energy is detected at bin 107 to declare a target. This correlates to a range of 490.25 feet (since the first bin is at zero range). The estimate of angle will come from the absolute voltage reading converted on the 108th sample as noted in the figure.

The software to activate the A/D converter and make it take the 112 sample set is quite simple. The problems with regards to real time come when the 112 sample array has to be scanned for targets and the target information of time, range, angle voltage, and return magnitude saved in another array. The final software configuration to accomplish this is a program called RADAT.CAR shown in appendix B. The main points of the program will be presented here.

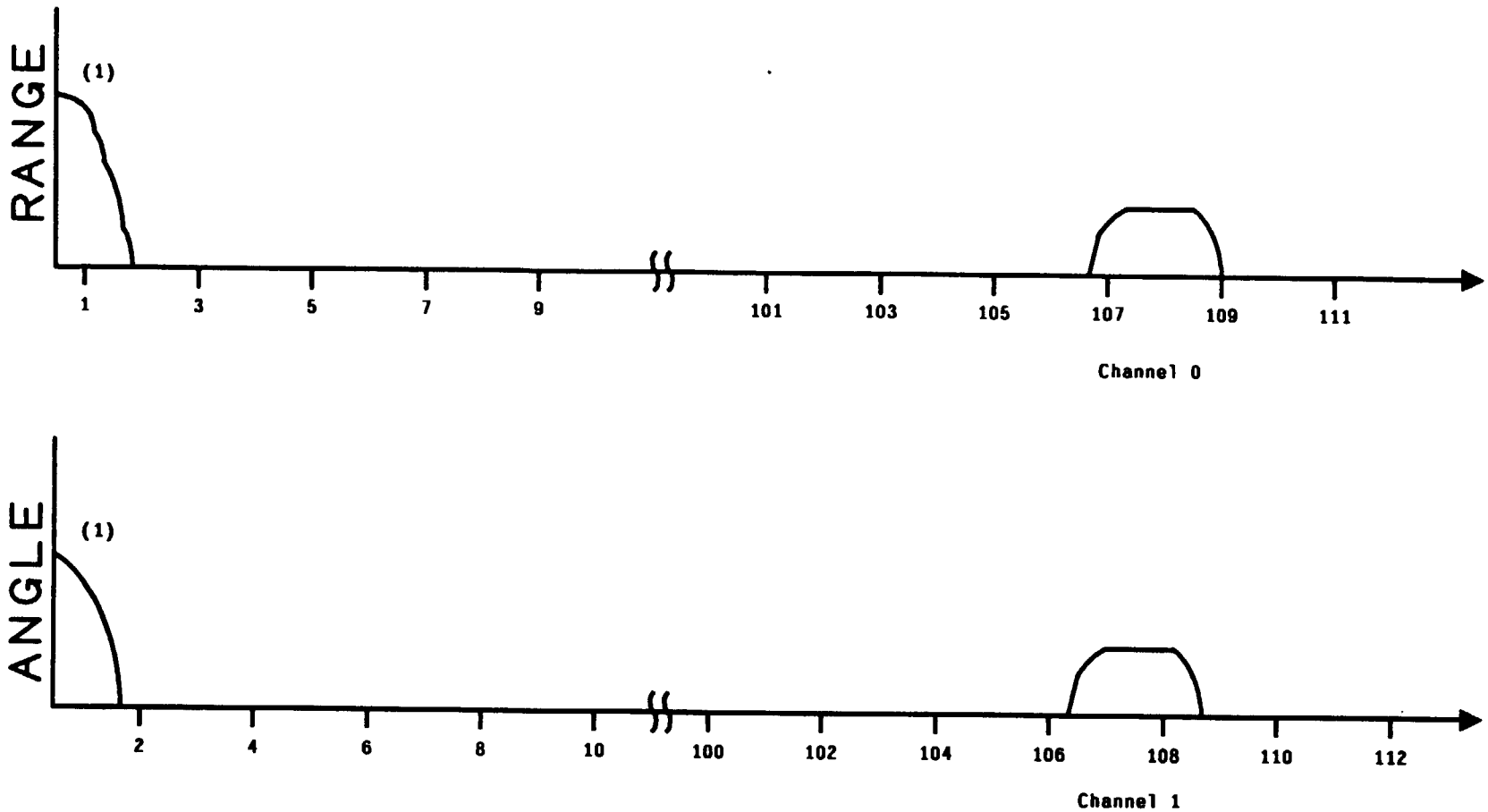

Target at bin 107: range = (107-1) x 4.625 = 490.25 feet
Angle at bin 108: angle is proportional to absolute voltage

NOTE: (1) Transmit energy leakage into receiver

Figure 9-5.- Correlation of sample bin number to range and angle.

The A/D converter fills the 112 sample array called INDATA. For each INDATA received, the array is scanned and all detected targets are separated from the array and stored in an output array of 61,280 bytes called OUTDAT. For every transmitted pulse (every INDATA input) at least one target information set will be stored. If no real targets are found, INDATA sample 1 will be stored to keep track of time. The information stored in OUTDAT is transmitter number (ticks of a clock), range bin or target, angle voltage (binary representation), and target magnitude (also binary). A separate counter is run counting the number of times OUTDAT is accessed. When this counter reaches 7500, the run is terminated.

Termination is necessary because of limits on the largest array that can be handled by ASYST. When this limit is reached, or approached, but never reached here, real time data acquisition terminates and the data stored to that point is written to a disk file. RADAT.CAR accomplishes this file generation and also prompts the operator as to the first and last transmitted pulses processed since the tape playback started. This allows the tape to be rewound to the beginning and when RADAT.CAR is run, the operator can tell the computer which transmitted pulse to start on and data acquistion will not begin until the tape has reached the point where the previous data acquisition pass had terminated.

The only complication to this software was the ability to handle more than one target being present in the INDATA array when it is processed. The processing of each target takes time and with the input data rate to the A/D converter being one datum every 88 ms, only so many targets can be processed within this time interval. Measurements in the lab showed this number to be four targets. If more than four targets are present, they all will be processed, but the A/D converter will not be re-enabled in time to take the next radar data set. This data will be lost. The procedure was evolved to accept the data loss, but to update the time count artificially if more than 4 targets are found correlated with a given tranmitted pulse. By this method, four targets are handled without data loss and some 20 targets can be handled without loss of time sense. This concept could be extended further if necessary, but system evaluation never reached the point of needing this multi-target feature.

In summary, the real time data processing software, RADAT.CAR, can process multiple targets and will generate disk files of this captured radar data. More than one disk file may be necessary to cover all the data in the test, but the software provides features of syncing the stops and starts of files such that the data are consecutive. The threshold criteria is operator selectable at runtime.

Multiple Target Tracking Software

The second level of CAR radar data processing is software to access the data files written by the real time pre-processing software and identify the individual targets detected by the system. The ultimate goal is to separate the targets from one another in both range and angle and establish a tracking history for each. The target history file will be used to extrapolate future locations, smooth over individual data points to try to improve accuracy, and to accommodate the expected short-term dropout due to target noise or multi-

path. It should be pointed out that with the monopulse scheme used for angle measurement, two targets located at the same range, but at different angles will appear as one target at some composite angle.

Since angle calibration data did not exist for the CAR system at the time this second level software was being written, separation of targets by range only was accomplished. The first step in separating targets in range is to decide that all adjacent range bins exceeding threshold are target returns from a single target, i.e., this is a target extended in range. If two range bins exceed threshold, but have at least one range bin between them that does not exceed threshold, then these two threshold detects arise from two separate targets. This was the criteria used to identify separate targets in range. The last decision was to minimize target information carried by reducing all targets extended in range to their closest point to the CAR radar, i.e., track only the smallest bin range. When angular resolution and sensitivity information was available, the line-of-sight (LOS) angle information would be incorporated into the decision process so that the true LOS minimum distance would be tracked.

The program TARID.CAR in appendix B was the software under development to accomplish this task. It has incorporated into it the ability to reduce range extended targets to their closest point to the radar. Initial thoughts were being developed to incorporate a target memory for each detected separate target, but this effort was halted to support system testing. Multiple target tracking was simulated by using the brain and eye to identify individual targets in plot routines.

Both TARID.CAR and RADAT.CAR were checked out by simulation software which generated appropriate inputs simulating a radar output. Simulations of one and two target scenarios were run and correctly processed by the software.

Systems Test Software

The initial effort in the systems area was to calibrate the angel channel response so that volts could be converted to line-of-sight angle to the target. This was acoomplished by the prgram STATS.CAR in appendix B. This program was written to take a 100 sample set of a target configuration (e.g., the target located 1.5 degrees to the right of boresight). The target can be at any range. The computer operator can select a range bin (target location) and the software will automatically calculate and output to the screen the mean and standard deviation of the sample set of voltage in the range bin and voltage in the angle bin. This gives a measurement of the magnitude of the noise process in each channel.

To calibrate the angel channel, it is necessary to perform tests as above for many angles. For instance, the CAR radar angle response was calibrated from 9 degrees right in 0.5 degree increments. STATS.CAR was used to accomplish this by utilizing the correct macro in the software. This macro allows the operator to save the mean and standard deviations from individual data points and plot the entire sequence at the end of the test run. For the angle calibration tests, the elapsed time to calibrate over 18 degrees is approximately 6 hours. At the end of the test, plots of the angle and range channels means

and standard deviations can be made by calling the appropriate plot routines with STATS.CAR.

A real time data acquisition piece of software, called TESTSEG.CAR (appendix B), was written to acquire and write to disk file, tests of short duration and medium memory requirements. Under this latter requirement, a multisegmented disk file was not necessary and a single segmented data file can be used and re-accessed more conveniently. The heart of TESTSEG.CAR is from the operational software program, RADAT.CAR, previously discussed, but memory/array usage is limited to 16,160 bytes. This limits test times to less than 3 minutes for single targets. Realistically, tests of less than 2 minutes in the normal multitarget environment were supported.

The conclusion of TESTSEG.CAR was a disk file containing time, range bin, angle voltage, and target voltage. The software DISSEG.CAR (appendix B) is a follow-on software set that accesses the data file written by TESTSEG.CAR, identifies individual targets, and discriminates extended targets to their closest point. Multitarget plots can be made from the discriminated data. Since only data points are plotted (and not line-connected points), the human eye/brain determines the individual targets and their specific time trajectories.

The static target case was also run with TESTSEG.CAR and those data files were accessed by SELBIN.CAR, also in appendix B. The output of SELBIN.CAR is a point plot of the time history of any operator-selected range bin and its corresponding angle bin. This was used to present the time consecutive data and visually assess the amount of channel noise.

APPENDIX A

PANASONIC PV-9000 VIDEO CASSETTE RECORDER

RECORDING ANALOG PULSE DATA

INTRODUCTION

The recorder contains a high fidelity stereo sound system in addition to the standard monophonic channel. The stereo and monophonic channels are automatically recorded at the same time. The monophonic channel is a mix of the two stereo channels. The monophonic channel is recorded on an edge track of the tape while the stereo channels are recorded in the same area as the video. It is the two stereo channels, with their wider bandwidth, that is of interest for recording analog data.

PROBLEM

The audio channels contain automatic gain controls which do not respond well to narrow pulses. As a result, the gain is automatically set to near maximum. This causes a poor signal-to-noise ratio and clipping of the higher amplitude pulses. For successful recording of narrow and widely-spaced pulses, it is necessary to disable some of the AGC circuitry.

MODIFICATION

Switches have been added to the stereo channels for bypassing AGC circuitry. The slide switches are mounted to the circuit board above the tape transport and behind the cassette. They can be operated with a long screwdriver while the cassette holder is raised and the cassette removed. Look to the right-of-center for the black handles which point downward.

The left-hand switches operates the left channel and the right-hand switch the right channel. Place the switches in the right-hand position to bypass the AGC (pulse mode) or in the left-hand position to return operation to normal.

CIRCUIT OPERATION

Recording

The microphone inputs are much too sensitive for most signal sources. The stereo line adaptor contains a 300:1 attenuator and is recommended for use between the signal source and the microphone inputs. The stereo line adaptor plugs directly into the microphone and video output jacks. The video connection is needed to pick up a second ground for the input signal return. Separate ground connections are used for the signal source and the input attenuator. This is part of a scheme to reduce interference from cable noise pickup.

The signals enter the recorder at the jack panel. Refer to the motor drive and jack panel schematic in the PV-9000 service manual. The signals are amplified by a preamplifier (IC6901) which has a gain of 50. From here the signals are passed to the FM audio circuit board.

On arrival at the FM audio board, the left channel signal is processed by IC4203 and the right channel by IC4204. These are hard limiting AGC circuits that only become active for large input signals, and at that point, limit the signal to a precise level. Their time constants have a fast attack and very slow decay characteristics. When switches S1 (left channel) and S2 (right channel) are in the normal position and with typical input signal levels, these circuits have a fixed gain of 10. Refer to switch sections S1A and S2A on the modified FM audio schematic. When the switches in the pulse position, the gain is reduced to 1. This allows the input signals to be increased by a factor of 10, for a better signal-to-noise ratio and without activating the AGC action. The signals leave IC4203 and IC4204 through pin 27. From here, IC4208 and IC4209 route the left and right channels to the second AGC.

The second AGC circuits (IC4205) have a soft action, for a limited effect on gain and have medium attack and decay characteristics. This is a dynamic noise reduction system that compresses the signal amplitude range during record, and later, expands the range to normal during playback. In this kind of operation, the gain control is always active, and therefore, should be disabled for pulse recording. Switch sections S1B and S2B bypass the gain control stages when placed in the pulse position.

The signals now go to IC4202 for an additional amplification of 20, and then return to IC4203 and IC4204 for frequency modulation of carriers. The left channel modulates a 1.3 MHz carrier and the right channel modulates a 1.7 MHz carrier.

After modulation, the carriers pass through lowpass filters, are mixed, and then amplified by the record amplifier. The record amplifier includes transistors Q4219 through Q4222 and drives two FM audio heads. These heads are located on opposite sides of the cylinder, as are the video heads.

For monitoring of the recorded signals, a second output (pin 1) is taken from IC4203 and IC4204. These signals are routed by IC4211 to the output amplifiers (IC4215). These amplifiers drive the headphone jack.

Playback

The two FM audio heads used for recording are also used for playback. During playback, the signal carriers go to the FM audio circuit board and IC4201. This IC contains preamplifiers, an electronic switch, and AGC. The electronic switch is synchronized to the cylinder rotation. A constant signal is fed to the electronics by switching to each head as it comes in contact with the tape. The AGC provides the correct carrier amplitude to the following circuits.

The output of IC4201 passes through bandpass filters to separate the left and right channel carriers. The left channel carrier (1.3 MHz) is amplified and fed to IC4203. The right channel carrier (1.7 MHz) is amplified and fed to IC4204. The integrated circuits contain several functions including limiters and frequency demodulators.

The demodulated signals pass through lowpass filters and de-emphasis networks. IC4208 and IC4209 route the left and right channel signals to IC4205.

The AGC circuits of IC4205 function the same during playback as they did during record. For playback of analog pulse data, the AGC should be disabled. Set switches S1 and S2 to the right-hand (pulse) position, as they were for recording.

The signals are amplified by IC4202 and routed by IC4203, IC4204, and IC4211. IC4211 is controlled by the audio selector switch. Set the switch, which is located on the right side panel, to the L/R position. This makes both stereo channels available at the output. From IC4211, the signals go to the output amplifiers (IC4215) and then leave the recorder through the stereo headphone jack.

The audio-output cord is a handy adaptor which separates the left and right channels into two cords and terminates them in the more familiar RCA phone jacks. Set the adaptor switch to the stereo position to use both channels.

SPECIFICATIONS

Normal Operation

Place switches S1 and S2 in the left-hand position and refer to the specifications listed in the PV-9600 operating instructions manual. However, tests show the frequency response to be down 8 dB at the specified upper band-edge of 20 KHz.

Pulse Operation

Place switches S1 and S2 in the right-hand position.

Optimum record level:	0.4 volts peak, monitored at headphone jack
Input level:	1 volt peak typical, with 300:1 attenuator
Playback level:	0.4 volts peak, inverted, at headphone jack
Rise time:	35 μs

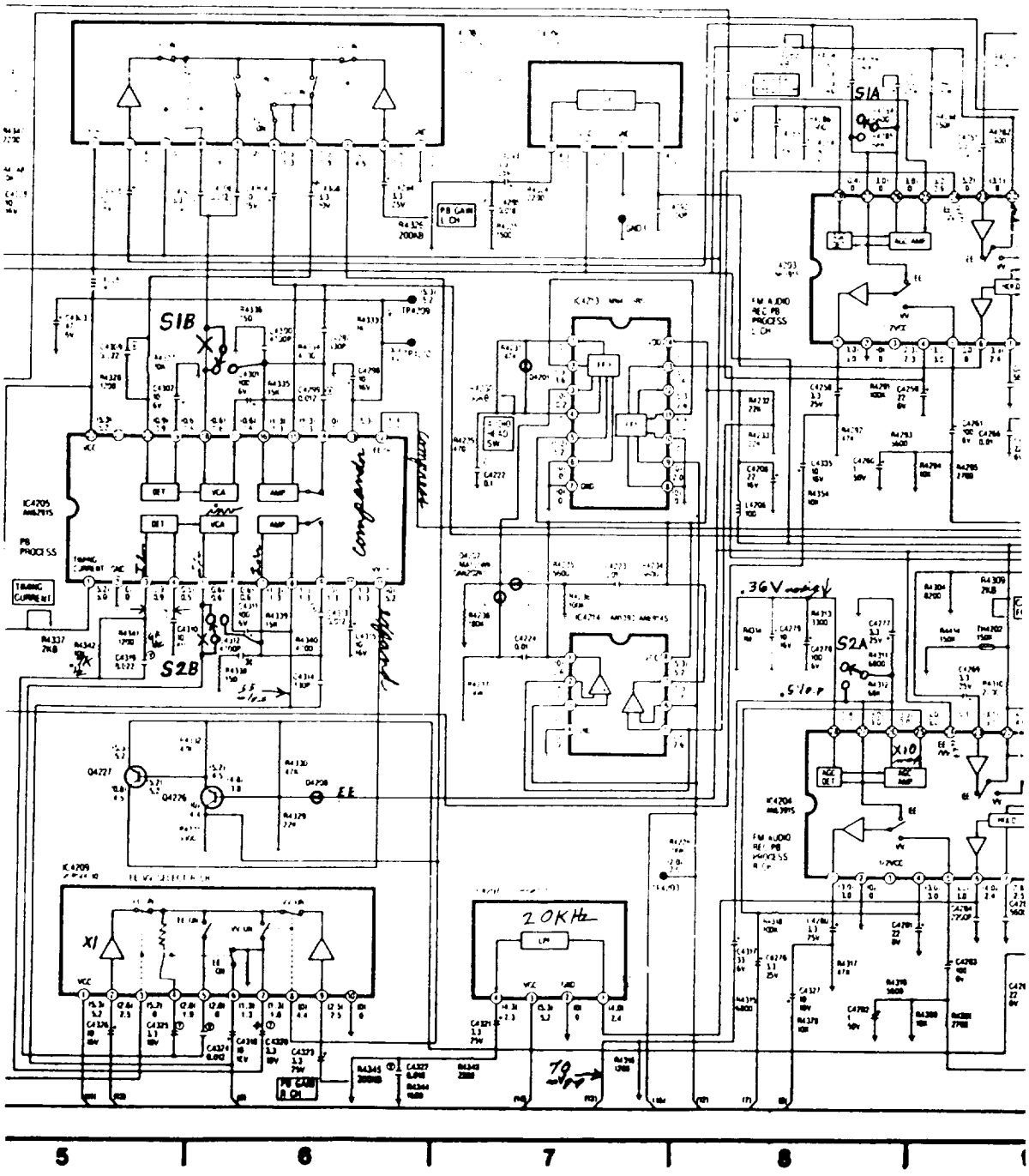

Panasonic PV-9000 video cassette recorder - FM audio circuit modifications (switches shown normal position).

APPENDIX B

CRASH AVOIDANCE RADAR

DATA ACQUISITION AND PRE-PROCESSING SOFTWARE

```
                    \ CRASH AVOIDANCE RADAR
          \ DATA ACQUISITION AND PRE-PROCESSING SOFTWARE
 \ WXC 8/21/85
 \ UPDATE 11/18/85 WXC
 \   UPDATE MASKS MAIN BANG USING A VARIABLE THRESHOLD.
 \ THIS PROGRAM ACQUIRES CAR RADAR DATA FROM THE AUDIO CHANNELS OF
 \ THE VIDEO RECORDER, PRE-PROCESSES FOR THRESHOLD DETECTION AND
 \ WRITES THE DATA SET TO MEMORY.  AFTER 60,000 BYTES HAVE BEEN
 \ STORED IN MEMORY THE PROGRAM TERMINATES WITH PROMPTS TO WRITE
 \ THE DATA TO A DISK FILE.
 \
 \ DEFINE INPUT & OUTPUT DATA ARRAYS AND COUNTERS
 DIM[ 112 ] DMA.ARRAY INDATA
 INTEGER DIM[ 7660 , 4 ] ARRAY OUTDAT
 INTEGER SCALAR EYE
 INTEGER SCALAR HITS
 INTEGER SCALAR BNUM
 INTEGER SCALAR ICOUNT
 INTEGER SCALAR CNDX
 INTEGER SCALAR BFIRST
 \
 \ DEFINE HIT ARRAY, THRESHOLDS AND RANGE/ANGLE INDICES
 \ SET UP FOR OUTPUT FILENAME
 INTEGER DIM[ 56 ] ARRAY HARRAY
 INTEGER SCALAR THRSH
 INTEGER SCALAR RNDX
 INTEGER SCALAR ANDX
 INTEGER SCALAR THRSH1
 14      STRING FILENAME
 \
 \ SET UP THE A/D CONVERTER PARAMETERS
 0 1 A/D.TEMPLATE ZERO.ONLY
 1 A/D.GAIN
 .037 CONVERSION.DELAY
 EXT.TRIG
 A/D.INIT
 INDATA DMA.TEMPLATE.BUFFER
 \
 \ SET THRESHOLDS AND ZERO ARRAYS/CONSTANTS
 : INITIALIZE
 0 BNUM :=
 0 EYE :=
 0 ICOUNT :=
 0 OUTDAT :=
 0 HARRAY :=
 0 HITS :=
 CR ." INPUT THRESHOLD VALUE: "
 BEGIN
 #INPUT NOT
 WHILE
 " INVALID NUMBER, REENTER: "
 REPEAT
 DUP THRSH1 :=
 1 - THRSH :=


 ASYST Version 1.5
 Page 1     c:radat.car    03/13/86    10:06
```

```
;
\
\ ROUTINE FOR WAITING FOR PROPER TRANSMITTER PULSE
: WAITONE
CNDX 1 - CNDX :=
CNDX 0 =
IF EXIT THEN
CNDX 0 DO
A/D.INIT
ZERO.ONLY A/D.IN>ARRAY(DMA)
BEGIN ?DMA.ACTIVE NOT UNTIL
BNUM 1 + BNUM :=
BNUM .
LOOP
;
\
\ ROUTINE TO SYNC TO DATA TAPE
: SYNC
CR ." INPUT THE NUMBER OF THE NEXT TRANSMITTED PULSE: "
BEGIN
#INPUT NOT
WHILE
" INVALID NUMBER, REENTER: "
REPEAT
CNDX :=
CNDX BFIRST :=
WAITONE
CR ." BNUM = " BNUM .
CR ." STARTING DATA SAVE ON NEXT TRANSMITTER PULSE. "
;
\
\ BEGIN THE DATA ACQUISITION LOOP UNTIL MEMORY FULL
: SCANSTORE
BEGIN
\
\ TAKE A DATA SET ( FILL INDATA ARRAY )
A/D.INIT
ZERO.ONLY A/D.IN>ARRAY(DMA)
BEGIN ?DMA.ACTIVE NOT UNTIL
\ UPDATE TRANSMITTED PULSE COUNTER
BNUM 1 + BNUM :=
\ SCAN THE INPUT ARRAY FOR NUMBER OF HITS
THRSH1 INDATA [ 1 ] :=
\ SET VARIABLE THRESHOLD INSIDE MAIN BANG HOLDOVER
THRSH INDATA [ 3 ] :=  \ 3 IS THROWN AWAY ALWAYS
\ 5 IS SET TO 5 VOLTS
INDATA [ 5 ] 4500 <
IF
  THRSH INDATA [ 5 ] :=  \ 5 CAN EXIST
THEN
\ 7 IS SET FOR 5 VOLTS
INDATA [ 7 ] 4500 <
IF
  THRSH INDATA [ 7 ] :=  \ 7 IS ELIMINATED
```

```
 THEN
 \ 9 IS SET FOR 5 VOLTS
 INDATA [ 9 ] 4500 <
 IF
   THRSH INDATA [ 9 ] :=  \ 9 IS ELIMINATED
 THEN
 INDATA SUB[ 1 , 110 , 2 ] THRSH [>] \ THIS CHANGED 12/10/85
 TRUE.INDICES
 1 []DIM HITS :=
 REV[ 1 ]
 2 * 1 -
 HARRAY SUB[ 1 , HITS , 1 ] :=
 HITS 1 >
 \ IF NUMBER OF HITS > ONE THEN DO ONE LESS
 \    (HIT ARRAY HAS BEEN REVERSED)
 IF
 HITS 1 - HITS :=
 THEN
 \ ENTER MEMORY WRITE LOOP
 HITS 0 DO I
 1 + EYE :=
 ICOUNT 1 + ICOUNT :=
 BNUM
 HARRAY [ EYE ]
 DUP DUP
 RNDX :=
 1 + ANDX :=
 INDATA [ ANDX ]
 INDATA [ RNDX ]
 \ WRITE DATA TO MEMORY
 OUTDAT [ ICOUNT , 4 ] :=
 OUTDAT [ ICOUNT , 3 ] :=
 OUTDAT [ ICOUNT , 2 ] :=
 OUTDAT [ ICOUNT , 1 ] :=
 LOOP
 0 HARRAY SUB[ 1 , HITS , 1 ] :=
 \  EXIT WHEN >= TO 7500
 ICOUNT 7500 >= UNTIL EXIT
 ;
 \
 \ A ROUTINE TO PLOT THE INPUT ARRAY. NOT CURRENTLY CALLED.
 : DMAP
 INDATA
 0 10 A/D.SCALE
 Y.AUTO.PLOT
 ;
 \
 \ ROUTINE TO INVOKE WRITING THE COLLECTED DATA TO
 \ A DISK FILE.  FILE SIZE IS BASED ON THE ACTUAL DATA
 \ COUNT "ICOUNT" AND WILL BE APPROXIMATELY 60,000 BYTES
 : WRFILE
 FILE.TEMPLATE
 1 COMMENTS
 INTEGER DIM[ 766 , 4 ] SUBFILE
```

```
10 TIMES
END
CR ." TO WRITE THE DATA TO DISK ENTER A 1 "
CR ." OTHERWISE ENTER A ZERO. "
BEGIN
#INPUT NOT
 WHILE
 " NOT A NUMBER, REENTER: "
   REPEAT
0 =
IF EXIT
  THEN
CR ." NAME OF DATA FILE? "
"INPUT FILENAME ":=
FILENAME DEFER> FILE.CREATE
FILENAME DEFER> FILE.OPEN
CR ." YOU HAVE 64 CHARACTERS TO INPUT THE TOTAL DATA COUNT "
CR ." (ICOUNT); THE FIRST TRANSMITTED PULSE NUMBER; AND THE "
CR ." LAST TRANSMITTED PULSE NUMBER.  INCLUDE SOME TEST NAME ALSO: "
CR ." REMEMBER A CARRIAGE RETURN ENDS THIS INPUT! "
CR
"INPUT
1 >COMMENT
1 SUBFILE
OUTDAT SUB[ 1 , 766 ; 1 , 4 , 1 ] ARRAY>FILE
2 SUBFILE
OUTDAT SUB[ 767 , 766 ; 1 , 4 , 1 ] ARRAY>FILE
3 SUBFILE
OUTDAT SUB[ 1533 , 766 ; 1 , 4 , 1 ] ARRAY>FILE
4 SUBFILE
OUTDAT SUB[ 2299 , 766 ; 1 , 4 , 1 ] ARRAY>FILE
5 SUBFILE
OUTDAT SUB[ 3065 , 766 ; 1 , 4 , 1 ] ARRAY>FILE
6 SUBFILE
OUTDAT SUB[ 3831 , 766 ; 1 , 4 , 1 ] ARRAY>FILE
7 SUBFILE
OUTDAT SUB[ 4597 , 766 ; 1 , 4 , 1 ] ARRAY>FILE
8 SUBFILE
OUTDAT SUB[ 5363 , 766 ; 1 , 4 , 1 ] ARRAY>FILE
9 SUBFILE
OUTDAT SUB[ 6129 , 766 ; 1 , 4 , 1 ] ARRAY>FILE
10 SUBFILE
OUTDAT SUB[ 6895 , 766 ; 1 , 4 , 1 ] ARRAY>FILE
FILE.CLOSE
CR
;
\
\ THE EXECUTIVE ROUTINE THAT ACTUALLY MAKES ALL THIS RUN
\ IN A SEQUENCE.
: EXEC
  INITIALIZE
  SYNC    \ CALLS WAITONE
   SCANSTORE
CR ." THE LAST DATA SET NUMBER IN MEMORY WAS " ICOUNT .
CR ." THE FIRST TRANSMITTED PULSE WAS " BFIRST .
CR ." THE LAST TRANSMITTED PULSE WAS " BNUM .
    WRFILE
CR
;
F9 FUNCTION.KEY.DOES EXEC


ASYST Version 1.5
Page 5    c:radat.car    03/13/86    10:07
```

```
                \ CRASH AVOIDANCE RADAR
\          TARGET POINTER PROGRAM
     SECOND LEVEL RADAR DATA PROCESSING - - TARGET ID
\ WXC 9/27/85
\ THIS SOFTWARE ACCESSES THE PRE-PROCESSED RADAR DATA FILES AND
\ ESTABLISHES IDENTITIES OF INDIVIDUAL TARGETS SEEN DURING THE
\ DATA RUN.  TARGET RANGE EXTENT IS ABOLISHED AND A TARGET IS
\ DEFINED BY ITS CLOSEST POINT.
\
\ THE TARGET IS DENOTED BY A POINTER WHICH SHOWS
\ WHERE THE VALID TARGETS ARE WITHIN THE ORIGINAL
\ DATA ARRAY OR FILE SEGMENT.
INTEGER DIM[ 766 , 4 ] ARRAY FILSEG
INTEGER DIM[ 20 ] ARRAY TARA
INTEGER DIM[ 766 ] ARRAY TME
INTEGER DIM[ 766 ] ARRAY PTAR
INTEGER SCALAR SFILNUM
INTEGER SCALAR ISTART
INTEGER SCALAR ILIM
INTEGER SCALAR IC
INTEGER SCALAR ICT
INTEGER SCALAR IPT
INTEGER SCALAR TSTART
INTEGER SCALAR HDX
INTEGER SCALAR NDX
INTEGER SCALAR II
INTEGER SCALAR HITS
INTEGER SCALAR TOTHITS
INTEGER SCALAR ITEMP
FILE.TEMPLATE
1 COMMENTS
INTEGER DIM[ 766 , 4 ] SUBFILE
10 TIMES
END
14 STRING FILENAME
: OPENF
CR ." INPUT NAME OF DATA FILE? "
"INPUT FILENAME ":=
FILENAME DEFER> FILE.OPEN
;
\
\ SET UP AND RE-ESTABLISH CONSTANTS/COUNTERS
: INITIALIZE
0 SFILNUM :=
0 ISTART :=
0 ILIM :=
0 IC :=
0 ICT :=
0 IPT :=
0 TSTART :=
0 HDX :=
0 NDX :=
0 II :=
0 HITS :=


ASYST Version 1.5
Page 1    c:tarid.car    03/14/86    11:30
```

```
0 FILSEG :=
0 TARA :=
0 TME :=
0 TOTHITS :=
0 PTAR :=
;
\
\ SIZEFIND EXAMINES THE FILE SEGMENT JUST READ TO ESTABLISH
\ THE NUMBER OF ENTRIES.  THE FULL SEGMENT IS 766 4-ELEMENT
\ ENTRIES.  THE RESULT OF SIZEFIND IS THE PARAMETER ILIM.
\ IT MAY BE 766 OR LESS.  PROCESSING OF DATA FROM THE SEGMENT
\ SHOULD USE ILIM TO PROPERLY TRUNCATE THE FILE.
: SIZEFIND
TME [ 1 ] ISTART :=
  BEGIN
   IC 1 + IC :=
   IC 766 >
    IF
      0 IC :=
      766 ILIM :=
      EXIT
    THEN
      TME [ IC ] ISTART <
        IF
          IC 1 - ILIM :=
          0 IC :=
          EXIT
        THEN
  AGAIN
;
\
\ ONEPULSE ESTABLISHES ALL THE RADAR RETURNS THAT ARE
\ ASSOCIATED WITH A TRANSMITTED PULSE.  ICT IS THE
\ NUMBER OF RETURNS FOR THAT TRANSMITTED PULSE.  THE
\ PARAMETER IPT IS THE CORRECT POINTER FOR THE NEXT FILE
\ SEGMENT ELEMENT.
: ONEPULSE
0 ICT :=
TME [ IPT ] TSTART :=
IPT ILIM =
 IF
   1 IPT + IPT :=
   1 ICT + ICT :=
   EXIT
 THEN
 BEGIN
        1 IPT + IPT :=
         IPT ILIM >
         IF
            EXIT
         THEN
       1 ICT + ICT :=
        IPT ILIM =
        IF
```

```
            TME [ IPT ] TSTART >
             IF
               EXIT
             THEN
            IPT 1 + IPT :=
            ICT 1 + ICT :=
           EXIT
         THEN
        TME [ IPT ] TSTART >
 UNTIL
;
\
\ TARSEP IS THE ROUTINE TO EXAMINE ALL RETURNS FROM A
\ SINGLE TRANSMITTED PULSE AND IDENTIFY INDIVIDUAL TARGETS.
\ A TARGET WITH EXTENDED RANGE RETURN IS TRUNCATED SUCH THAT
\ ITS VALUE IS ITS CLOSEST RANGE.  IN THE A/D CONVERTER ARRAY
\ THIS MEANS THE DIFFERENCE IN RANGE BIN VALUE MUST BE
\ GREATER THAN TWO.  IF THERE ARE TWO TARGETS SIDE-BY-SIDE
\ AND OCCUPYING TWO ADJACENT RANGE BINS, ONLY THE CLOSEST
\ TARGET WILL BE IDENTIFIED UNTIL THEIR SEPARATION SPANS
\ MORE THAN TWO BINS.
: TARSEP
0 HITS :=
1 HDX :=
IPT ICT - NDX :=
NDX TARA [ HDX ] :=
NDX 1 + IPT =
 IF
   EXIT
 THEN
BEGIN
     FILSEG [ NDX , 2 ]
     NDX 1 + NDX :=
      NDX IPT =
      IF
        EXIT
      THEN
     FILSEG [ NDX , 2 ] - 2 >
     IF
       1 HDX + HDX :=
       NDX TARA [ HDX ] :=
     THEN
NDX 1 + IPT =
UNTIL
;
\
\ POINTER ARRAY WRITE ROUTINE
: WRARAY
HITS 0 DO I
1 + II :=
II TOTHITS + ITEMP :=
TARA [ II ] PTAR [ ITEMP ] :=
LOOP
;

ASYST Version 1.5
Page 3    c:tarid.car    03/14/86    11:30
```

```
\
\ FOR NOW THIS IS RUNNING AS THE MAIN CALLING SEGMENT.
  READF
INITIALIZE
1 COMMENT>
"TYPE
CR ." INPUT SUBFILE NUMBER TO BE PROCESSED: "
BEGIN
#INPUT NOT
WHILE
" INVALID NUMBER, REENTER: "
REPEAT
SFILNUM :=
SFILNUM SUBFILE
FILE>UNNAMED.ARRAY
FILSEG :=
FILSEG XSECT[ ! , 1 ] TME :=
TME [ 1 ] ISTART :=
ISTART 0 =
IF
   CR ." THIS FILE SEGMENT IS EMPTY. "
ELSE
SIZEFIND
1 IPT :=
BEGIN
0 TARA :=
  ONEPULSE
  TARSEP
   TARA TRUE.INDICES
   1 []DIM HITS := DROP
   WRARAY
   HITS TOTHITS + TOTHITS :=
  IPT ILIM >
UNTIL
THEN
CR ." JOB IS DONE! "
;
F9 FUNCTION.KEY.DOES OPENF
F10 FUNCTION.KEY.DOES READF
F5 FUNCTION.KEY.DOES FILE.CLOSE
```

```
8 4 FIX.FORMAT
REAL DIM[ 100 , 5 ] ARRAY XAB  \ ABSCISSA,RMEAN,RSIG,AMEAN,ASIG
INTEGER DIM[ 100 , 112 ] ARRAY DSET
INTEGER DIM[ 112 , 2 ] ARRAY MVSET
DIM[ 112 ] DMA.ARRAY INDATA
REAL DIM[ 112 ] ARRAY TME
REAL DIM[ 56 ] ARRAY RMEAN
REAL DIM[ 56 ] ARRAY RSIG
REAL DIM[ 56 ] ARRAY AMEAN
REAL DIM[ 56 ] ARRAY ASIG
INTEGER SCALAR II
INTEGER SCALAR JJ
INTEGER SCALAR RBIN
INTEGER SCALAR ABIN
INTEGER SCALAR DCOUNT
6 STRING PRETAPE
16 STRING TAPENAME
" TAPE: " PRETAPE ":="
6 STRING PRESEG
16 STRING TESTSEG
" TEST: " PRESEG ":="
22 STRING LABXAB
TME []RAMP
TME 4.625 * 4.625 - TME :=
: INITIALIZE
0 II :=
0 JJ :=
;
0 1 A/D.TEMPLATE ZERO.ONLY
1 A/D.GAIN
.037 CONVERSION.DELAY
EXT.TRIG
A/D.INIT
: DMAZERO
0 INDATA :=
INDATA DMA.TEMPLATE.BUFFER
A/D.INIT
ZERO.ONLY A/D.IN>ARRAY(DMA)
BEGIN ?DMA.ACTIVE NOT UNTIL
;
: SMAP
GRAPHICS.DISPLAY
CURSOR.OFF
" *" SOLID&SYMBOL
TME SUB[ 1 , 112 , 2 ]
INDATA SUB[ 1 , 112 , 2 ]
.0012207 *
XY.AUTO.PLOT
NORMAL.COORDS
.4 .05 POSITION
" RANGE (FEET) " LABEL
270 LABEL.DIR
.01 .85 POSITION
" RANGE CHAN VOLTS " LABEL


ASYST Version 1.5
Page 1    c:stats.car    03/17/86    09:17
```

```
0 LABEL.DIR
0 0 POSITION

: DIFMAP
GRAPHICS.DISPLAY
CURSOR.OFF
" *" SOLID&SYMBOL
TME SUB[ 2 , 112 , 2 ]
INDATA SUB[ 2 , 112 , 2 ]
.0012207 *
XY.AUTO.PLOT
NORMAL.COORDS
.4 .05 POSITION
" RANGE (FEET) " LABEL
270 LABEL.DIR
.01 .85 POSITION
" ANGLE CHAN VOLTS " LABEL
0 LABEL.DIR
0 0 POSITION
;
: INPNUM
  BEGIN
  #INPUT NOT
  WHILE
  " INVALID NUMBER, REENTER: "
  REPEAT
;
  GETSET
 BEGIN
  1 JJ + JJ :=
  DMAZERO
   112 0 DO I
   1 + II :=
   INDATA [ II ] DSET [ JJ , II ] :=
   LOOP
 100 JJ =
 UNTIL
;
: COLLECT
CR ." ENTER THE VALUE OF THE ABSCISSA: " INPNUM
DCOUNT 1 + DCOUNT :=
XAB [ DCOUNT , 1 ] :=
DSET XSECT[ ' , RBIN ] DUP
MEAN .0012207 * XAB [ DCOUNT , 2 ] :=
SAMPLE.VARIANCE SQRT .0012207 *
XAB [ DCOUNT , 3 ] :=
DSET XSECT[ ' , ABIN ] DUP
MEAN .0012207 * XAB [ DCOUNT , 4 ] :=
SAMPLE.VARIANCE SQRT .0012207 *
XAB [ DCOUNT , 5 ] :=
;
: ONEBIN
  CR ." INPUT THE RANGE BIN NUMBER ( 1 - 55 ): "
  INPNUM


ASYST Version 1.5
Page 2    c:stats.car    03/17/86    09:17
```

```
  2 * 1 - RBIN :=
RBIN 111 >
     IF
        CR ." RANGE BIN TOO LARGE, 1 TO 55 ONLY! "
        INPNUM
     THEN
 RBIN 1 + ABIN :=
DSET XSECT[ ' , RBIN ] DUP
CR ." MEAN TARGET VOLTAGE = " MEAN .0012207 * .
CR ." STANDARD DEVIATION ( IN VOLTS ) = "
SAMPLE.VARIANCE SQRT .0012207 * . CR
DSET XSECT[ ' , ABIN ] DUP
CR ." MEAN ANGLE VOLTAGE = " MEAN .0012207 * .
CR ." STANDARD DEVIATION ( IN VOLTS ) = "
SAMPLE.VARIANCE SQRT .0012207 * .
CR ." IF YOU WISH TO SAVE FOR PLOTTING ENTER A 1 "
CR ." OTHERWISE ENTER A 0. "
INPNUM
0 =
IF
  EXIT
THEN
  COLLECT
;
: SUMMARIZE
0 MVSET :=
0 JJ :=
BEGIN
  1 JJ + JJ :=
  DSET XSECT[ ' , JJ ] DUP
  MEAN MVSET [ JJ , 1 ] :=
  SAMPLE.VARIANCE SQRT MVSET [ JJ , 2 ] :=
  112 JJ =
UNTIL
MVSET .0012207 * SUB[ 1 , 112 , 2 ; 1 , 2 , 1 ] DUP
XSECT[ ' , 1 ] RMEAN :=
XSECT[ ' , 2 ] RSIG :=
MVSET .0012207 * SUB[ 2 , 112 , 2 ; 1 , 2 , 1 ] DUP
XSECT[ ' , 1 ] AMEAN :=
XSECT[ ' , 2 ] ASIG :=
;
: RANHP
AXIS.DEFAULTS
HP7470
PLOTTER.DEFAULTS
" *" SOLID&SYMBOL
TME SUB[ 1 , 112 , 2 ] DUP
RMEAN
XY.AUTO.PLOT
" o" SOLID&SYMBOL
RSIG
XY.DATA.PLOT
.015 .058 CHAR.SIZE
NORMAL.COORDS


ASYST Version 1.5
Page 3    c:stats.car    03/17/86    09:18
```

```
.4 .075 POSITION
" RANGE (FEET) " LABEL
)0 LABEL.DIR
.07 .35 POSITION
" RANGE CHAN VOLTS " LABEL
0 LABEL.DIR
.007 .04 CHAR.SIZE
.85 .3 POSITION
" ¥ MEAN VALUE " LABEL
.85 .275 POSITION
" 0 STANDARD DEV. " LABEL
0.4 0.9 POSITION
.012 .04 CHAR.SIZE
PRETAPE TAPENAME "CAT
LABEL
.4 .87 POSITION
PRESEG TESTSEG "CAT
LABEL
;
: ANGHP
AXIS.DEFAULTS
HP7470
PLOTTER.DEFAULTS
" *" SOLID&SYMBOL
TME SUBI 2 , 112 , 2 ) DUP
AMEAN
XY.AUTO.PLOT
" o" SOLID&SYMBOL
ASIG
XY.DATA.PLOT
.015 .058 CHAR.SIZE
NORMAL.COORDS
.4 .075 POSITION
" RANGE (FEET) " LABEL
90 LABEL.DIR
.07 .35 POSITION
" ANGLE CHAN VOLTS " LABEL
0 LABEL.DIR
.007 .04 CHAR.SIZE
.85 .3 POSITION
" ¥ MEAN VALUE " LABEL
.85 .275 POSITION
" 0 STANDARD DEV. " LABEL
0.4 0.9 POSITION
.012 .04 CHAR.SIZE
PRETAPE TAPENAME "CAT
LABEL
.4 .87 POSITION
PRESEG TESTSEG "CAT
LABEL
;
: ANOTATE
CR ." ENTER TAPE ID ( 16 CHAR MAX ) "
"INPUT TAPENAME ":=


ASYST Version 1.5
Page 4    c:stats.car    03/17/86    09:18
```

```
CR ." ENTER TEST SEGMENT OR SUMMARY (16 LIMIT) "
"INPUT TESTSEG ":=
;
: CRANHP
AXIS.DEFAULTS
HP7470
PLOTTER.DEFAULTS
" *" SOLID&SYMBOL
XAB SUB[ 1 , DCOUNT , 1 ; 1 , 5 , 1 ] DUP
XSECT[ ! , 1 ] SWAP
XSECT[ ! , 3 ]
XAB SUB[ 1 , DCOUNT , 1 ; 1 , 5 , 1 ] DUP
XSECT[ ! , 1 ] SWAP
XSECT[ ! , 2 ]
XY.AUTO.PLOT
" O" SOLID&SYMBOL
XY.DATA.PLOT
.015 .058 CHAR.SIZE
CR ." ENTER ABSCISSA AXIS NAME: (22 CHAR MAX) "
"INPUT LABXAB ":=
NORMAL.COORDS
.4 .075 POSITION
LABXAB LABEL
90 LABEL.DIR
.07 .35 POSITION
" RANGE CHAN VOLTS " LABEL
0 LABEL.DIR
.007 .04 CHAR.SIZE
.85 .3 POSITION
" * MEAN VALUE" LABEL
.85 .275 POSITION
" O STANDARD DEV. " LABEL
.4 .9 POSITION
.012 .04 CHAR.SIZE
PRETAPE TAPENAME "CAT
LABEL
.4 .87 POSITION
PRESEG TESTSEG "CAT
LABEL
;
: CANGHP
AXIS.DEFAULTS
HP7470
PLOTTER.DEFAULTS
" *" SOLID&SYMBOL
XAB SUB[ 1 , DCOUNT , 1 ; 1 , 5 , 1 ] DUP
XSECT[ ! , 1 ] SWAP
XSECT[ ! , 5 ]
XAB SUB[ 1 , DCOUNT , 1 ; 1 , 5 , 1 ] DUP
XSECT[ ! , 1 ] SWAP
XSECT[ ! , 4 ]
XY.AUTO.PLOT
" O" SOLID&SYMBOL
XY.DATA.PLOT
```

```
.015 .058 CHAR.SIZE
CR ." ENTER ABSCISSA AXIS NAME: (22 CHAR MAX) "
 INPUT LABXAB "t=
NORMAL.COORDS
.4 .075 POSITION
LABXAB LABEL
90 LABEL.DIR
.07 .35 POSITION
" ANGLE CHAN VOLTS " LABEL
0 LABEL.DIR
.007 .04 CHAR.SIZE
.85 .3 POSITION
" * MEAN VALUE " LABEL
.85 .275 POSITION
" O STANDARD DEV. " LABEL
.4 .9 POSITION
.012 .04 CHAR.SIZE
PRETAPE TAPENAME "CAT
LABEL
.4 .87 POSITION
PRESEG TESTSEG "CAT
LABEL
;
: MAIN
  INITIALIZE
  GETSET
  SUMMARIZE
  CR ." JJ = " JJ .
;
F9 FUNCTION.KEY.DOES MAIN
F10 FUNCTION.KEY.DOES SMAP
F7 FUNCTION.KEY.DOES DIFMAP
F8 FUNCTION.KEY.DOES ONEBIN
F1 FUNCTION.KEY.DOES PANHP
F2 FUNCTION.KEY.DOES ANGHP
F3 FUNCTION.KEY.DOES CRANHP
F4 FUNCTION.KEY.DOES CANGHP
F5 FUNCTION.KEY.DOES ANOTATE
```

```
                \ CRASH AVOIDANCE RADAR
        \ TEST SEGMENT PROCESSING SOFTWARE
\ WXC 12/11/85
\ IT IS WRITTEN TO ACQUIRE A COMPLETE TEST SEQUENCE OF DATA AND
\ STORE IT AS A SIGLE-SEGMENTED DATA FILE ON DISK.  THIS EASES
\ THE JOB OF LATER ACCESSING THE DISK FILE FOR DATA MANIPULATING
\ AND/OR PLOTTING.  THE MAXIMUM TRANSMITTED PULSES, ASSUMING A
\ SINGLE TARGET RETURN PER TRANSMISSION, IS ABOUT 2000 PULSES.
\ THIS CORRELATES TO A TEST SEGMENT TIME OF 176 SECONDS.
\ SHORTER TEST SEGMENTS CAN BE ACCOMODATED BY STOPPING THE TAPE
\ AND DOING CONTROL/BREAK.  THE VARIABLE ICOUNT WILL INDICATE
\ THE SIZE OF THE DATA ARRAY.
\
\ DEFINE INPUT & OUTPUT DATA ARRAYS AND COUNTERS
DIM[ 112 ] DMA.ARRAY INDATA
INTEGER DIM[ 2020 , 4 ] ARRAY OUTDAT
INTEGER SCALAR EYE
INTEGER SCALAR HITS
INTEGER SCALAR BNUM
INTEGER SCALAR ICOUNT
INTEGER SCALAR CNDX
INTEGER SCALAR BFIRST
\
\ DEFINE HIT ARRAY, THRESHOLDS AND RANGE/ANGLE INDICES
\ SET UP FOR OUTPUT FILENAME
INTEGER DIM[ 56 ] ARRAY HARRAY
INTEGER SCALAR THRSH
INTEGER SCALAR RNDX
INTEGER SCALAR ANDX
INTEGER SCALAR THRSH1
14     STRING FILENAME
\
\ SET UP THE A/D CONVERTER PARAMETERS
0 1 A/D.TEMPLATE ZERO.ONLY
1 A/D.GAIN
.037 CONVERSION.DELAY
EXT.TRIG
A/D.INIT
INDATA DMA.TEMPLATE.BUFFER
\
\ SET THRESHOLDS AND ZERO ARRAYS/CONSTANTS
: INITIALIZE
0 BNUM :=
0 EYE :=
0 ICOUNT :=
0 OUTDAT :=
0 HARRAY :=
0 HITS :=
CR ." INPUT THRESHOLD VALUE: "
BEGIN
#INPUT NOT
WHILE
" INVALID NUMBER, REENTER: "
REPEAT


ASYST Version 1.5
Page 1    c:testseg.car    03/18/86    10:06
```

```
DUP THRSH1 :=
1 - THRSH :=
;
\
\ BEGIN THE DATA ACQUISITION LOOP UNTIL MEMORY FULL
: SCANSTORE
BEGIN
\
\ TAKE A DATA SET ( FILL INDATA ARRAY )
A/D.INIT
ZERO.ONLY A/D.IN>ARRAY(DMA)
BEGIN ?DMA.ACTIVE NOT UNTIL
\ UPDATE TRANSMITTED PULSE COUNTER
BNUM 1 + BNUM :=
\ SCAN THE INPUT ARRAY FOR NUMBER OF HITS
THRSH1 INDATA [ 1 ] :=
\ SET VARIABLE THRESHOLD INSIDE MAIN BANG HOLDOVER
THRSH INDATA [ 3 ] :=  \ 3 IS THROWN AWAY ALWAYS
THRSH INDATA [ 5 ] :=  \ 5 IS THROWN AWAY ALWAYS
THRSH INDATA [ 7 ] :=  \ 7 IS THROWN AWAY ALWAYS
THRSH INDATA [ 9 ] :=  \ 9 IS THROWN AWAY ALWAYS
THRSH INDATA [ 11 ] := \ 11 IS THROWN AWAY ALWAYS
THRSH INDATA [ 13 ] := \ 13 IS THROWN AWAY ALWAYS
THRSH INDATA [ 111 ] := \ 111 IS THROWN AWAY ALWAYS
INDATA SUB[ 1 , 112 , 2 ] THRSH [>]
TRUE.INDICES
1 []DIM HITS :=
REV[ 1 ]
2 * 1 -
HARRAY SUB[ 1 , HITS , 1 ] :=
HITS 1 >
\ IF NUMBER OF HITS > ONE THEN DO ONE LESS
\    (HIT ARRAY HAS BEEN REVERSED)
IF
HITS 1 - HITS :=
THEN
\ ENTER MEMORY WRITE LOOP
HITS 0 DO I
1 + EYE :=
ICOUNT 1 + ICOUNT :=
BNUM
HARRAY [ EYE ]
DUP DUP
RNDX :=
1 + ANDX :=
INDATA [ ANDX ]
INDATA [ RNDX ]
\ WRITE DATA TO MEMORY
OUTDAT [ ICOUNT , 4 ] :=
OUTDAT [ ICOUNT , 3 ] :=
OUTDAT [ ICOUNT , 2 ] :=
OUTDAT [ ICOUNT , 1 ] :=
LOOP
0 HARRAY SUB[ 1 , HITS , 1 ] :=


ASYST Version 1.5
Page 2    c:testseg.car    03/18/86    10:07
```

```
\  EXIT WHEN >= TO 2000
ICOUNT 2000 >= UNTIL EXIT
;
\
\ ROUTINE TO INVOKE WRITING THE COLLECTED DATA TO
\ A DISK FILE.  FILE SIZE IS BASED ON THE ACTUAL DATA
\ COUNT "ICOUNT" AND WILL BE APPROXIMATELY 60,000 BYTES
: WRFILE
FILE.TEMPLATE
1 COMMENTS
INTEGER DIM[ 2020 , 4 ] SUBFILE
END
CR ." TO WRITE THE DATA TO DISK ENTER A 1 "
CR ." OTHERWISE ENTER A ZERO. "
BEGIN
#INPUT NOT
 WHILE
 " NOT A NUMBER, REENTER: "
   REPEAT
0 =
IF EXIT
  THEN
CR ." NAME OF DATA FILE? "
"INPUT FILENAME ":=
FILENAME DEFER> FILE.CREATE
FILENAME DEFER> FILE.OPEN
CR ." YOU HAVE 64 CHARACTERS TO INPUT THE TOTAL DATA COUNT "
CR ." (ICOUNT); THE FIRST TRANSMITTED PULSE NUMBER; AND THE "
CR ." LAST TRANSMITTED PULSE NUMBER.  INCLUDE SOME TEST NAME ALSO: "
CR ." REMEMBER A CARRIAGE RETURN ENDS THIS INPUT! "
CR
"INPUT
1 >COMMENT
OUTDAT ARRAY>FILE
FILE.CLOSE
CR
;
\
\ THE EXECUTIVE ROUTINE THAT ACTUALLY MAKES ALL THIS RUN
\ IN A SEQUENCE.
: EXEC
  INITIALIZE
   SCANSTORE
CR ." THE LAST DATA SET NUMBER IN MEMORY WAS " ICOUNT .
    WRFILE
CR
;
F9 FUNCTION.KEY.DOES EXEC
```

```
\          COLLISION AVOIDANCE RADAR DATA PROCESSING PROG
\          TARGET DISCRIMINATE & PLOT PROGRAM
\   SECOND LEVEL RADAR DATA PROCESSING - - TARGET ID
\  WXC 12/11/85
\ THIS SOFTWARE ACCESSES DATA FILES WRITTEN BY TESTSEG.CAR AND
\ ESTABLISHES IDENTITIES OF INDIVIDUAL TARGETS SEEN DURING THE
\ DATA RUN.  TARGET RANGE EXTENT IS ABOLISHED AND A TARGET IS
\ DEFINED BY ITS CLOSEST POINT.
\
\ THE TARGET IS DENOTED BY A POINTER WHICH SHOWS
\ WHERE THE VALID TARGETS ARE WITHIN THE ORIGINAL
\ DATA ARRAY OR FILE SEGMENT.
8 4 FIX.FORMAT
INTEGER DIM[ 2020 , 4 ] ARRAY FILSEG
INTEGER DIM[ 20 ] ARRAY TARA
INTEGER DIM[ 2020 ] ARRAY TM1
INTEGER DIM[ 2020 ] ARRAY TME
INTEGER DIM[ 2020 ] ARRAY RAN
INTEGER DIM[ 2020 ] ARRAY ANG
INTEGER DIM[ 2020 ] ARRAY PTAR
INTEGER SCALAR SFILNUM
INTEGER SCALAR ISTART
INTEGER SCALAR ILIM
INTEGER SCALAR IC
INTEGER SCALAR ICT
INTEGER SCALAR IPT
INTEGER SCALAR TSTART
INTEGER SCALAR HDX
INTEGER SCALAR NDX
INTEGER SCALAR II
INTEGER SCALAR HITS
INTEGER SCALAR TOTHITS
INTEGER SCALAR ITEMP
INTEGER SCALAR I3
INTEGER SCALAR I4
FILE.TEMPLATE
1 COMMENTS
INTEGER DIM[ 2020 , 4 ] SUBFILE
END
14 STRING FILENAME
1 STRING SYMPLT
22 STRING TESTSEG
: OPENF
CR ." INPUT NAME OF DATA FILE? "
"INPUT FILENAME ":=
FILENAME DEFER@ FILE.OPEN
;
\
\ SET UP AND RE-ESTABLISH CONSTANTS/COUNTERS
: INITIALIZE
0 SFILNUM :=
0 ISTART :=
0 ILIM :=
0 IC :=


ASYST Version 1.5
Page 1    c:disseg.car    03/17/86    09:20
```

```
0 ICT :=
0 IPT :=
0 TSTART :=
0 HDX :=
0 NDX :=
0 II :=
0 HITS :=
0 FILSEG :=
0 TARA :=
0 TM1 :=
0 TME :=
0 RAN :=
0 ANG :=
0 TOTHITS :=
0 PTAR :=
;
\
: SMAP
GRAPHICS.DISPLAY
CURSOR.OFF
DOTTED
TME SUB[ 1 , TOTHITS ] .088 *
RAN SUB[ 1 , TOTHITS ] 4.625 *
XY.AUTO.PLOT
NORMAL.COORDS
.4 .05 POSITION
" TIME (SEC) " LABEL
270 LABEL.DIR
.01 .85 POSITION
" RANGE (FEET) " LABEL
0 LABEL.DIR
0 0 POSITION
;
: DIFMAP
GRAPHICS.DISPLAY
CURSOR.OFF
DOTTED
TME SUB[ 1 , TOTHITS ] .088 *
ANG SUB[ 1 , TOTHITS ] .0012207 *
XY.AUTO.PLOT
NORMAL.COORDS
.4 .05 POSITION
" TIME (SEC) " LABEL
270 LABEL.DIR
 .01 .85 POSITION
" ANG CHAN VOLTS " LABEL
0 LABEL.DIR
0 0 POSITION
;
: ANNOTATE
CR ." ENTER THE TEST TITLE/NAME (22 CHAR MAX) "
"INPUT TESTSEG ":=
CR ." INPUT THE HP PLOT SYMBOL DESIRED (PT PLOTS ONLY HERE) "
"INPUT SYMPLT ":=


ASYST Version 1.5
Page 2    c:disseg.car    03/17/86    09:20
```

```
;
: RANHP
AXIS.DEFAULTS
HP7470
PLOTTER.DEFAULTS
SYMPLT SYMBOL
TME SUB[ 1 , TOTHITS ] .088 *
RAN SUB[ 1 , TOTHITS ] 4.625 *
XY.AUTO.PLOT
.015 .058 CHAR.SIZE
NORMAL.COORDS
.4 .075 POSITION
" TIME (SEC) " LABEL
90 LABEL.DIR
.07 .35 POSITION
" RANGE (FEET) " LABEL
0 LABEL.DIR
.4 .9 POSITION
.012 .04 CHAR.SIZE
TESTSEG LABEL
;
: ANGHP
AXIS.DEFAULTS
HP7470
PLOTTER.DEFAULTS
SYMPLT SYMBOL
TME SUB[ 1 , TOTHITS ] .088 *
ANG SUB[ 1 , TOTHITS ] .0012207 *
XY.AUTO.PLOT
.015 .058 CHAR.SIZE
NORMAL.COORDS
.4 .075 POSITION
" TIME (SEC) " LABEL
90 LABEL.DIR
.07 .35 POSITION
" ANG CHAN VOLTS " LABEL
0 LABEL.DIR
.4 .9 POSITION
TESTSEG LABEL
;
\
\ SIZEFIND EXAMINES THE FILE SEGMENT JUST READ TO ESTABLISH
\ THE NUMBER OF ENTRIES.  THE FULL SEGMENT IS 766 4-ELEMENT
\ ENTRIES.  THE RESULT OF SIZEFIND IS THE PARAMETER ILIM.
\ IT MAY BE 766 OR LESS.  PROCESSING OF DATA FROM THE SEGMENT
\ SHOULD USE ILIM TO PROPERLY TRUNCATE THE FILE.
: SIZEFIND
TM1 [ 1 ] ISTART :=
  BEGIN
   IC 1 + IC :=
   IC 2020 >
    IF
      0 IC :=
     2020 ILIM :=
```

```
      EXIT
    THEN
      TM1 [ IC ] ISTART <
        IF
          IC 1 - ILIM :=
          0 IC :=
          EXIT
        THEN
  AGAIN
;
\
\ ONEPULSE ESTABLISHES ALL THE RADAR RETURNS THAT ARE
\ ASSOCIATED WITH A TRANSMITTED PULSE.  ICT IS THE
\ NUMBER OF RETURNS FOR THAT TRANSMITTED PULSE.  THE
\ PARAMETER IPT IS THE CORRECT POINTER FOR THE NEXT FILE
\ SEGMENT ELEMENT.
: ONEPULSE
0 ICT :=
TM1 [ IPT ] TSTART :=
IPT ILIM =
 IF
   1 IPT + IPT :=
   1 ICT + ICT :=
   EXIT
 THEN
 BEGIN
        1 IPT + IPT :=
         IPT ILIM >
         IF
            EXIT
         THEN
       1 ICT + ICT :=
        IPT ILIM =
        IF
           TM1 [ IPT ] TSTART >
            IF
              EXIT
            THEN
           IPT 1 + IPT :=
           ICT 1 + ICT :=
           EXIT
        THEN
       TM1 [ IPT ] TSTART >
 UNTIL
;
\
\ TARSEP IS THE ROUTINE TO EXAMINE ALL RETURNS FROM A
\ SINGLE TRANSMITTED PULSE AND IDENTIFY INDIVIDUAL TARGETS.
\ A TARGET WITH EXTENDED RANGE RETURN IS TRUNCATED SUCH THAT
\ ITS VALUE IS ITS CLOSEST RANGE.  IN THE A/D CONVERTER ARRAY
\ THIS MEANS THE DIFFERENCE IN RANGE BIN VALUE MUST BE
\ GREATER THAN TWO.  IF THERE ARE TWO TARGETS SIDE-BY-SIDE
\ AND OCCUPYING TWO ADJACENT RANGE BINS, ONLY THE CLOSEST
\ TARGET WILL BE IDENTIFIED UNTIL THEIR SEPARATION SPANS
```

```
\ MORE THAN TWO BINS.
: TARSEP
0 HITS :=
1 HDX :=
IPT ICT - NDX :=
NDX TARA [ HDX ] :=
NDX 1 + IPT =
 IF
   EXIT
 THEN
BEGIN
     FILSEG [ NDX , 2 ]
     NDX 1 + NDX :=
      NDX IPT =
      IF
        EXIT
      THEN
     FILSEG [ NDX , 2 ] - 2 >
     IF
       1 HDX + HDX :=
       NDX TARA [ HDX ] :=
     THEN
NDX 1 + IPT =
UNTIL
;
\
\ POINTER ARRAY WRITE ROUTINE
: WRARAY
HITS 0 DO I
1 + II :=
II TOTHITS + ITEMP :=
TARA [ II ] PTAR [ ITEMP ] :=
LOOP
;
\
: READF
INITIALIZE
1 COMMENT>
FILE>UNNAMED.ARRAY
FILSEG :=
FILSEG XSECT[ ' , 1 ] TM1 :=
TM1 [ 1 ] ISTART :=
ISTART 0 =
IF
   CR ." THIS FILE SEGMENT IS EMPTY. "
ELSE
SIZEFIND
THEN
;
: MAIN
 INITIALIZE
 READF
1 IPT :=
BEGIN
```

```
0 TARA :=
  ONEPULSE
  TARSEP
   TARA TRUE.INDICES
   1 []DIM HITS := DROP
   WRARAY
   HITS TOTHITS + TOTHITS :=
  IPT ILIM >
UNTIL
0 I3 :=
TOTHITS 0 DO I
1 + I3 :=
PTAR [ I3 ] I4 :=
FILSEG [ I4 , 1 ] TME [ I3 ] :=
FILSEG [ I4 , 2 ] RAN [ I3 ] :=
FILSEG [ I4 , 3 ] ANG [ I3 ] :=
LOOP
CR ." JOB IS DONE! "
;
F9 FUNCTION.KEY.DOES OPENF
F10 FUNCTION.KEY.DOES MAIN
F7 FUNCTION.KEY.DOES SMAP
F8 FUNCTION.KEY.DOES DIFMAP
F1 FUNCTION.KEY.DOES RANHP
F2 FUNCTION.KEY.DOES ANGHP
F5 FUNCTION.KEY.DOES FILE.CLOSE
F6 FUNCTION.KEY.DOES ANNOTATE
```

```
\          COLLISION AVOIDANCE RADAR DATA PROCESSING PROG
\ WXC 1/7/86
\ THIS SOFTWARE ACCESSES DATA FILES WRITTEN BY TESTSEG.CAR AND
8 4 FIX.FORMAT
INTEGER DIM[ 2020 , 4 ] ARRAY FILSEG
INTEGER DIM[ 2020 ] ARRAY TM1
INTEGER DIM[ 2020 ] ARRAY RAN
INTEGER DIM[ 2020 ] ARRAY ANG
INTEGER DIM[ 2020 ] ARRAY PTAR
INTEGER SCALAR SFILNUM
INTEGER SCALAR ISTART
INTEGER SCALAR ILIM
INTEGER SCALAR IC
INTEGER SCALAR TSTART
INTEGER SCALAR RBIN
INTEGER SCALAR ICT
INTEGER SCALAR IOUT
INTEGER SCALAR ITEMP
FILE.TEMPLATE
1 COMMENTS
INTEGER DIM[ 2020 , 4 ] SUBFILE
END
14 STRING FILENAME
1 STRING SYMPLT
22 STRING TESTSEG
: OPENF
CR ." INPUT NAME OF DATA FILE? "
"INPUT FILENAME ":=
FILENAME DEFER> FILE.OPEN
;
\
\ SET UP AND RE-ESTABLISH CONSTANTS/COUNTERS
: INITIALIZE
0 SFILNUM :=
0 ISTART :=
0 ILIM :=
0 IC :=
0 TSTART :=
0 FILSEG :=
0 TM1 :=
0 RAN :=
0 ANG :=
0 PTAR :=
0 RBIN :=
0 ICT :=
0 IOUT :=
0 ITEMP :=
;
\
: SMAP
GRAPHICS.DISPLAY
CURSOR.OFF
DOTTED
TM1 SUB[ 1 , IOUT ] .088 *


ASYST Version 1.5
Page 1    c:selbin.car    03/17/86    09:25
```

```
RAN SUB[ 1 , IOUT ] 4.625 *
XY.AUTO.PLOT
NORMAL.COORDS
.4 .05 POSITION
" TIME (SEC) " LABEL
270 LABEL.DIR
.01 .85 POSITION
" RANGE (FEET) " LABEL
0 LABEL.DIR
0 0 POSITION
;
: DIFMAP
GRAPHICS.DISPLAY
CURSOR.OFF
DOTTED
TM1 SUB[ 1 , IOUT ] .088 *
ANG SUB[ 1 , IOUT ] .0012207 *
XY.AUTO.PLOT
NORMAL.COORDS
.4 .05 POSITION
" TIME (SEC) " LABEL
270 LABEL.DIR
 .01 .85 POSITION
" ANG CHAN VOLTS " LABEL
0 LABEL.DIR
0 0 POSITION
;
: ANNOTATE
CR ." ENTER THE TEST TITLE/NAME (22 CHAR MAX) "
"INPUT TESTSEG ":=
CR ." INPUT THE HP PLOT SYMBOL DESIRED (PT PLOTS ONLY HERE) "
"INPUT SYMPLT ":=
;
: RANHP
AXIS.DEFAULTS
HP7470
PLOTTER.DEFAULTS
SYMPLT SYMBOL
TM1 SUB[ 1 , IOUT ] .088 *
PTAR SUB[ 1 , IOUT ] .0012207 *
XY.AUTO.PLOT
.015 .058 CHAR.SIZE
NORMAL.COORDS
.4 .075 POSITION
" TIME (SEC) " LABEL
90 LABEL.DIR
.07 .35 POSITION
" RANGE CHAN VOLTS " LABEL
0 LABEL.DIR
.4 .9 POSITION
.012 .04 CHAR.SIZE
TESTSEG LABEL
;
: ANGHP


ASYST Version 1.5
Page 2    c:selbin.car    03/17/86    09:25
```

```
AXIS.DEFAULTS
HP7470
PLOTTER.DEFAULTS
SYMPLT SYMBOL
TM1 SUB[ 1 , IOUT ] .088 *
ANG SUB[ 1 , IOUT ] .0012207 *
XY.AUTO.PLOT
.015 .058 CHAR.SIZE
NORMAL.COORDS
.4 .075 POSITION
" TIME (SEC) " LABEL
90 LABEL.DIR
.07 .35 POSITION
" ANG CHAN VOLTS " LABEL
0 LABEL.DIR
.4 .9 POSITION
TESTSEG LABEL
;
\
\ SIZEFIND EXAMINES THE FILE SEGMENT JUST READ TO ESTABLISH
\ THE NUMBER OF ENTRIES.  THE FULL SEGMENT IS 766 4-ELEMENT
\ ENTRIES.  THE RESULT OF SIZEFIND IS THE PARAMETER ILIM.
\ IT MAY BE 766 OR LESS.  PROCESSING OF DATA FROM THE SEGMENT
\ SHOULD USE ILIM TO PROPERLY TRUNCATE THE FILE.
: SIZEFIND
TM1 [ 1 ] ISTART :=
  BEGIN
   IC 1 + IC :=
   IC 2020 >
    IF
      0 IC :=
     2020 ILIM :=
      EXIT
    THEN
      TM1 [ IC ] ISTART <
        IF
          IC 1 - ILIM :=
          0 IC :=
          EXIT
        THEN
  AGAIN
;
\
: READF
INITIALIZE
1 COMMENT>
FILE>UNNAMED.ARRAY
FILSEG :=
FILSEG XSECT[ ! , 1 ] TM1 :=
TM1 [ 1 ] ISTART :=
ISTART 0 =
IF
   CR ." THIS FILE SEGMENT IS EMPTY. "
ELSE


ASYST Version 1.5
Page 3    c:selbin.car    03/17/86    09:26
```

```
SIZEFIND
THEN
;
: PICKOUT
BEGIN
 1 ICT + ICT :=
 ICT 2020 >=
  IF
     EXIT
  THEN
 FILSEG [ ICT , 2 ] RBIN =
  IF
     1 IOUT + IOUT :=
     FILSEG [ ICT , 1 ] TM1 [ IOUT ] :=
     FILSEG [ ICT , 2 ] RAN [ IOUT ] :=
     FILSEG [ ICT , 3 ] ANG [ IOUT ] :=
     FILSEG [ ICT , 4 ] PTAR [ IOUT ] :=
  THEN
     ILIM 10 - ITEMP :=
     ICT ITEMP >=
UNTIL
;
: MAIN
 INITIALIZE
 READF
CR ." INPUT THE DESIRED RANGE BIN VALUE: "
BEGIN
#INPUT NOT
WHILE
" INVALID NUMBER, RE-ENTER: "
REPEAT
RBIN :=
PICKOUT
0 PTAR [ 1 ] :=
5. PTAR [ 2 ] :=
0 ANG [ 1 ] :=
5. ANG [ 2 ] :=
CR ." MAIN IS DONE! "
;
F9 FUNCTION.KEY.DOES OPENF
F10 FUNCTION.KEY.DOES MAIN
F7 FUNCTION.KEY.DOES SMAP
F8 FUNCTION.KEY.DOES DIFMAP
F1 FUNCTION.KEY.DOES RANHP
F2 FUNCTION.KEY.DOES ANGHP
F5 FUNCTION.KEY.DOES FILE.CLOSE
F6 FUNCTION.KEY.DOES ANNOTATE
```

SECTION 10
SYSTEMS TEST

A general test plan for testing the CAR radar system was outlined in the memorandum of October 18, 1985, enclosed in the appendix. The system test effort was designed to fulfill these objectives. However, when it became obvious that the system could not perform adequately, continuance of the testing served no useful or evaluative purpose and the testing ceased.

This section will address the test environment, tests conducted, and data summaries.

TEST RANGE DESCRIPTION

The test range used for the systems tests is located at the rear of the facility in which the radar was developed. The range begins with a narrow two-lane road running west for approximately 600 feet. At the end of the 600-foot road the concrete broadens to a considerable expanse and continues west for some 1800 additional feet. When viewed from the air, the two-lane road appears as the shaft of an arrow and the broadened concrete area as an arrowhead. The land is flat and without trees. Thus, there were minimal clutter returns during the tests.

Some 500 feet of the two-lane road was measured and marked at range intervals of 50 feet. At the zero range mark, the footprint of the four tires of the van carrying the radar was painted with the van looking west along the centerline of the road. From this vantage point all the static calibration data was taken as well as some of the dynamic data. In general, the entire 2400-foot range was used to acquire the dynamic data taken.

HARDWARE CONFIGURATION

Figure 9-1 in the previous section shows the initial hardware configuration used during systems tests. Many static tests for calibration were done in this configuration and all the dynamic tests were done this way.

As the next sections will discuss, the reduction of system measurement errors to an acceptable level required that the VCR be removed from the system. Since no other recording medium was available, the AT&T 6300 and peripherals had to be installed in the radar van. All testing after this installation was with the radar van stationary.

ANGLE CALIBRATION TESTING

The initial end-to-end system test for the CAR radar was the angle channel calibration to establish the transfer function from voltage in the difference (angle) channel to LOS angle to the target in degrees. The target for these tests was a Luneburg lens with wide angular response. It was chosen for this spatial property plus the fact that it appears as a point target.

Figure 10-1 shows the results of the first attempt at calibrating the angle channel. The Luneburg lens was taken out to a range of 300 feet and moved from -8.5 degrees (left=minus) to +6.5 degrees. At each angle location a sample set of 100 A/D converter arrays was taken and the mean and standard deviation of that sample set calculated. The accumulation of these means and standard deviations are the points plotted in the figure.

In running this test the target lens was mounted on a tripod and raised some 3 feet off the ground. It is believed that this target height above the ground introduced significant effects from multipath propagation. These effects may explain the sawtoothed appearance in areas of the plot of figure 10-1.

The major property of the data plot in figure 10-1 that generated interest for further investigation was the standard deviation. A quick study of the plot shows that the measurement error increases with increasing channel voltage. Just the opposite should occur. The estimate of signal value should become more consistent as signal power increases. This inconsistency prompted a lengthy investigation of the angle channel.

The investigation started with a second angle calibration test. This time data sets were collected every 0.25 degrees for an angular interval from -3 to +3 degrees in front of the radar. During the test the possibility of multipath degrading the data was minimized by placing the target on the ground. Figure 10-2 is the plot of the angle channel response from this test.

The figure shows a shift between mechanical boresight (0.0 degrees on the axis) and peak electrical response from the radar's angle channel. This angular misalignment occurred when the radar was remounted on the van. As long as the error is known it can be accounted for and subtracted from the data.

In figure 10-2, the mean and standard deviation plotted at each angular interval are calculated from a set of 100 samples of measurements taken consecutively from the radar. Figure 10-3 shows the sample set from the 2 degree point of figure 10-2. The data points are plotted in the time order in which they were taken from the system which is why the abscissa is in seconds of time. From the figure it is obvious that the constancy of the measurement is not good. Thinking that the error was the result of inadequate signal power, additional measurements were done with 10 dB more signal power. The results were only marginally better meaning the error source is not limited power.

The follow-on troubleshooting centered on eliminating, systematically, portions of the system to isolate the origin of the error. The radar front-end through the video detectors was replaced by two high quality pulse generators. These two generators were externally triggered by the radar transmit trigger and then their outputs added to yield a double pulse resembling a radar "main bang" and a target at some range. Figure 10-4 shows an oscilloscope photograph taken of the output of the generator configuration.

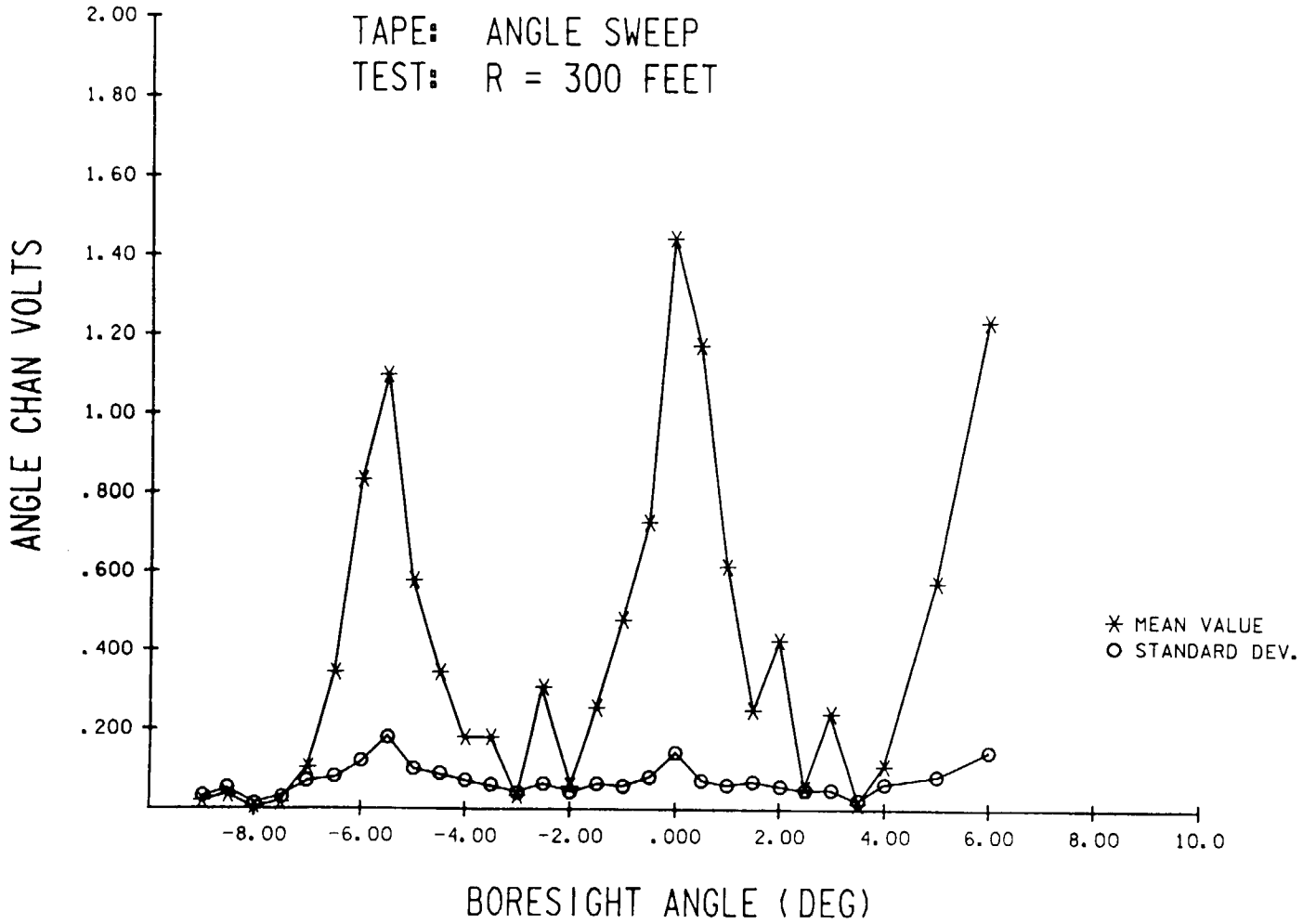

Figure 10-1.- Angle calibration curve (point target).

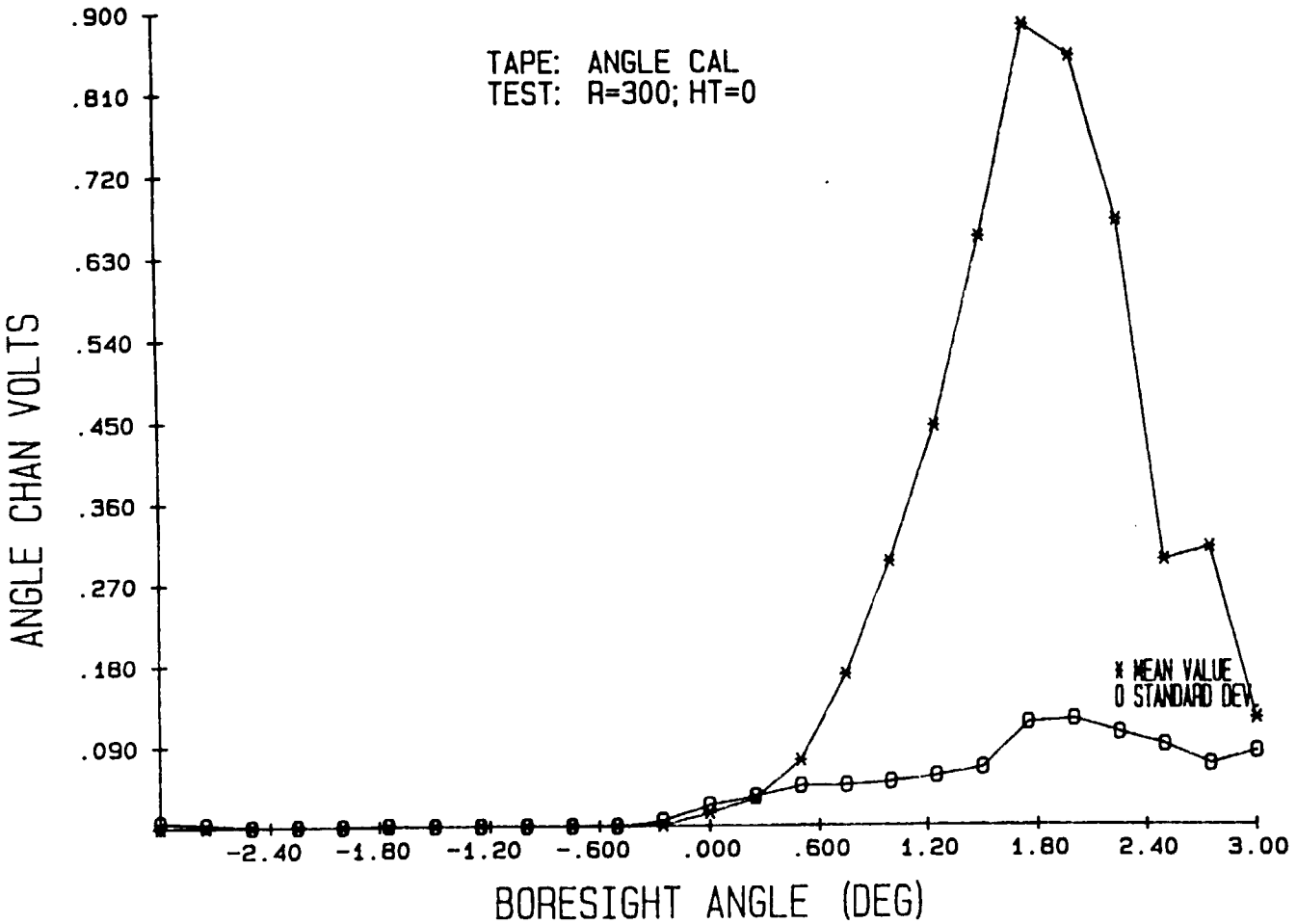

Figure 10-2.- Retest of angle channel with 0.25 degree resolution.

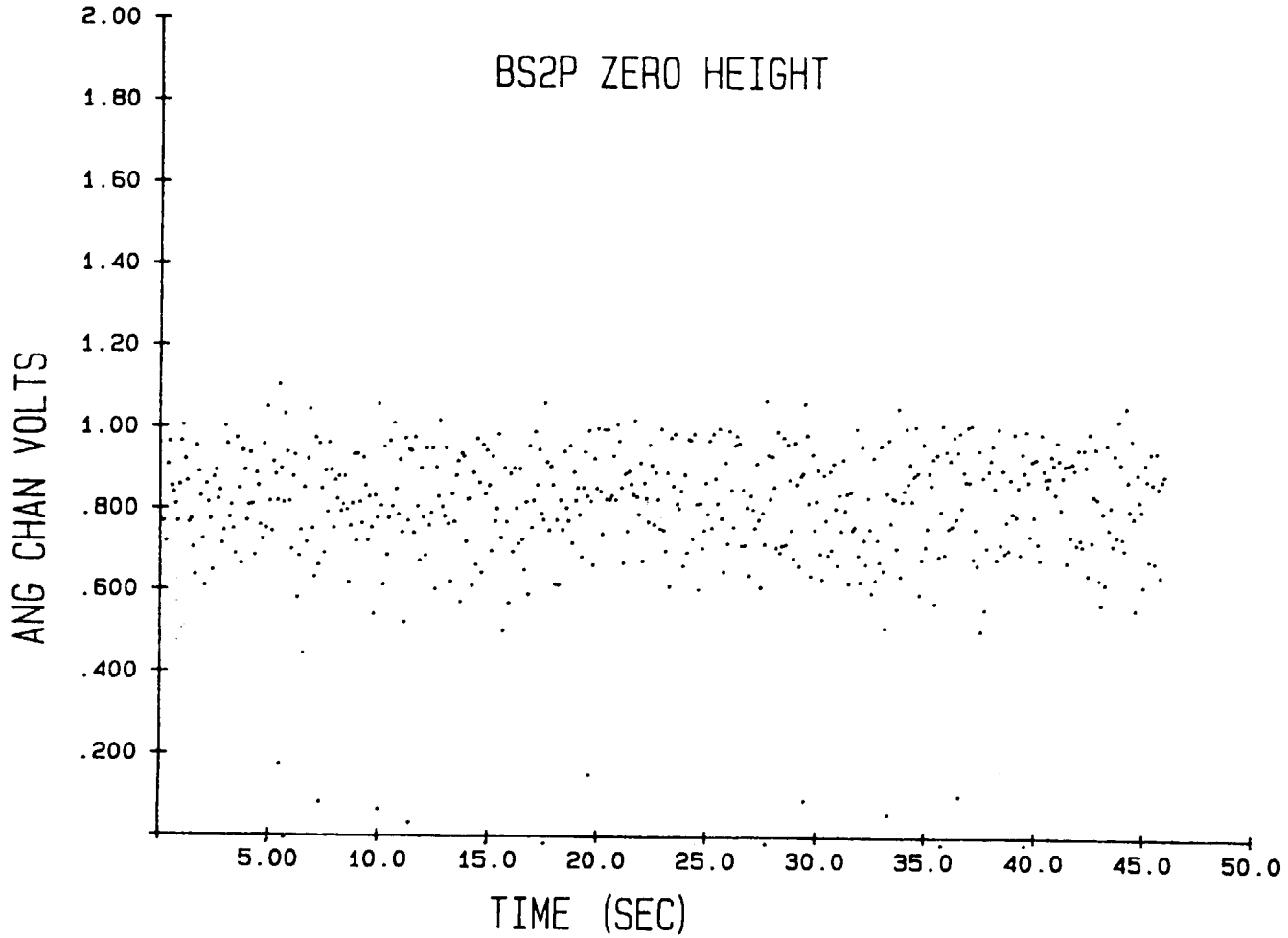

Figure 10-3.- Time history of angle channel voltage at 2.0 degrees from mechanical boresight.

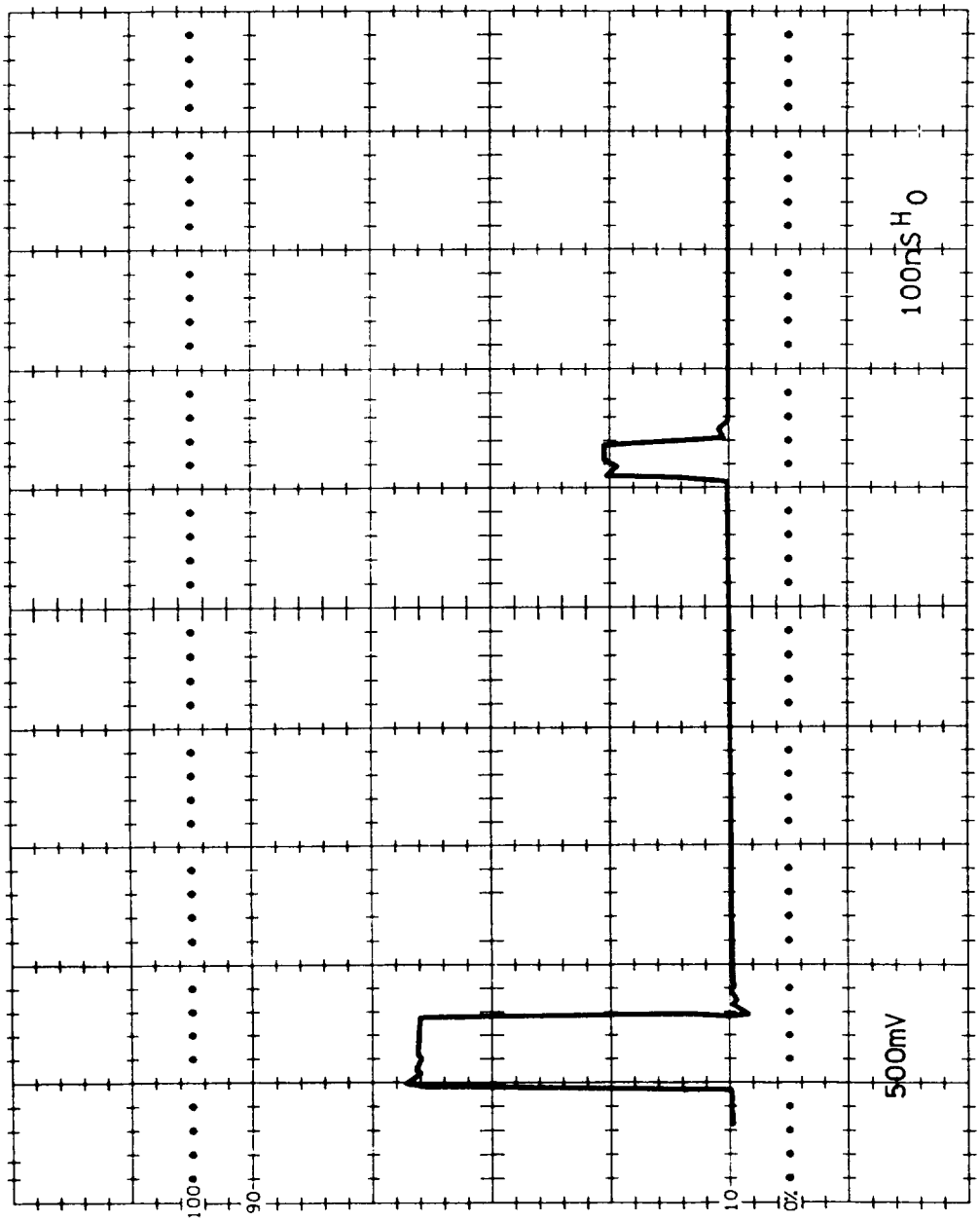

Figure 10-4.- Pulse generator reference for evaluating data acquisition system performance.

The signal shown in figure 10-4 became the basis for assessing the performance of the data acquisition system. While there are some line reflections that are present, the distortions are not great. The sharp crisp rise and fall times of the pulses greatly exceed the capability of the rest of the system to resolve. The clean, constant baseline is more than adequate as a reference. This signal was fed into both channels of the time expander system and signal quality was established at different points in the data acquisition chain.

Figure 10-5 shows the two channel output of the time expander board when driven by the input signal shown in figure 10-4. There are bandwidth limitations seen in the rise and fall times, but the baseline stability and signal-to-noise ratio are excellent. The top trace in figure 10-5 is the sum channel containing the range estimation. It is buffered through the matching amplifier (fig. 9-1) before driving the right channel of the stereo audio system of the VCR. It is also used as a reference to normalize the angle channel response to achieve an angle voltage independent of range and target size. The bottom trace in figure 10-5 is the difference channel output used to derive the angle channel when differenced from the sum channel. The resultant is the input to the left audio channel of the VCR.

Figure 10-6 is a photograph of the outputs of the amplifiers driving the VCR. The top trace is the range channel. The uncertainties seen in the rise and fall times of the bottom trace arise from time variances in the two waveforms being differenced to form the normalized angle channel. Except for these uncertainties, the shape of the target response is roughly the same as the target pulse in the top trace.

Testing of the VCR effects on the waveforms showed that the recorder was not adequate in its response to support the CAR radar effort. Its deficiencies were two: low frequency noise on the order of 100 to 200 millivolts probably from the IC's used and the effect of the ac-coupling on trying to read absolute voltages. Figure 10-7 shows this latter phenomenon in particular. Of interest in the figure are the bottom traces in each of the two photographs. They are the angle channel outputs. The top photo is the return from a point target at 75 feet in range (the target is just below the 2 volt symbolic indicator). The bottom photo is the same target at 300 feet in range (the target is in the center of the trace). The zero volt baseline in each case is the gridline just above the trace. Since the ac-coupling in the audio channel balances the area above and below the zero reference, the target at 75 feet has a greater apparent undershoot. This, plus the roughly 100 millivolt noise on the baseline, forced the decision to eliminate the VCR until such time as the angle channel calibration could be completed and verified.

Removal of the VCR forced a redesign of the signal conditioner unit in figure 9-1 and it forced a move of the computer from the lab to the radar van. These changes were accomplished and testing using pulse inputs to the time expander boards was continued. The objective of the testing was to achieve the usable angle channel response.

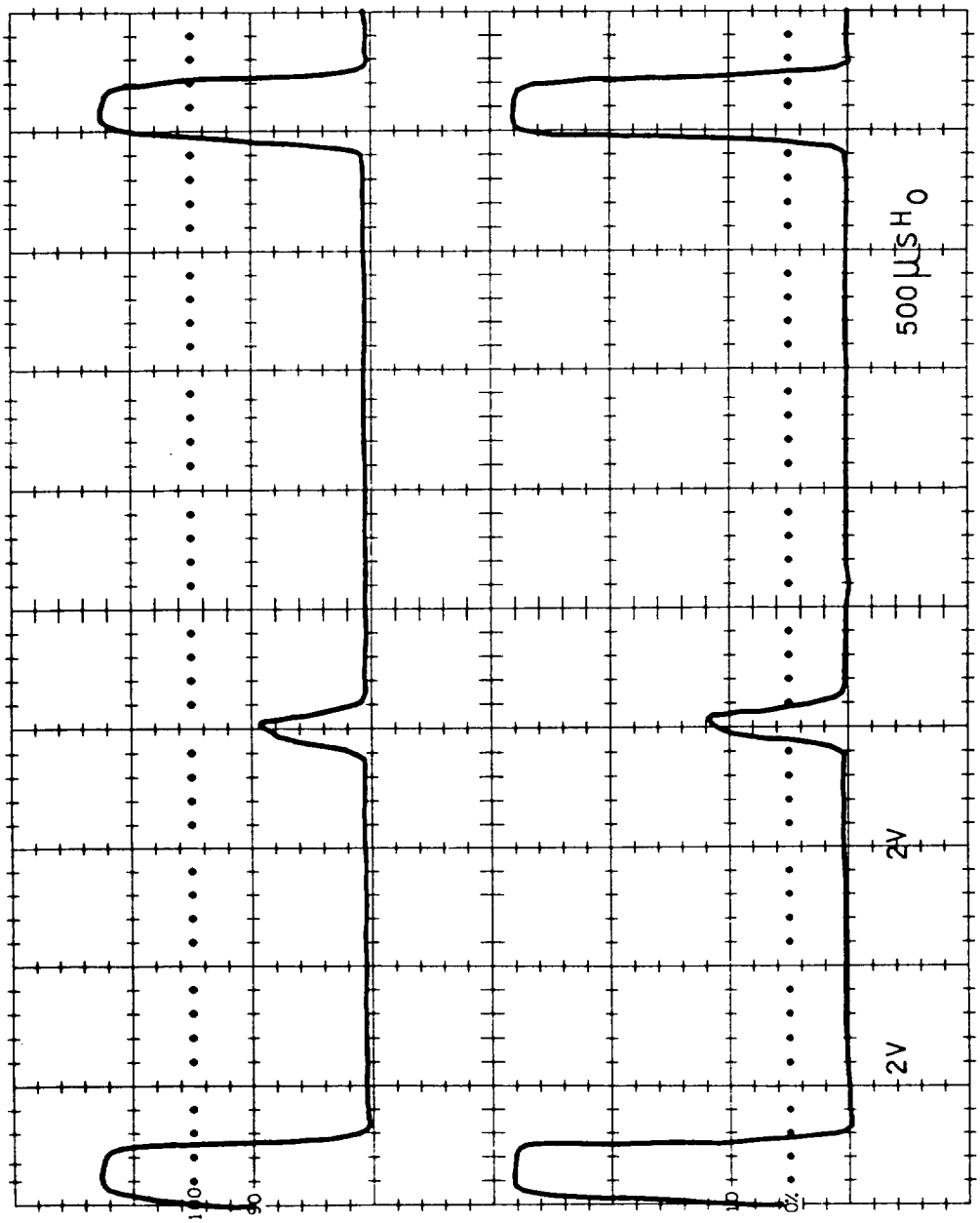

Figure 10-5.- Time expander board output when driven with input of figure 10-4. Top trace is range channel while bottom is angle channel.

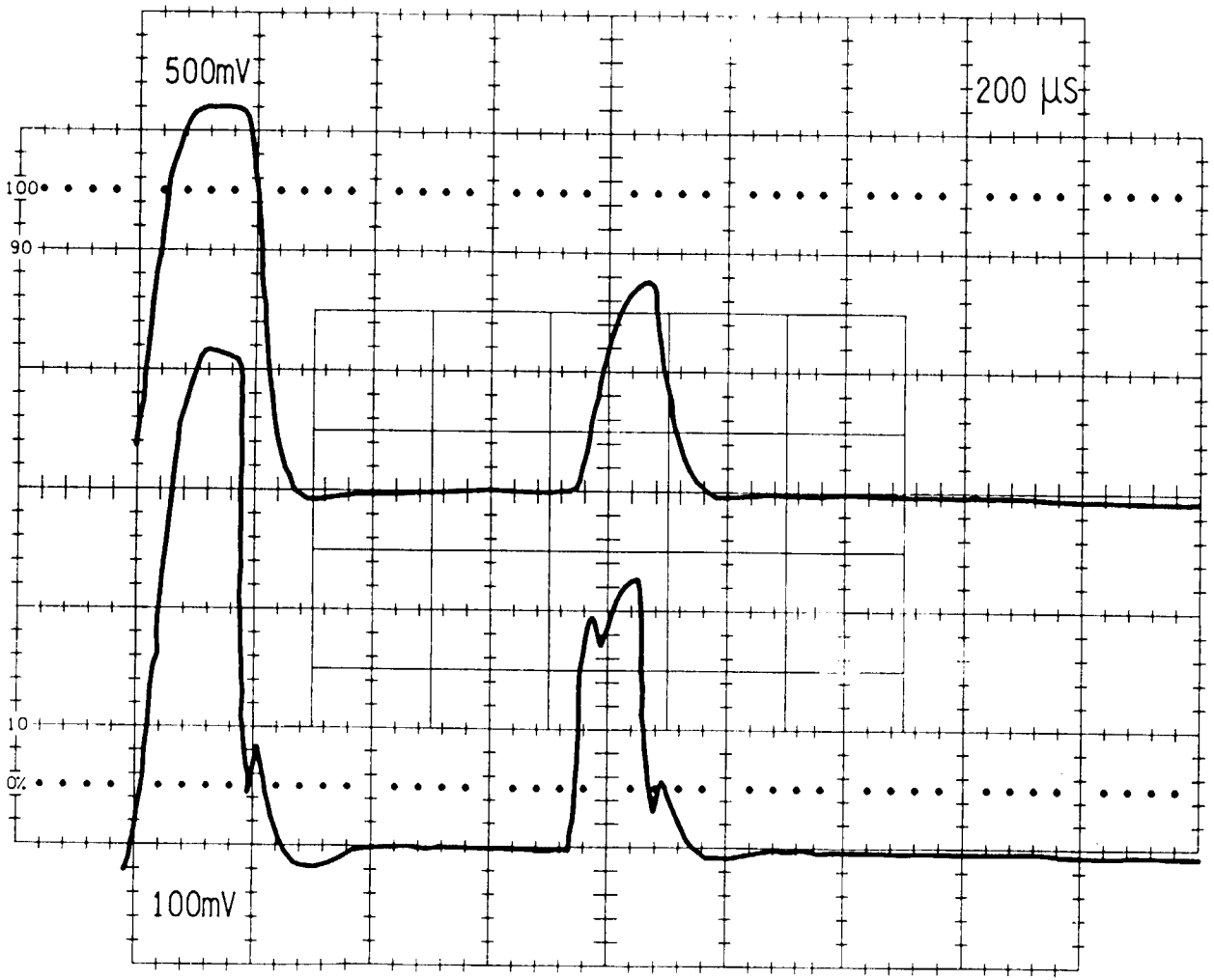

Figure 10-6.- Signal inputs to the VCR. Top trace is range. Bottom trace is angle.

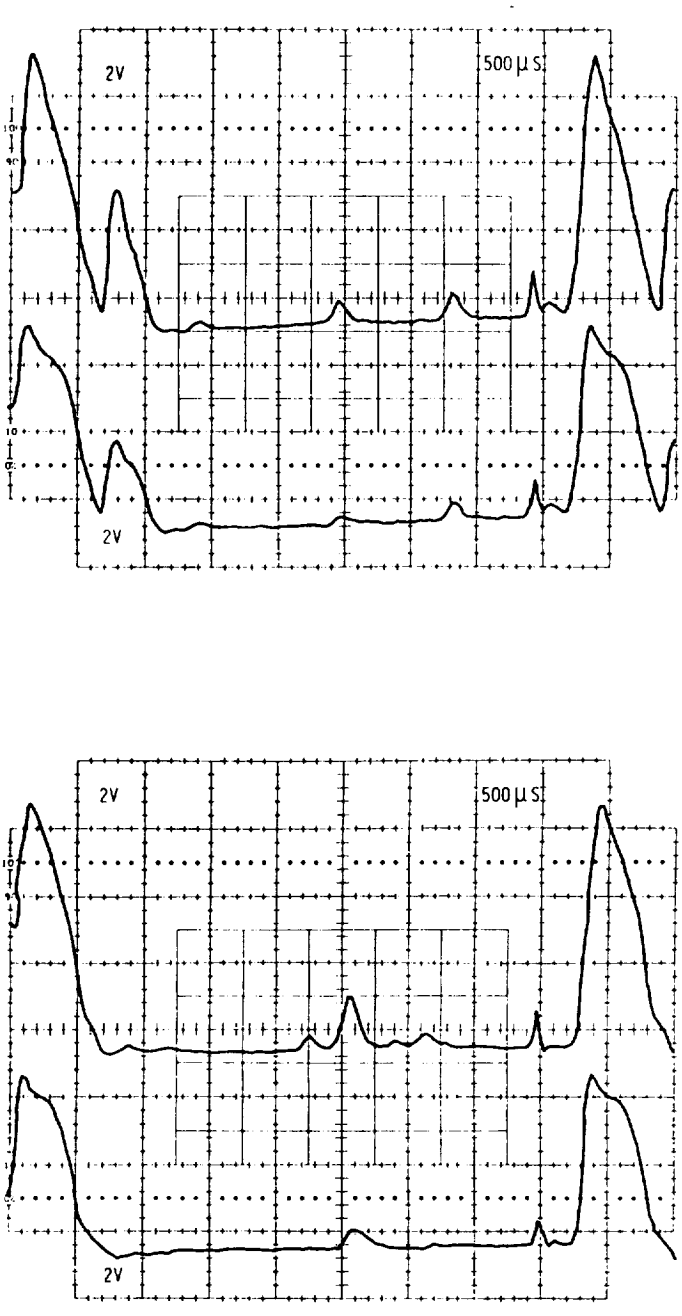

Figure 10-7.- Coupling effects in the VCR. Top photo is a point target at 75 feet. Bottom is the same target at 300 feet. Note baseline shift as a function of channel energy.

C-3

The pulse configuration of figure 10-4 was retested with the VCR out of system with the range and angle channel responses shown in figures 10-8 and 10-9, respectively. These are plots of the mean and standard deviation over a sample set of 100 for each range and angle bin. It is encouraging to note that the standard deviations are low and that apparently they do not increase with signal power. They do increase in regions of transitions. This, plus the low standard deviation at the measurement in the "center" of the target pulse, represents a significant improvement in performance over what had been seen earlier.

The angle measurement with the midpulse smallest standard deviation in figure 10-9 is associated with (or is the next A/D sampled after) range bin 53. The time history of this angle bin is plotted in figure 10-10. The peak-to-peak excursion of this measurement is roughly 100 millivolts. The improvement over the measurements in figure 10-3 is approximately a factor of four in voltage amplitude.

The next logical step in the testing was to increase the pulse width and the next data set taken was for a target pulse 60 ns wide. Figure 10-11 shows the angle channel response for this condition (the range response is similar and not shown here). These are now two angle measurements within the target return with low standard deviations. They are associated with range bins 53 and 55. Their time histories are plotted in figures 10-12 and 10-13, respectively. Figure 10-12 shows a peak-to-peak signal of significantly less than 100 millivolts and obvious improvement over figure 10-10. Figure 10-13 is obviously the best and represents a good estimate of the signal. This would be usable angle data from which to calibrate the channel.

The end in improvement by increasing pulse width needed to be found and thus the pulse width was increased from 60 to 70 ns. Fiugre 10-14 shows the angle channel response to that pulse width. It is noted that there are three data points within the target return that have low deviations on the measurements. These are the measurements associated with range bins 53, 55, and 57. (The range channel response is the same as the angle channel, but range will be indicated by the signal exceeding some threshold so that absolute voltage measurement is not required.) Figures 10-15, 10-16, and 10-17 show the time history for the angle estimates of the targets. The error in bin 53 is approximately the same as seen in the 60 ns case and bin 55 shows improvement over bin 53 as might be expected from the 60 ns case. Of particular interest is that bin 57 really doesn't show any appreciable error reduction over bin 55. There really was no point in increasing pulse widths any further and testing with the pulse generator was concluded.

The conclusions of the tests just discussed are that removal of the VCR was necessary and that increasing the transmitted pulse widths was also necessary. The first was necessary to maintain dc level in order to measure absolute voltage with a single-ended A/D converter input. The second was necessary to allow the limited-bandwidth, limited-sample rate system time enough to estimate the angle voltage.

The radar RF portion and the data acquisition system were connected and the transmitter modulator adjusted for a longer pulse width. The desired pulse width was 70 ns, but a modulator width of approximately 55 ns turned out to

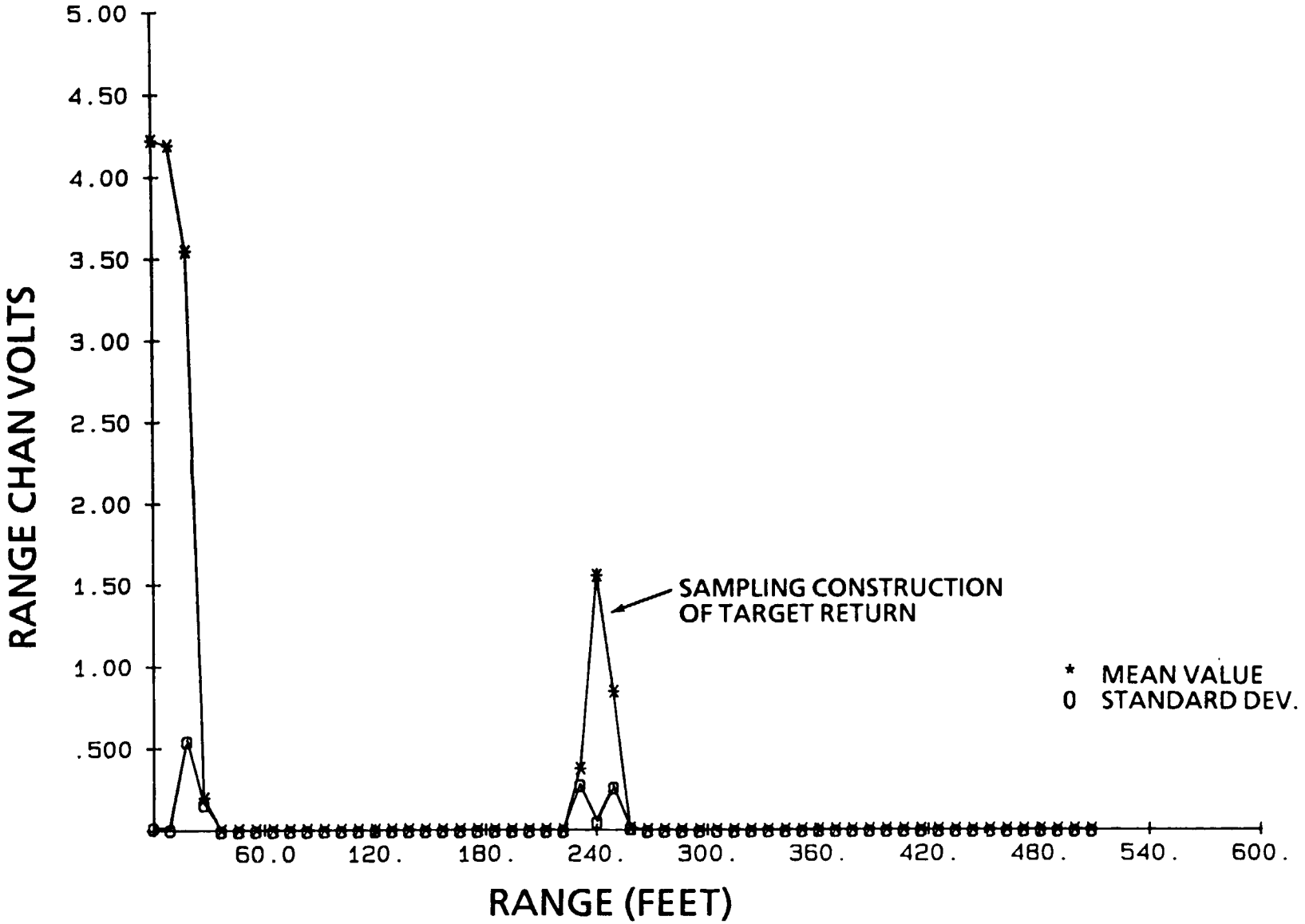

Figure 10-8.- Range channel response to pulse generator input with 30 ns target pulse width.

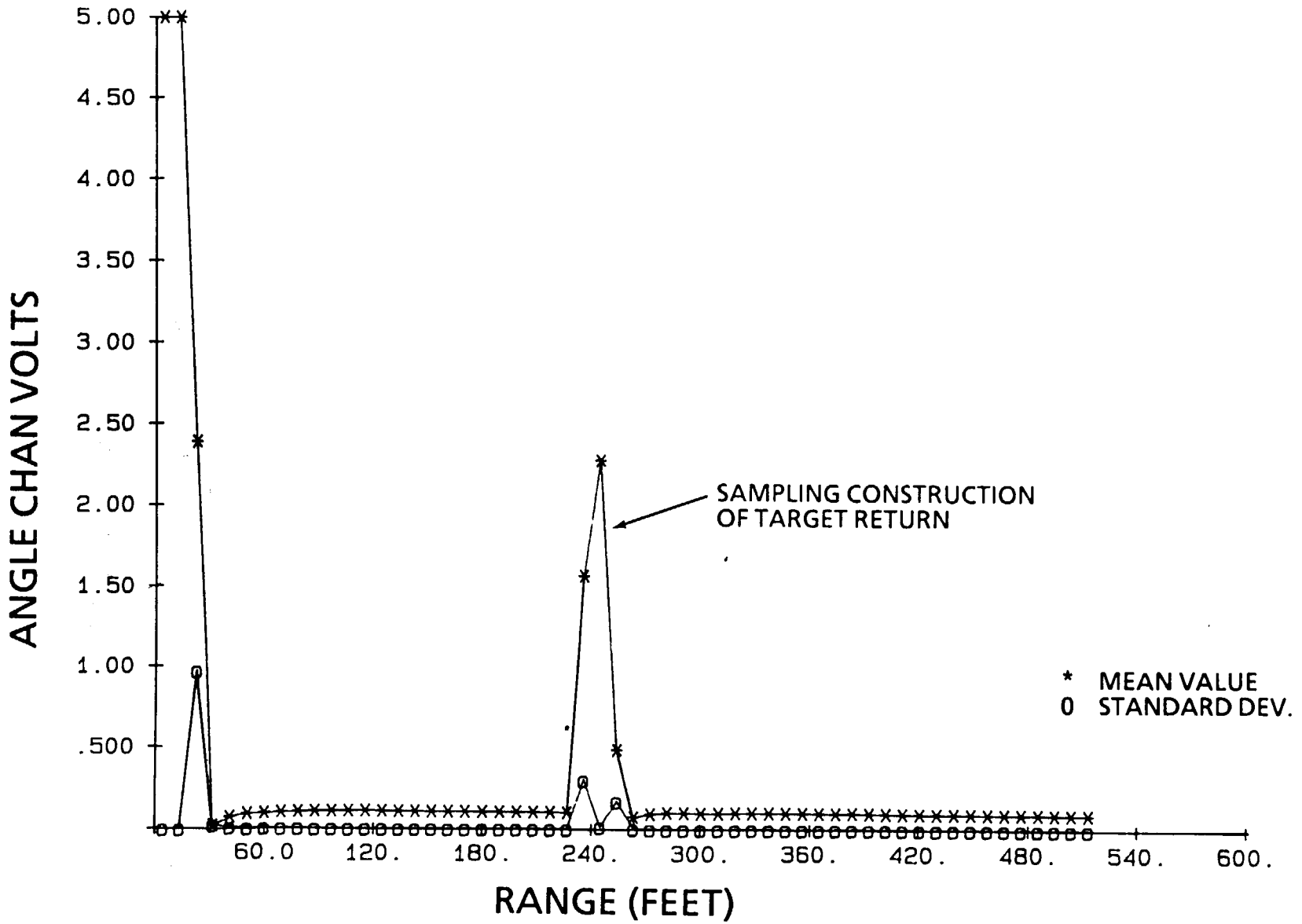

Figure 10-9.- Angle channel response to pulse generator input with 30 ns target pulse width.

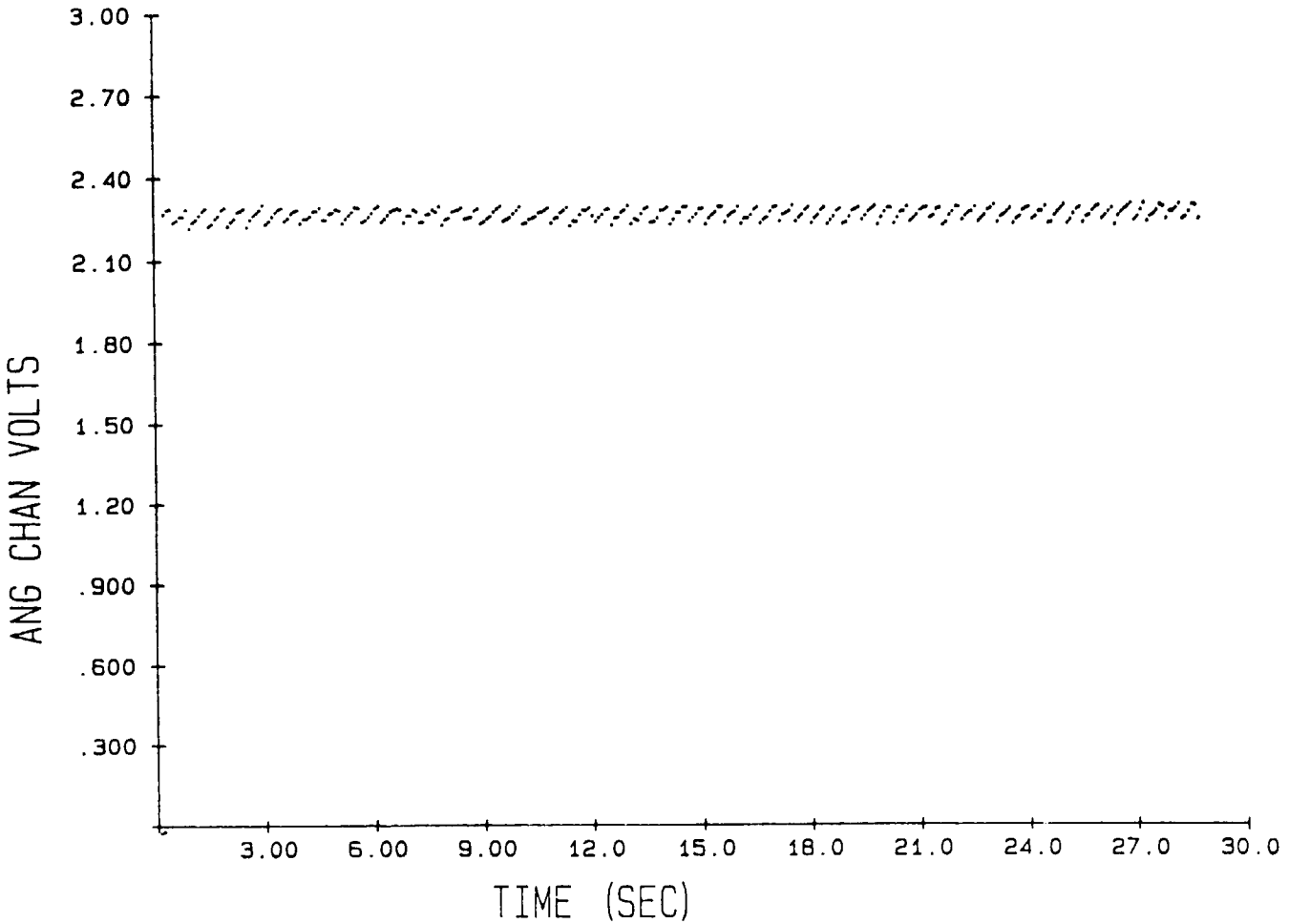

Figure 10-10.- Best angle channel estimation for a 30 ns target pulse from a pulse generator.

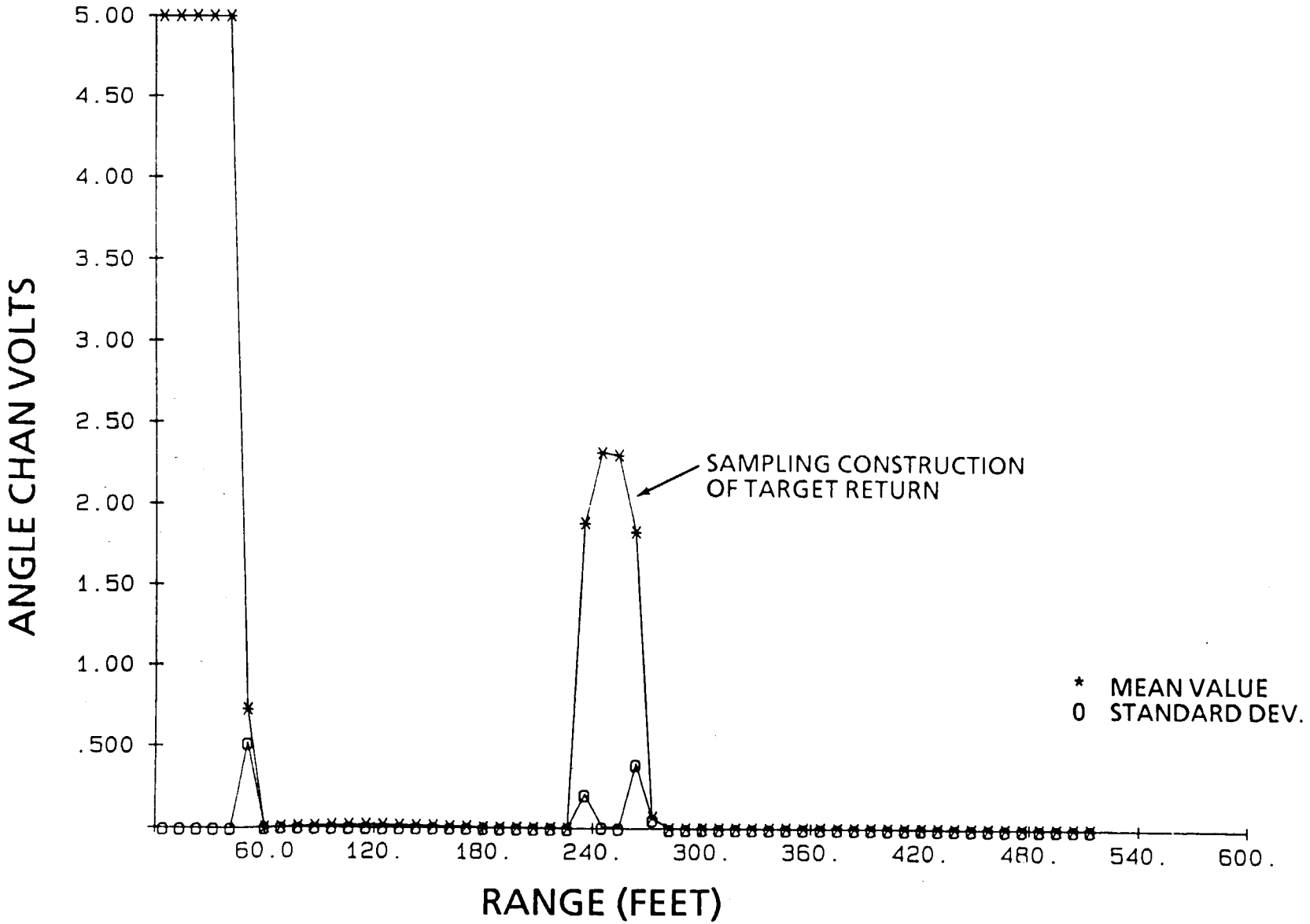

Figure 10-11.- Angle channel response to pulse generator input with a 60 ns target pulse width.

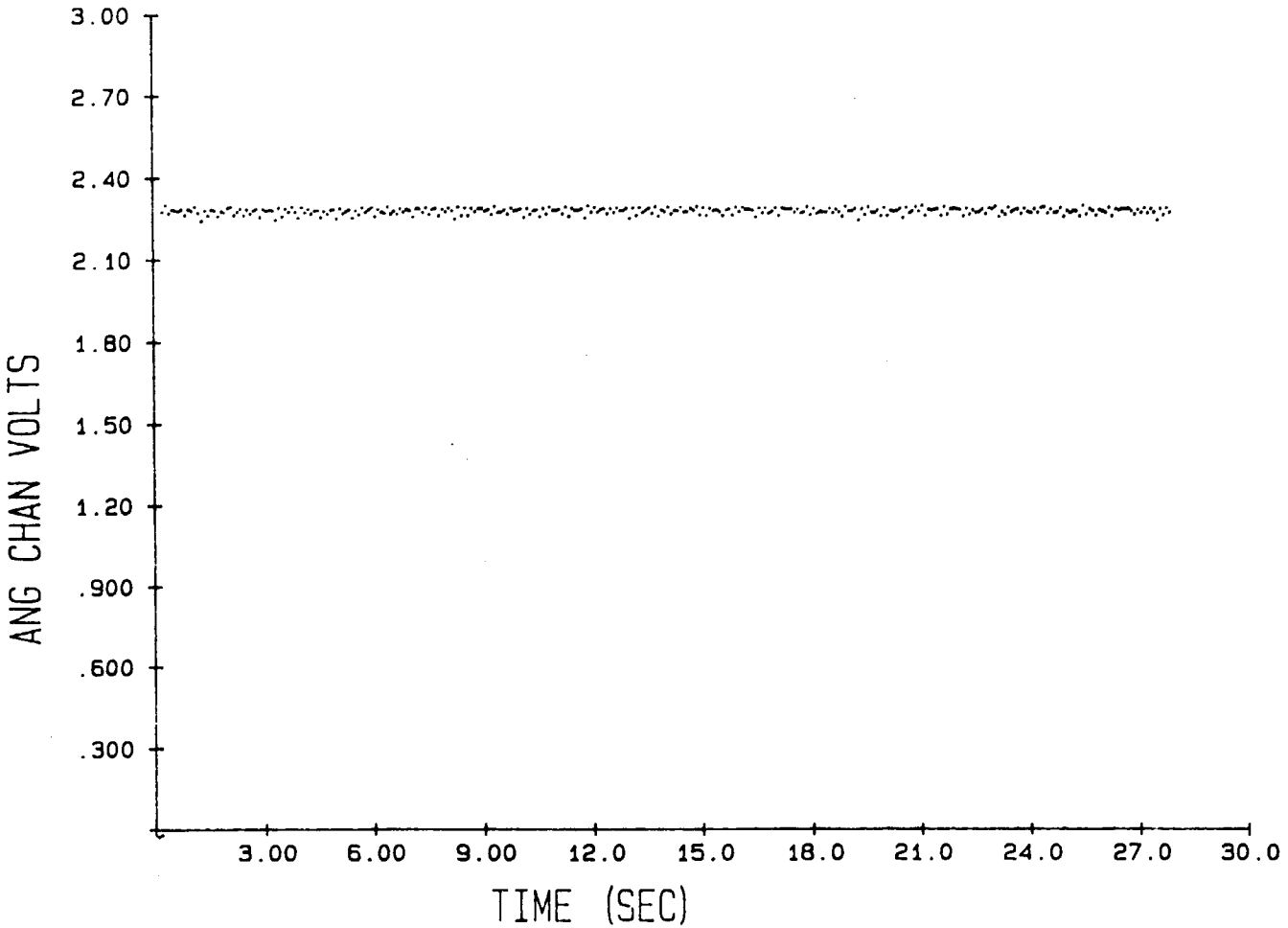

Figure 10-12.- Angle channel estimation for a 60 ns target pulse for range bin 53.

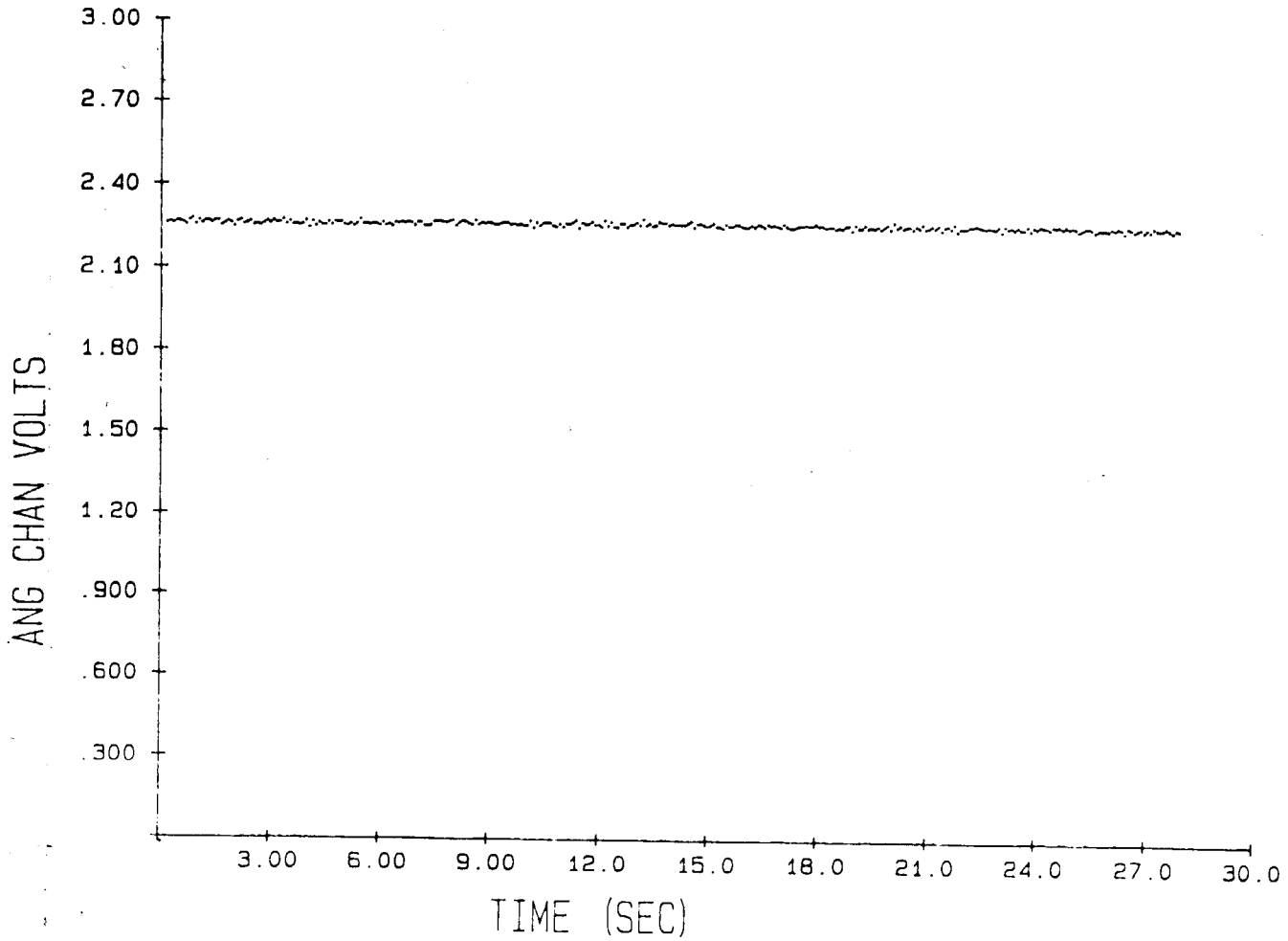

Figure 10-13.- Angle channel estimation for a 60 ns target pulse for range bin 55.

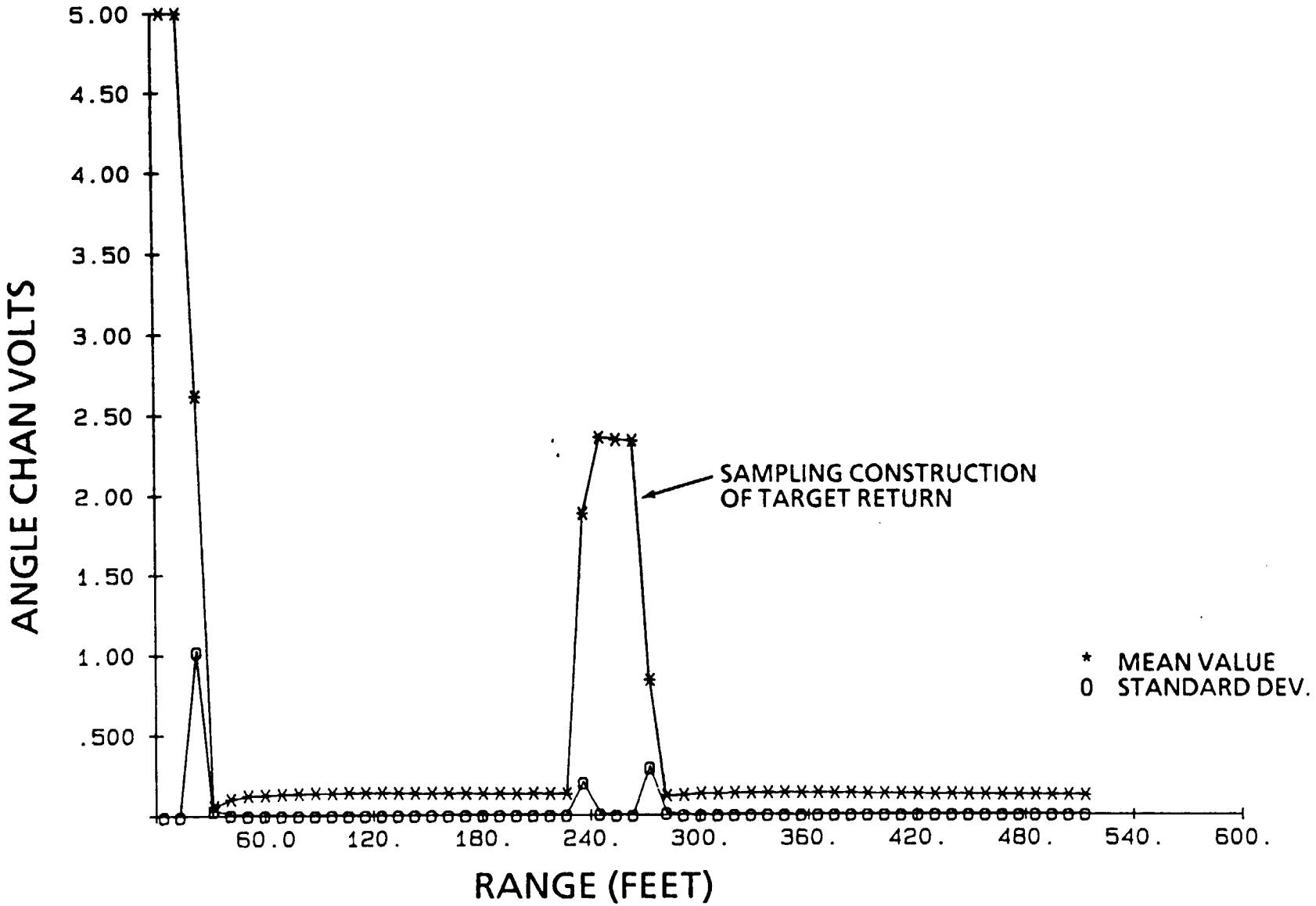

Figure 10-14.- Angle channel response to pulse generator input with a 70 ns target pulse width.

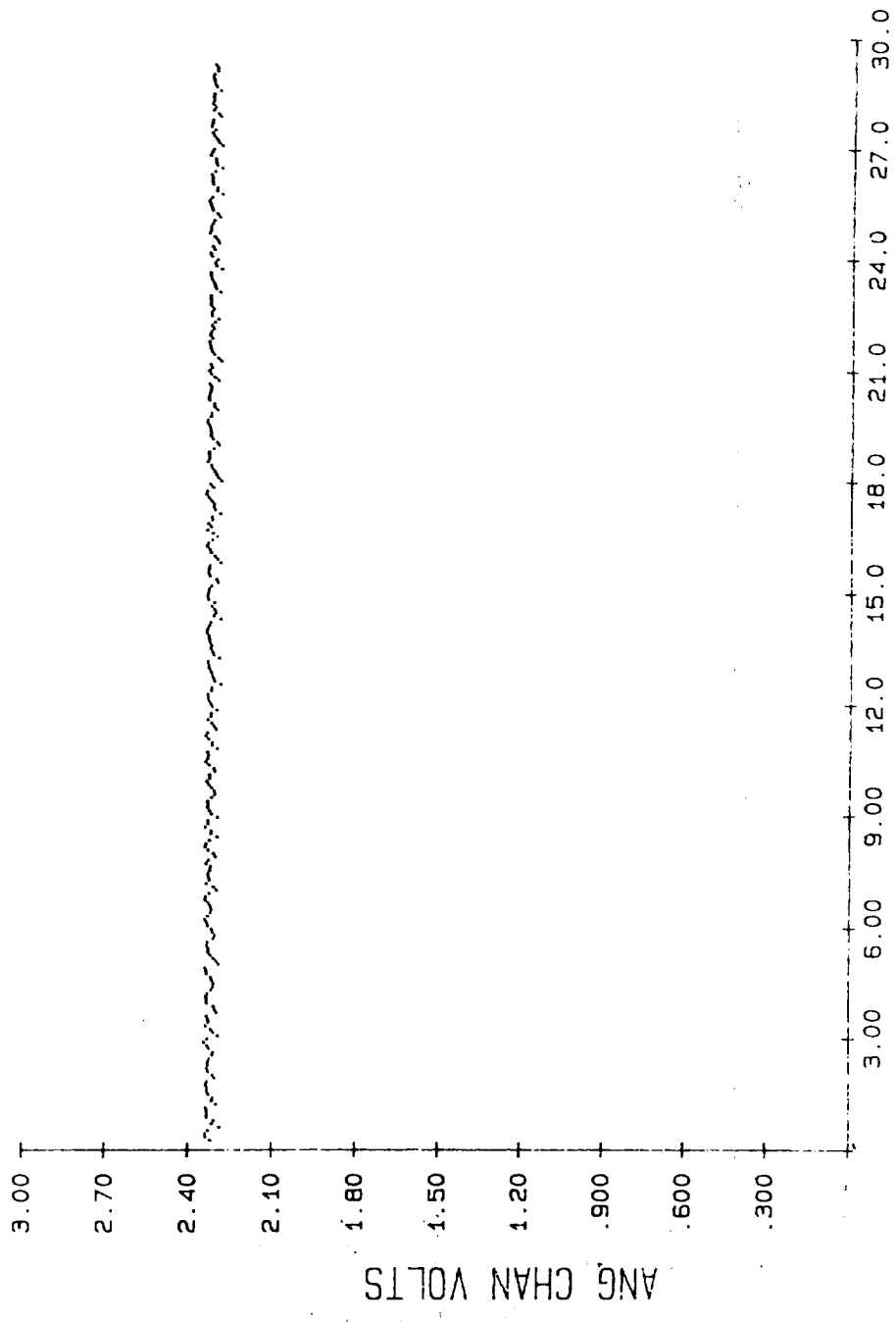

Figure 10-15.- Angle channel estimation for a 70 ns target pulse for range bin 53.

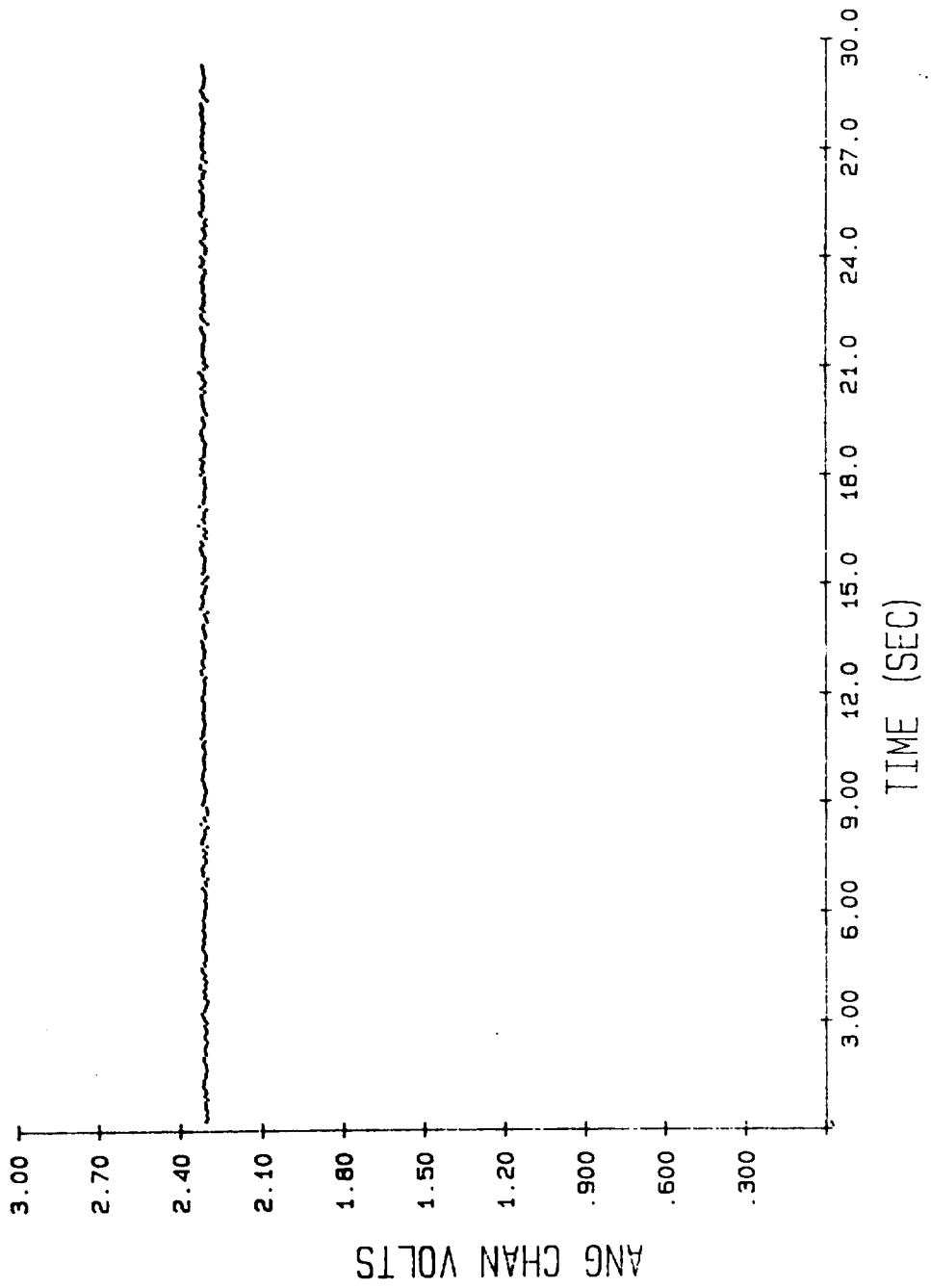

Figure 10-16.- Angle channel estimation for a 70 ns target pulse for range bin 55.

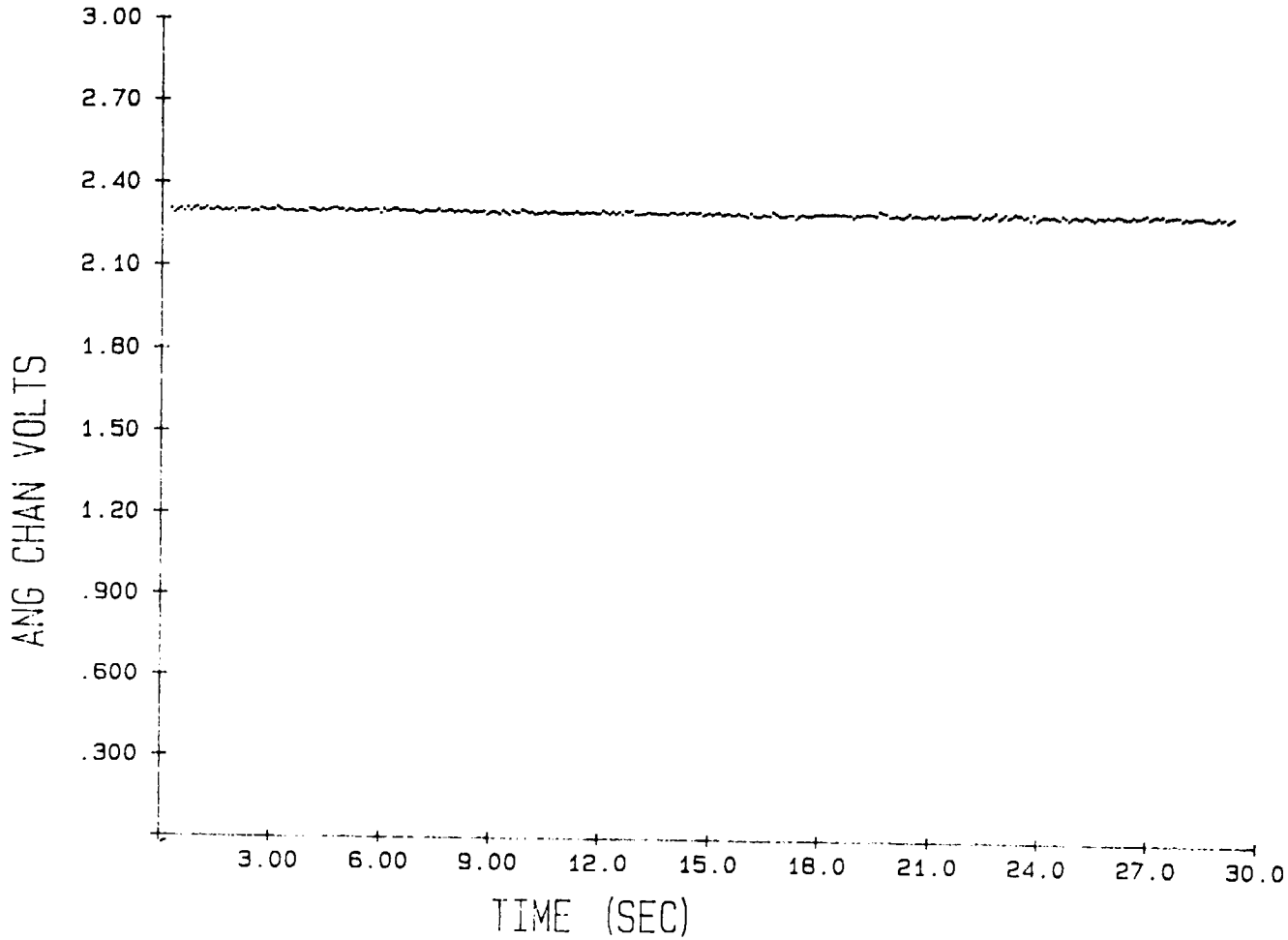

Figure 10-17.- Angle channel estimation for a 70 ns target pulse for range bin 57.

be the hardware limit. The point target Luneburg lens was used to test this configuration to see if angle channel response had been improved. Because of inclement weather the radar van had to remain indoors and measurements were made with the target placed outside the door and not on the original test range. The clutter in this new environment was quite high and the results presented here should be weighed against that fact. The system response in the angle channel is shown in figure 10-18. The target is located at a range of roughly 100 feet. Looking at the standard deviations it is seen that one of two points at the peak of the target return should yield the best voltage estimation. It so happens that the best estimation is in bin 23. A time history plot of this measurement is shown in figure 10-19. The results displayed here are encouraging also.

At this point in the system test, it appeared that a decent angle calibration could be accomplished with this modified configuration. Thus, when the weather cleared and with the computer, plotter, and printer all mounted inside the van, the system was moved back to the range. Here the angle calibration sequence, as performed to generate figure 10-1, was repeated. This time multipath was minimized by placing the point target on the ground.

Figure 10-20 is a plot of this calibration. The results and improvements of modifying the radar system by eliminating the VCR and increasing the pulse width can be seen by examining the standard deviation of each measurement. Instead of the standard deviation increasing with increased signal as was seen in figures 10-1 and 10-2, the measurement error decreases and stabilizes. This is the performance trend that is proper for this system.

Figure 10-20 also shows only one main response where three significant responses were noted in figure 10-1. In the earlier case the target had been some 3 feet off the ground and in the case of figure 10-20, the target was placed on the ground to minimize multipath. It is felt that the lowering of the target put it beneath the illuminating beam in the transmit antenna for the off-axis cases. The result is the single response noted around the zero degree electrical boresight.

The shift between mechanical boresight and electrical boresight that was shown in figure 10-2 is still present in this last calibration curve. It is emphasized in figure 10-20 by the two abscissa axes that are plotted to define the relationship between physical angle from the radar/vehicle to the target and the radar angle channel electrical voltage. This combination becomes the angle calibration for a point target.

The next section shows the effects of an extended target on this point target calibration curve.

STATIC TESTS - EXTENDED TARGETS

After successfully achieving the point target calibration curve for the angle channel, it was necessary to establish angle channel to a representative extended angle target. The target used was a 1977 midsized automobile (MSA) supplied by the Department of Transportation for the test program. The first test run was a static head-on test. The automobile was placed head-on to the radar along the electrical boresight. A statistical sample set of

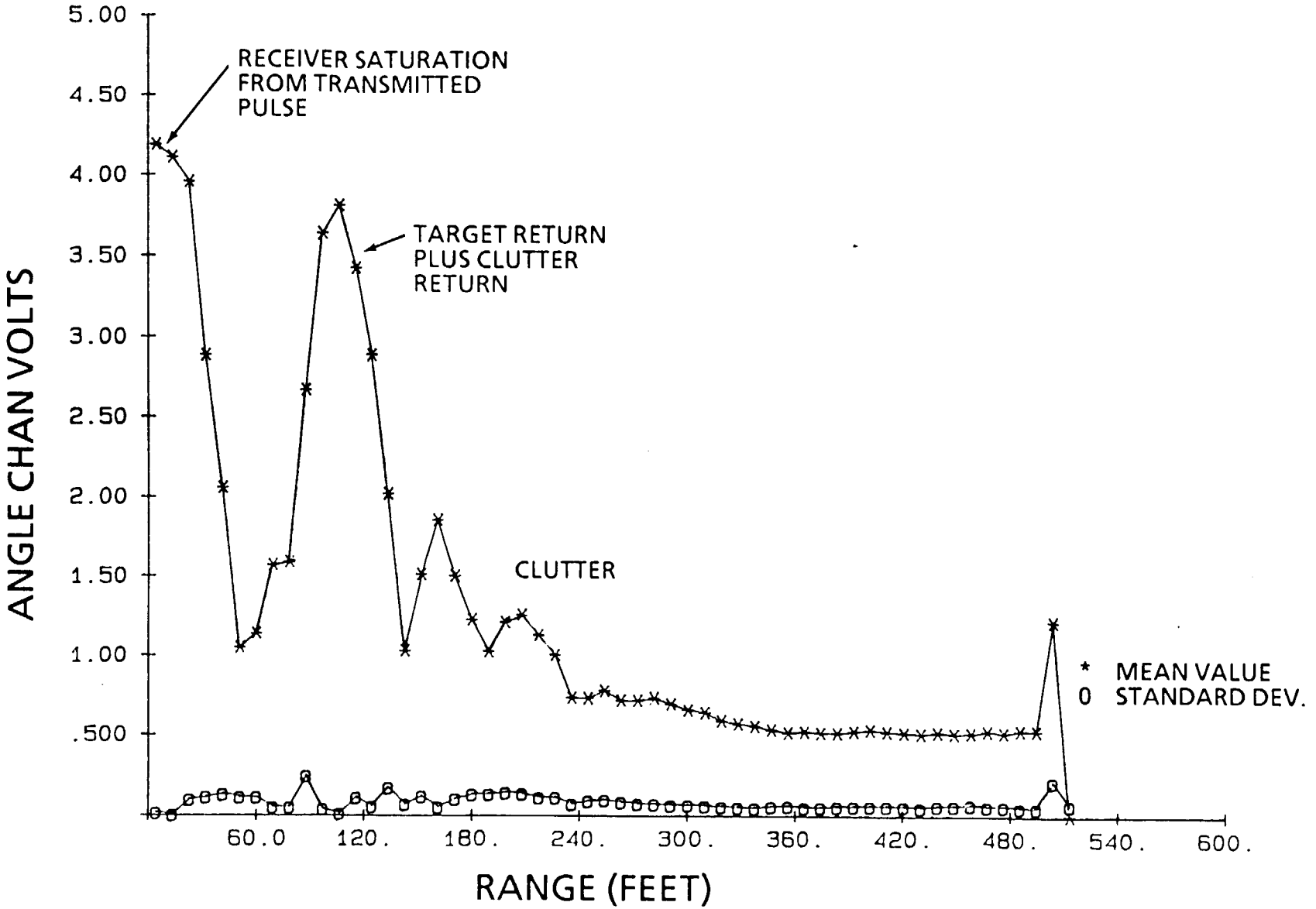

Figure 10-18.- Angle channel response to the Luneburg lens in a cluttered environment, with a transmitted pulse width = 55 ns, and a target range of approximately 100 feet.

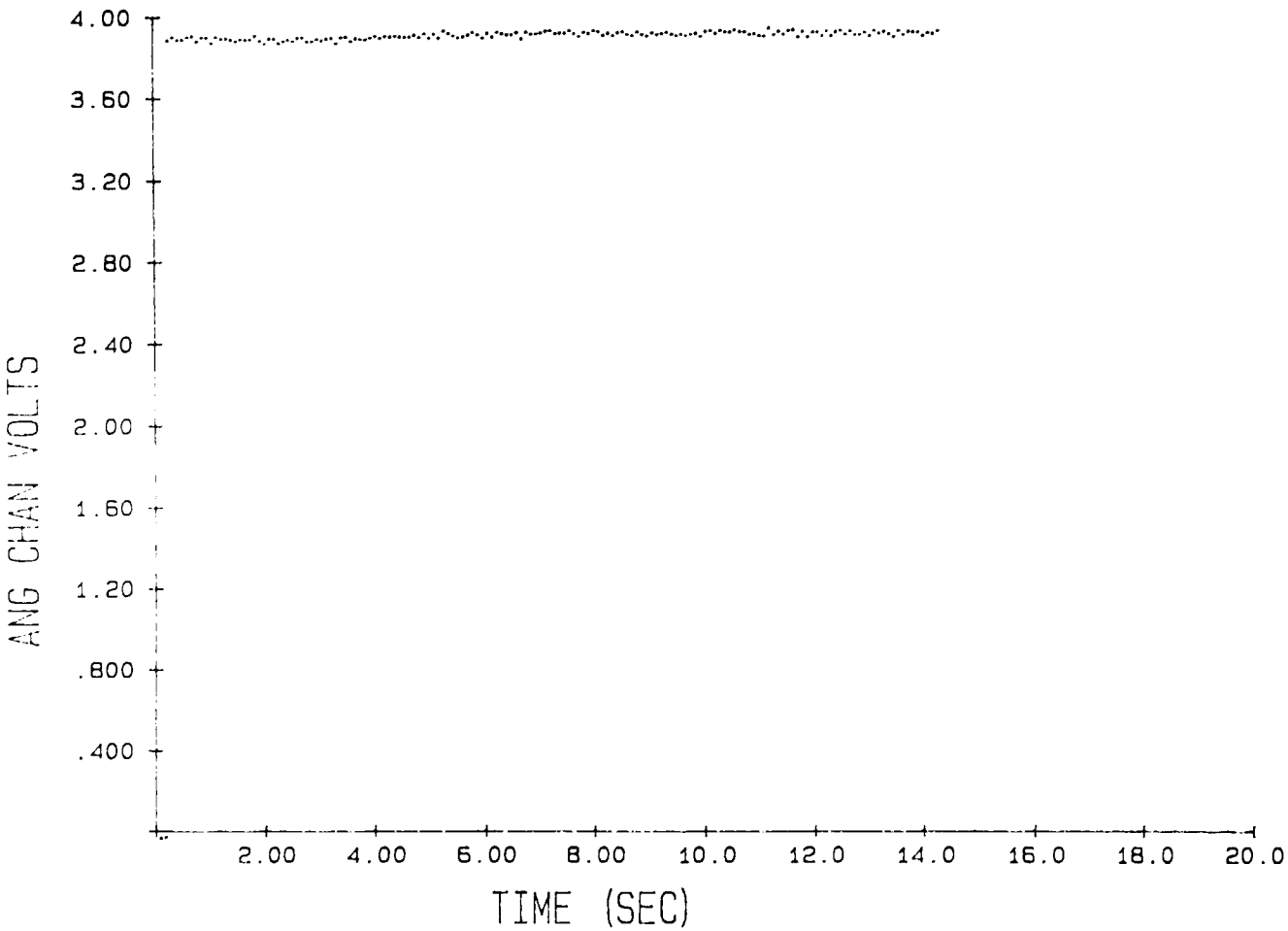

Figure 10-19.- Angle channel estimation for a point target in a cluttered environment with a 55 ns pulse.

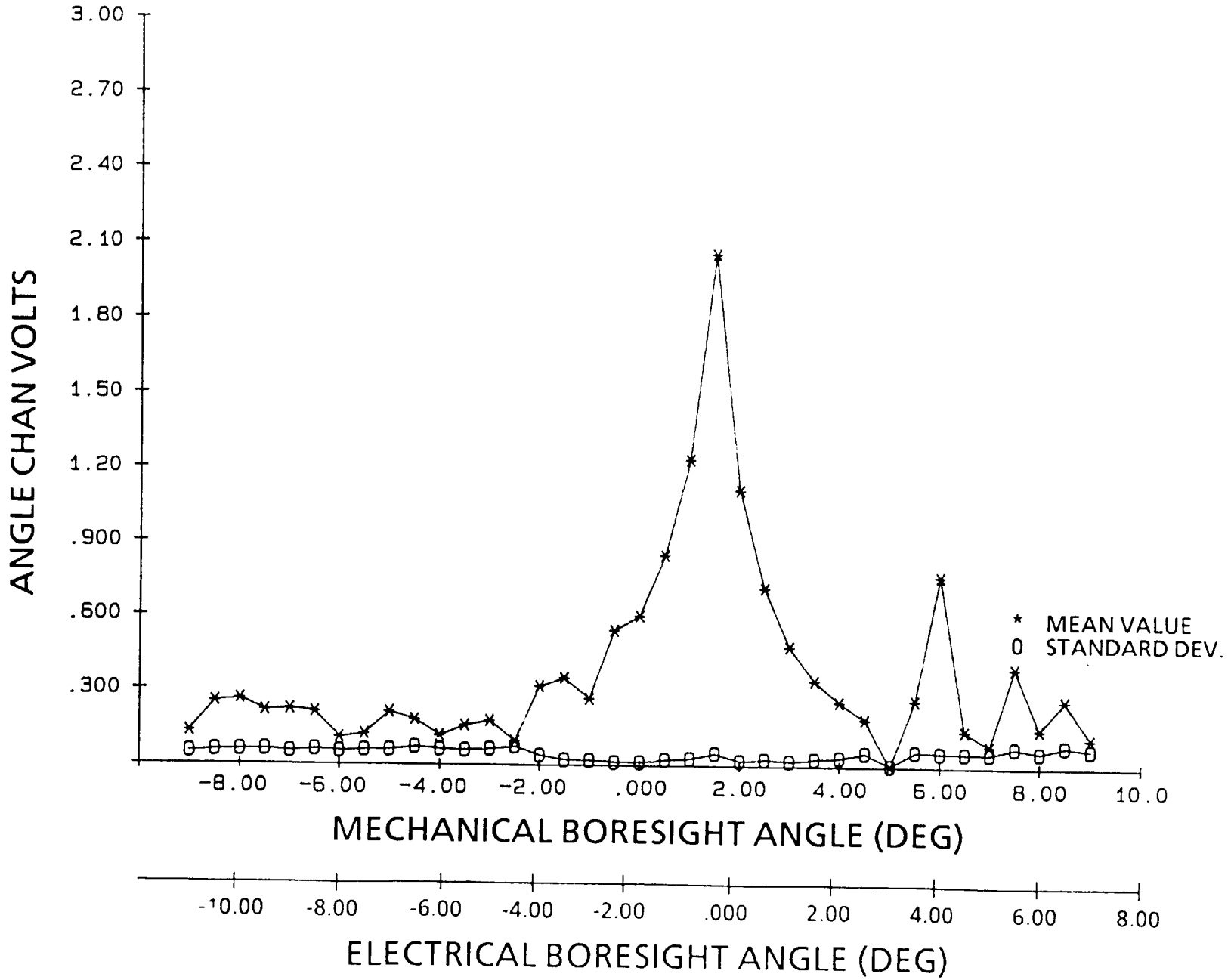

Figure 10-20.- Angle channel calibration for the modified radar system working against a point target. Multipath has been minimized by placing the target on the ground.

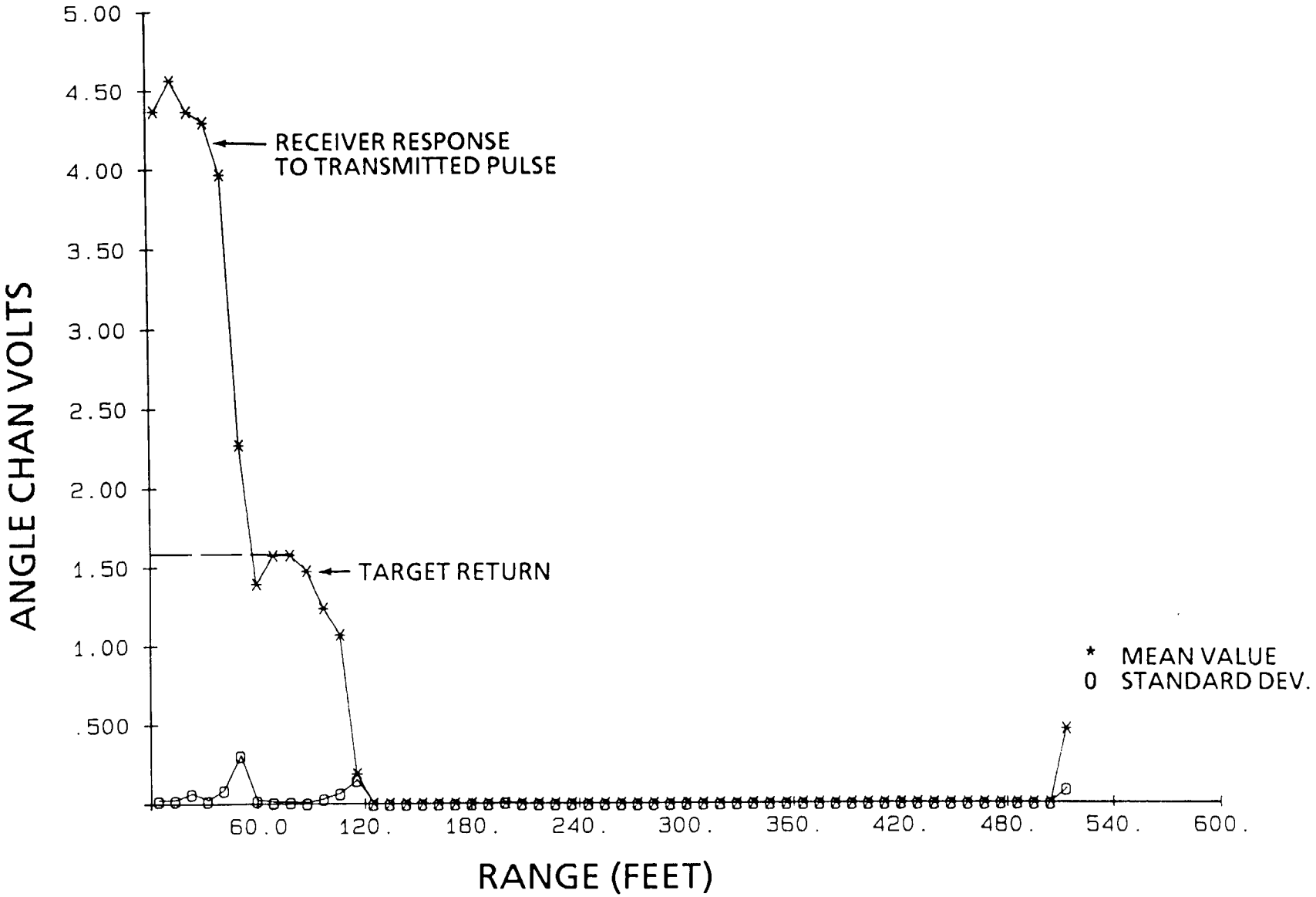

Figure 10-21.- Angle response for midsized automobile at 50 feet. Orientation is head-on.

radar response was taken and processed for mean and standard deviation of the measurements. The car was then placed along the same LOS, but at a different range. Figures 10-21 through 10-25 are plots of the angle channel responses for ranges of 50, 100, 150, 200, and 300 feet, respectively. Since angle is determined by absolute voltage, a line has been drawn from the ordinate to the peak voltage in the target return. The variation of these peaks should be noted. Also, for this static case, it should be noted that the variance of any one measurement set is at least on the order of the point target case.

Figures 10-26 through 10-30 show the angle channel response for the same automobile over the same range interval, but this time the car is positioned broadside to the radar electrical boresight. The peak voltage in the target return is marked here also. Of interest is the appearance of one to two more "targets". These are thought to be multibounce between the radar van and the large broadside area of the automobile. These bounces are further masked by the theoretical 2000-foot range of the radar (250 kHz PRF) and the roughly 500-foot processing range of the time expander board. In any event, the radar would detect and try to process at least some of these multibounce, false targets. And finally, in this set of figures, note the change in peak voltage from figure to figure.

The peak target responses for the automobile in figures 10-21 through 10-30 are summarized in figure 10-31. The curve in the figure is the point target calibration curve from figure 10-20. Along the electrical boresight of this calibration, arrows are plotted to show the voltages induced in the angle channel when the automobile was on boresight. On the left of the peak are the cases for the car head-on to the radar and on the right are the broadside cases. On both sides the range from the radar to the automobile is indicated for each test case (figs. 10-21 through 10-30).

It would have been ideal if the automobile had generated the same voltage on electrical boresight for each orientation and for all ranges. If this voltage had also been equal to the point target peak (approximately 2 volts), then the automobile would have the same radar cross-section as the point target. Figure 10-31 shows results that are entirely different, however. The voltage in the angle channel changes with automobile orientation and range. It also changes in ways that are not predictable. This lack of consistency is the result of the automobile being extended in angular size so that it is not valid to try to describe its location by a single line-of-sight angle. The monopulse angle estimating technique tries to make this single angle description - and fails.

Figure 10-31 shows that the monopulse radar has trouble with the angular size of the automobile even as far out as 300 feet. Unfortunately, this is within the region of prime concern for collision avoidance and is the region where angular precision is necessary in identifying collision cases. Based on these results, one conclusion must be that the monopulse technique for angle measurement is not proper for this application.

The results associated with figure 10-31 are the prime drivers for terminating the testing of this radar.

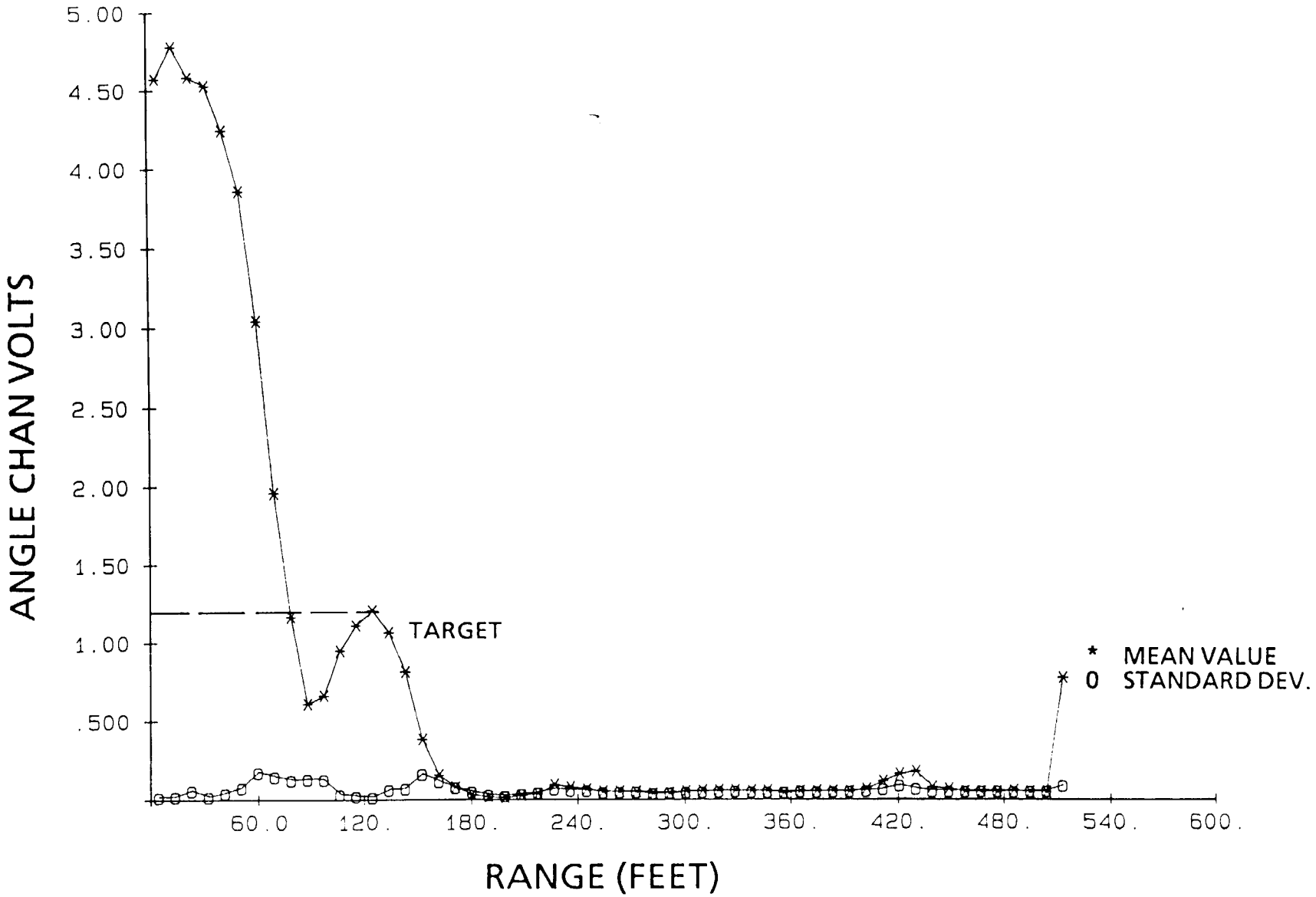

Figure 10-22.- Angle response for midsized automobile at 100 feet. Orientation is head-on.

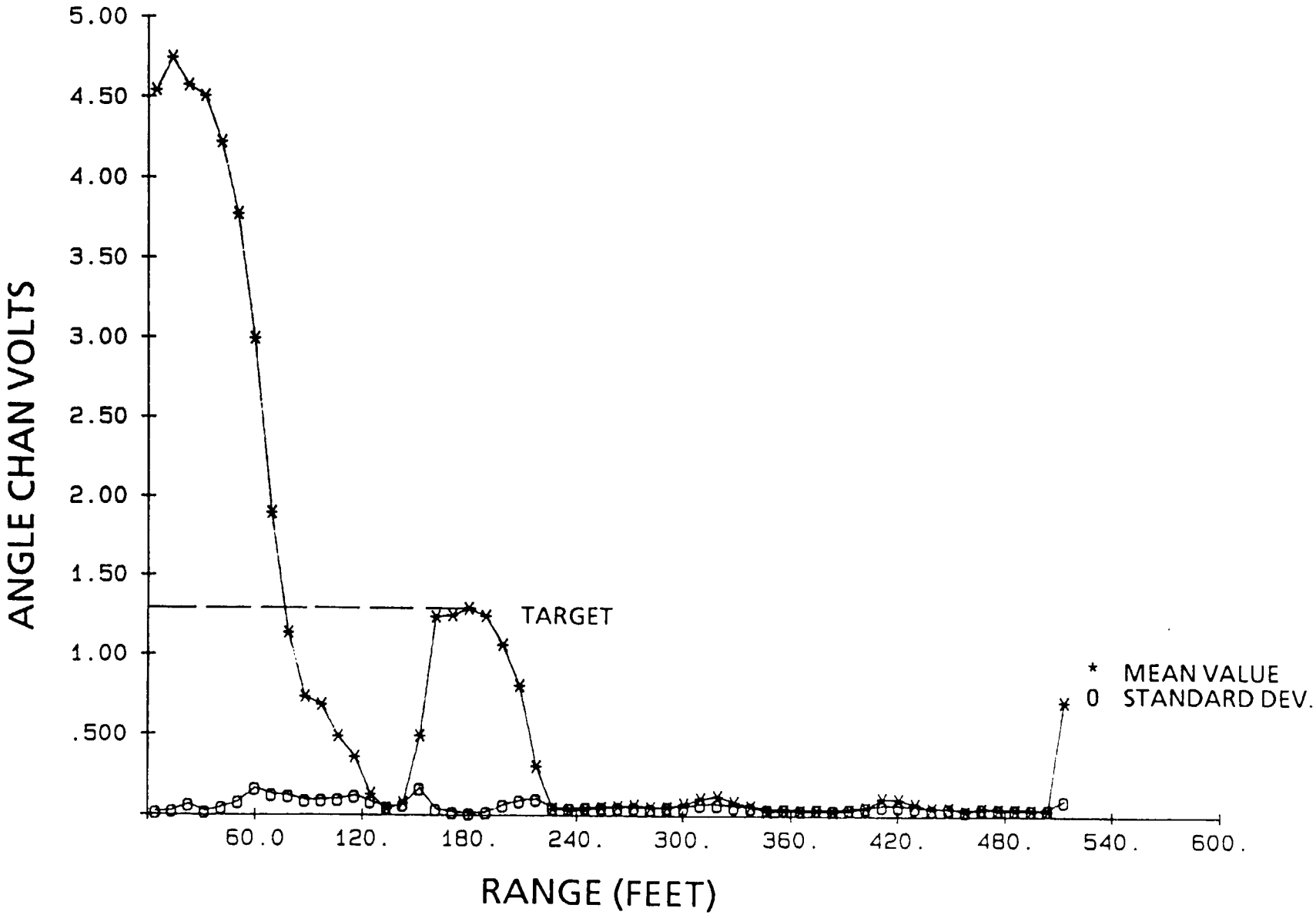

Figure 10-23.- Angle response for midsized automobile at 150 feet. Orientation is head-on.

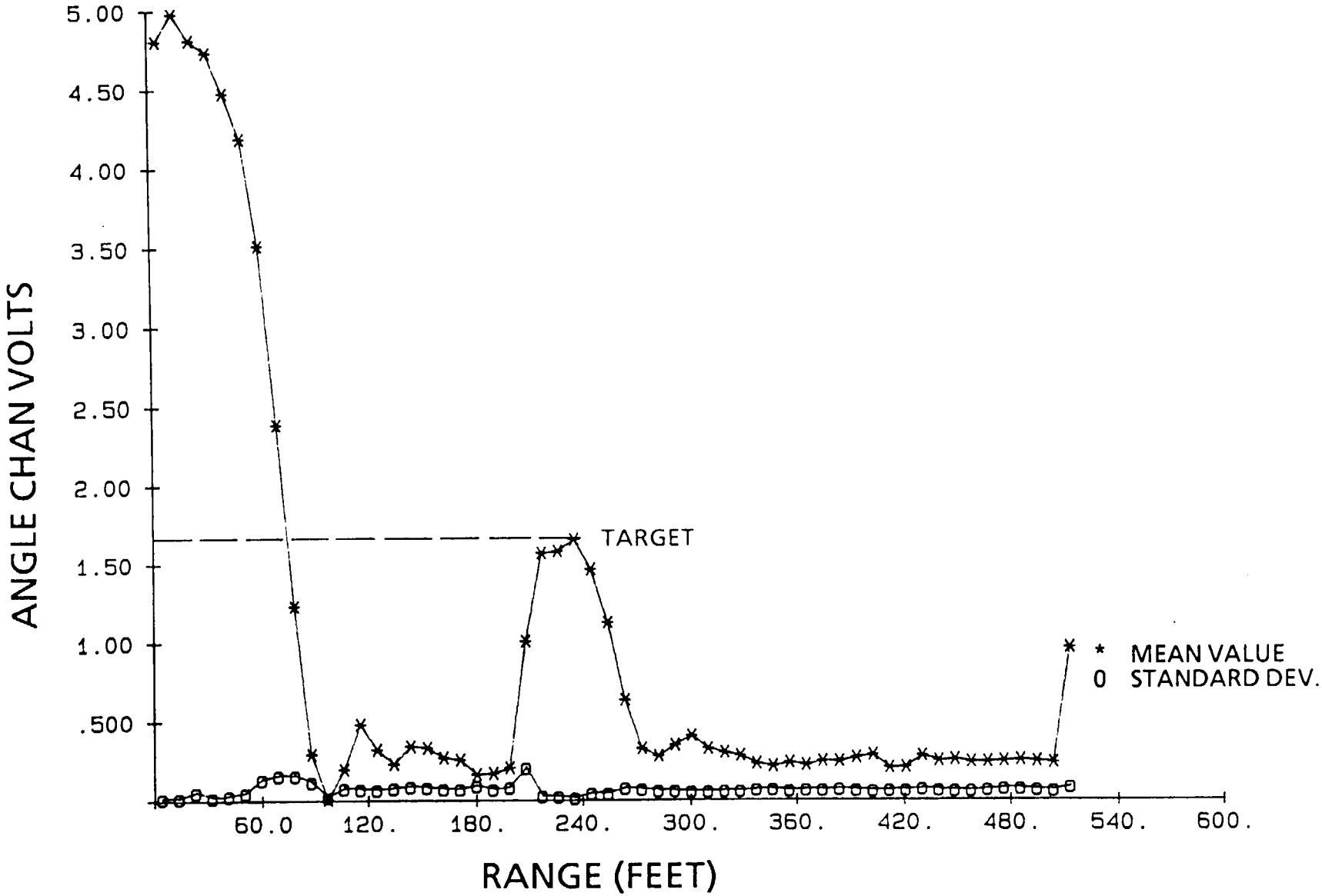

Figure 10-24.- Angle response for midsized automobile at 200 feet. Orientation is head-on.

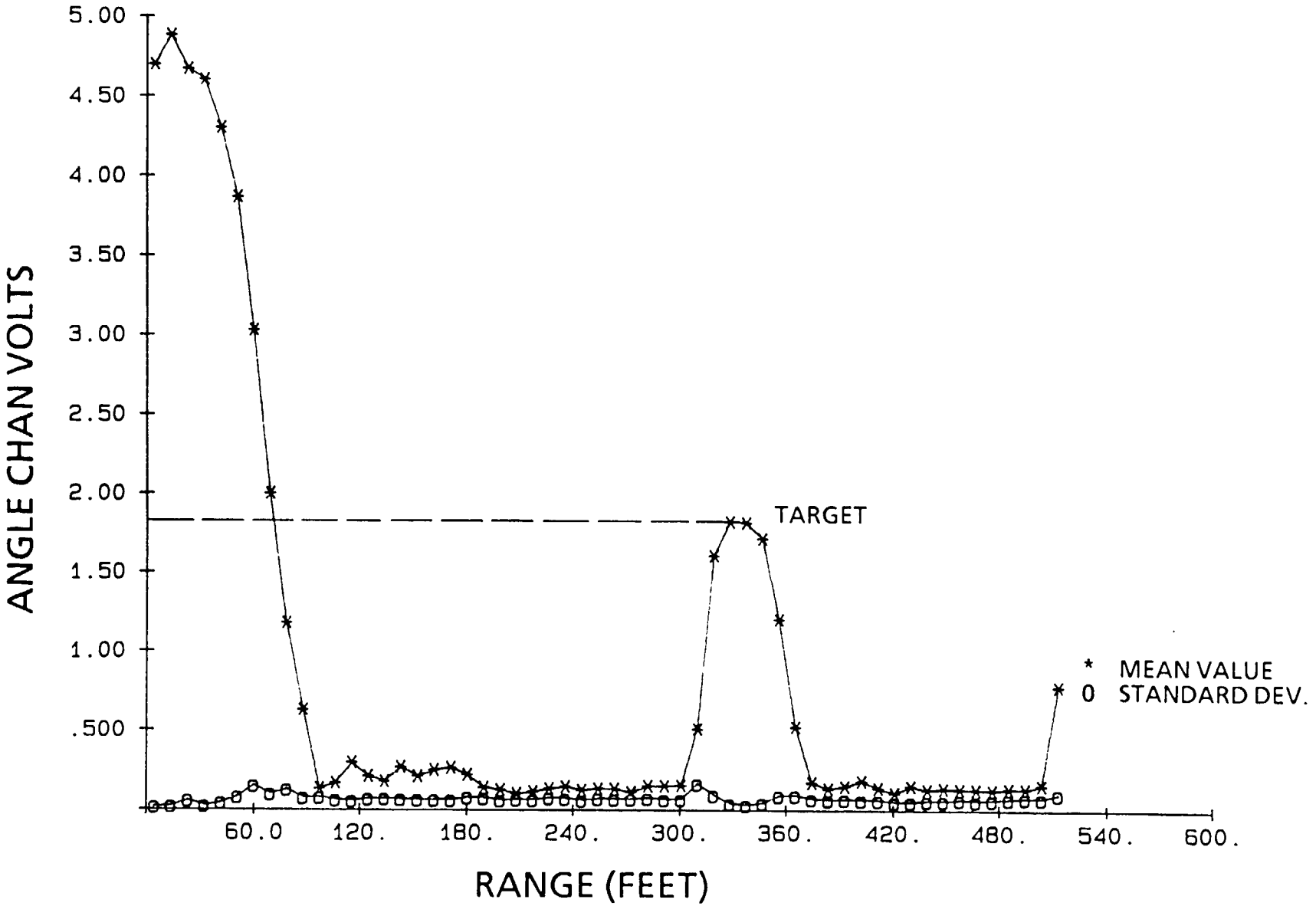

Figure 10-25.- Angle response for midsized automobile at 300 feet. Orientation is head-on.

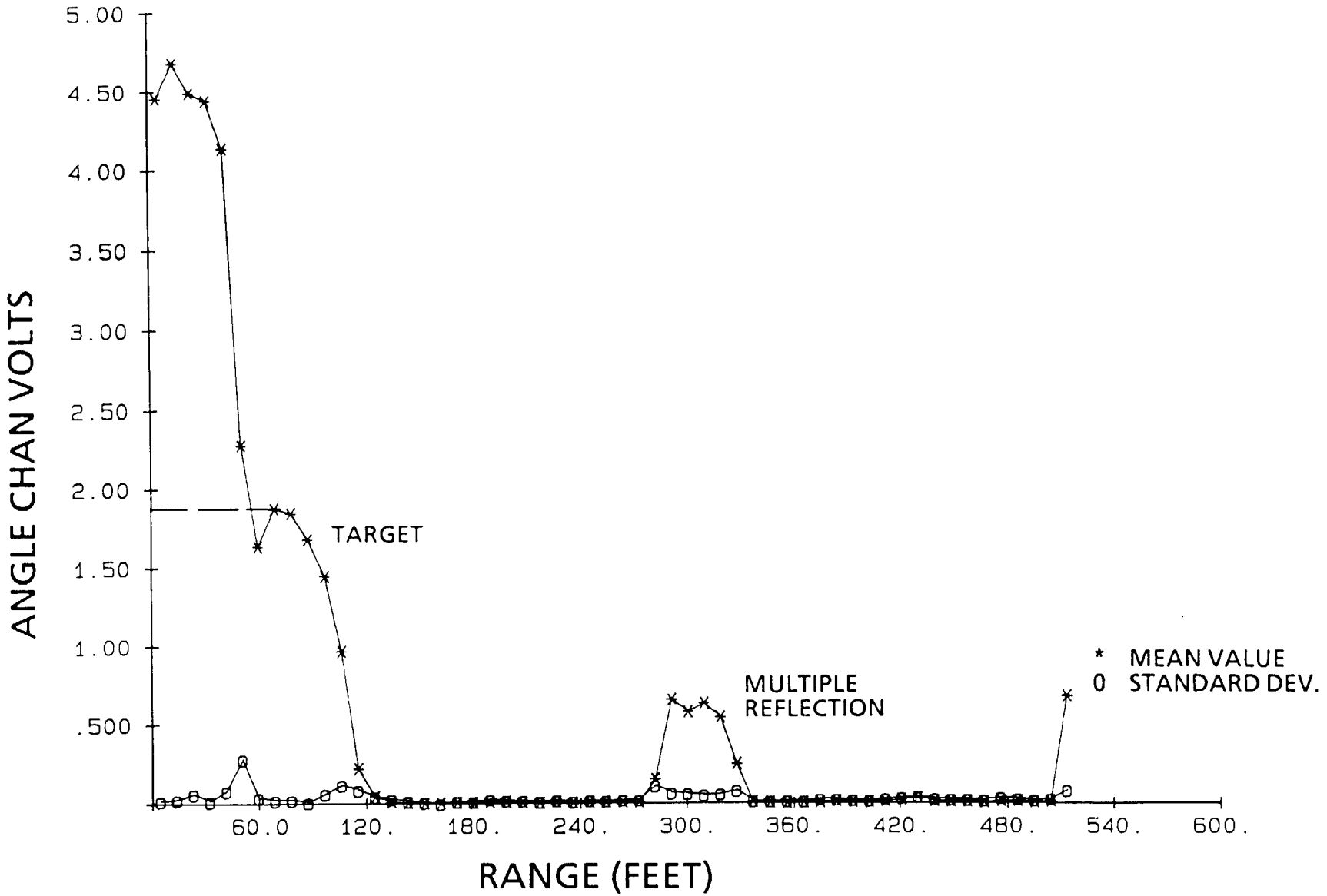

Figure 10-26.- Angle channel response for midsized automobile at 50 feet. Orientation is broadside.

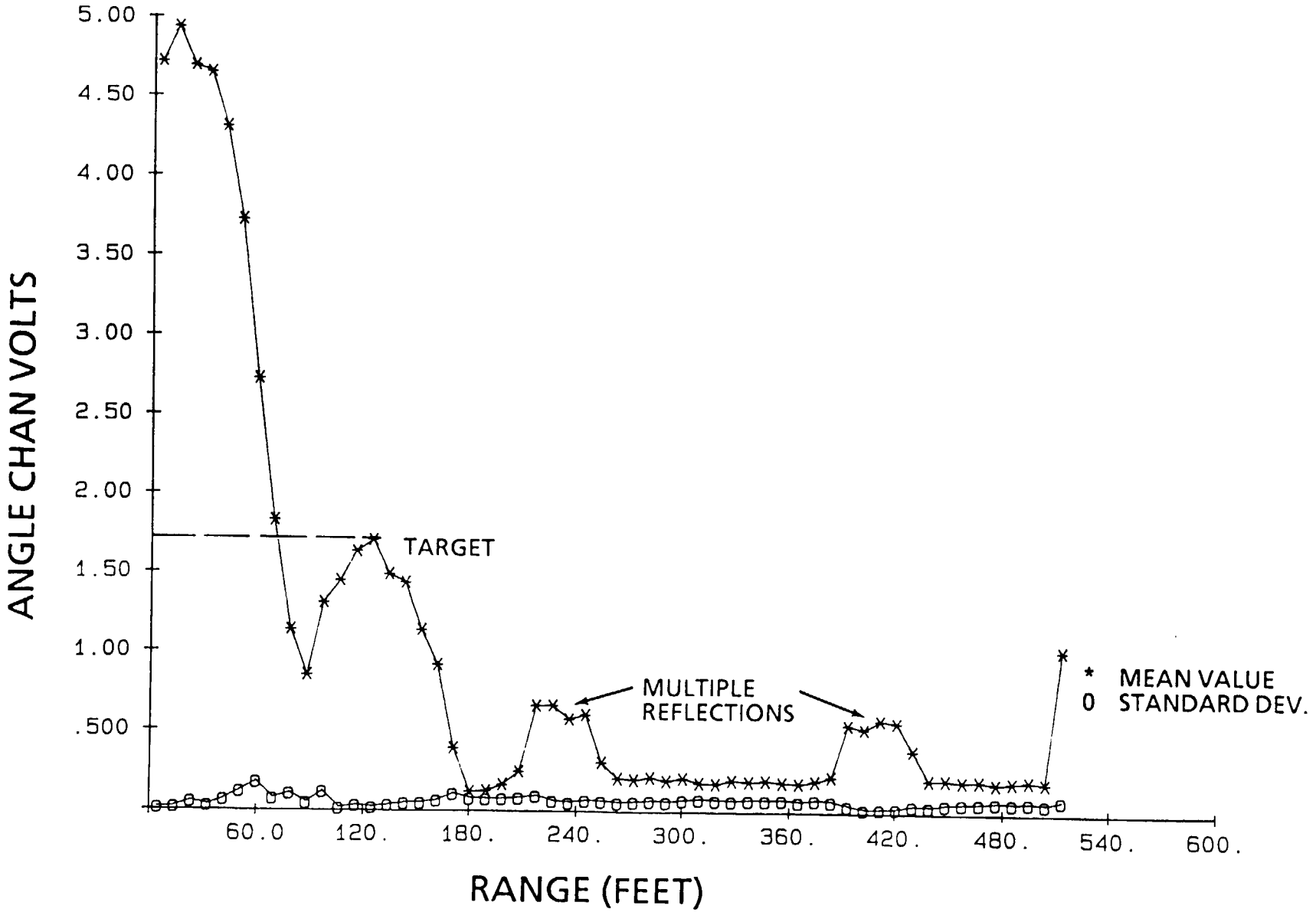

Figure 10-27.- Angle channel response for midsized automobile at 100 feet. Orientation is broadside.

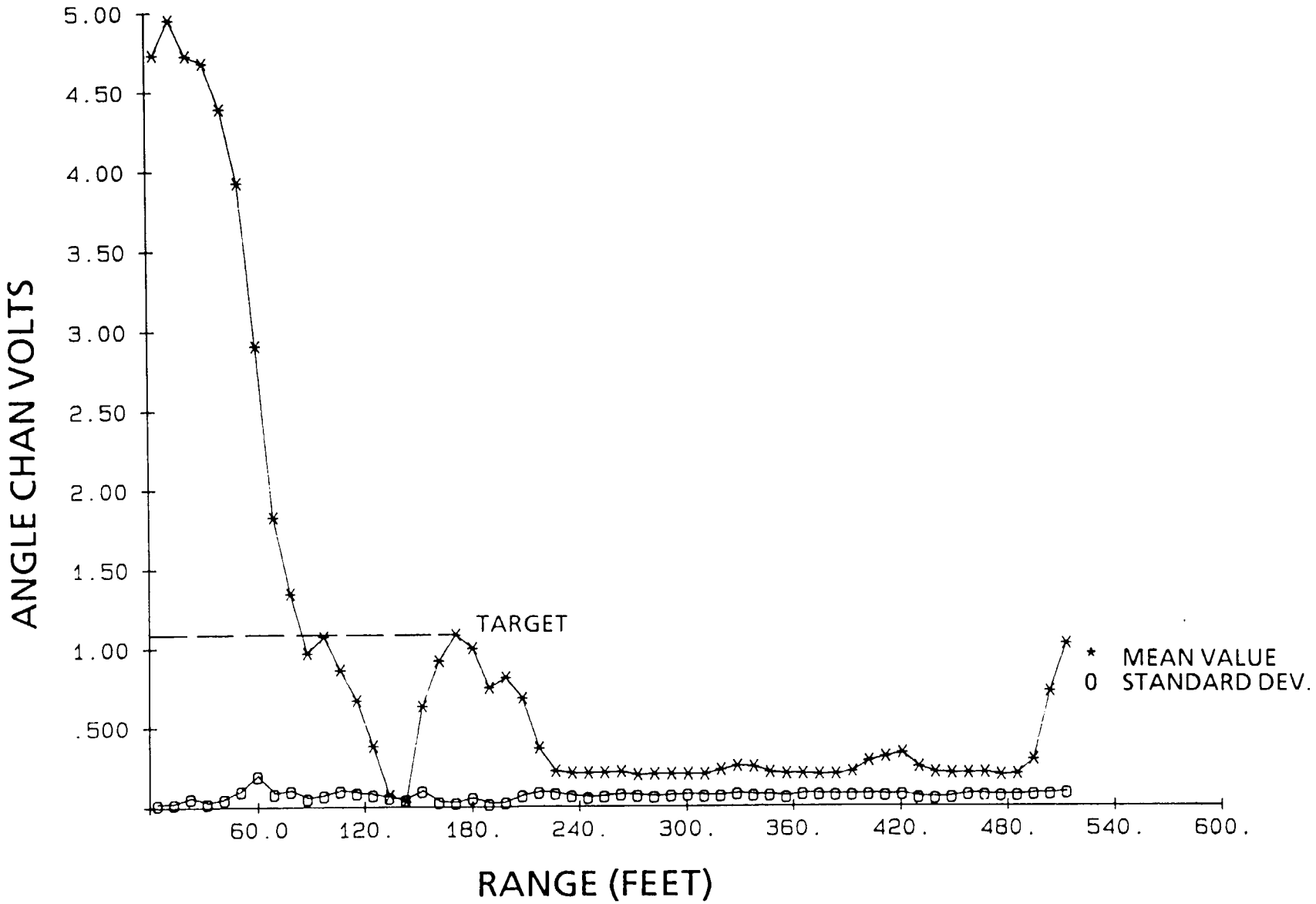

Figure 10-28.- Angle channel response for midsized automobile at 150 feet. Orientation is broadside.

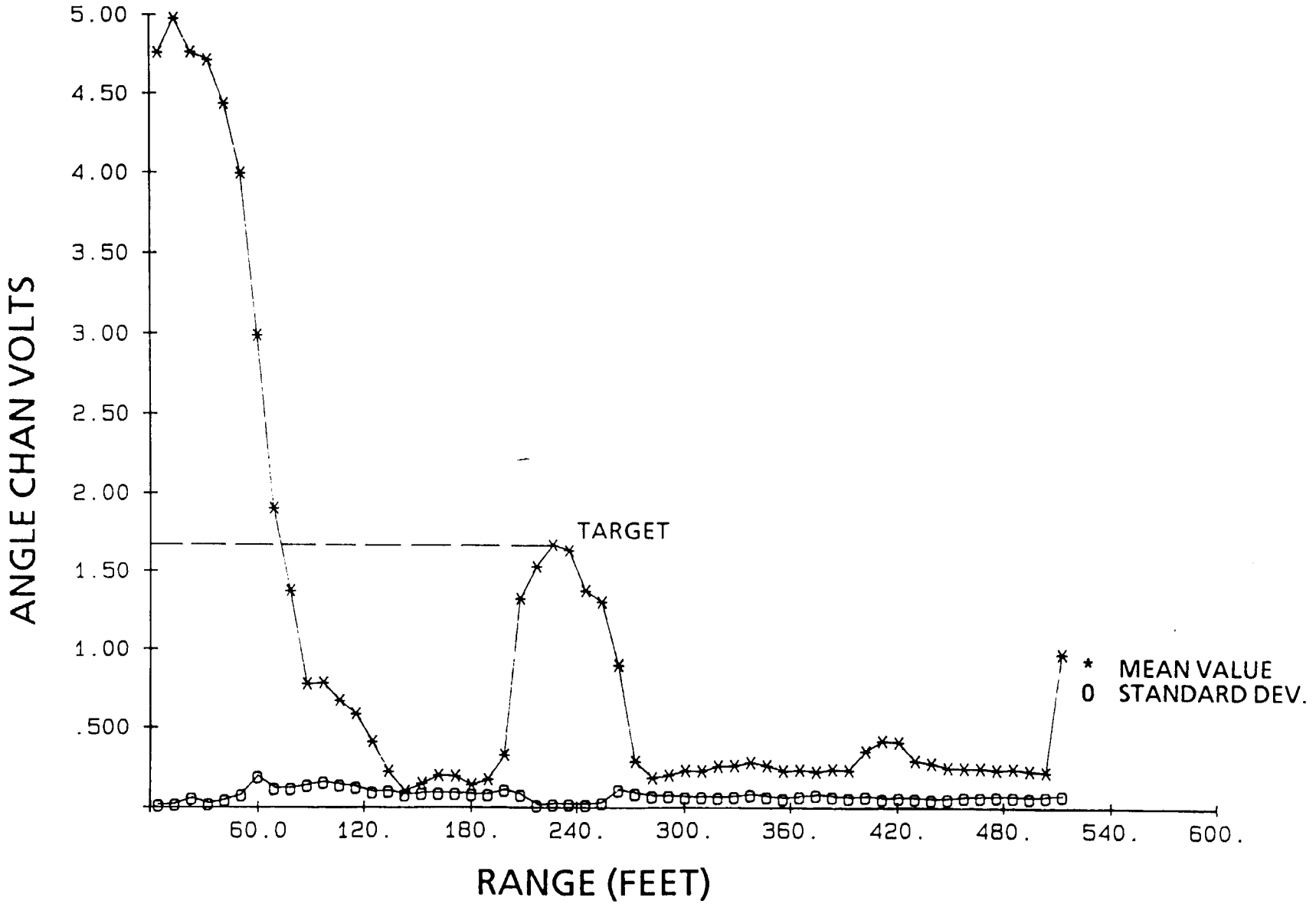

Figure 10-29.- Angle channel response for midsized automobile at 200 feet. Orientation is broadside.

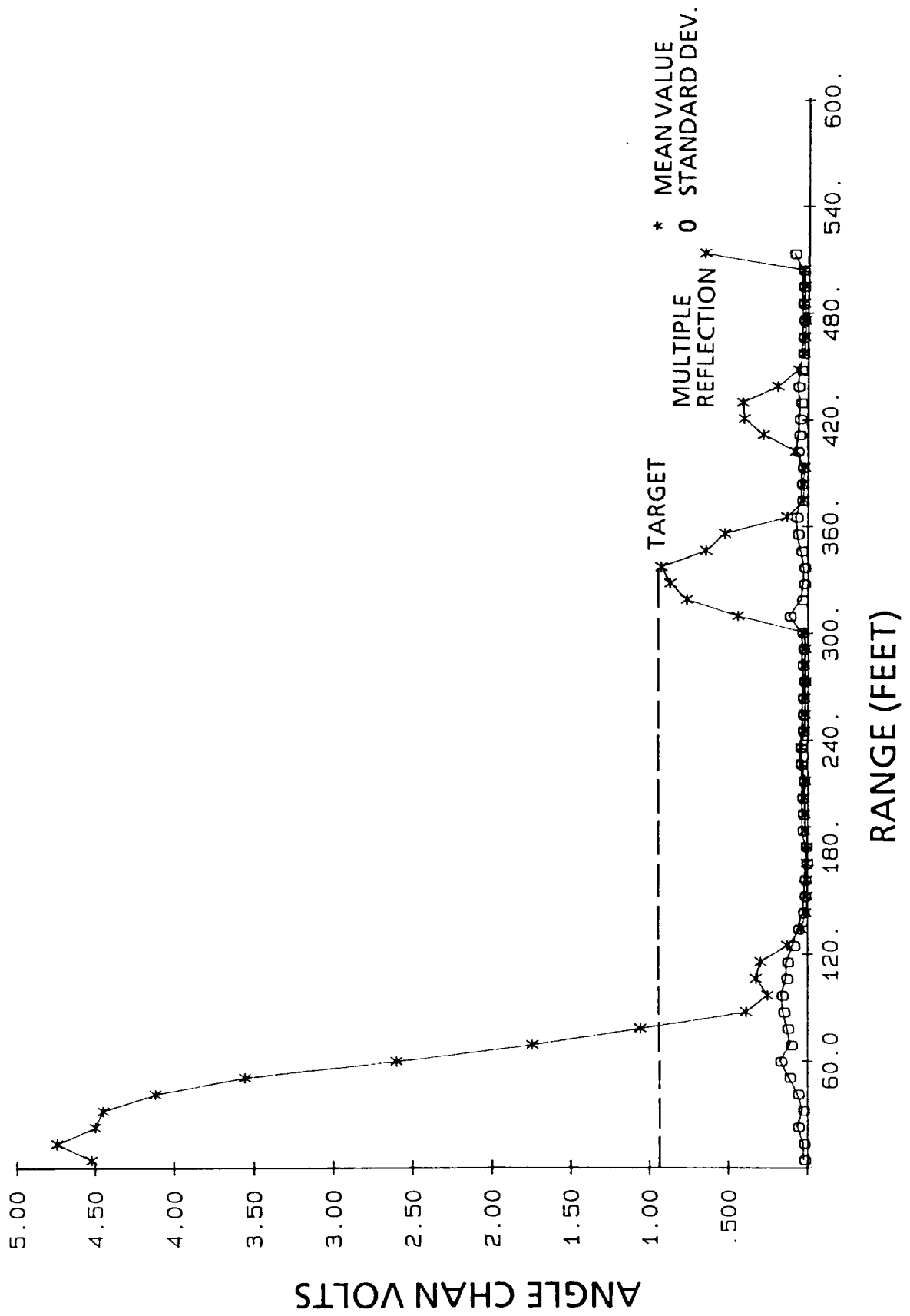

Figure 10-30.- Angle channel response for midsized automobile at 300 feet. Orientation is broadside.

DYNAMIC TESTS - EXTENDED TARGETS

Prior to the removal of the VCR from the data acquisition system, some trial dynamic runs were made with the radar system to assess, in general, the end-to-end operation of the system. The video tapes of these runs were retained as archival and documentary with little thought of utilizing them in analysis of system performance. At the end of the angle calibration trials, when the VCR has been eliminated for the reasons given and the program had really reached the terminating point, it was found that these tapes represented the only history of dynamic response.

Review of these tapes has yielded useful information and insight into both the range performance of the radar and into the angular response of the system.

Ranging to Dynamic Targets

Test runs were made with the MSA approaching and driving away from the radar at different speeds. Figure 10-32 shows the range channel response for the automobile approaching at 10 miles per hour (mph), passing the radar on one side, turning around and departing at 10 mph.

In the figure the MSA is detected approaching at roughly 500 feet and tracked into some 50 or 60 feet where it passes from the radar field-of-view. The automobile turns around and passes the radar again and is picked up by the radar as it departs. It is tracked out to roughly 500 feet. The software used to process the raw data tracked only the closest point of the car to the radar, so that for any instant of time there is only one point plotted to represent the automobile. There are points plotted along the abscissa or zero range. These points denote no target was detected, but they also represent the radar data system keeping track of time. Except for the turnaround interval, the most significant data dropouts occur at roughly a time 56 seconds and greater. No explanation for this is offered.

The range bin concept of the radar is noted in the figure by the groups of consecutive range readings of the same value. If the next range reading is different, it will be different by at least the range bin interval of approximately 9 feet. If the data acquisition system could sample faster, this range bin interval would be smaller.

Figure 10-33 shows the range versus time plot for the automobile approaching the radar at 55 mph maximum. With the automobile speed this high, the limited sampling rate only allows one range reading per range bin in some cases. The speed of 55 mph is probably close to the maximum velocity to be run against the sample rate of this system. The first 4 to 5 seconds of this run were at speeds of 55 mph. After that the driver began to slow the automobile for safety in passing on the narrow road.

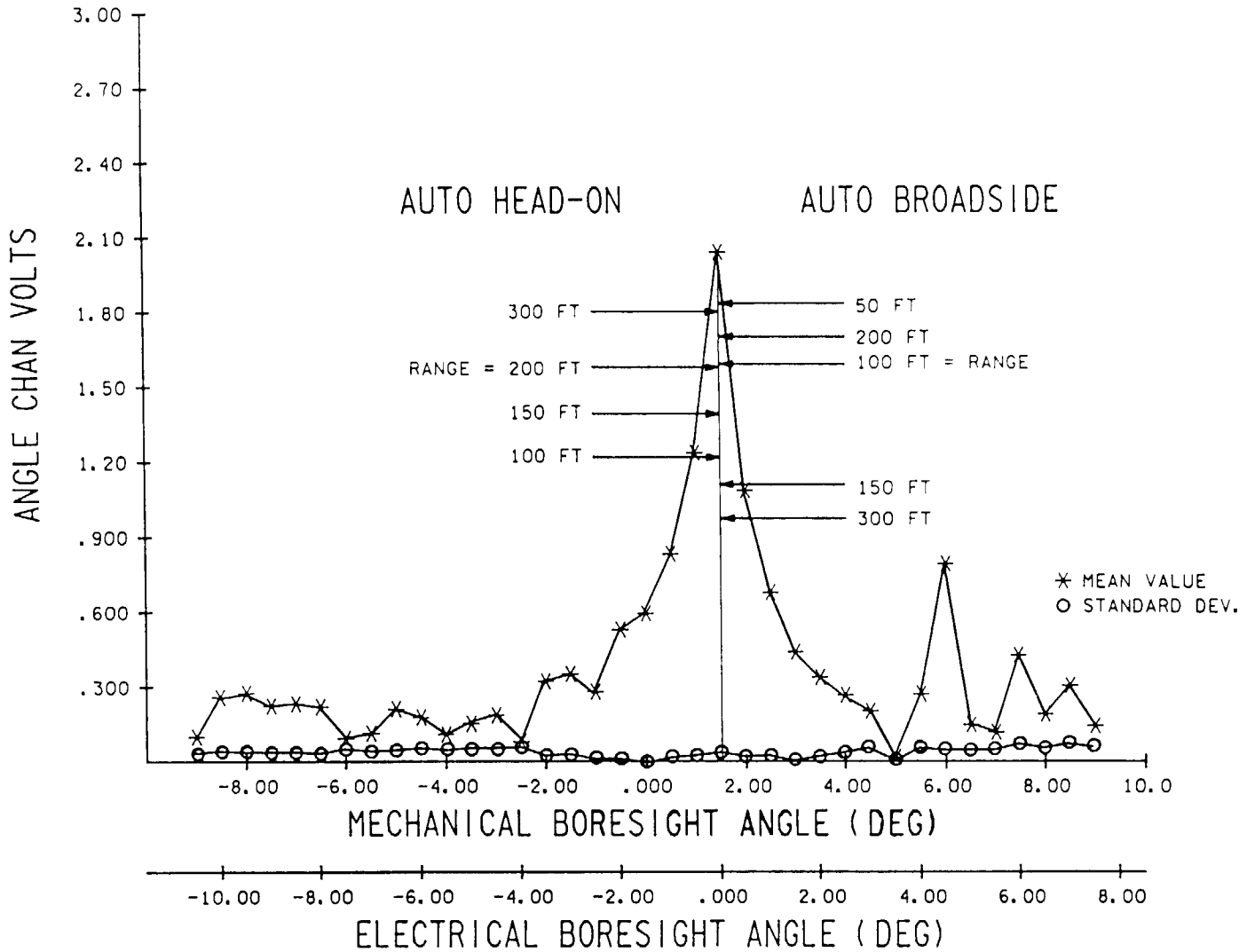

Figure 10-31.- Angle channel voltage response to an automobile or electrical boresight. (Reference curve is the point target angle calibration curve in figure 10-20).

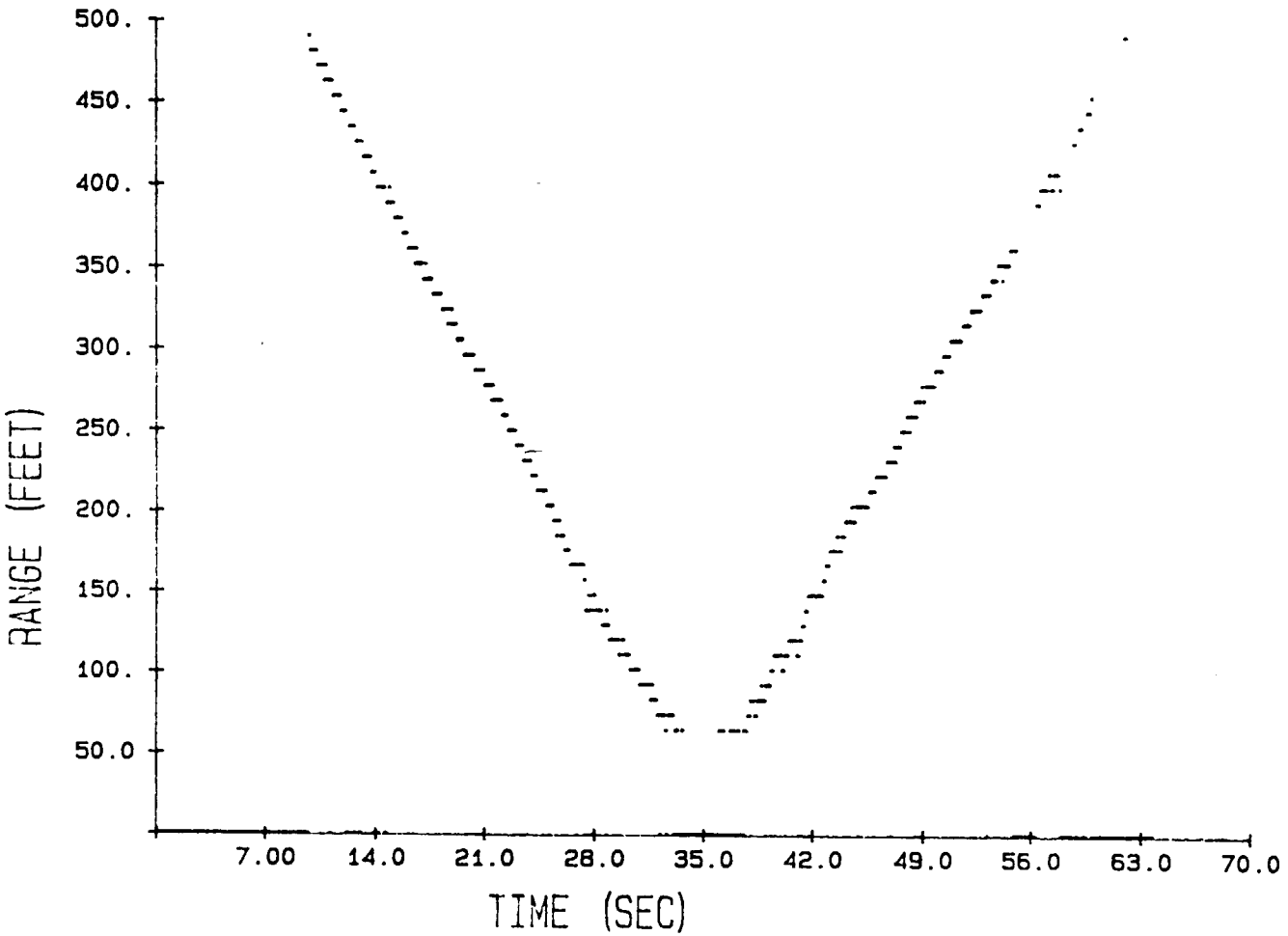

Figure 10-32.- Range channel response to a midsized automobile approaching and then departing. Speed is 10 mph.

Angle Response to Dynamic Targets

The response of the angle channel in these documentary tapes was reviewed with some interesting results. In looking at this set of data it must be remembered that correlation of the angle channel voltage with an absolute angle is not possible. First, because the VCR is still in the string of instrumentation, and second, in the case of the extended target, the system response is too complicated. So the caveat on this information is that the data sets represent trends in system response and not absolute, quantative system response.

Further comments about the figures that follow are in order also. First, these figures present channel voltage as a function of range to the target. Both the angle channel and the range channel are shown. This is done because the angle channel voltage shown has been normalized to the range channel voltage level. Understanding the angle channel response requires knowledge of the status of the range channel at the same instant of time.

Finally, the figures represent the peak target voltage at the indicated range. These peak voltages were sketched by hand from the face of a Tektronix 7633 storage oscilloscope. Many, many reruns of portions of tests were required in order to assimilate a sketch of a single test run. In some cases the frequency of voltage fluctuation was too fast to document and in these cases, the maximum excursion of voltage was sketched as accurately as possible. Other details relating to a specific test case are discussed with the appropriate figure.

Figure 10-34 shows the radar system response recorded at the point target, laying on the ground, was approached at roughly 10 mph. The baseline of the VCR voltage should be noted in both the range channel response and the angle channel. The actual channel voltage at any range is algebraic substraction of the baseline voltage from the peak voltage. The range voltage is seen to increase as the target is approached, until ranges of less than 150 feet occur. Past this interval the voltage fluctuates as seen. Explanation of this fluctuation is not offered though antenna pattern is probably the cause.

The angle channel response should have remained fairly constant since this has a straight approach and stop. Some degree of consistency is seen in the interval of 100 to 300 feet.

Of more interest than the details of figure 10-34 is the comparison of that performance with the point target against the extended target. Figure 10-35 shows the latter case. Here the MSA is approached from the rear at 10 mph. The curves as plotted stop at roughly 75 feet range because the MSA was passed on the right. Up until that range the automobile was in the direct path of the radar. In general, the radar range channel response was increasing as in the point target case. Fluctuations started at roughly 100 feet as before, but perhaps delayed because the extended target remains longer in the beam width of the antenna. The angle channel response is uncomplicated in appearance and relatively constant from roughly 300 to 100 feet; but it should be because the angle to the target was essentially constant.

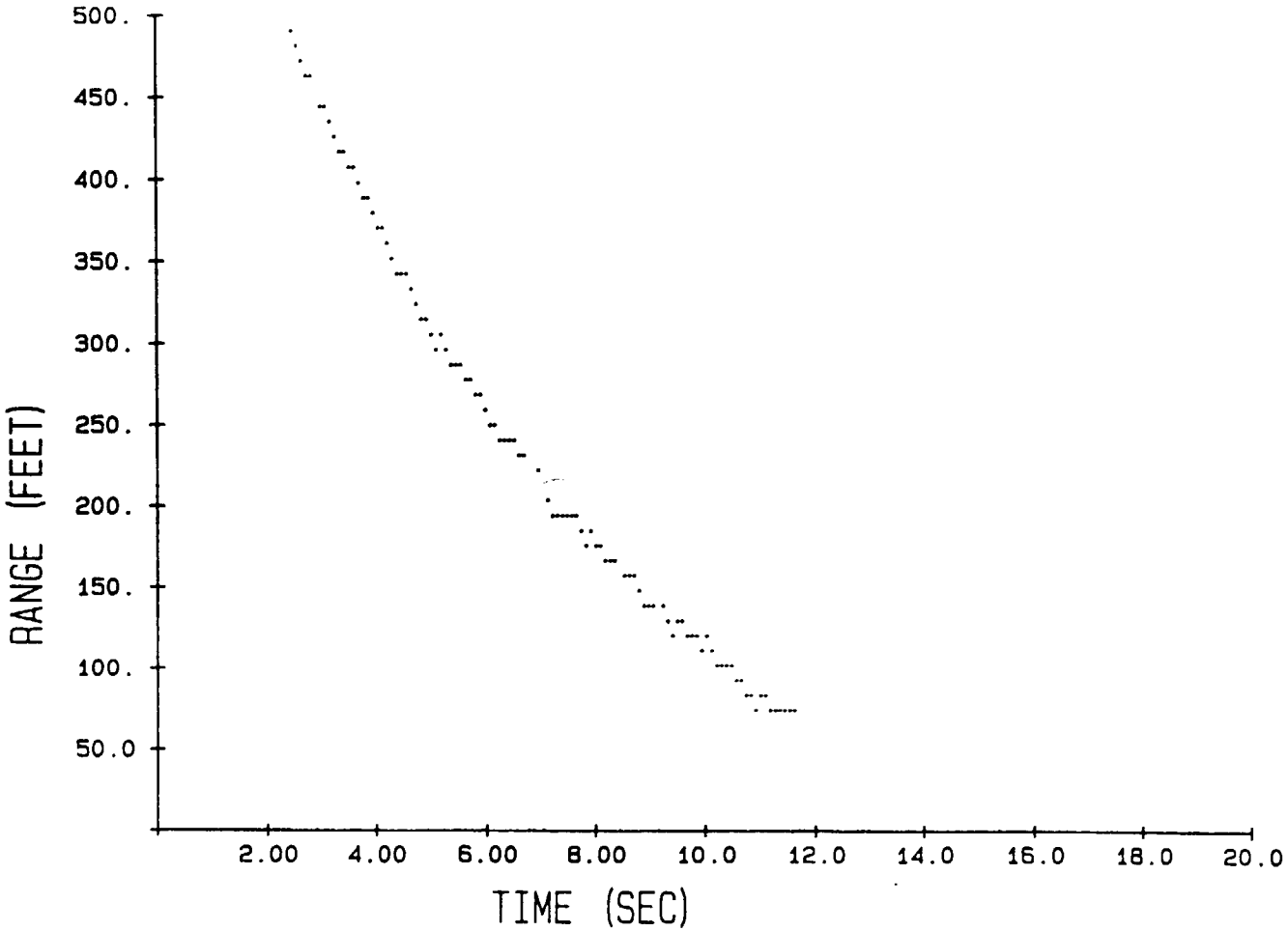

Figure 10-33.- Range channel response to a midsized automobile approaching at 55 mph.

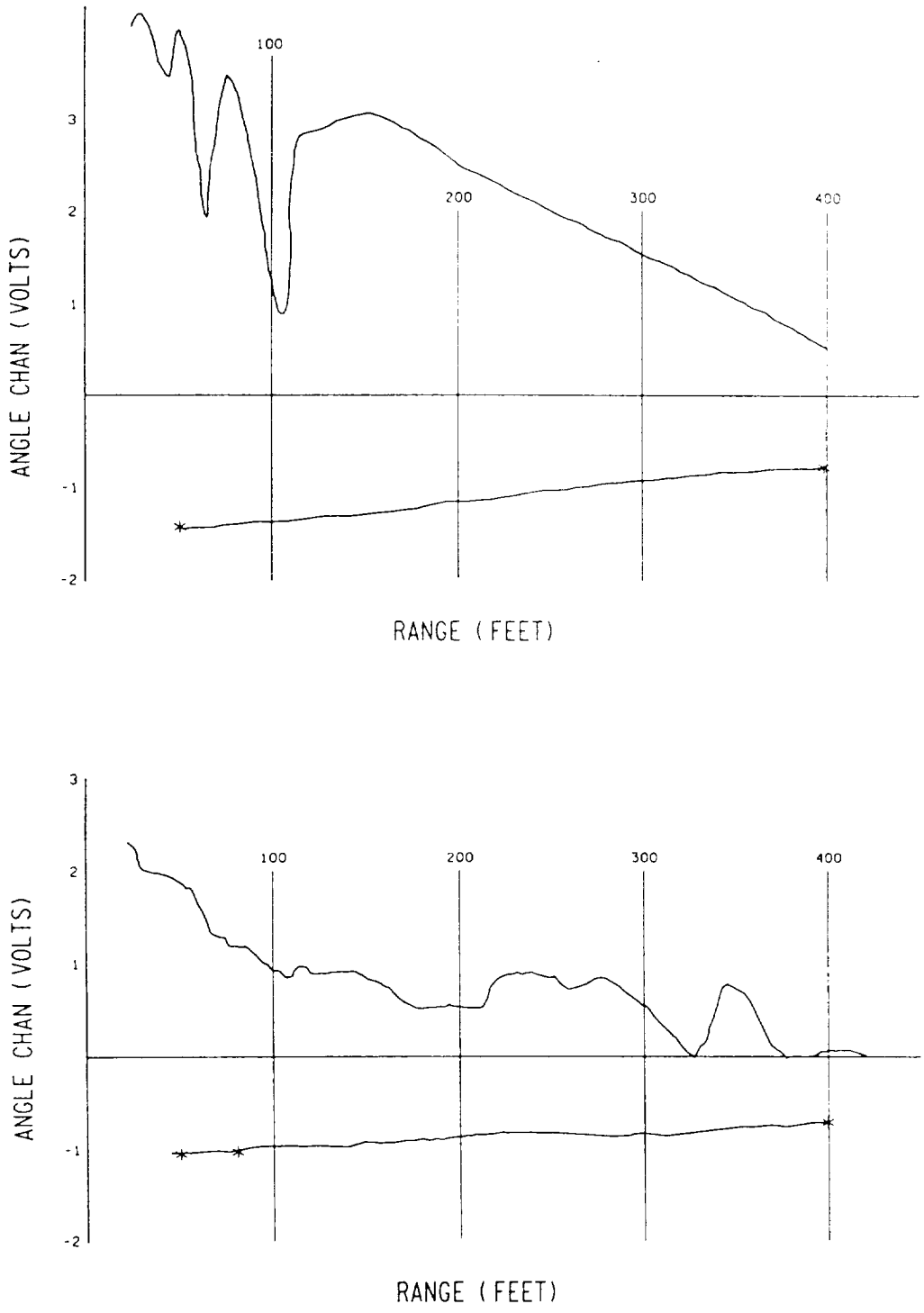

Figure 10-34.- Range channel response to a midsized automobile approaching the point target at 10 mph.

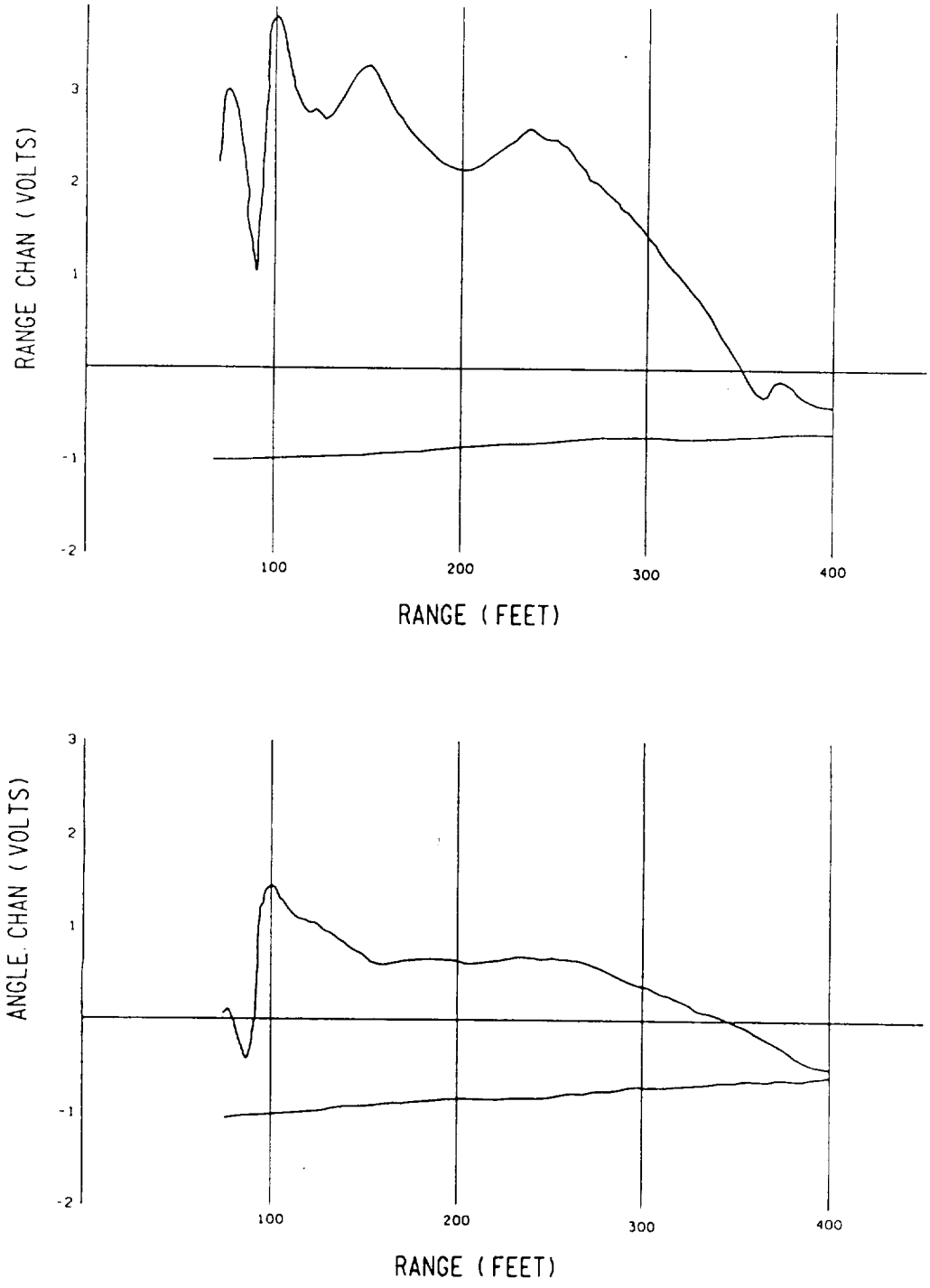

Figure 10-35.- Range channel response approaching a midsized automobile from the rear at 10 mph.

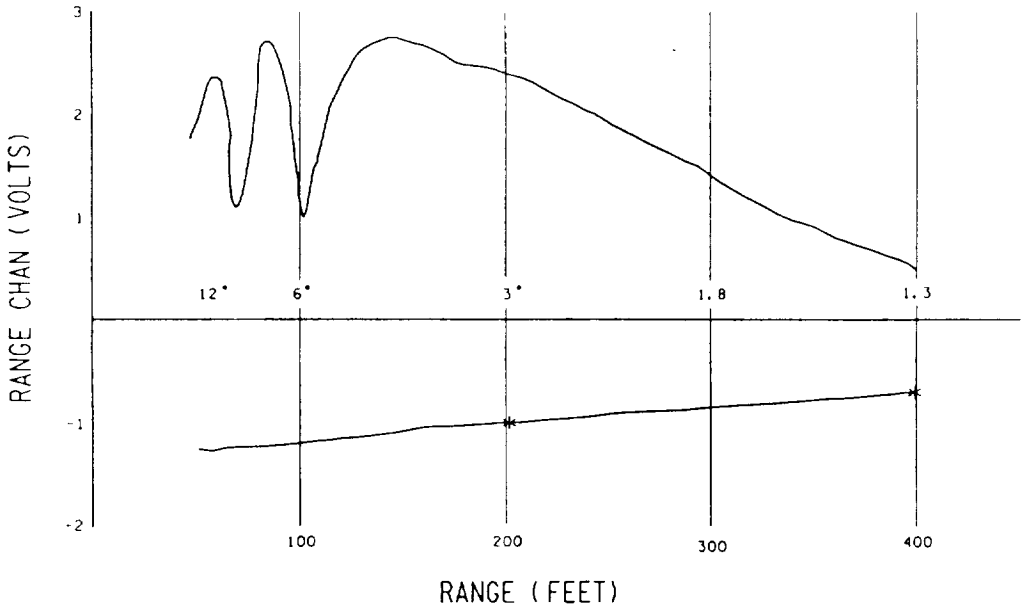

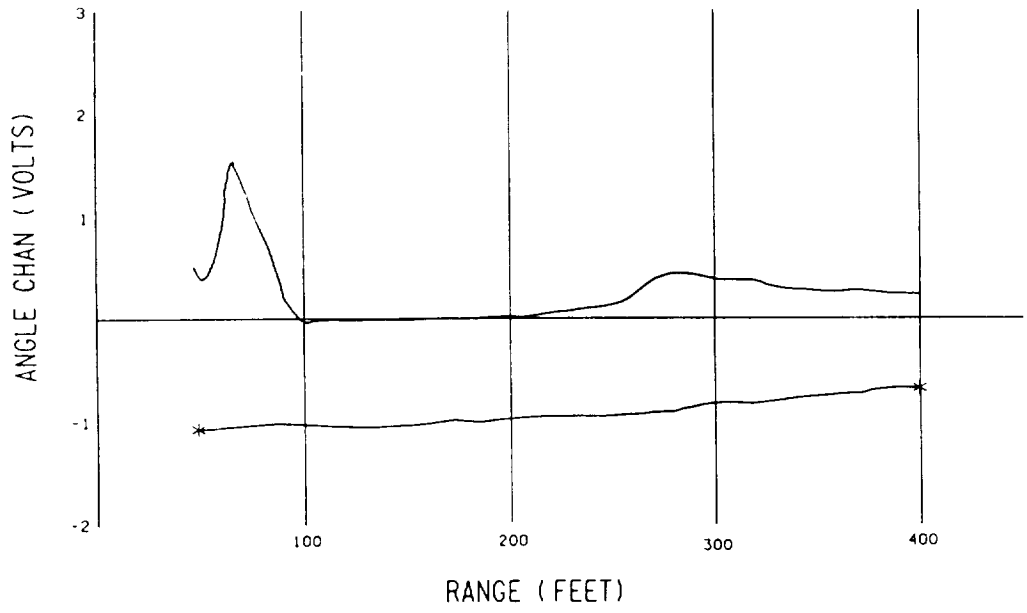

Figure 10-36.- Range channel response to a point target drive-by at 10 mph.

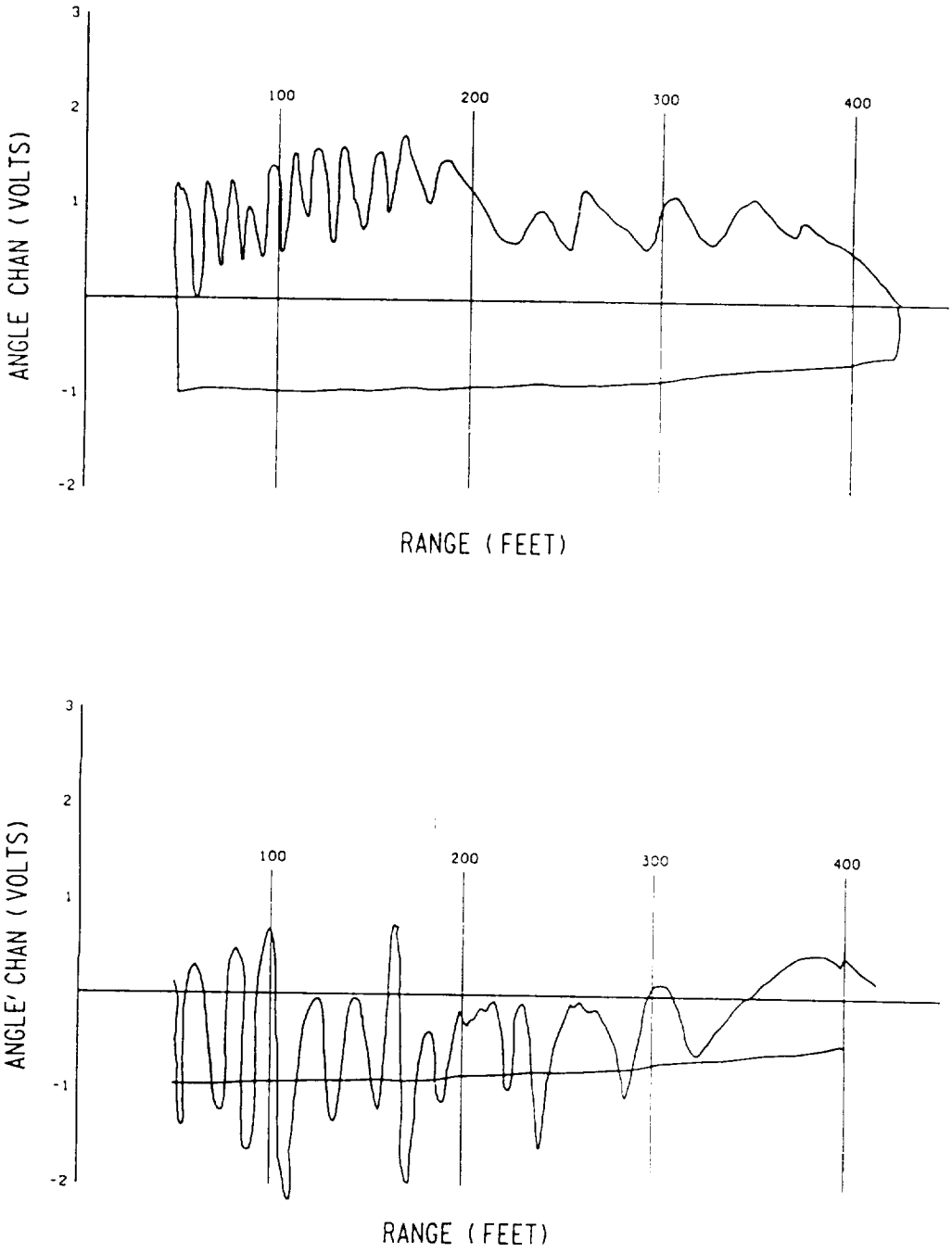

Figure 10-37.- Range channel response to a midsized automobile drive-by at 10 mph.

The last two cases considered are driving by the point target at 10 mph and driving by the MSA at 10 mph. Figure 10-36 shows the point target case. Superimposed on the abscissa of the range channel response is an estimate of the line-of-sight angle to the point target at specific ranges. The performance of both the range channel and the angle channel seems, in general, to be quite reasonable with similarities, appropriately, to characteristics noted in figures 10-34 and 10-35.

Figure 10-37 shows radar system performance when driving past the MSA at 10 mph. While there is sufficient signal energy to detect the target in the range channel and perform the ranging function, the angle channel has completely degraded. The frequency of the fluctuations seen in the angle channel are far too rapid to be correctly represented in the figure. The maximum excursions of the signal are reasonably reproduced, however.

Looking at the angle channel, there are instances where the channel voltage actually goes below the VCR baseline. This can occur only if the raw angle voltage is higher than the raw range voltage. For point targets without multipath this cannot happen. However, the figure shows that for the monopulse radar attempting to process the extended target, it does happen and with disastrous results.

APPENDIX

TEST PLAN FOR INITIAL TESTING

OF THE

CRASH AVOIDANCE RADAR (CAR)

Lockheed Engineering and Management Services Company, Inc.

INTERDEPARTMENTAL COMMUNICATION

DATE: October 18, 1985

TO	C. E. Coe	DEPT./ ORGN.	21-40	BLDG./ ZONE	J14	PLANT/ FAC.	Houston	
FROM	W. X. Culpepper	DEPT./ ORGN.	21-40	BLDG./ ZONE	J14	PLANT/ FAC.	Houston	EXT. 3547

SUBJECT: TEST PLAN FOR INITIAL TESTING OF THE CRASH AVOIDANCE RADAR (CAR)

This short paper describes what is felt to be the initial tests required to be performed when the in-house CAR system is first brought on-line. These tests will define the end-to-end transfer functions and first order limitations of the system. The system in this case includes the RF, time expansion sampling, data acquisition and data reduction subsystems. Some parameters which will be defined in these tests are the conversion constants necessary to complete the end-to-end data flow.

The preliminary tests are shown in Table 1 and show both the transfer functions and the basic dynamic response characteristics needing definition. The results will be the end-to-end capability and response of the system. An important aspect of this test not emphaized in the table is the system ability to detect mimimum dynamics, i.e. range rates and angle rates near zero.

Table 2 shows a list of basic situational tests. The criteria of avoiding collisions in all these situations are well known. That is not the purpose here. The purpose here is to establish the ability of this CAR system to react appropriately to each of these cases. Once this information is gathered and understood more exotic tests can be formulated. That will be the basis for a test plan for advanced testing.

W. X. Culpepper

W. X. Culpepper

WXC/jdt
cc: H. Erwin C. Lichtenberg H. Nitschke

FORM LEMSCO 426 1

TABLE 10-1.- PRELIMINARY TESTS

TRANSFER FUNCTIONS:

1. Range Channel

   - Accuracy
   - Range resolution
   - Extended target response
   - Magnitude versus cross-section

2. Angle Channel

   - System response (volts/degree)
   - Accuracy
   - Useful angular range
   - Resolution
   - Extended target response

RESPONSE TO DYNAMIC SITUATIONS:

1. Range rate

   - Zero to 120 mph at zero angle rate

2. Angle range

   - Zero to TBD degrees/seconds at zero range rate

3. Combined range rate and angle rate at TBD values

TABLE 10-2.- BASIC SITUATIONAL TESTS

1. Roadside

   - Angle rate response is prime concern.
   - Absolute angle accuracy is secondary concern.

2. Head-on

   - Maximum range is prime concern.
   - Angle rate response is secondary concern.

3. Follow-after

   - Range rate response is prime concern.
   - Absolute range is secondary concern.

4. Angular-collision

   - Angle rate response is prime concern.
   - Absolute range is secondary concern.

SECTION 11
CONCLUSIONS AND RECOMMENDATIONS

Testing of the Phase 1 radar at the Johnson Space Center was intentionally terminated prior to completion of the previously planned investigations. The overriding cause terminating the tests was the effects of the extended target on radar performance.

APPLICABILITY OF MONOPULSE RADAR

The history of successful use of monopulse radar is long and noteworthy. It is, however, a point target tracking radar system and a single target tracking system. Of course, large targets have been tracked, but at ranges where their included angle classifies them as a good point target approximation. The tests done on the Phase 1 radar also displayed good point target tracking capability when used against the Luneburg lens. It also showed improving performance as the included angle of the extended targets became smaller with increasing range.

It is felt by considering these tests that the monopulse radar will not have adequate performance to handle the collision avoidance radar case, however. The small ranges and large extended targets are just beyond the capability of the technique. Therefore, it is concluded that the monopulse radar approach is not readily adaptable to this problem. Another technique designed to handle extended targets must be implemented. Additional investments into the monopulse technique do not appear warranted at this time.

SUGGESTED ALTERNATIVE

A first approach in coping with this extended target environment is to make all decisions yes or no. In other words, don't make an absolute energy level measurement to estimate a parameter. In the monopulse radar the range channel already was doing this, i.e., if the sum channel energy exceeds a predetermined threshold, the answer is yes to target presence. Time delay then determined range. There was no dependence on absolute energy. This same type of approach should be implemented in the angle channel.

The threshold approach is applicable if a narrow beam scanning antenna is implemented. In this system the antenna beam will be scanned over some larger angular interval and for each beam position a ranging pulse will be transmitted. If enough energy comes back from a target to exceed threshold, the range to the target is calculated from the time delay (just as in the Phase 1 system), but now the angle is deduced from the beam position at the time of transmission. If the target is large compared to the antenna beam width, then target detects will be seen in adjacent beam positions. The target actually is "painted" by the scanning beam and this new radar will have information concerning both target location and size.

This is the alternative approach recommended for any follow-on effort in CAR radar development at the Johnson Space Center. While some suspicions exist now as to the implementation of this new approach, e.g., very narrow beam, electronically scanned, millimeter wave, etc., the following steps are recommended as the proper course of development:

1. Perform computer simulations of scenarios to establish performance requirements, i.e., time available to measure and warn, parameter dynamic range (maximum angular change, range rate change), etc.

2. Convert the results of item 1 to system requirements, i.e., repetition rate, antenna beam width, scan rates, data rates, etc.

3. Convert item 2 into critical subsystem development and pursue development to completion, e.g., the antenna and data processor.

4. With critical subsystem performance known (or estimated based on better predictions), complete specifications for an advanced CAR radar.

5. Implement and test the advanced system.

It is felt that the scanning beam system in the extended target environment is the best hope of success in developing a radar that can function outside of the one-lane radar. No wavelength is implied as proper and all are candidate. Proper development as outlined above must be followed to ensure success in minimum time.

SECTION 12
SUMMARY

PRELIMINARY DESIGN REQUIREMENTS ASSESSMENTS

A large amount of collision avoidance radar work has occurred since about 1970. Much of the effort was conducted by separate independent labs such as RCA, Rashid, CA Research, and Bendix. Unfortunately, only one-dimensional, non-angle sensing radars were researched and developed to any extent. The attendant problems with these simpler non-angle sensing radars include high false alarm rates, lack of multiple target detection and tracking, and unacceptably narrow coverage areas. In addition, these non-angle sensing radars cannot compute target path trajectories, which means that a target crossing the radar beam will often trigger an alarm even though it is not on a collision trajectory. This effect primarily contributes to the false alarm problem. Angle tracking can be used to alleviate these false alarms. There are systems under development to provide some level of angle tracking, such as the Nissan microwave radar. However, commercialization has not occurred, and we are suspicious that the Nissan system may suffer similar disturbances which affected our phase monopulse approach, i.e., extended target and multipath interference.

The operating environment for a collision avoidance radar is complicated by the multitude of radar reflecting objects, some of which are collision hazards and some of which are not. A radar that can sense and track all these objects and predict a possible collision between the radar and any of these objects appears to be the best approach. This is in contrast to the previously investigated simpler, non-angle sensing, single target tracking radars.

TRAFFIC ACCIDENT REPORT ANALYSES' CONCLUSIONS

Traffic accident data could be very useful for determining system specifications for a collision avoidance radar. Unfortunately, sufficiently detailed traffic accident data are not yet available to support the subtler system specification requirements such as beam width as determined from the crash distributions for each degree of angle off of boresight. Only general system characteristics can be deduced from currently available data, which for example, only gives frequency of accidents occurring within each 30 degree sector.

DATA COLLECTION RADAR SYSTEM (RF/IF)

A data collection radar system was designed and fabricated. The emphasis was placed on system specifications which seemed most likely to be used in later developmental models if the approach taken should have proved to be viable. Major features of this system included 24 GHz narrow pulsed transmitter, dual channel receiver, logarithmic IF amplification, large receiver dynamic range, and moderately low receiver noise figure.

Design values for peak transmitter power were not able to be attained within the alloted time; this necessitated a change in antenna components to provide compensation. In addition, a higher gain antenna system was recognized to be required to provide adequate signal levels for the angle channel.

PREDICTED RESPONSE FOR DATA COLLECTION RADAR

An analysis was performed on the radar design implemented for data collection. Predicted (ideal) response patterns were generated for the sum and angle channels. The normalized angle channel response was generated for the standard gain horn array as well as the slotted waveguide array.

WEATHER EFFECTS ON RADAR PERFORMANCE

A study was performed addressing nine areas of concern for radar design and performance vis-a-vis atmospheric conditions. The areas considered were (1) effect of index of refraction changes, (2) transmitter modulation type effects, (3) antenna polarization effects on precipitation cancelling, (4) gaseous attenuation, and (5) rain, fog, snow, hail, and sandstorm/dust-storm interference to radar operation. Heavy rates of rain or partially melted hail/snow could cause disruptions in radar operation. The effect of slushly accumulations over the antenna face could be investigated at some point.

DATA ACQUISITION SYSTEM

A data acquistion system was assembled for collecting radar receiver output data. This system comprises time sampler boards used for bandwidth compression, analog amplifiers, stereo video cassette recorder and camera interface timing boards, analog-to-digital converters, microcomputer plus plotters, printers, etc., and special software. This system represents a significant capability given the time allotted. A bandwidth limitation of less than 20 KHz is a problem with this system. It will be upgraded for any future data acquisition/analysis activities.

SYSTEMS TEST

A series of static tests were performed using a special radar reflector and a midsized auto (1977 Granada). A designated and marked off 600-foot concrete road was the test site. Limited dynamic testing was performed using the entire 2400-foot road. After encountering several problems with the data collection system, changes were made to alleviate the disturbances and to allow collecting meaningful data. Response plots were generated from the collected data.

The tests revealed that multipath effects are present which disturb target illumination and return signal reception. In addition, the extended, or large when compared to the far field distance of the target ($2\ D^2/\lambda$),* nature of the midsized auto disrupts the behavior of the angle sensing channel. The angle sensing capability of the radar is degraded to an unusable extent due to these effects.

CONCLUSIONS AND RECOMMENDATIONS

Based on systems tests and discussions held subsequently with other researchers in this field, it is felt that a modified approach to the collision avoidance problem is required. While the monopulse is in general appropriate to far field tracking radar problems, it appears to be incapable of providing the higher quality angle information required by us.

It is recommended that additional effort be expended to develop more extensive radar parameter requirements, then to redesign a radar approach based on these requirements. The insight and expertise gained during this project effort being reported on now will prove very valuable for future efforts.

RADIATION HAZARDS CONSIDERATIONS FOR THE COLLISION AVOIDANCE RADAR SYSTEM

A study was performed addressing the thermal effects of microwave exposure due to one or more radar systems. Microwave levels for a typical candidate radar implementation were considered. The expected levels due to one radar's radiation were calculated for the antenna aperture to well into the far field. Multiple radiator configurations were proposed, and their effects were calculated using worst case values which arise from overly ideal assumptions regarding radiated power efficiency, phase coherency, and spatial summation. The current U.S. standard is not exceeded nor is a more strict proposed U.S. standard. The conservative U.S.S.R. standard maximum levels are only exceeded in a few, unlikely situations which are based on overly ideal propagation conditions.

MODELING AND ACCURACY CONSIDERATIONS

A report was prepared addressing decision logic for collision trajectory models. Items addressed included vehicular minimum stopping distances, equations of vehicle motion, and collision detection logic.

*where D = largest dimension of target and λ = .49 inches

SECTION 13
COMPREHENSIVE BIBLIOGRAPHY

COLLISION AVOIDANCE RADAR

1. Grimes, D. M. and V. P. McGinn, "Automotive Radar: Practicality and Effectiveness," SAE Government-Industry Conference, Washington, D.C., May 1984.

2. McGinn, V. P., "A Beam Steerable Microwave Antenna for Automotive Radar Application," Ph.D. Dissertation, The Pennsylvania State University, 1984.

3. "Final Report (Evaluating Two 1977 Automobiles Equipped with Bendix Radar Systems) to the DOT-NHTSA on Contract No. DTNH22-81P-07211," The Pennsylvania State University, Department of Electrical Engineering, January 1983.

4. Belohoubec, E. F., et al., "Radar Control for Automotive Collision Mitigation and Headway Spacing," IEEE, VI-31, May 1982.

5. Mainz, Barry E., "A Parabolic Dish Antenna for Every Bumper," Microwaves 21 (Nov. 1982), pp. 27-28.

6. Nogami, T., Toyota Motor Co., and T. Sakamoto, Fujitsu Ten Ltd., "Automotive Warning System Using 50-GHz Band Radar," The Ninth International Technical Conference on Experimental Safety Vehicle, Kyoto, Japan, November 14, 1982.

7. Tachibana, A., et al., "Stereo Radar System for Automobile Collision Avoidance," Nissan Motor Co., Ltd., Ninth International Technical Conference on Experimental Safety Vehicles, Kyoto, Japan, November 1-4, 1982,

8. "Collision Avoidance System Cost-Benefit Analysis," Volume I - Technical Report, Kinetic Research, DOT-HS-806-242, September 1981.

9. "Collision Avoidance System Cost-Benefit Analysis," Volume III, DOT-HS-806-244, Kinetic Research, September 1981.

10. Laugenie, J-M., "Simulation of Detection in Automotive Radar," The Pennsylvania State University, MS Thesis, 1981.

11. Pruvot, H., "Propagation Systems in Automotive Radar," The Pennsylvania State University, M.S. Thesis, 1981.

12. Redmond, D., V. Ausherman, and V. Costa, "Methodology for the Computation of Fatality and Injury Loss Reduction Accruing from the Installation of Radar Controlled Brakes on Passenger Cars," for use on Contract No. DTNH22-80-C-07530, 'Collision Avoidance System Cost-Benefit Analysis', Kinetic Research Technical Report KR-TR-106, July 1981.

13. Takenhana, T., et al., "Automotive Radar Using m.m. Wave," I. Mech. E., C178/81, 1981.

14. Ausherman, V. and K. Friedman, "Review of Collision Avoidance Cost-Benefit Analyses," Kinetic Research Technical Report KR-TR-073, November, 1980.

15. Ausherman, V. and A. Khadildar, "Selection of Accident Data Base and Accident Analysis Approach for Collision Avoidance System Benefit-Cost Analysis," Kinetic Research Technical Report KR-TR-083, December 1980.

16. Belohoubek, E., J. J. Risko, et al., "Electronic Subsystems for the Research Safety Vehicle (RSV) Phase III," RCA Laboratories Report PRRL-80-CR-8, March 1980.

17. Dougan, P. and K. Friedman, "User's Manual for the Kinetic Research Accident Environment Simulation and Projection (KRAESP) Model, Version 3," Kinetic Research Technical Report KR-TR-066, December 1980.

18. "Electronic Subsystems for the Research Safety Vehicle (Phase III)," RCA Laboratories, Report No. NHTSA-79-001, Contract No. DOT-HS-7-01552, March 1980.

19. Hahn, L., Further Development of Autarkic Headway Warning Radar Systems, VDO Adolf Schindling AG, January 1980.

20. Redman, D., "Calculation of the Projected Benefits of Upgraded Restraint-Structure System Performance Using the KRAESP Model," Kinetic Research Technical Report KR-TR-067, September 1980.

21. Redmond, D. and K. Friedman, "Introduction to the Kinetic Research Accident Environment Simulation (KRAESP) Model," Kinetic Research Technical Report KR-TR-041, January 1980.

22. Belohoubek, E., "Radar-Controlled Functions in the U.S. Research Safety Vehicle," 7th International Technical Conference on Research Safety Vehicles, Paris, France, June 1979.

23. "Collision Avoidance Radar Braking Systems Investigation - Phase III Study," The Bendix Corporation Research Laboratories, Report No. 8940, Contract No. DOT-HS-6-01450, June 1979.

24. Der Bundesminister für Forschung und Technologie, Entwicklungslinien in Kraftfahrzeugtechnik und Strassenverkehr, Forschungsbilanz, Verlag TUV Rheinland Gmbh, 1979.

25. Flannery, J. B., et al., "An Improved Radar Anticollision Device," SAE 790456, Detroit, March 1979.

26. Fujikawa, T., et al., A Study of the Automatic Braking System Central Engineering Laboratories, Nissan Motor Corporation, June 1979.

27. Grimes, D. M., "Recent Autonomous Collision Avoidance Systems in the USA," International Symposium on Traffic and Transportation Technologies, IVA 1979, Hamburg, Germany, June 1979.

28. Hahn, L., "Advances in the Development of Headway Radar Using Pulse Techniques," Second International Conference on Automotive Electronics, London, November 1979.

29. Jones, T. O. and D. M. Grimes, "Some Automotive Radar System Considerations," Second International Conference on Automotive Electronics, London, October 29-November 2, 1979.

30. Jones, T. O. and D. M. Grimes, "Some Automotive Radar System Considerations," Microwave Journal, 1979.

31. Kiyoto, M., N. Fujiki, et al., "A Study of the Automatic Braking System," 7th International Conference on Experimental Safety Vehicle - Paris, June 1979.

32. "Neininger, G., Gerätetechnische Voraussetzungen zur Durchführung eines Erprobungsprogrammes für Radarabstandswarngeräte," SEL. BMFT Forschungsbilanz, pp. 153-168, 1979.

33. Redmond, D., "Implementation and Preliminary Analysis of 1979 State of North Carolina Accident Data," for use on Contract DTNH22-80-C-07530, 'Collision Avoidance System Cost-Benefit Analysis', Kinetic Research Technical Report KR-TR-103.

34. Der Bundesminister für Forschung und Technologie, Entwicklungslinien in Kraftfahrzeugtechnik und Strassenverkehr, Forschungsbilanz, Verlag TUV Rheinland Gmbh, 1978.

35. Duell, E. H. and H. J. Peters, "Collision Avoidance System for Automobiles," SAE Technical Paper 780263, 1978.

36. Friedman, D. and E. Belohoubek, "The Near-Term Prospect for Automotive Electronics: Minicars' Research Safety Vehicle," Proc. Int. Conf. Auto. Electronics, Dearborn, MI, pp. 120-130, September 1978.

37. Friedman, R. E., "PRICE - A Parametric Cost Modeling Methodology," RCA Government and Commercial Systems, May 1978.

38. Funke, J. L., "Target Identification Capability of Swept Frequency Automobile Radar," SAE 780261, Detroit, March 1973.

39. Neininger, G. "35-GHz Radarabstands Warnsystem mit Mikroprozessor Unterstützter Signal Auswertung - Entwicklungs Stand, Messergebnisse," SEL, BMFT Forschungsbilanz, pp. 550-558, 1978.

40. Rose, G. F., "A Baseband Radar Sensor for Auto Braking Applications," SAE Int. Auto. Eng. Congress, Detroit, March 1978.

41. Tamama, T., A. Iwabe, K. Ban, M. Tsudo, S. Mitsui, of Mitsubishi Electric Corporation, and K. Baba, M. Kiyoto, H. Endo, N. Fujiki, of Nissan Motor Co., Ltd., "Radar Sensor for Automotive Collision Prevention," International Microwave Symposium, MTT-IEEE, Ottawa, Canada, October 1978.

42. Willins, W., "Auto Anticollision Radar Accelerates Away from the Lab Backburner to Global Test Sites," Microwaves, January 1978.

43. Belohoubek, E., J. Cusak, J. Risko, J. Rosen, "Microcomputer Controlled Radar Display For Cars," Paper 770267, Presented at The Society of Automotive Engineers International Automotive Engineering Congress and Exposition, Detroit, February 28-March 4, 1977.

44. Chandler, R. A. and L. E. Wood, "System Consideration for the Design of Radar Braking Sensors," IEEE VT-26, May 1977.

45. Friedman, K., "BRAKE Algorithm Documentation," KRI-TR-020, December 1977.

46. Zur Heiden, D. and H. Oehlen, "Radar Anticollision Warning System for Road Vehicles," SEL, Stuttgart, Electrical Communication, Volume 52, pp. 141-145, 1977.

47. Neininger, G., "An FM/CW Radar with High Resolution in Range and Doppler; Application for Anti-Collision Radar for Vehicles," Standard Elektrik Lorenz AG, D, 7000 Stuttgart, West Germany, 1977.

48. Raudonat, U. and F. Sautier, "Mehrzielfähiges FM/CW Radar zur eindeutigen Messung von Entfernung und Geschwindigkeit," Nachrichtentechnische Zeitschrift, Vol. 3, pp. 255-260, 1977.

49. Ross, G. F. and K. Robbins, "Baseband Radar Braking System for Automobile Application," Final Report to U.S. Department of Commerce under Contract No. 07-0142, June 1977.

50. Tambas, N. S., J. R. Treat, S. T. McDonald, "An Assessment of the Accident Avoidance and Severity Reduction Potential of Radar Warning, Radar Actuated, and Anti-Lock Braking Systems," SAE Paper 770266, 1977.

51. Storwick, R. M., "Review of Target Discrimination Techniques for Automobile Radar Applications," SAE 770264, Detroit, March 1977.

52. Troll, W. C., et al., "Results from a Collision Avoidance Radar Braking System Investigation," SAE 770265, Detroit, March 1977.

53. Zimdaj, W., "Simulationsuntersuchungen zu Problemen der Abstandswarnung in Kraftfahrzeugen," Regelungstechnik, No. 6, 1977.

54. The Bendix Corporation, "Collision Avoidance Radar Braking Systems Investigation--Phase II Study, Volume I--Summary Report," Contract No. DOT-HS-4-00913, February 1976.

55. The Bendix Corporation, "Collision Avoidance Radar Braking Systems Investigation--Phase II Study, Volume II--Technical Reports," Contract No. DOT-HS-4-00913, September 1976.

56. Köhler, U. and H. Zackor, "Abstands-Warngeräte. Eine Möglichkeit zur Erhöhung der Verkehrssicherheit." StraBenverkehrstechnik, No. 6, 1976.

57. Lindner, K. and W. Wiesbeck, "35 GHz Impulsradarsensor zur Verwendung in Abstandswarngeräten für Kraftfahrzeuge," NTZ, Vol. 29:9, pp. 667-672, 1976.

58. Radtke, Th., "Autarkes Abstandswarngerät zu Erhöhung der Sicherheit im StraBenverkehr," 4th Status Seminar on the Vehicle and Road Traffic Engineering of the Federal Ministry of Research and Technology, 10-12.11.76 in Berlin.

59. Wocher, B., "Beschreibung der Auswertelogik für ein Abstandswarngerät - Betriebserfahrungen," 4th Status Seminar on the Vehicle and Road Traffic Engineering of the Federal Ministry of Research and Technology, 10-12.11.76 in Berlin.

60. "Analysis of Problems in the Application of Radar Sensors to Automotive Collision Prevention," DOT-HS-801-453, Institute of Telecommunications Sciences, March 1975.

61. Chandler, R. A., et al., "A Review of Philosophical Considerations in the Development of Radar Brake Systems," SAE 750086, Detroit, February 1975.

62. Jones, T. O. and D. M. Grimes, "A Review of Automotive Station Keeping and Braking Radars," Microwave Journal, October 1975.

63. Kaplan, G. S., F. Sterzer, "Dual-Mode Automobile Collision Avoidance Radar," Paper 750087, Presented at the Society of Automotive Engineers International Automotive Engineering Congress and Exposition, Detroit, February 24-26, 1975.

64. Krage, Mark K., "Binaural Automobile Radar," Automotive Engineering and Exposition, Paper 750089, February 24-28, 1975.

65. Nagy, L. L. and J. A. M. Lyon, "An Ultrashort Pulse Radar Sensor for Vehicular Precollision Obstacle Detection," IEEE VT-24, November 1975.

66. Nicolson, A. M. and G. F. Ross, "A New Radar Concept for Short Range Application," Symposium Record, IEEE 1975 International Radar Conference, pp. 146-151, April 1975.

67. Storwick, R. M. and L. Nagy, "Automobile Radar Signature Studies," SAE 750088, Detroit, February 1975.

68. Tresselt, C. P., "Variable Range Cutoff System for Dual Frequency CW Radar," U.S. Patent 3,898,655, dated August 5, 1975.

69. "Tri-Level Study of the Causes of Traffic Accidents: Interim Report II (Volume II: Radar and Anti-Lock Braking Payoff Assessment." Indiana University, DOT-HS-801-631, June 1975.

70. "Collision Avoidance Radar Braking Systems Investigation: Phase I Study," Bendix Research Labs, DOT-HS-801-253, October 1974.

71. Flannery, J. B., "Automotive Braking by Radar," presented at the SAE Automotive Engineering Congress, Paper #740094, February 25-March 1, 1974.

72. Grimes, D. M. and T. O. Jones, "Automotive Radar: A Brief Review," Proceedings of the IEEE, Volume 62, Number 6, June 1974.

73. Ives, A. P. and P. M. Jackson, "A Vehicle Headway Control System Using Q-Band Primary Radar," Paper #740097 presented at the SAE Automotive Engineering Congress, February 25-March 1, 1974.

74. "Potential Payoff of Radar and Anti-Lock Braking Systems in Preventing Accidents and Reducing their Severity," Institute for Research in Public Safety, Indiana University, Preliminary Report, July 1974.

75. Ross, G. F., "Barbi, A New Concept for Precollision Sensors," Sperry Research Center, Sudbury, Mass., Research Report SCRC-RP-74-12, April 1974.

76. Shefer, J., R. J. Klensch, H. C. Johnson, and G. S. Kaplan, "A New Kind of Radar for Collision Avoidance," Paper #740096 presented at the SAE Automotive Engineering Congress, February 25-March 1, 1974.

77. Troll, William C., "Automotive Radar Brake," Bendix Corp., presented at the Automotive Engineering Congress in Detroit, Michigan, Society of Automotive Engineers, New York, February 25-March 1, 1974.

78. "Analysis of Problems on the Application of Radar Sensors to Automotive Collision Prevention," DOT-HS-801-011, Institute for Telecommunications Sciences, December 1973.

79. The Bendix Corporation, "Braking Performance Analysis," Contract #PO-A-33529, July 1973.

80. Holmstrom, F. R., J. B. Hopkins, A. T. Newfell, and E. F. White, "A Microwave Anticipatory Crash Sensor for Activation of Automobile Passive Restraints," IEEE Trans. Vehicle Technology, Vol. VT-22, pp. 46-54, May 1973.

81. Hopkins, John D., "Anticipatory Sensors for Collision Avoidance and Crash Protection as Applied to Vehicle Safety Research," U.S. Department of Transportation, Transportation System Center; Proceedings of the Vehicle Safety Research Integration Symposium, NHTSA, May 30 and 31, 1973.

82. Hyltin, T. M., T. D. Fuchser, H. B. Tyson, and W. R. Regueiro, "Vehicular Radar Speedometer," SAE Paper 730125, January 1973.

83. Johnson, H. C. and A. Presser, "Automotive Doppler Radar Speed Sensor," RCA Corporate Engineering Services, 1973.

84. Jones, T. O., D. M. Grimes, R. A. Dork, and W. R. Reguiero, "Automotive Radar-Problems and Promises," in WESCON, Professional Program, September 1973.

85. Shefer, J. and R. J. Klensch, "Harmonic Radar for Automobile Collision Avoidance," IEEE Spectrum 10, May 1973.

86. "System Construction, Functional Theory, and Performance of the Toyota Air Bag Radar Sensor (FM/CW)," Toyota Motor Co., Ltd., August 1973.

87. Tresselt, C. P., "Range Cutoff System for Dual Frequency CW Radar," U.S. Patent 3,766,554, dated October 26, 1973.

88. Troll, W. C. (Bendix Research Labs., Detroit, Mich.), "Automotive Radar," Presented at the University of Michigan Automotive Electronics Course, March 12, 1973.

89. Wood, L. E., et al., "Analysis of Problems on the Application of Radar Sensors to Automotive Collision Prevention," DOT-HS-801-010: TEA 6090.W66, December 1973.

90. Hazel, M. E., et al., "A Microwave Anticipatory Crash Sensor for Automobiles, SAE Paper 720423, May 1972.

91. Jones, T. O., et al., "A Critical Review of Radar as a Predictive Crash Sensor," SAE 720424, Second Int. Conference on Passive Restraints, Detroit, May 1972.

92. Jones, T. O., O. T. McCarter, and R. N. Oglesby, "Comparative Analysis of Crash Sensors," SAE Paper 720035, January 1972.

93. Responses to National Highway Traffic Safety Administration, Docket 72-1, "Automatic Braking System," July 27, 1972.

94. Stevens, J. E. and L. L. Nagy, "Diplex Doppler Radar for Automotive Obstacle Detection," Presented at the IEEE Vehicular Technology Group Conference, Dallas, Texas, December 1972.

95. Takahashi, T., T. Makine, and K. Sato, "Development of a Radar Sensor for Inflatable Occupant Restraint System," SAE Paper 720422, May 1972.

96. NHTSA - DOT to NMVSAC DOT, "Transcript of Comments on Automotive Braking," September 1972.

97. Lare, L. B. and W. E. Weber, "A Benefit - Cost Analysis of Auto Safety Features," Applied Economics, Vol. 2, No. 4, 1970.

98. Carp, R. W., J. G. Elliott, and J. S. Weidman, "Adaptive Speed Control and Automobiles," Bendix Technical Journal, Autumn 1969.

99. Boyer, W. D., "A Diplex Doppler Phase Comparison Radar," IEEE Transactions on Aerospace and Navigation Electronics, pp. 27-33, March 1963.

100. Versace, J., L. Gau, and G. Platzer, "Driver Response to Radar Brakes," presented at the Highway Research Board Annual Meeting, Washington, D.C., January 1958.

GENERALLY RELATED REFERENCES

1. "Atmospheric Absorption of Millimeter Waves," Microwave System Designer's Handbook, 1985.

2. Bernstein, Mary, "BEMS Hears Evidence of Health Risk," Microwaves and RF, August 1985.

3. Cember, Herman, Introduction to Health Physics, New York, NY: Pergamon Press, 1983.

4. Potson, David, "Extremely Fast Log Amp Handles Narrow Pulses," Microwave and RF, April 1985.

5. Stilwell, G. W., A. M. Madni, Dr. L. A. Wan, "Sensitivity Analysis of a 15.0 GHz Monopulse Radar Receiver Using Logarithmic Amplifier Detector Scheme," IEEE MTT-S Digest, 1985.

6. "Fatal Accident Reporting - 1982," DOT-HS-806-566 May 1984.

7. "National Accident Sampling System - 1982," DOT-HS-806-530, March 1984.

8. "The Economic Cost to Society of Motor Vehicle Accidents," DOT-HS-806-342, January 1983.

9. Jessop, G. R., "VHF/UHF Manual," Radio Society of Great Britain, 1983.

10. Klimko, L., "Development of an AIS to Delta-V Relationship for Vans and Light Trucks," Kinetic Research Technical Report KR-TR-905, January 1981.

11. Redmond, D., "Adjustments Made to the 1979 North Carolina Data to Make it Nationally Representative," Kinetic Research Technical Note KR-TN-013, May 1981.

12. Klimko, L. and K. Friedman, "Preliminary Results on the Feasibility and Application of the SASE Methodology to the Derivation of AIS to Delta-V Relationships from State Data," for use on Contract DOT-HS-9-02096, Kinetic Research Technical Report KR-TR-057, April-1980.

13. Liao, S. Y., Microwave Devices and Circuits, Prentice-Hall, NJ, 1980.

14. Wood, P. J., Reflector Antenna Analysis and Design, Peregrinus, 1980.

15. Larsen, H. J., B. O. Shubert, Probabilistic Models in Engineering Sciences, Vol. I, John Wiley and Sons, 1979.

16. Proctor, Gene, NISOH Draft Report, "Recommended Standard on RF/Microwave Radiation," NISOH, 1979.

17. Robel, M. C., "Prediction of Atmospheric Refraction Angular Error by a Computer Raytrace Program with Application to the Space Shuttle MSBLS," LEC-16619, December 1979.

18. Rudduck, R. C. and S. H. Lee, Numerical Electromagnetics Code (NEC) - Reflector Antenna Code, Part I: User's Manual, The Ohio State University, September 1979.

19. Rudduck, R. C. and S. H. Lee, Numerical Electromagnetics Code (NEC) - Reflector Antenna Code, Part II: Code Manual, The Ohio State University, September 1979.

20. "1977 Annual Report - Fatal Accident Reporting System," U.S. Department of Transportation, DOT-HS-301-954, November 1973.

21. "Highway Safety 1977", U.S. Department of Transportation, DOT-HS-303-372, June 1973.

22. Carver, K. R., "Notes on Microwave Antennas," Las Cruces, NM, January 1978.

23. Raff, S. J., Microwave System Engineering Principles, Pergamon Press, 1977.

24. Faigin, B. M., "1975 Societal Costs of Motor Vehicle Accidents," U.S. Department of Transportation, DOT-HS-302-119, December 1976.

25. Rückstrahlortungsgerät mit Frequenzmodulation: German Patent Application No. 2611321, March 17, 1976.

26. Rückstrahlortungsgerät zur gleichzeitigen Messung von Entfernung und Relativgeschwindigkeit: German Patent Application No. P 2514868, April 4, 1975.

27. Barton, D. K., Low Angle Radar Tracking, Proc. IEEE 62, No. 6, pp. 687-704, June 1974.

28. Bradley, S. G. and C. D. Stow, "The Measurement of Charge and Size of Raindrops," Journal of Applied Meteorology, February 1974.

29. "How Tough is the Environment for Auto Electronics?," SAE Automotive Eng., January 1974.

30. McCarter, D. T., Environmental Guidelines for the Designer of Automotive Electronic Components, No. 740017, SAE Automotive Engineering Congress.

31. Nagy, L. L., "Electromagnetic Reflectivity Characteristics of Road Surfaces," IEEE Transactions on Vehicular Technology, VT-23, No. 4, pp. 117-124, September 1974.

32. Andrews, G. B., "Control of the Automotive Electrical Environment," SAE Paper 730045, January 1973.

33. Local Climatological Data, Detroit, Michigan, Metropolitan Airport, U.S. Department of Commerce, 1973.

34. Martin, E. E., "Dual Polarized Radar Cross-Section Measurements of Vehicles and Roadway Obstacles at 16 GHz and 70 GHz." Eng. Exp. Station, Georgia Tech, November 1973.

35. Maxam, G. L., O. T. McCarter, and D. E. Schofield, "Electromagnetic Interference and the Automobile," SAE Paper 730129, January 1973.

36. McCarter, O. T., "An Electronic Systems Viewpoint of the Automobile Environment, Presented at the 11th Electrical/Electronics Insulation Conf., IEEE-NEMA, September 1973.

37. Nagy, L. L., "Electromagnetic Reflectivity of Road Surfaces," General Motors Corp. Rcs. Rep. 1341, June 1973.

38. Ross, G. F. (Sperry Research Center), The New York Times, Business and Finance Section, May 26, 1973.

39. Augustine, C. F., "A Doppler Radar Using the Janus Principle as a True Ground Speed Indicator," Presented at the University of Michigan Workshop on Automotive Radar, June 26, 1972.

40. CCIR, Conclusions of the Interim Meeting of Study Group 5 (Propagation in Non-Ionized Media), International Telecommunications Union, Geneva, Switzerland, 1972.

41. Gazis, D. G., "Traffic Flow and Control: Theory and Applications," Amer. Sci., Vol. 60, pp. 414-424, 1972.

42. Herman, R., T. Lam, and I. Prigogine, "Kinetic Theory of Vehicular Traffic: Comparison with Data," Transpri. Sci., Vol. 6, pp. 440-452, November 1972.

43. Michealson, S. M., "Human Exposure to Non-Ionizing Radiant Energy - Potential Hazards and Safety Standards," Proceedings, IEEE, pp. 389-421, April 1972.

44. State of Colorado, Roadway Design Manual, State Department of Highways, 1972.

45. Cowley, M., S. Hamilton, and R. J. Riezman, "Cut the Costs of Doppler Radars," Electron. Des., Vol. 13, pp. 48-53, June 24, 1971.

46. Brown, W. M. and J. F. Riordan, "Resolution Limits with Propagation Phase Errors," IEEE Trans. Aerosp. Electron. Syst., Vol. AES-6, pp. 657-662, September 1970.

47. Cox, D. R., "The Analysis of Binary Data," Halsted Press, a division of John Wiley and Sons, New York, 1970.

48. Skolnick, M. I., Radar Handbook, McGraw-Hill Book Co., 1970.

49. Barton, D. K., Radar System Analysis, Prentice-Hall Inc., 1969.

50. Collin, R. E. and F. J. Zucker, Antenna Theory, McGraw-Hill, New York, 1969.

51. Compton, R. T. Jr. and R. E. Collin, "Open Waveguides and Small Horns," in Antenna Theory, Part I, R. E. Collin and F. J. Zucker, eds. New York: McGraw-Hill, 1969.

52. W. J. Evans and G. I. Haddad, "Frequency Conversion in IMPATT Diodes," IEEE Trans. Electron Devices, Vol. ED-16, pp. 78-87, January 1969.

53. McGillem, C. D., G. R. Cooper, and W. B. Wittman, "Use of Wideband Stochastic Signals for Measuring Range and Velocity," EASCON Record, pp. 305-311, 1969.

54. Nathanson, F. E., Radar Design Principles, McGraw-Hill, 1969.

55. Rihaczek, A. W., Principles of High Resolution Radar, McGraw-Hill, Inc., 1969.

56. Crispin, J. W., K. M. Siegel, Methods of Radar Cross-Section Analysis, Academic Press, 1968.

57. Jordan, E. C. and K. G. Balmain, Electromagnetic Waves and Radiating Systems, Prentice-Hall, 1968.

58. Weeks, W. L., Antenna Engineering, McGraw-Hill, 1968.

59. Crane, R. K., "Microwave Scattering Parameters for New England Rain," MIT Lincoln Lab Report 426, Lexington, Mass., 647798, October 3, 1966.

60. Herman, R., "Theoretical Research and Experimental Studies in Vehicular Traffic," in 3rd Conf. of the Australian Research Board, Vol. 3, Pt. 1, pp. 25-56, 1966.

61. Ross, R. A., "Radar Cross-Section of Rectangular Flat Plates as a Function of Aspect Angle," Transactions on Antennas and Propagation, Vol. AP-14, No. 3, 330-335, May 1966.

62. Schetzen, M., "The Power Density Spectrum of the Echo from an Airborne Doppler Radar," M.I.T. Instrumentation Lab. Rep. R-541, March 1966.

63. United States of America Standards Institute (USASI), "Safety Level of Electromagnetic Radiation with Respect to Personnel," C95.1, November 1966.

64. Born, M. and E. Wolf, Principles of Modern Optics, 3rd ed., New York: Pergamon, 1965.

65. Kerr, D. E., "Propagation of Short Radio Waves," New York: Dover, 1965.

66. Matthews, P. A. and A. L. Cullen, "A Study of the Field Intensity at an Axial Focus of a Square Microwave Lens," IEEE Monograph No. 186R, pp. 449-456, July 1965.

67. Silver, S., Microwave Antenna Theory and Design. New York: Dover, 1965.

68. Valley, Shea L. ed., Handbook of Geophysics and Space Environments, McGraw-Hill, 1965.

69. Yeh, C., "Reflection and Transmission of Electromagnetic Wave by a Moving Dielectric Medium," J. Appl. Phys., Vol. 36, pp. 3513-3517, November 1965.

70. Beckmann, P., and A. Spizzichino, The Scattering of Electromagnetic Waves from Rough Surfaces, Pergamon Press, New York, NY, 1963.

71. Gardels, K. and K. Herman, "Vehicular Traffic Flow," Sci. Amer. 1963.

72. Keller, J. B., Geometrical Theory of Diffraction, J. Opt. Soc. Am., 1962.

73. Nilssen, O. K., "New Methods in Range Measuring Doppler Radar," IRE Trans. Aerosp. Navig. Electron., Vol. ANE-9, pp. 255-265, January 1962.

74. Rubin, W. L., and S. K. Kamen, "SCAMP - A Single-Channel Monopulse Radar Signal Processing Technique, IRE Trans. MIL-6, pp. 146-152, April 1962.

75. Skolnik, Merril I., Introduction to Radar Systems. New York, NY: McGraw-Hill, 1962.

76. Fradin, A. Z., Microwaves Antennas, New York: Pergamon, 1961.

77. Jasik, H., Antenna Engineering Handbook, New York: McGraw-Hill, 1961.

78. Saunders, W. K., "Post-War Developments in Continuous-Wave and Frequency-Modulated Radar," IRE Trans. Aerosp. Navig. Electron., Vol. ANE-9, pp. 7-18, March 1961.

79. Huebner, G. J. Jr., "Engineering for Safety with a Psychological Yardstick," Presented at the SAE Greenbriar Meeting, White Sulphur Springs, W. Va., September 1960.

80. Thourel, L., The Antenna, New York; Wiley and Sons, 1960.

81. Andrews, G. B. and H. A. Bazydlo, "Crystal Noise Effects on Zero IF Receiver," Proceedings, IRE, pp. 2018-2019, November 1959.

82. Dunn, J. H., D. D. Howard, and A. M. King, Phenomena of Scintillation Noise in Radar Tracking Systems, Proc. IRE, 47, pp. 855-836, May 1959.

83. Peake, W. H., "Theory of Radar Return from Terrain," IRE Conv. Rec., Part I, pp. 27-41, 1959.

84. Rhodes, D. R., Introduction to Monopulse, New York: McGraw-Hill, Inc., 1959.

85. Taylor, R. C., "Terrain Return Measurements at X, Ku, and Ka Band," IRE Conv. Rec., Part I, pp. 19-26, 1959.

86. Urquhart, L. C., Civil Engineering Handbook, New York: McGraw-Hill, Inc., 4th ed., 1959.

87. Schultz, F. V., R. C. Burgener, and S. King, "Measurement of the Radar Cross-Section of a Man," Proc. IRE, 46, 476-481, 1958.

88. van de Hulst, H. C., Light Scattering by Small Particles, New York: Wiley, 1957.

89. Bullington, K., "Reflection Coefficients of Irregular Terrain," Proc. IRE, Vol. 43, pp. 1258-1262, August 1954.

90. Gunn, K. L. S. and T. W. R. East, "The Microwave Properties of Precipitation Particles," Mc. Gill University, Montreal, July 1954.

91. Freedman, J., Resolution in Radar Systems, Proc. IRE 39, No 7, pp. 813-818, July 1951.

92. Jordan, Edward C., Electromagnetic Waves and Radiating Systems, Englewood Cliffs, NJ, 1950.

93. Kaplan, Wilford, Advanced Calculus, Reading, Mass., 1952.

94. Kras, J. D., Antennas, McGraw-Hill, 1950.

95. Haddock, F. T., Scattering and Attenuation of Microwave Radiation through Rain, Naval Research Laboratories, Washington, 1948.

96. Marshall, J. S. and W. Palmer, "The Distribution of Raindrops with Size," Journal of Meteorology, pp. 165-166, August 1948.

97. Hansen, W. W., in Radar System Engineering, R. N. Ridenour, ed., New York: McGraw-Hill, 1947.

98. Silver, S., Microwave Antenna Theory and Design, MIT Radiation Lab Series, New York: McGraw-Hill, Inc., December 1947.

99. Sokolnikoff and Sokolnikoff, Higher Mathematics for Engineers and Physicists, New York: McGraw-Hill, 1941.

100. "Pedestrian Involvement, Multidisciplinary Accident Investigation," University of Houston, DOT-HS-087-1-117, U.S. Department of Transportation, National Highway Traffic Safety Administration.

101. Kustom Electronics, Inc., Lenexa, Kansas.

102. Decatur Electronics, Decatur, Illinois.

103. Federal Signal Corporation, Signal Division, University Park, Illinois.

104. M.P.H. Industries, Inc., Chanute, Kansas.

1. Report No	2. Government Accession No.	3. Recipient's Catalog No.
NASA TM 58275		

4. Title and Subtitle	5. Report Date
Application of Radar for Automotive Collision Avoidance Volume 1: Technical Report Volume 2: Development Plan and Progress Reports	April 1987
	6. Performing Organization Code

7. Author(s)	8. Performing Organization Report No.
C. L. Lichtenberg (Editor)	S-555
	10. Work Unit No.

9. Performing Organization Name and Address	11. Contract or Grant No.
NASA-Lyndon B. Johnson Space Center Tracking and Communications Division Houston, Texas 77058	DTNH22-85-X-07163
	13. Type of Report and Period Covered

12. Sponsoring Agency Name and Address	Technical Memorandum (FINAL) 11/84 through 12/85
U.S. Department of Transportation National Highway Traffic Safety Administration Washington, D.C. 20590	14. Sponsoring Agency Code

15. Supplementary Notes

16. Abstract

The purpose of this project was to investigate, delineate, develop, and perform tasks related to the development of an automobile collision avoidance radar system. Items within the scope of this 1-year effort were to (1) review previous authors' work in this field; (2) select a suitable radar approach; (3) develop a system design; (4) perform basic analyses and observations pertinent to radar design, performance, and effects; (5) fabricate and collect radar data from a data collection radar; (6) analyze and derive conclusions from the radar data; and (7) make recommendations about the likelihood of success of the investigated radar techniques.

The major finding was that the application of radar to the automobile collision avoidance problem deserves continued research and development even though the specific approach investigated in this effort did not perform adequately in its angle measurement capability. Additional findings were that (1) preliminary performance requirements of a candidate radar system are not unreasonable; (2) a significant number of traffic accidents and/or their severity could possibly be lessened by using a collision avoidance radar system which observes a fairly wide field-of-view ahead of the radar-equipped vehicle (approximately ± 10 degrees or wider; (3) the health radiation hazards of a probable radar design are not significant even when a large number of radar-equipped vehicles are considered; (4) effects of inclement weather on radar operation can be accommodated in most cases by judicious system design; (5) the phase monopulse radar technique as implemented and tested here demonstrated inferior angle measurement performance which warrants the recommendation of investigating alternative radar techniques; and (6) extended target and multipath effects, which presumably distort the amplitude and phase distribution across the antenna aperture, are responsible for the observed inadequate phase monopulse radar performance.

17. Key Words (Suggested by Author(s))	18. Distribution Statement
Collision avoidance Accident prevention Radar Warning systems Safety devices	Unclassified - Unlimited Subject category: 85

19. Security Classif. (of this report)	20. Security Classif. (of this page)	21. No. of pages	22. Price*
Unclassified	Unclassified	254	

*For sale by the National Technical Information Service, Springfield, Virginia 22161